Final Report

Investigation of the Ability of Filters to Stop Erosion through Cracks in Dams

Subcontract Number: DEN33411

Performance Period: January 1, 2001 to December 31, 2003

Prepared by

Youngjin Park
Thomas L. Brandon
J. Michael Duncan

Department of Civil and Environmental Engineering
200 Patton Hall
Virginia Tech
Blacksburg, VA 24061

Chapter 1. Introduction

1.1. Background

Since Terzaghi (1922) developed grain size criteria for granular soils in dam filters, many researchers have studied embankment dam filters. The major function of the filter is to prevent erosion and piping. In order to have this ability, filters must restrain the particles of the protected soil (the base soil) and allow water to pass freely out of the base soil. Sherard et al. (1984) modified these criteria for cohesive soils, and developed the concept of "critical filters," that can prevent erosion even under the severe condition where the base soil is cracked, and where concentrated flow occurs through the crack.

In addition to grain size criteria that ensure restraint of the base soil while allowing free passage of water, a filter must also be graded so that the filter itself will not crack. To ensure that filters will not support cracks, most current filter gradation criteria require that no more than 5% of the filter material should be finer than the #200 sieve, and that the fines within the filter should be non-plastic. However, it is not clear that this criterion is sufficient. At Ochoco Dam shown in Figure 1.1, a sinkhole developed in a filter that was designed to have a maximum of 3% passing the #200 sieve. This incident at Ochoco Dam gave rise to renewed interest in filter criteria, and resulted in sponsorship of the research described in this dissertation. This research was designed to investigate the crack-preventing and crack-stopping abilities of filters, and to develop criteria that can be relied upon to ensure that a filter will perform its essential function even when subjected to deformations that cause cracks in the adjacent core.

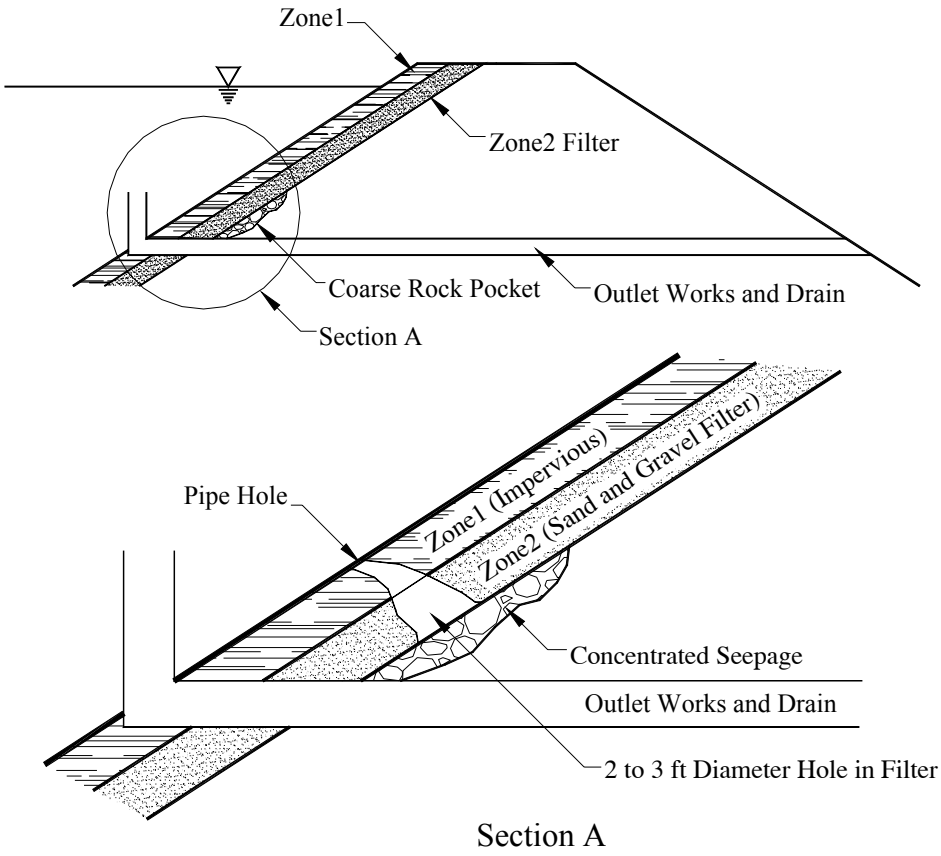

Figure 1.1 Ochoco Dam Piping Problem

1.2. Transverse Cracks in Dams

Transverse cracks in embankment dams can develop as a result of post-construction settlement (Hsu, 1981) or earthquake deformations (USCOLD, 1992). These cracks result from differential settlements or deformations. A related and equally serious problem can occur where settlements or earthquake - induced deformations cause separation between an embankment dam and an adjacent concrete structure.

Hsu (1981) reported that piping through settlement–induced transverse cracks has occurred in Apishapa Dam (1923), Stockton Dam (1950), Cougar Dam (1963), Round Butte Dam (1964), Yard's Creek Dam (1963), Matahina Dam (1966), and Viddalsvatn Dam (1971). In Yard's Creek Dam, Matahina Dam, and Viddalsvatn Dam, the cracks extended through the filters as well as the core, because the filters contained excessive amounts of fines (Hsu, 1981).

USCOLD (1992) reported two instances of transverse cracks in dams resulting from earthquake deformations. Matahina Dam (New Zealand) suffered settlements and cracking as a result of the Magnitude 6.3 Edgecumbe Earthquake on May 2, 1987. Trenching showed that the cracks were shallow, and that they did not extend across the core. The trenching exposed a large cavity which was thought to be related to earlier core cracking, seepage and internal erosion. The rate of seepage through the dam increased as a result of the earthquake. Austrian Dam (California) suffered deformations and cracking as a result of the Magnitude 7.1 Loma Prieta Earthquake on October 17, 1989. A transverse crack was traced 30 ft down the left abutment, and transverse cracking and separation of the embankment from the spillway occurred to a depth of 23 ft on the right abutment. Water levels in the embankment, measured in open well piezometers, increased as a result of the earthquake.

1.3. Filters and Crack-Stoppers

It is commonly assumed that filters downstream of the cores in dams will prevent erosion and piping through transverse cracks in dams (Sherard and Dunnigan, 1989). This assumption is based on the concept that the filter will be cohesionless, and that it will not support a crack. However, as shown by observations at Yard's Creek, Matahina, and Viddalsvatn Dams, this is not always the case.

The ability of a filter to provide a reliable line of defense against erosion and piping depends on the cohesionless nature of the filter material, and its own inability to support a

crack. The same is true of upstream crack-stoppers – zones of sand upstream from the core, designed to wash into and fill cracks. If they crack and do not wash into the crack in the core, they will not perform their intended function.

1.4. Objectives of the Research

This research to investigate the ability of filters to stop cracks has four principal elements:

- A review of the literature concerned with filters, and particularly the crack-stopping ability of filters.
- Development of a laboratory filter test device for testing composite specimens with cracks formed through both the filter and the base coarse material.
- Development of procedures for processing base and filter materials, in order to have precise control over their grain-size distribution.
- Performing tests on composite specimen to explore (1) the effect of the compaction water content, (2) the effects of the density to which the filter material is compacted, (3) the effect of the width of the crack that extends through the base and filter material, and (4) the effects of the percentage of fines in the filter material.

Chapter 2. Literature Review

2.1. Introduction

In this chapter, previous laboratory research, theoretical studies, and discussions are summarized and reviewed. Table 2.1 shows summary of references that are related with this research. The most significant finding from these previous studies are described in Section 2.2.1 - 2.2.12.

2.2. Significant finding from previous studies

2.2.1. Sherard (1979)

In several cases, sinkholes have formed in dams as a result of piping of well-graded core soils. These broadly-graded cores were glacial in origin with nearly linear gradations. The filtration of the silt-sized fraction is critical when these soils are used for dam cores. The filter should be fine sand to medium fine sand. In order to assess the stability of the broadly graded soils, Sherard suggests splitting the gradation curve at the 1.0 mm particle size and analyzing it as two separate gradations.

Table 2.1 Literature Review Summary

Reference	Title	Type of Study	Principal Findings
Bertram, G.E. (1940)	An Experimental Investigation of Protective Filters	• Lucite tube with a diameter of 2inches and a length of 6inches used as a permeameter • Base materials were compacted to 70% standard Proctor • Natural sands, Ottawa sand, and Quartz sand were tested as base and filter materials • Hydraulic gradients with mean values 7 and 19 were used for all materials • Permeability of each base / filter combination was measured for time durations between 6-8 hrs. • Transport of the base materials into the filter were determined through pre-test and post - test comparisons of base material	• $D_{15F} / D_{85B} = 6$ for stability • D_{15F} / D_{85B} is independent of the shape of the soil particles • $D_{15F} / D_{85B} = 6$ is acceptable criteria for tests with hydraulic gradients ranging from 6 to 20
Arulanandan, K., Loganathan, P. & Krone, R.B. (1975)	Pore and Eroding Fluid Influences On Surface Erosion of Soil	• Yolo Loam was used throughout testing. 1.5 Kilogram samples were prepared with varying Sodium Adsorption Rates (SAR) • Rotating Cylinder Test Apparatus designed to induce shear stress on the soil sample • Soil sample had dimensions equal to 3inches in diameter and 3.2inches in length. • Outer cylinder of test apparatus could be rotated at speeds up to 1500rpm. • Eroding fluid, with varying concentrations of Sodium was placed in between the soil sample and outer rotating cylinder	• Flocculated clay materials are produced at high sodium concentrations. It required a higher critical shear stress, τ_c, to induce erosion at higher sodium contents • Dispersion of the Yolo loam increased with increasing sodium adsorption ratio (SAR). This dispersion caused swelling of the particles and thus a decrease of inter-particle bonding.

Table 2.1 Literature Review Summary (cont.)

Reference	Title	Type of Study	Principal Findings
Vaughan, P.R. (1978)	Design of Filters For the Protection of Cracked Dam Cores Against Internal Erosion	• Discussion: Failure of Balderhead Dam in Northern England	• The manner in which the Balderhead core behaved during failure suggests that filter design criteria based on intact clay cores are invalid • Suggests that permeability of the filter material is a good measure for filter design. Mentioned average values of permeability for effective filters are $7*10^{-5}$ cm/s for uniform filters and $2*10^{-5}$ cm/s for graded filters. • At least 2.5% of the filter material should pass the #200 sieve in order to be effective in retaining the smallest particles of the clay core • Determined the size of the smallest clay particles by running hydrometer tests. • Suggests running "Sand Castle Tests" to determine the amount of cohesion in a filter. The test is performed by overturning a bucket of sand on a tray and running water over it. If the sand collapses to it's true angle of repose, it is not cohesive.
Arulanandan, K. (1978)	Erosion in Relation to Filter Design Criteria for Earth Dams	• Discussion of current filter design practice • Review of previous testing regarding erosion • A procedure for designing filters is given	• Terzaghi's design criteria do not consider erodibility characteristics of fines in the base material • Dispersive / Nondispersive behaviors do not accurately quantify whether a soil is erodible • Erodibility can be described using τ_c, the critical shear stress • For cores with fines, erodible soils have $\tau_c \leq 4$, moderately erodible soils have $4 \leq \tau_c \leq 9$, and erosion resistant soils have $\tau_c > 9$ • Procedure involves assuming that the core will crack, determining τ_c , performing flume and rotating cylinder tests, determining the head necessary for hydraulic fracturing, and finally selecting a filter to prevent the passage of fines and prevent cracking

Table 2.1 Literature Review Summary (cont.)

Reference	Title	Type of Study	Principal Findings
Sherard, J.L. (1979)	Sinkholes in Dams of Coarse, Broadly Graded Soils	• Cites case histories and references of sinkholes forming in dams having coarse soils as cores. • Suggests mechanism for erosion in cores having broad gradations	• Filtration of the silt-sized fraction very important • Problems soils are usually glacial in origin and have linear gradation curves • Can assess stability by examining gradation curves for the soil imagined to be split at 1mm particle size. • Should use fine to medium fine sands for filters
U.S. Department of the Interior (1980) 3rd Ed. (1998)	Earth Manual (2nd Ed.)	• Brief overview of the purpose and function of protective filters • Criteria for filter design and construction are given	• D_{50F}/D_{50B} = 5 to 10 for uniform filters • Use the minus #4 fraction if there is gravel in base soil • May need to use a graded filter
Hsu, S.J.C (1981)	Aspects of Piping Resistance To Seepage in Clayey Soils	• Review of Previous Studies: Discussion and Comparison of previous filter criteria theories	• No unique findings.
Vaughan, P.R. & Soares, H.F. (1982)	Design of Filters for Clay Cores of Dams	• Tests performed on potential filters for the Cow Green Dam • 50mm diameter acrylic tube 450mm in length was set up vertically • A plug of pre-saturated filter material was compacted at the bottom of the tube • Flocculated Clay was introduced with water flowing through the tube to and visually monitoring of the out-flowing water was performed to determine success or failure of the filter • The filter was deemed successful if the out-flowing water was free of clay particles	• Suggest that permeability should be the main measure of filter performance • Performed "Sand Castle" tests to determine whether or not a filter is cohesionless • Suggests that the amount of material passing the #200 sieve in a filter should be determined by the size of the smallest flocculated base particle.
Arulanadan, K. & Perry E.B. (1983)	Erosion in Relation to Filter Design Criteria in Earth Dams	Review of Previous Studies: Discussion of Current Filter Criteria and erosion of base materials	• With reference to Terzaghi, filter criteria for D_{15}, the void volume and permeability of the filter material decreases with increasing width of gradation. The

Table 2.1 Literature Review Summary (cont.)

Reference	Title	Type of Study	Principal Findings
			permeability of the filter can then become equivalent to that of the base material. • The consequences of a widely graded sand-gravel filter is that if it contains a significant percentage of fines passing the #200 sieve, combined with particle interlock, the filter may be able to sustain a crack. • The main dilemma is that it is necessary to have some percentage of fines in the filter material to prevent erosion but this in turn allows the filter to behave as a cohesive material • Base materials erode due to a surface shear stress caused by water flow through the materials.
Hillis, S.F. & Truscott, E.G. (1983)	Magat Dams: Design of Internal Filters & Drains	• Filter tests were performed specifically for the Magat dams • Permeameter constructed of a 580mm diameter oil drum. A glass window was installed on the side for observation of the soil behavior • A constant head of 5m was applied to the base and filter sample. The permeameter could be positioned for either vertical or horizontal flow • The core material tested was a broadly graded residual sand and gravel. The plasticity of the material was similar to some glacial tills • A perforated outflow pipe was installed through the base material to simulate field drainage conditions • Horizontal flow tests were inconclusive so a 500mm square flume with a length equal to 2000mm was constructed • A crack was placed in the base material by	• Visual observations of out-flowing water and base material migration proved success or failure of the filter • Cohesive base materials form arches at the filter/core interface and the gradation of the filter material to be used for design depends on the size of these arches.

Table 2.1 Literature Review Summary (cont.)

Reference	Title	Type of Study	Principal Findings
		placing two metal plates in the base area and compacting base material against them. The plates were then removed	
Lafleur, J. (1984)	Filter Testing of Broadly Graded Cohesionless Tills	• Tests performed on James Bay core material. • Permeameter tests performed with different gradations of the filter material • Tests were performed using a maximum value of hydraulic gradient equal to 8 • Base materials were compacted to less than 97% of the Standard Proctor, which, simulated field conditions that were worse than the minimum specifications for the James Bay dam. • Success or failure of a filter was based on visual inspection of the filter and by the change in permeability of the base/filter combination. A decrease in permeability was deemed a failure	• Suggests that permeability is a useful parameter in determining the success or failure of a filter • The degree of saturation of the base soil may affect the results of the tests. • Lower degrees of saturation can be useful in quantifying the apparent cohesion of a base material
Sherard, J.L., Dunnigan, L.P. & Talbot, J.R. (1984)	Basic Properties of Sand and Gravel Filters	• Filter test apparatus consisting of clear plastic cylinder with 10.16cm diameter. • Pressurized water system with approximately 4kg/cm^2 of pressure flowing through the cylinder. • 5.08-10.2cm thick base material compacted on top of 12.7-17.8cm filter material • Uniform sands were used as base materials. They were placed dry in 3 lightly tamped layers • Uniform sands and gravels were used as filter materials. They were compacted in a saturated condition to relative densities of 80-100%. D_{15F} size was approximately 1.0-10	• $D_{15F}/D_{85B} < 5$ is conservative for most uniform filters, but should continue to be used as the main criteria for judging filter performance. • D_{50F}/D_{50B} & D_{15F}/D_{15B} criteria established by USBR tests performed in 1955 are not supported by these experiments. • Angular particles and sub- rounded alluvial particles are both satisfactory for use as filter material. • The particle distribution of the filter material need not be the same as that of the base material. • Results from a side study to quantify pore size paths in graded filters indicate that for D_{15F} = 11mm, the minimum flow channel dimension is approximately (0.09-0.18) D_{15F}. Therefore, if above $D_{15F}/D_{85B} < 5$ is

Table 2.1 Literature Review Summary (cont.)

Reference	Title	Type of Study	Principal Findings
		mm. Uniform sand that was coarser than the base material and finer than the filter material was used as a "side material" to eliminate large voids at the base and filter / cylinder wall interfaces.	used, most base material will be captured by the filter.
Sherard, J.L. (1984)	Trends and Debatable Aspects in Embankment Dam Engineering	Discussion: Various issues in embankment Dam engineering	• Sands and gravelly sands with average D_{15F} values of 0.5mm or smaller are conservative filters for most fine-grained clays with D_{85B} size of 0.03 mm or larger • The D_{85B} size of the base material is normally 20 to 30 mm and thus requires a coarser filter material in order to satisfy the current $D_{85B}/D_{15F} \leq 5$ design criteria. These coarser materials tend to segregate when placed and can lead to large voids in the filter.
Sherard, J.L., Dunnigan, L.P. & Talbot (1984)	Filters for Silts & Clays	• Slot test using sand and gravel filters compacted to a relative compaction = 95% of the maximum Standard Proctor density. • Slurry test performed by mechanically breaking down the base material from slot tests and using the slurry as the base. • Tests run with hydraulic gradient varying from 1000-2000. • Pressure increased in increments of 0.5 kg/cm^2 until discoloration of flowing water was noticed. • Numerous variations of the base material were tested. Base materials consisted of CL, CH, ML, and CL-ML. • Numerous adaptations of filters with D_{15F} ranging from 0.3mm – 9.5mm.	• Slot Tests and Slurry Tests give identical results. • Atterberg limits of the base material have no influence on the selection of the filter material. • Critical value of D_{15F} is about 0.1mm smaller when distilled water is used during testing as opposed to tap water. • The slot test is severe because it allows higher velocities to flow through the crack than would be achieved in the field. • Current $D_{15F}/D_{85B} < 5$ criteria are in agreement with these test results.
Sherard, J.L. & Dunnigan, L.P. (1985)	Filters and Leakage Control in Embankment Dams	• No Erosion Filter Test • Same apparatus as slot and pinhole tests. The NEF test uses a diameter with a value	• On any given base soil with a filter finer than D_{15B} (boundary) there is no visible erosion in the pinhole • The filter boundary (D_{15B}) for typical silts and clays,

Table 2.1 Literature Review Summary (cont.)

Reference	Title	Type of Study	Principal Findings
		equal to 100mm for fine soils and 280mm for coarse soils • The base soil has a thickness of 25mm for fine soils and 100mm for coarse soils • A hole is formed in the base soil. The diameter of the hole has a value equal to 1.0mm for fine soils and a range in values from 5-10mm for coarse soils • The flow through the sample is in a downward direction at a pressure equal to 4kg/cm^2 • The base material / filter material performance is observed for 5 – 10minutes	defined by the NEF, is approximately 20-40% of that defined by the slot and slurry tests • Test results are influenced by grain size distributions only. They are not influenced by the plasticity of the soil. • Crack fillers, upstream sand filters with material finer than the base material should not be relied upon to stop cracks. Instead the downstream filter should be designed more conservatively • $D_{15F}/D_{85B} < 9$ is a recommended design criteria for base material with 85-100 % passing #200 sieve
Kenney, T.C., Chahal, R., Chiu, E., Ofoegbu, G.I., Omange, G.N., & Ume, C.A. (1985)	Controlling Constriction Sizes of Granular Filters	• Mathematical analysis of the maximum and minimum constriction sizes in a soil • Uses test results and discussions from previous studies	• The parameter D_c* is defined as the controlling constriction size of the filter, which is the same as the maximum particle size that can pass through a filter of particular thickness • The capability of a filter is dependent on the minimum constriction sizes along a flow path • Base particles larger than D_c* cannot pass through the filter • Base particles smaller than D_c* can pass through the filter depending on the seepage • Controlling constrictions sizes is useful in filter design but cannot be used alone • For cohesionless bases: $D_{50B} > D_{5F} / 4$ or $D_{50B} > D_{15F} / 5$; use coarser • For cohesive bases, filter performance is influenced strongly by hydrodynamic conditions in filter and constrictive sizes should be used only to aid in filter design
Kenney, T.C., & Lau, D. (1985)	Internal Stability of Granular Filters	• Seepage cells with diameters of 245mm and 580mm	• With respect to filter gradations, there are stable and unstable gradations

Table 2.1 Literature Review Summary (cont.)

Reference	Title	Type of Study	Principal Findings
		• Diameters of specimens were about 240mm and 550mm • Relative densities of the samples were close to 100 % • Various gradations used in filter materials • Vibration was induced during water flow through light tapping of cylinder with a rubber hammer	• Vibration of test samples causes a large increase in migration of smaller particles to the bottom of the sample
U.S. Army Corps of Engineers (1986) – Change 1: 30 Apr 1993	Engineering and Design: Seepage Analysis and Control for Dams, EM 1110-2-1901	Manual for fundamental design principles for seepage considerations	• Appendix D states filter criteria – current criteria is in 1993 Change • Design steps are the same as given by the Bureau of Reclamation (1994) and are the currently accepted criteria.
Townsend, F.C., Shiau, J. & Pietrus, T.J. (1987)	Piping Susceptibility and Filter Criteria for Sands	• Rectangular flume 1ft. x 1ft. x 7.5ft. with a transparent top used to observe piping effects on sands • Three filter design gradations and thicknesses were evaluated • Bedford sand used as base material for filter tests	• Smaller diameter pipes concentrate flows more, create higher hydraulic gradients and initiate piping more easily. • The current filter criteria $D_{15F}/D_{85B} \leq 4$ was verified for the cohesionless base tested. This criterion provides a factor of safety value approximately equal to 2.
Lowe, John III (1988)	Seepage Analysis	• Discussion and explanation of Terzaghi filter criteria based on Bertram's work • Explanation of how to use Terzaghi criteria for a gap-graded material • Gives guidelines regarding construction methods, types of filter sand to use, and thickness of filers	• No unique findings
Das Neves, E.M. (1989)	Analysis of Crack Erosion in Dam Cores: The Crack Erosion Test	• Semi-cylindrical base and filter material. The split cylinder sample represents a crack in the sample. The tested crack width was 5mm. • Material is placed in horizontal flow test	• When low flow velocities are passed through the crack, erosion may be dependent upon crack orientation. • Gravity plays an important role in erosion.

Table 2.1 Literature Review Summary (cont.)

Reference	Title	Type of Study	Principal Findings
		apparatus with a transparent plate to observe erosion of base material. • A geotextile material is placed on the upstream side of the base sample to prevent turbulent water flow through the apparatus. • Granite and schist materials are used as the base materials. The soils are compacted at optimum water content. • Two different filters were developed to test with each base material. Filter A possessed a D_{15F} = 2.3 mm and a Coefficient of Uniformity C_u = 1.6. Filter B possessed a D_{15F} = 0.95 mm and a C_u = 1.5. • Flow through the apparatus is laminar with Reynolds number varying between 100 and 125. The corresponding hydraulic gradient is $5 * 10^{-3}$ cm/sec	• Low flow velocities (2cm/s) are capable of transporting base materials to the front of the filter. • The ability of a base material to seal itself is partially dependent upon the material's ability to floc together (cohesion).
Honjo, Y. & Veneziano, D. (1989)	Improved Filter Criterion for Cohesionless Soils	Analytical Study: Use of Statistical Model to compare current filter criteria	• As per experiments performed by Mendez (1981), Soares (1980), and Southworth (1980), the stability of the base soil is controlled by the coarser particles. In the early stages of erosion, a self-healing layer forms at the base/filter interface • Statistical modeling verified the Terzaghi parameter of $D_{15F} / D_{85B} < 4\text{-}5$ • Statistical study agrees that the D_{50F} / D_{50B} is not a correct filter design parameter • A self healing index parameter is also useful in filter design. $D_{95B} / D_{75B} < 7$ is applicable for cohesionless base soils
Khor, C.H., & Woo, H.K. (1989)	Investigation of Crushed Rock Filters for Dam Embankment	• No Erosion Filter Test (NEF) with a diameter equal to 170mm and a length equal to 290mm • Base materials tested were low plasticity	• Test results agree with the findings of Sherard that D_{50B} criteria is inadequate for the sandy impervious soil • Results from tests ran with cracked bases give finer

Table 2.1 Literature Review Summary (cont.)

Reference	Title	Type of Study	Principal Findings
		silts taken from the core of the Sungai Malut Dam • Base soils were compacted to 95% Proctor density • Pinhole and induced crack tests were performed • Filters with varying gradations were tested to find the proper filter boundary, D_{15B}, for each base/filter combination	filter criteria than those with pinhole cracks • Test results lead the authors to believe that there is a better correlation than D_{15F}/D_{85B}. This new correlation relates the d_{85} to the percent finer than the # 200 sieve
Pinto, P.S. & Santana, T (1989)	Filters For Clay Cores of Embankment Dams	• Conventional filter tests with water flowing in the horizontal direction. Water pressures were increased from a value of 50kPa to a value of 200 kPa in time increments of 5minutes. • Slot filter tests. Water pressures were applied in the same manner as the conventional filter test. • Pinhole filter tests with a 1mm diameter hole. Water pressure was applied instantaneously at a pressure of 250kPa for approximately 20-25minutes. • Three types of base materials were tested: CH, SM, & CL. • Four types of filter materials were tested with each base. The D_{15F}/D_{85B} ratios varied from 0.3-17 depending upon the base-filter combinations. The C_u of the filters ranged from 2.4 –8.3. • Relative compaction of the base materials ranged from 90% - 100% Standard Proctor.	• When D_{15F}/D_{85B} <4, the filter did not fail. • Flow rate increased with decreasing Dr, resulting in failure. • The velocity attained in the slot tests was not high enough to cause any erosion of the base. (1 m/s). • In terms of pressure and gradient, laboratory tests are unconservative when compared to actual field studies.
Sherard, J.L. & Dunnigan, L.P. (1989)	Critical Filters for Impervious Soils	Review of Previous Studies: Summary of results of previous tests and soil conditions	• Tests were performed on numerous variations of base material and filter material. 28 different base samples with 4 different filters

Table 2.1 Literature Review Summary (cont.)

Reference	Title	Type of Study	Principal Findings
			• Successful & unsuccessful filters are independent of the hydraulic gradient used • The NEF test illustrates a worst case scenario in core material behavior • The water content and density of the core is not a big factor. The ratio of gradation between the base and filter is the main factor • Lists filter boundaries (D_{15B}) for different fines contents.
Goldsworthy, M. H. (1990)	Filter Tests- Direct or Indirect	Review of Previous Studies: Comparison of Pinhole Erosion Tests and smallest particle measurements to determine erosion rates of base materials	• Vaughn and Soares recommended an indirect method of measuring the erosion of base materials through filters in 1982. This method is based on measurement of the smallest particle of the core material. • The size of the smallest particle that would arrive at the filter is dependent on the flocculation of base material. • Methods of directly determining erosion rates of base materials are based on the previous work performed by J. Sherard. • Results of this study show that the critical filter size predicted indirectly from the base materials floc size is larger than those obtained from direct filter tests.
Leonards, G.A., Huang, A.B., & Ramos, J (1991)	Piping and Erosion Tests at Conner Run Dam	• Constant head permeability test capable of applying high gradients • Clay base materials compacted to 95% of the maximum standard Proctor dry density. The clays had plasticity indexes ranging from 13 to 21 • Pinhole tests were performed to observe internal erosion of the base materials	• For the base materials tested, plasticity had no influence on the resistance to internal erosion • When the base materials were compacted to 100% of the maximum Standard Proctor dry density, the range of hydraulic gradient at which piping was initiated increased from • $40 < i < 80$ to $160 < i < 240$

Table 2.1 Literature Review Summary (cont.)

Reference	Title	Type of Study	Principal Findings
Chapuis, R.P. (1992)	Similarity of Internal Stability Criteria for Granular Soils	• Comparisons between recommendations of Kezdi, Sherard, and Kenney & Lau are made • A brief explanation of each of these methods is given	• The criteria given by the three methods are similar; all give minimum slopes for grain size distribution curves for when a soil is no longer self-filtering • The three methods can be replaced with minimum values for the secant slope of the grain size distribution curve • Experience and caution is needed to use this minimum slope value
Talbot, J.R. & Deal, C. (1993)	Rehabilitation of Cracked Embankment Dams	Review of Previous Studies: Dam construction	• Many dams constructed in the 1950's and 1960's contained no defensive measures against cracking. • These dams were designed without transitions or filters and drainage zones. • Most dams studied used collapsible soils that are found in the arid west and Great Plains of the U.S. • These soils exhibit a rapid loss of strength and large volume change when saturated. • SCS results have shown that a properly designed filter can be effective in preventing concentrated leaks and eventual failure due to erosion in these dams. Filter criteria as per Sherard. • Swelling of the base material seals most minor cracks in clay dams. • Limit equilibrium analysis techniques were first used to determine the factor of safety for embankment dams. There are two problems with this approach: This method requires predetermined, assumed failure surfaces which generally don't represent the failure surface that will develop as a result of a foundation collapse. In addition, the c and ϕ values used in the analysis are not appropriate. At a "critical moisture condition", cohesion decreases with an increase in the internal friction angle. • Proposed using finite element analyses to model

Table 2.1 Literature Review Summary (cont.)

Reference	Title	Type of Study	Principal Findings
			cracking and differential settlement of embankment dams.
Åberg, B. (1993)	Washout of Grains from Filtered Sand and Gravel Materials	• A model for self-filtering during washout was developed based on both theory and previous experiments • The model applies to cohesionless materials only and describes the self-filtering behavior of a material, not the interaction between two materials	• Using this model, the self-filtering during washout of a soil can be accurately modeled provided that the hydrodynamic number, R', is greater than 15 or 20. • There are two causes for grading instability: 1) loose grains traveling relatively large distances through the soil and 2) washout of fixed grains, such as with a gap-graded material. This model addresses the second type only. • A disadvantage to the model is that it requires five empirical coefficients
U.S. Bureau of Reclamation (1994)	Design Standards No. 13: Embankment Dams	Design standards are given for earth dams; filter criteria is given in sections 5.7 to 5.12	• An eight step procedure for filter design is given • The criteria is based on four soil categories which are defined by % passing the #200 sieve
McCook, D. K & Talbot, J. (1995)	NRCS Filter Design Criteria – A Step By Step Approach	A condensed version of the results of the research performed by the SCS in 1980-1985	• A twelve-step procedure for designing a filter is given • Procedure includes current USBR criteria
Indraratna, B., Vafai, F., & Haque, M.A. (1996)	Laboratory and Analytical Modeling of Granular Filters	• Conventional filter test apparatus • A constant head of about 2 m was applied to the sample at a mean gradient of 8 to 10 • Uniform and well graded sandy filters were tested • Filters were fine, medium and coarse with values of Coefficient of Uniformity (C_u) ranging in values from 1.34 to 1.40 • Gap-graded base materials were tested for erosion potential by using a screen as the filter. • Lateritic residual soils with values of Coefficient of Uniformity (C_u) greater than 4	• Uniform sand filters of fine to medium grain sizes are effective in establishing a self-filtering interface • Uniform coarse sand filters are ineffective in establishing a self-filtering interface due to their permeability and porosity. • The concept of a gap-graded ratio was defined as the ratio between the upper and lower bound of the gradation curve gap for a base material • A gap-graded ratio equal to 4 is considered to be the critical ratio

Table 2.1 Literature Review Summary (cont.)

Reference	Title	Type of Study	Principal Findings
		were tested as base materials	
Terzaghi, K., Peck, R.B., & Mesri, G. (1996)	Soil Mechanics in Engineering Practice, 3rd Ed.	Excerpt from a textbook; briefly explains how a filter functions	• Particle migration and erosion are the causes for most catastrophic earth dam failures • Filter voids are small enough to block passage of fine materials and large enough to allow water to escape • Filters should not be broadly graded or gap graded • Filter materials should be checked to ensure internal stability
Fenton, G.A. & Griffiths, D.V. (1997)	Extreme Hydraulic Gradient Statistics in Stochastic Earth Dam	Two earth dam cross sections were studied to determine how internal hydraulic gradients are effected if there is spatial variability in the dam's permeability	• Constant permeability of the dam produces more conservative results than if the permeability is spatially varying; for constant permeability, the elevation of the downstream exit point is higher. • The free surface does not change significantly when there is special variability in permeability. • Drains with permeability at least 120 times the dam permeability proved to be successful • It was found that since special variability of permeability does not change the probability of higher internal gradients, the current soil stability design criteria is conservative
Reddi, L.N., Ming, X. & Lee, I.M. (2000)	Permeability Reduction of Soil Filters due to Physical Clogging	• Experiments were run to observe the reduction in filter permeability due to clogging. A model was also developed to predict this behavior. • For the experiment, concrete sand was used as the filter and the influents were particles suspended in water. Both kaolinite and polystyrene microspheres were used as influent.	• The filter permeability reduced more than one order of magnitude after the filtering of 300 to 600 pore volumes • Increasing the influent particle concentration leads to a faster permeability reduction • Changing the flow rate does not appear to change the clogging behavior • The model developed fits the experimental data well

Table 2.1 Literature Review Summary (cont.)

Reference	Title	Type of Study	Principal Findings
Locke, M., Indraratna, B. & Adikari, G. (2000)	Erosion and Filtration of Cohesive Soils	• Permeameter with a diameter equal to 150 mm • Soil sample is compacted in five, 40 cm thick layers with a 90% Standard Proctor density. The sample is 150mm in diameter and 200mm long • Pinhole with a diameter equal to 3 mm is pushed through the sample • Modified pinhole test • Water supply producing flow velocities through the samples with values ranging from 0.7 to 3.5 m/s • Out-flowing water is collected on an aluminum foil sheet and oven dried. The remaining sediment is scraped from the sheet • Particle size diameters of the scraped sediment are determined using a Melvern Particle Size Analyzer (PSA)	• The resistance to surface erosion of a cohesive soil is dependent primarily on the inter-particle bonding forces • Erosion is strongly influenced by the Sodium Adsorption Ratio (SAR) of the soil • It requires approximately 2-3 days after the pinhole is made for the sample to gain full strength and be ready for an erosion test • The modified pinhole test provides a reasonable method to model erosion in base materials • Before dispersion, eroded particles are significantly larger than the primary particles of the soil. This indicates that erosion occurs as aggregates of materials
Ramos, F.D. & Locke, M (2000)	Design of granular filters: Guidelines & Recommendations	• Comparison of empirical data, mathematical models, and Test procedures to predict filter performance • Description of common problems associated with the NEF test and recommendations to alleviate these problems	• Empirical methods can quickly determine safe filters during project investigation and development. However there are some limitations in application and these methods are not conservative • Mathematical models are adequate for predicting erosion within the filter materials as a function of time and their seepage rates • Increasing the fines content in a filter greatly improves the filter effectiveness. • Removal of the fines in a filter produces more conservative testing. • Compaction of the filter material can lead to breakage and thus more fines. This leads to a deviation in the gradation curve and therefore can produce false results

Table 2.1 Literature Review Summary (cont.)

Reference	Title	Type of Study	Principal Findings
			• Materials finer than those in the filter particle size distribution should not be used as a "side" material in the NEF test. These materials can be washed into the filter and produce false results • The authors recommend the use of modeling clay as a side material to prevent the above conditions from occurring • The base material should only contain the fraction passing the 4.75mm sieve, as the coarser fraction has no influence on filtration • Both standard sieve analysis and hydrometer tests should be performed on the base material to determine the tendency for the base to form flocs. • Distilled water should be used if the base material is determined to be dispersive • Coarse filter materials should not be present at the base / filter interface. These materials may clog the pinhole and produce false results • Erosion of the base soil usually occurs within the first 20 minutes of testing, therefore tests of longer duration are not necessary • The NEF test is very sensitive. The border between success and failure can be detected to within a filter size of 0.1mm.
Foster, M & Fell, R. (2000)	Use of Event Trees to Estimate the Probability of Failure of Embankment Dams by Internal Erosion and Piping	• The paper provides a summary of relevant literature on event trees and includes analysis of 17 dams that experienced either accidents or failure. • Qualitative guidance is given about the effect of certain factors on the likelihood of three events: the initiation of internal erosion, piping, and breaching. • Embankments studied are assumed to be	• For a detailed study of estimating the probability of failure by piping, event trees should be used. Historical performance methods can be limited. • Several tables (4 through 14) were developed to show the influence of certain factors on the likelihood of a particular event. • When assessing the likely performance of a filter, three branches should be used to represent the three possible filter behaviors: 1) seal without erosion, 2)

Table 2.1 Literature Review Summary (cont.)

Reference	Title	Type of Study	Principal Findings
		functioning under normal conditions (no seismicity). • The intent of the paper is to give guidance to experts when assigning conditional probabilities to their event trees.	seal with some erosion, and 3) excessive or continuing erosion. • Table 15 gives the relative importance of design and construction details on the likelihood of internal erosion and piping in terms of low, medium, and high importance. • Table 16 provides a linkage between verbal description of a risk and a numerical value for probability. • Historical trends are explained; for example, historically dams with good filters have very low likelihood of failure by piping.
Hurcomb, D. (2001)	Petrographic Examination of Exhumed Filter Sand-Horsetooth Dam Modifications-Colorado-Big Thompson Project, Colorado	Review of Study: Cementation Effects on Granular Materials	• The clay minerals that are present in sand filters cement together due to lack of water and are able to form bridges that capture sand particles. • The cemented sand and clay minerals collapse when they come into contact with water • Petrographic analysis was used to observe the structure of the cemented particle bridges • Semctite, illite/mica, and kaolinite minerals were present in the cemented samples
Foster, M & Fell, R. (2001)	Assessing Dam Filters That Do Not Satisfy Design Criteria	• A method is proposed to assess existing filters that do not satisfy current Sherard and Dunnigan criteria. • The study was based on lab test results performed by Sherard and Dunnigan and others as well as dams that experienced piping but not failure. • The proposed method can be used to define three boundaries: no-erosion, excessive-erosion, and continuing-erosion. • This method is intended for existing dams only; for new filter design, the modern	• Many existing dams have filters that are either too coarse by modern standards or became segregated during construction. It is possible for these filters to perform satisfactorily in some cases. • Dams with poor filter performance in general have broadly-graded cores (15% - 85% fines in base; $D_{95B} >$ 2mm) and filters with $D_{15F} > 1.0$mm on average. • Dams with good filter performance in soil group 2 had on average $D_{15F} \leq 0.5$mm. • The proposed criteria are given in Table 6; criteria are given for each of the three boundaries for each of the four soil types. Factors of safety are not included,

Table 2.1 Literature Review Summary (cont.)

Reference	Title	Type of Study	Principal Findings
		Sherard and Dunnigan criteria should be used	as this is only a method to assess existing filters.
Indratatna, B. & Radampola, S. (2002)	Analysis of Critical Hydraulic Gradient for Particle Movement in Filtration	• Analytic and laboratory study to determine the critical gradient for movement of a base particle through a filter. • Solution considered gravity, viscous drag, and frictional resistance between particle and pore channel. • Conventional laboratory filter tests were conducted. • Specimen diameter. = 15.5cm and ht = 24.5cm • Filter thickness = 6cm • Sand used as base material and gravel used as filter	• Critical hydraulic gradient function of minimum pore diameter, length of pore channel (filter), grain-to-grain friction angle, base material particle diameter, density of base material, and orientation of flow.

2.2.2. Vaughan and Soares (1982)

Filter experiments were run to test potential filters for the Cow Green Dam. Information from the failure at Balderhead Dam was used since the cores were made of similar clay. Also, lab tests in a 50 mm diameter by 450 mm long tube were run; a pre-saturated filter was first compacted in the tube and then clay flocs were introduced with flowing water. The amount of clay in the outflow was observed. Successful tests had outflow without clay particles. The authors suggest that permeability is the main measure of filter performance. The filter design for the percent passing the #200 sieve is governed by the size of the smallest flocculated base particle. Also, filters should be cohesionless to ensure that the filter itself cannot sustain a crack. A simple "sand castle" test was suggested for testing the cohesion of the filter material.

2.2.3.Sherard, Dunnigan, and Talbot (1984a)

Sand and gravel filters were tested in the lab to analyze the effectiveness of current filter criteria. A 10.16 cm diameter permeameter was used with a 13 cm to 18 cm thick filter beneath a 5 cm to 10 cm thick base. Results indicate that the criteria D_{15F}[1] /D_{85B} < 5 is conservative and should be the main criteria in judging filter performance. Upper case D refers to grain size of the filter. Numerical subscription indicates the percentage of the material that is finer than the indicated size. Subscription F and B means filter and base material. Criteria for D_{50F}/D_{50B} and D_{15F}/D_{15B} established by the USBR were not supported

[1] The USBR (1994) uses the following notation:

$D_{15}F$ where 15 is the % passing and F indicates filter (capital B indicates base)

The USACE (1993) uses the following notation:

d_{85} where lower case d represents the base particle size and 85 indicates the % passing

D_{15} where upper case D represents the filter particle size and 15 represents the % passing

To avoid confusion, this dissertation uses the following notation consistently throughout:

D_{15F} for a filter particle size of 15% passing

D_{85B} for a base particle size of 85% passing

by these experiments. Both angular and sub-rounded particles behaved well as filters. It was also seen that the shape of the filter gradation curve does not need to be the same as that for the base soil.

2.2.4. Sherard, Dunnigan, and Talbot (1984b)

In order to test the effectiveness of current criteria on silt and clay bases, slot and slurry tests were performed. Sand and gravel filters were used in the experiments. The slurry tests used base material from the slot tests to form the slurry base. Base materials consisted of CL, CH, ML, and CL-ML. The D_{15F} of the filters ranged from 0.3 mm to 9.5 mm. The results from both types of tests were identical. The slot test represents a more severe case such that velocities are higher through the crack than achieved in the field. A difference in critical value of D_{15F} was observed depending on the type of water used; distilled water caused the value to be about 0.1 mm smaller than when tap water is used. It was also found that the Atterberg limits of the base material did not influence the filter selection. The criteria, $D_{15F} / D_{85B} < 5$, agree with the results of these tests.

2.2.5. Sherard and Dunnigan (1985)

A "No Erosion Filter" test (NEF test) was developed to test the effectiveness of filters. It uses the same apparatus as the pinhole test and the slot test; the permeameter diameter is 100 mm for fine soils and 280 mm for coarse soils. The hole formed through the base soil is 1.0 mm for fine soils and 5 to 10 mm for coarse soils. Flow due to a water pressure of 4 kg/cm^2 was observed for 5 to 10 minutes. It was observed that for a base soil with a filter finer than D_{15B}, no visible erosion took place. For the NEF test, the largest successful D_{15B} was approximately 20% to 40% of the value defined by slot and slurry tests. It was also found that only the soil gradation influenced test results and not the plasticity of the soil. A main conclusion was that upstream sand filters should not be relied upon to stop cracks; instead, the downstream filter should be designed more conservatively. The

recommended criterion is $D_{15F} / D_{85B} < 9$ when 85% to 100% of the base soil passes the #200 sieve.

2.2.6. Kenney, Chahal, Chiu, Ofoegbu, Omange, and Ume (1985)

Mathematical analysis of the maximum and minimum constriction sizes in a soil is useful when designing granular filters. The capability of a filter depends on the minimum constriction sizes along a flow path. A parameter called D_c* is defined as the controlling constriction size of the filter. In other words, D_c* is the maximum particle size that can pass through a filter of a particular thickness. Base particles larger than D_c* cannot pass through the filter, and base particles smaller than D_c* can pass through the filter depending on the seepage conditions. For cohesionless bases, D_c* is the coarser of ($D_{50B} > D_{5F} / 4$) and ($D_{50B} > D_{15F} / 5$). Controlling constriction sizes in this way is useful in filter design but cannot be used alone. Especially in the case of cohesive bases, controlling constriction sizes is only an aid to filter design since filter performance for cohesive bases is strongly influenced by hydrodynamic conditions in the filter.

2.2.7. Das Neves (1989)

A crack erosion test was developed to test filters. Experiments were run using base materials of granite and schist and two filters, A and B. Filter A had D_{15F} = 2.3 mm and C_u[2] = 1.6 while filter B had D_{15F} = 0.95 mm and C_u = 1.5. The apparatus consisted of a cylindrical permeameter with a transparent plate for observation. The split cylinder represents a crack of width 5 mm. The material is placed so that flow is horizontal through the apparatus. A geotextile is placed on top of the base to prevent turbulent flow. With low velocities through the crack, erosion is dependent on the crack orientation. Also, gravity plays an important role in erosion. It was found that low velocities (2 cm/s) are capable of

[2] C_u: Coefficient of uniformity, $C_u = \frac{D_{60}}{D_{10}}$

transporting material to the filter interface. The ability of the base material to be self-healing is partly dependent on the cohesion of the soil or its ability to flocculate.

2.2.8. Honjo and Veneziano (1989)

An analytical study was conducted to compare various filter criteria. Experimentation by Mendez (1981), Soares (1980), and Southworth (1980) confirmed that the stability of the base soil is controlled by the coarser particles. Also, this experimentation show that in the early stages of erosion, a self-healing layer forms at the interface of the base and filter. Statistical modeling was used to confirm the Terzaghi criterion ($D_{15F} / D_{85B} < 4$ to 5). The statistical analysis also supports the conclusion that the D_{50F} / D_{50B} criteria are not useful in filter design. In filter design, a useful parameter is the self-healing index; for cohesionless bases, $D_{95B} / D_{75B} < 7$ indicates that material will be self-healing.

2.2.9. Khor and Woo (1989)

In order to investigate crushed rock filters, no erosion filter tests (NEF) were run. The base material used was low plasticity silts obtained from the core of the Sungai Malut Dam. Both pinhole and induced crack tests were run. A variety of filters were used to determine the proper filter boundary, D_{15B}, for each combination of filter and base. It was found that the D_{50B} criteria are inadequate, which is consistent with other results. Those samples with cracked bases required a finer filter than those with a pinhole. A conclusion made as a result of this testing was that there exists a better correlation than D_{15F} / D_{85B}. A better correlation relates the D_{85B} to the percent passing the #200 sieve.

2.2.10. Sherard and Dunnigan (1989)

Tests were performed on 28 different base samples and 4 filters. By comparing the data, it can be seen that success or failure of a filter is independent of the hydraulic gradient. The no erosion filter test (NEF) is a worst-case scenario of core material behavior. The water content and the density of the core are not controlling factors in filter success. The main factor is the ratio of filter gradation to base gradation.

2.2.11. Indraratna, Vafai, and Haque (1996)

Laboratory testing and analytical modeling were performed to assess the behavior of gap-graded base materials. In the testing, both uniform and well-graded sandy filters were used. The coefficient of uniformity, C_u, of the filters ranged from 1.34 to 1.40. The base materials used were gap-graded lateritic residual soils with C_u values greater than 4. It was found that uniform sand filters of fine to medium sands are effective in establishing a self-filtering interface. This was not the case with coarse sand filters; their inability to form a self-filtering interface is due to the permeability and porosity. A gap-graded ratio was defined as the ratio between the upper and lower bound of the gradation curve gap of the base material. The critical gap-graded ratio is considered to be equal to 4.

2.2.12. Locke, Indraratna and Adikari (2000)

A modified pinhole test was used to study erosion of base materials. The permeameter for this investigation had a diameter of 150 mm and a length of 200 mm. Soil was compacted in five each 40 cm thick layers. The pinhole diameter was 3 mm. After the pinhole was pushed through the soil, approximately 2 to 3 days were required for the sample to return to its original strength and be ready for testing. The outflowing water was collected and oven dried. The diameters of the sediment particles were then determined using a Melvern Particle Size Analyzer (PSA). This modified pinhole test provides a reasonable model of erosion in base materials. It was found that the resistance to surface

erosion of a cohesive soil is mainly dependent on inter-particle bonding forces. Also, erosion is influenced strongly by the sodium adsorption ratio (SAR) of the soil. It was determined that erosion occurs as aggregates of materials since before dispersion, eroded particles are significantly larger than the primary soil particles.

2.3. Current Filter Criteria

2.3.1. Gradation-based Filter Criteria

The history of research conducted on filter criteria for earth dams extends back almost 100 years. Design parameters for filters were published as early as 1910 (Hsu, 1981). However, the basis of the current form of filter design criteria can be attributed to work done by Terzaghi in the 1920's and Casagrande in the 1930's (Arulanandan and Perry, 1983; Hsu, 1981). It was recognized at that time that a filter must perform two separate tasks:

- It must prevent the migration of the core or base material into other zones of the dam, and
- It must possess a large enough hydraulic conductivity so that excess pore pressures are not developed in the dam and flow is channeled to the appropriate locations of the dam.

The criteria that Terzaghi proposed, still in use in a similar form today, was based on the gradation of the core or base soil to be protected. In order to satisfy the first criterion above, the following condition had to be met:

$$\frac{D_{15F}}{D_{85B}} < 4$$

where D_{15F} = grain size diameter of the filter where 15% by weight of the soil particles are smaller in diameter, and D_{85B} = the grain size diameter where 85% of the base or filter soil is smaller in diameter. In order to satisfy the second criterion, Terzaghi suggested that:

$$\frac{D_{15F}}{D_{15B}} > 4$$

where D_{15B} = the grain size diameter of the base or core where 15% by weight of the soil particles are smaller in diameter.

The first criterion provides a point on the gradation curve representing the coarsest allowable filter, and the second criterion provides a point on the gradation curve of the finest allowable filter.

The original Terzaghi criteria have been subjected to close scrutiny in the last 70 years. Laboratory tests and theoretical analysis have examined the validity of his choice of grain sizes and the minimum and maximum ratios of the two criteria. A good summary of these criteria was provided by Hsu (1981), and these are shown in Table 2.2 along with additional criteria developed since the publication of Hsu's paper.

Table 2.2 Filter criteria developed (after Hsu, 1981), modified to include more recently developed criteria

Author	Soil Type/Comments	Criteria
Terzaghi (1922)		$\frac{D_{15F}}{D_{85B}} \le 4, \quad \frac{D_{15F}}{D_{15B}} \ge 4$
Bertram (1940)	Silt, fine sand	$\frac{D_{15F}}{D_{85B}} \le 6, \quad \frac{D_{15F}}{D_{15B}} \le 9$
Hurley and Newton (1940)	Well-graded gravelly sand	$\frac{D_{15F}}{D_{15B}} \le 32, \quad \frac{D_{15F}}{D_{50B}} \le 15$

Table 2.2 Filter criteria developed (after Hsu, 1981), modified to include more recently developed criteria

Author	Soil Type/Comments	Criteria
U.S. Army Corps of Engineers (1941-1955)	Fine to coarse uniform sands	$4 \le \frac{D_{15F}}{D_{15B}} \le 20$, $\frac{D_{50F}}{D_{50B}} \le 25$, $\frac{D_{15F}}{D_{85B}} \le 5$
	Cohesive soils	$\frac{D_{15F}}{D_{15B}} > 5$, $\frac{D_{50F}}{D_{50B}} \le 25$, $\frac{D_{15F}}{D_{85B}} \le 5$
USBR (1947-1974)	Natural, sub-rounded, uniform materials	$5 \le \frac{D_{50F}}{D_{50B}} \le 10$
	Natural graded filters	$12 \le \frac{D_{50F}}{D_{50B}} \le 58$, $12 \le \frac{D_{15F}}{D_{15B}} \le 40$
	Crushed rock filters	$9 \le \frac{D_{50F}}{D_{50B}} \le 30$, $6 \le \frac{D_{15F}}{D_{15B}} \le 18$
Sherard and Dunnigan (1985)	Group 1 85%-100% fines	$\frac{D_{15F}}{D_{85B}} \le 9$
	Group 2 40%-85% fines	$D_{15F} \le 0.7\,\text{mm}$
	Group 3 0-15% fines	$\frac{D_{15F}}{D_{85B}} \le 4$
	Group 4 15-40% fines	Intermediate between groups 2 and 3 depending on fines content
Honjo and Veneziano (1989)	Soils with $\frac{d_{95B}}{d_{75B}} \le 7$	$\frac{D_{15F}}{D_{85B}} \le 5.5 - 0.5\frac{D_{95B}}{D_{75B}}$

As indicated by Table 2.2, many of the filter criteria are based on the ratio of D_{15F} to D_{85B}. Plotting the logarithm of D_{15F} versus the logarithm of D_{85B} allows a visual comparison of some of these filter criteria, as well as an assessment of the applicability of the criteria to the data collected. This plot is shown in Figure 2.1.

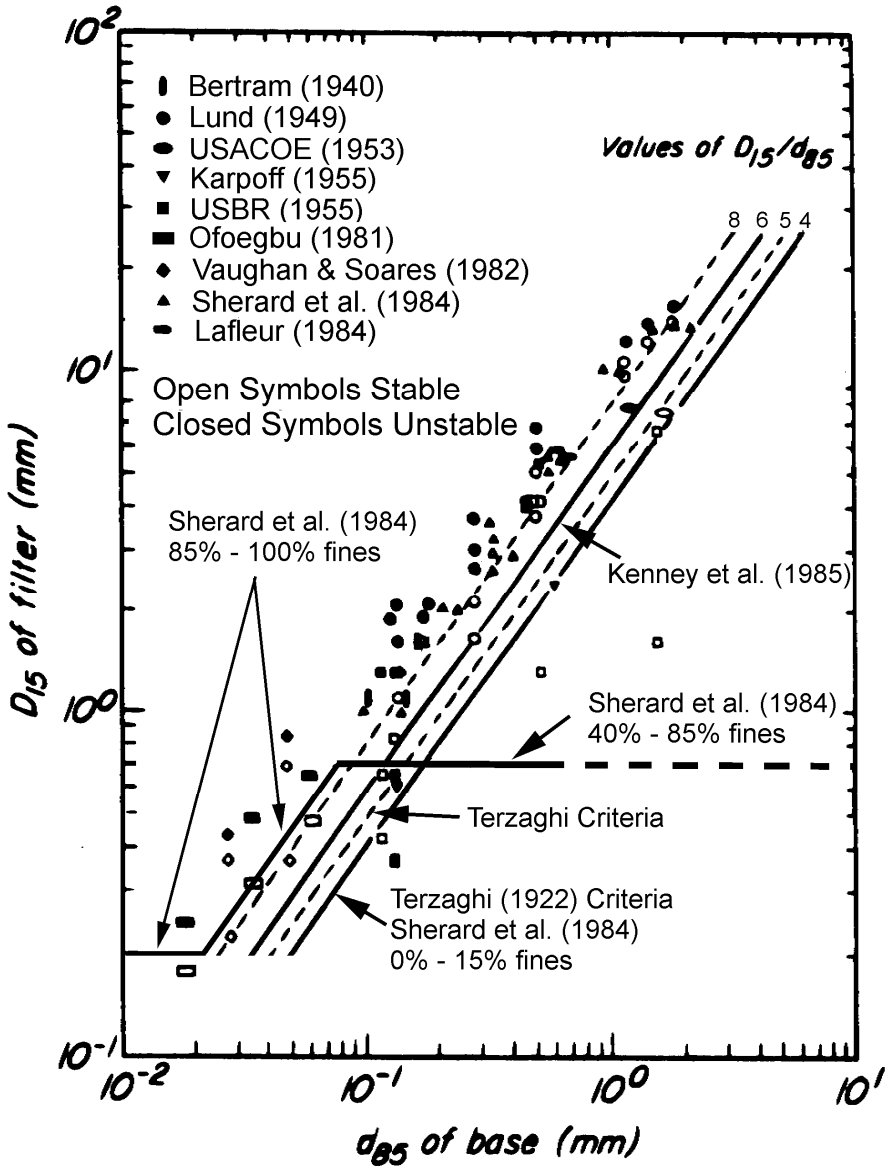

Figure 2.1 Filter criteria based on the ratio of D_{15F} to D_{85B} (after Terzaghi et al., 1996)

2.3.2. Current USBR Filter Criteria (after USBR, 1994)

In this research, the filter criteria by USBR were used as standard filter criteria during tests. Table 2.3 shows base soil categories were defined by percent fines content in base material.

Table 2.3 Criteria for filters and base soil categories (after USBR, 1994)

Base soil category	Percent finer than 0.074 mm (#200 sieve)	Base soil description	[1/] Filter criteria
1	> 85	Fine silts and clays	[2/] $D_{15F} \le 9 \times D_{85B}$
2	40 – 85	Sands, silts, clays, and silty and clayey sands	$D_{15F} \le 0.7\,\text{mm}$
3	15 – 39	Silty and clayey sands and gravels	[3,4/] $D_{15F} \le 0.7\,\text{mm} + \frac{(40 - A) * 4 \times D_{85B} - 0.7\,\text{mm})}{25}$
4	< 15	Sands and gravels	[5/] $D_{15F} \le 4 \times D_{85B}$

[1/] Filters are to have a maximum particle size of 2 inches (50 mm) and a maximum of 5 percent passing the No. 200 (0.074 mm) sieve, after compaction, with the PI (plasticity index) of the fines equal to zero. PI is determined on the material passing the No. 40 (0.425 mm) sieve in accordance with USBR 5360, Earth Manual. To ensure sufficient permeability, filters are to have a D_{15F} size equal to or greater than $5 \times D_{15B}$ but no smaller than 0.1 mm.
[2/] When $9 \times D_{85B}$ is less than 0.2 mm, use 0.2 mm.
[3/] A=percent passing the No. 200 sieve after any regarding.
[4/] When $4 \times D_{85B}$ is less than 0.7 mm, use 0.7 mm.
[5/] In category 4, the D_{85B} may be determined from the original gradation curve of the base soil without adjustments for particles larger than 4.75 mm, provided that the soil is not gap-graded or broadly graded.

The USBR also suggests ratios of D_{90F} / D_{10F} to obtain a gradation curve that provides a relatively uniform distribution of particle size in order to prevent segregation during placement. For coarser filters (sands and gravels), the criterion used by the USBR is given in Table 2.4.

Table 2.4 Gradation limits for prevention of segregation for coarse filters (USBR, 1994)

Minimum D_{10F} (mm)	Maximum D_{90F} (mm)
< 0.5	20
0.5 – 1.0	25
1.0 – 2.0	30
2.0 – 5.0	40
5.0 – 10	50
10 – 50	60

Chapter 3. Filter Test Concept

3.1. Introduction

The objective of this research was to determine under what conditions distressed filters will be able to prevent erosion of base materials. The major focus of the investigation was development of test equipment and procedures to investigate the ability of filters to prevent erosion of cracked base materials, even if the filter initially contains a crack. Sherard and his colleagues performed *pinhole tests* to investigate a similar phenomenon. The major differences between this research and Sherard's studies were (1) cracks rather than pinholes were used to simulate more closely what may occur in the field, and (2) the cracks extended through the filter as well as the base. The test specimens were compacted in filter test devices of two sizes, with pre-formed cracks between the soil and the wall of the test devices, as shown in Figure 3.1. The basic technique employed in these tests was to perform experiments wherein the specimens were subjected to flow of water through the pre-formed cracks, and to determine by observation whether the filter was able to collapse, close the crack, and retain the base soil.

Cross sections through the filter test devices used in this investigation are shown in Figure 3.2(a) and (b). The aluminum void-forming plates shown in the figures were removed after compaction to leave a "crack" or void through the base and the filter. Tests of this type were performed with void-forming plates of various thicknesses with filter materials containing various quantities of fines, which were compacted to various densities. The closure plates were replaced with clear plastic panels after compaction so that movements of soil particles could be observed.

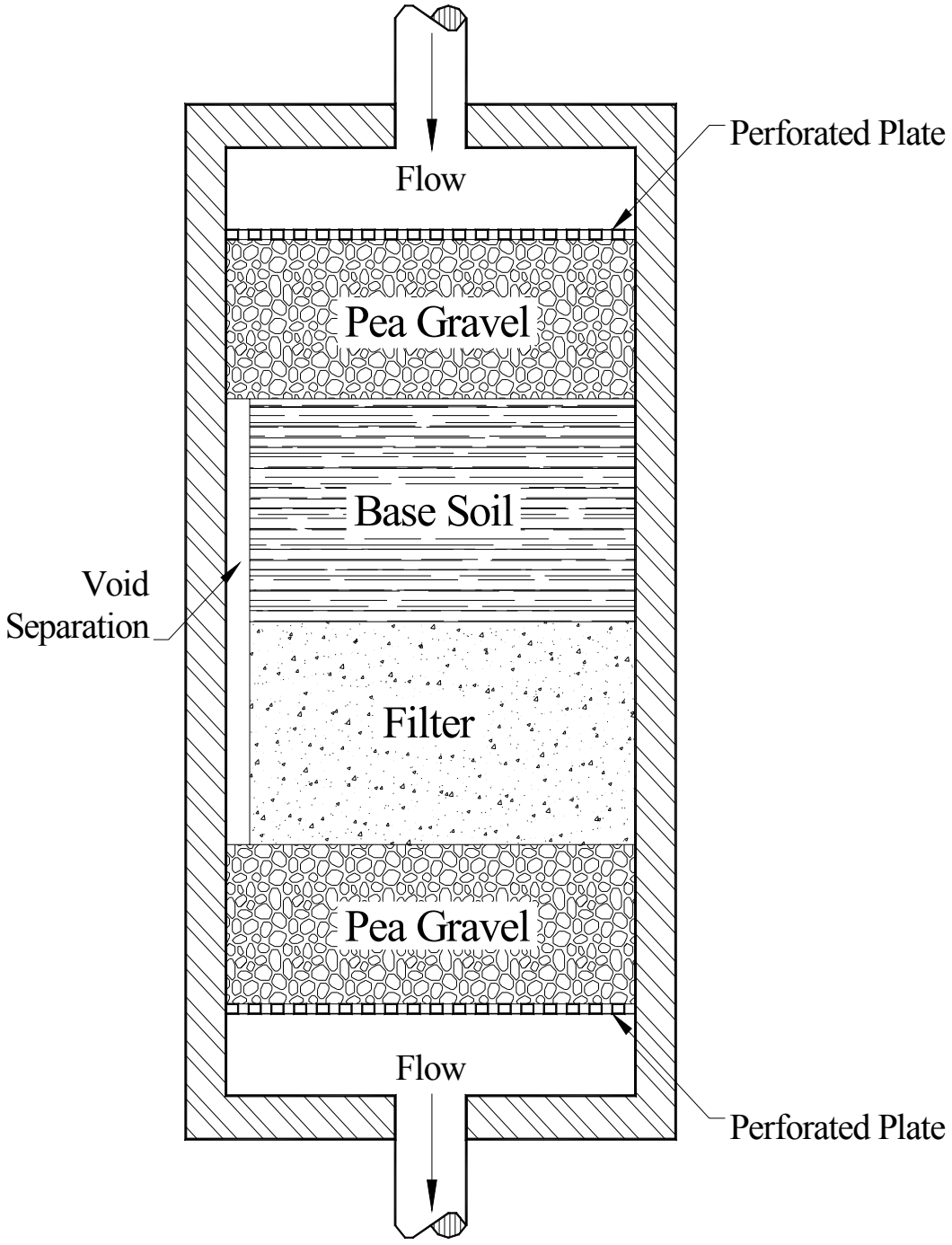

Figure 3.1 Filter test concept

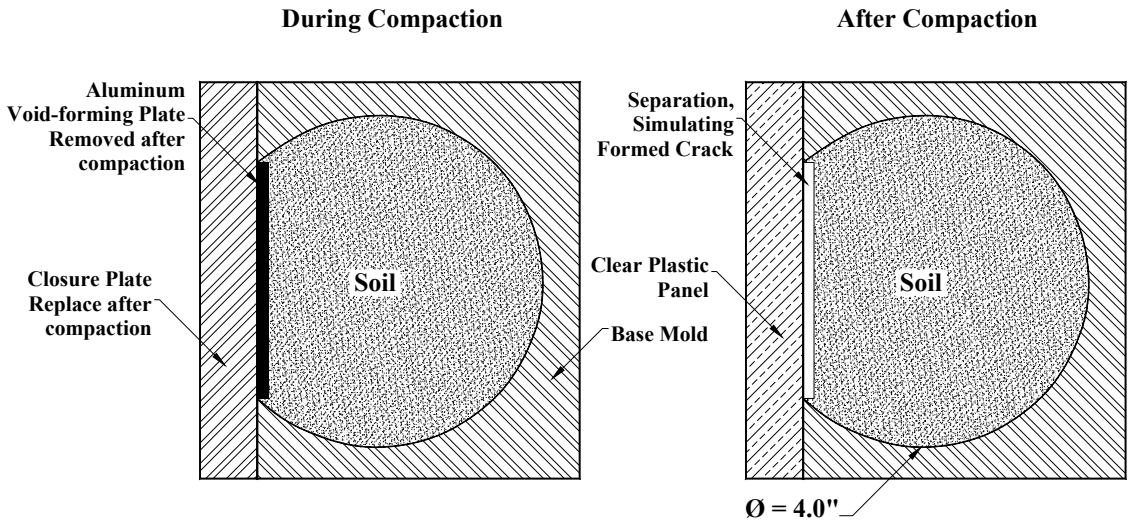

(a) 4-inch diameter filter test device

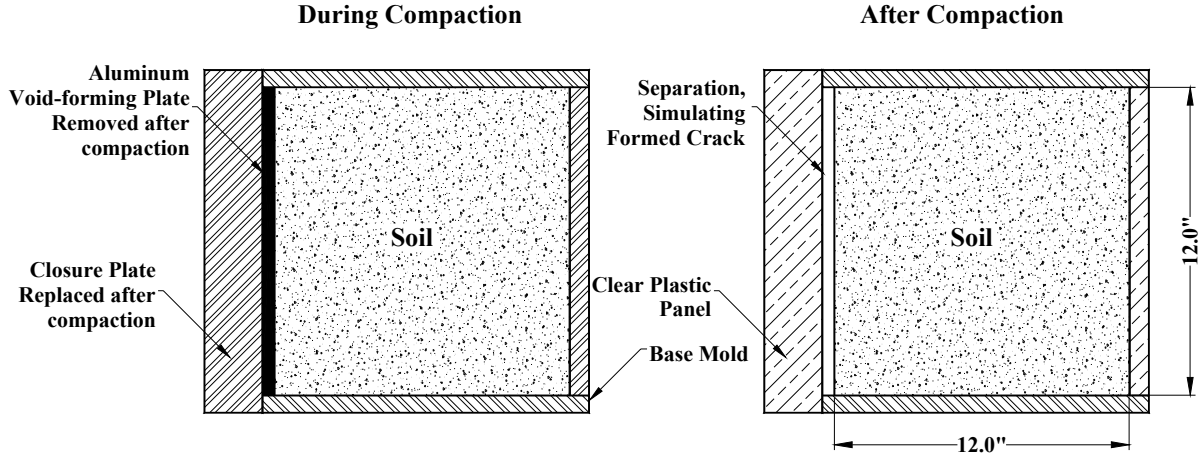

(b) 12-inch square filter test device

Figure 3.2 Cross sections through 4-inch and 12-inch filter test devices

3.2. Water Supply and Data Acquisition Systems

Figure 3.3 shows the water supply and data acquisition systems that were used in the tests. The measurements made during the tests included pressure, flow, and visual records in digital movie files. For pressure measurement, a pressure transducer was used. It was located in the water supply line upstream of the filter device. A turbine type sensor was used for flow measurement.

Pressurized water was introduced at the upstream ends of the filter test devices through a three-way control valve. Initial tests were performed using the tap water in the laboratory as the source of water, controlling the pressure using a water pressure regulator. However, it proved not to be possible to maintain a constant pressure in this way. To overcome this difficulty, a water tank pressurized with regulated air pressure was used for subsequent tests. The pressure at the upstream end of the specimen was maintained at about 5 psi, which corresponds to hydraulic gradients through the base material varying from 39 to 46. The pressure transducer and flow rate sensor were connected to a data acquisition card in a personal computer. Observations of particle movements and the cloudiness or clarity of the effluent during the tests were recorded using a digital camera.

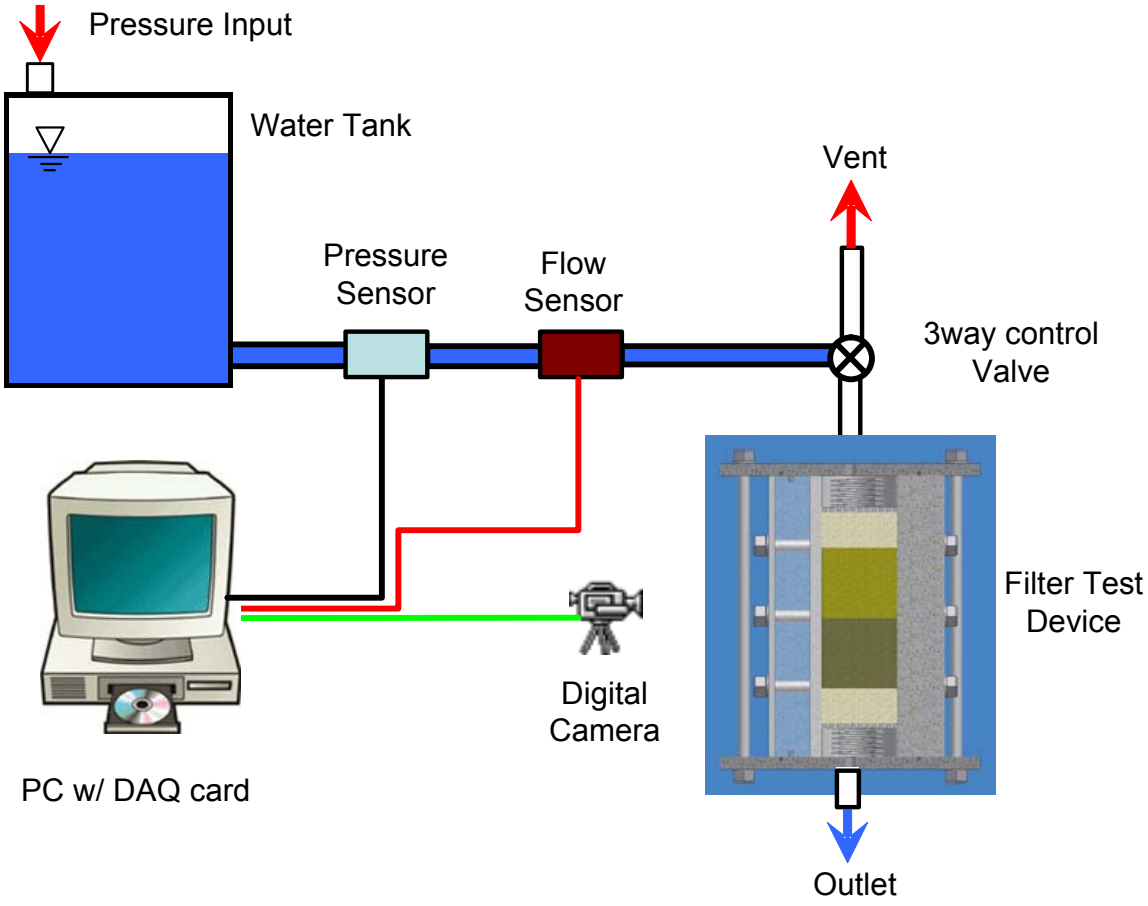

Figure 3.3 Schematic of Data Acquisition System

3.3. Crack Orientations and Flow Directions

Tests were performed using two crack orientations (horizontal and vertical) and two flow directions (horizontal and vertical) as shown in Figure 3.4. It was found that these orientations had a significant effect on the test results. Horizontal flow through a vertically oriented crack represents perhaps the most likely field condition, and the major emphasis was placed on the results of these tests.

	4-inch Filter test device	12-inch Filter test device
HH	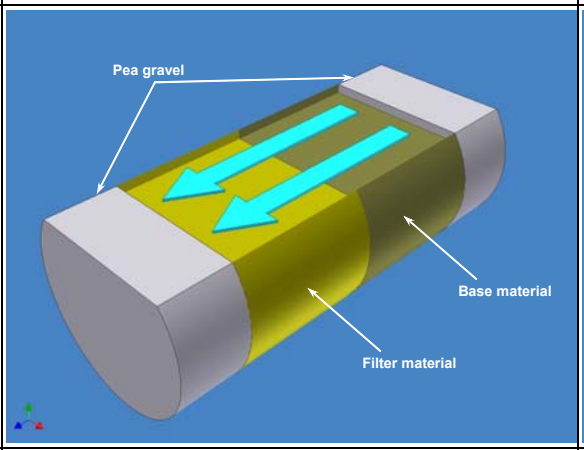	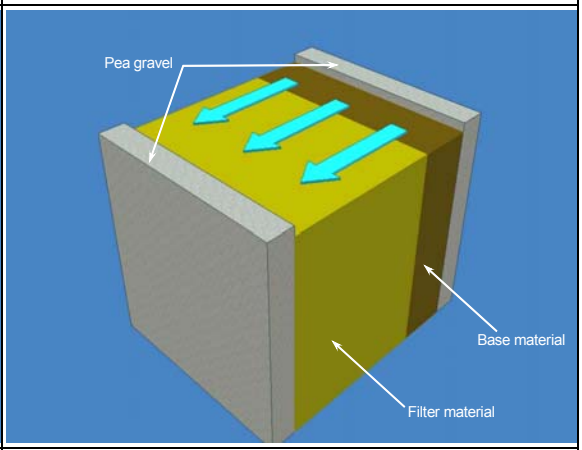
VH	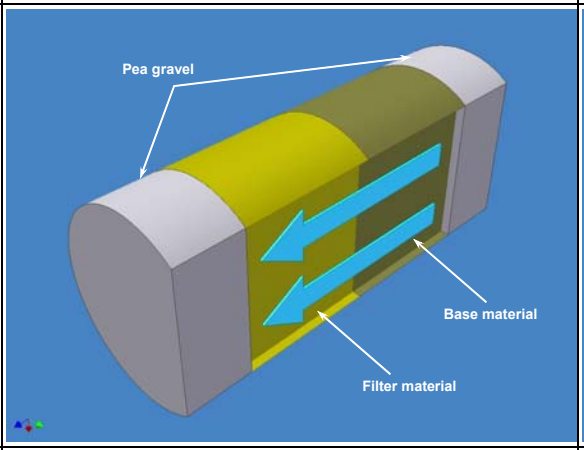	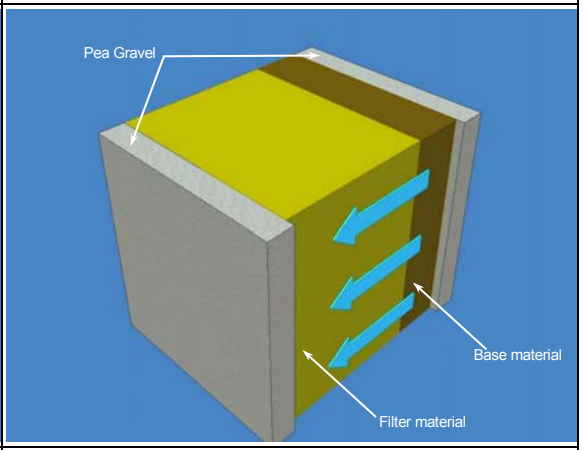
VV	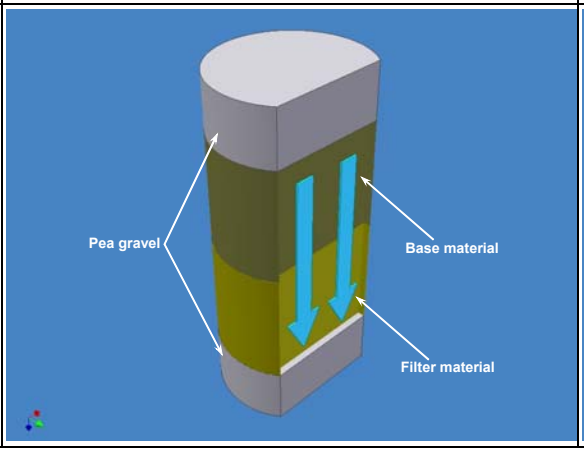	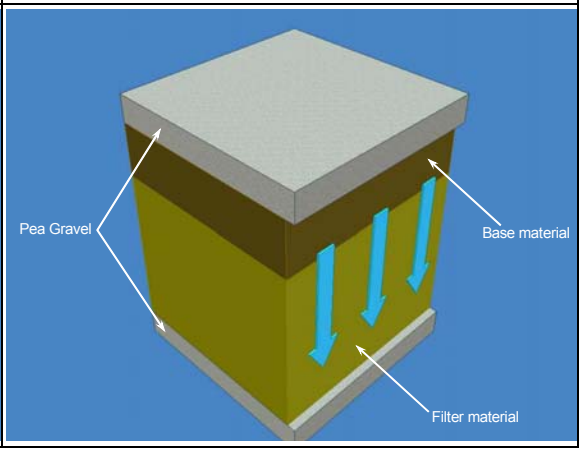

Figure 3.4 Crack orientation and Flow direction

3.4. Clogging Mechanism

By observing particle movements through the Lucite side panels during the tests, it was possible to understand the clogging mechanism through which an initially cracked filter is able to collapse and stop erosion of a cracked base. The mechanism is illustrated in Figures 3.5(a) through 3.5(d).

As shown in Figure 3.5(a), particles of the base material began to be eroded and move with the flowing water within 1 to 2 seconds. Within another one to two seconds particles of the filter material were also eroded and moved with the flowing water and were retained by the pea gravel below the filter, as shown in Figure 3.5(b). It is important that the pea gravel is able to retain the filter material.

As shown in Figures 3.5(b) and (c), the process of erosion and movement of particles continued and resulted in an accumulation of particles of both the filter and the base material within the preformed crack, which then prevented particles of the base material from being washed into the pea gravel. (It may be noted that a test in which the filter material was replaced with pea gravel, complete failure occurred by continuous erosion of the base material through the pea gravel, because the pea gravel did not satisfy filter requirements for restraint of the base material.) As shown in Figure 3.5(d), during the next few minutes, the conditions stabilized with an accumulation of base and filter material in the preformed crack. The flow rate decreased to a small value, and the effluent from the device became clear.

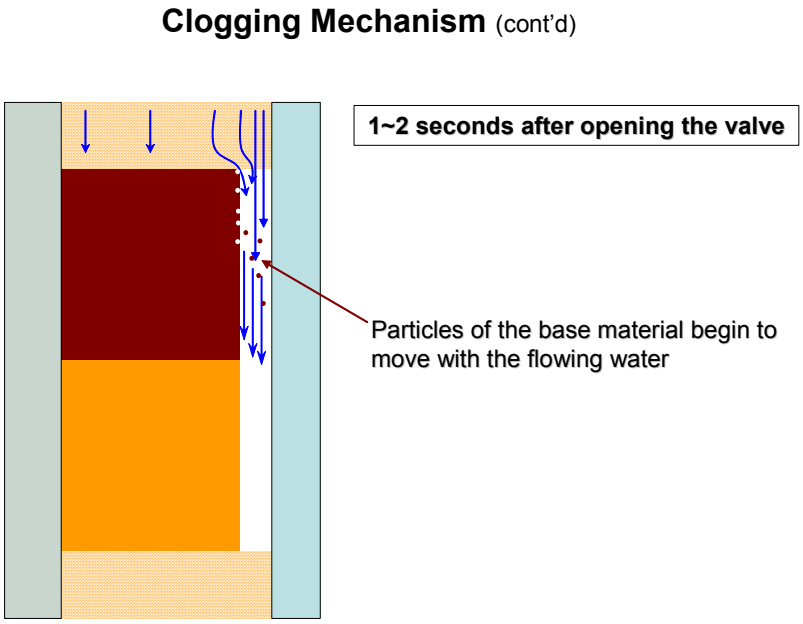

(a)

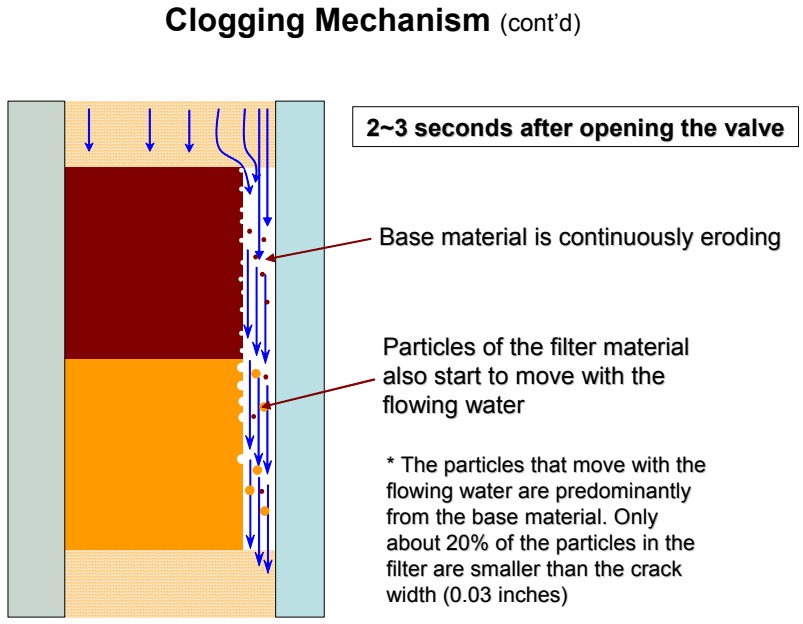

(b)

Figure 3.5 (a) and (b) Early stages of clogging by erosion of base and filter

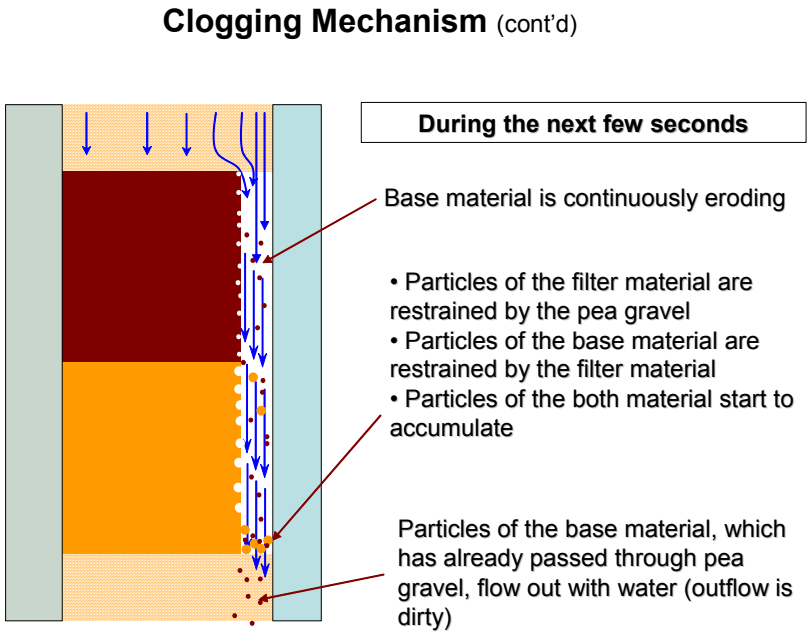

(c)

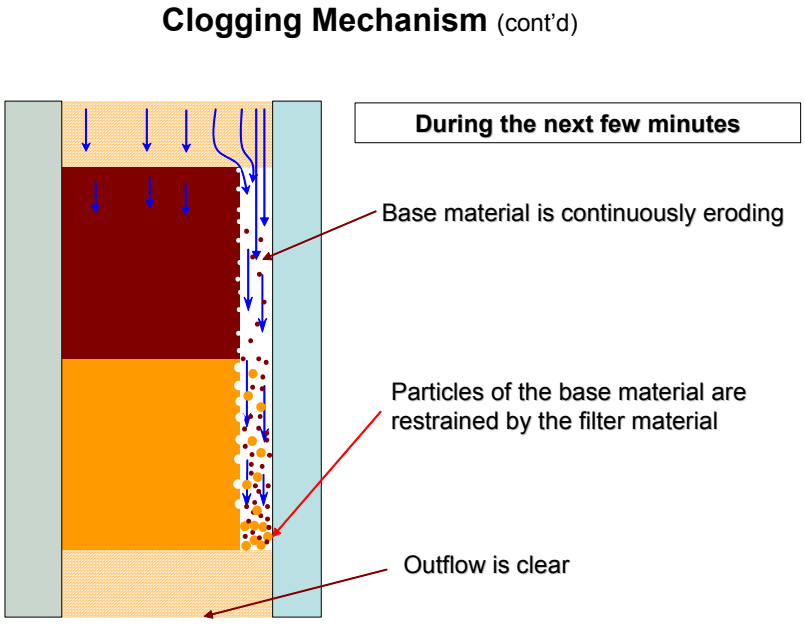

(d)

Figure 3.5 (c) and (d) Later stages of clogging – eroded particles restrained by pea gravel

3.5. Summary

The concept and procedures described above were used in designing two filter test devices, one 4 inches in diameter; and the other 12 inches square in cross section. These devices were used to investigate the effects of the amount and type of fine material in the filter, the density of the filter, the crack width, and the water content of the filter, as described in the Chapter 5 and 6.

Chapter 4. Materials Tested

4.1. Introduction

Index and property tests were conducted on the base and filter materials used in the filter tests. These tests included the following:

- Specific Gravity
- Grain size distribution (sieve and hydrometer)
- Atterberg Limits
- Standard Proctor compaction test
- Consolidated-Undrained triaxial tests
- Flexible wall permeability tests

4.2. Tests on Teton Dam Core Material (Base Material)

Specific gravity tests were conducted in accordance with ASTM D854. A value of specific gravity, G_s, equal to 2.699 was determined for the Teton Dam core material. The value of specific gravity was required in order to reduce the hydrometer test data.

The grain size distribution was determined using sieve and hydrometer tests in accordance with ASTM D422. The test specimen was first passed through at #10 sieve, and the material passing was subjected to a hydrometer analysis. After the hydrometer test was concluded, the entire test specimen was washed over a #200 sieve, and a sieve analysis was conducted on the material that was retained after the washing process. The grain size distribution of the Teton Dam core material is shown in Figure 4.1.

The Teton Dam core material, used as the base material in all filter tests, has a maximum particle size of about 2 mm and about 75% fines. The soil has about 25% sand, 65% silt, and 10% clay-sized particles. From the gradation curves, the particles sizes pertinent to filter design, which are listed in Table 4.1.

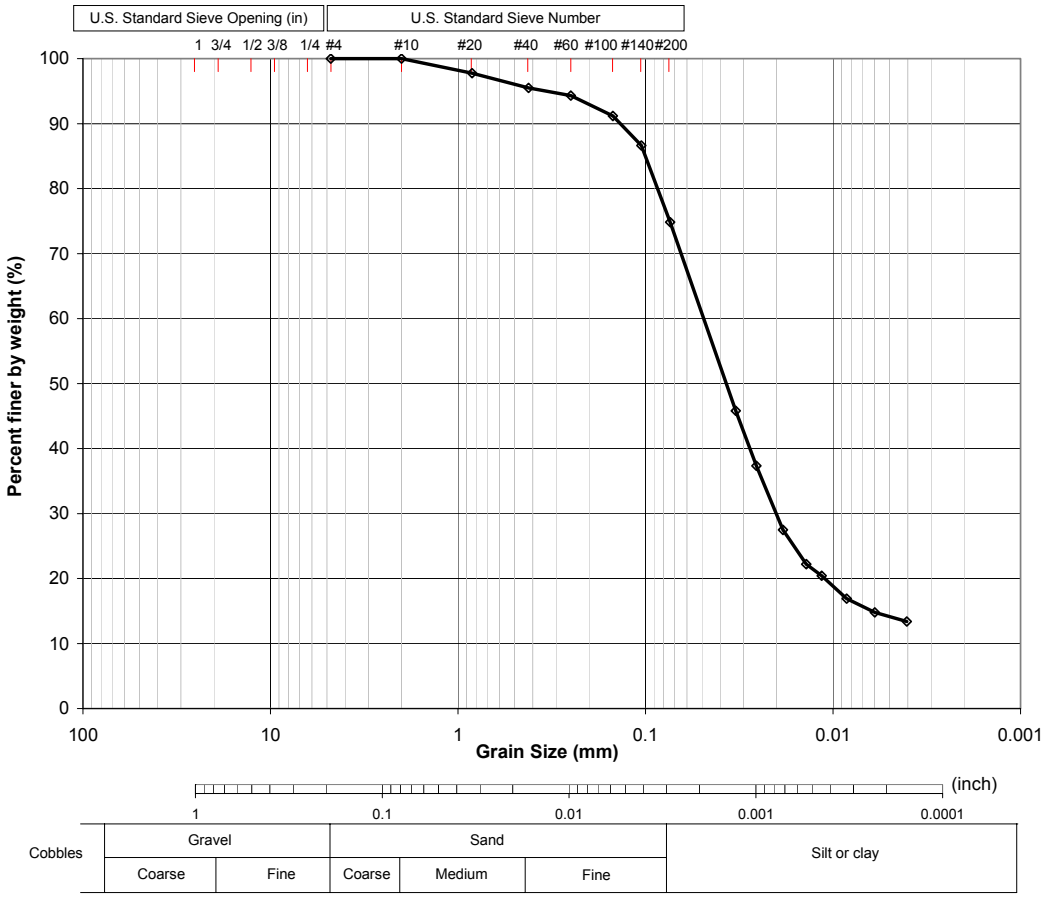

Figure 4.1 Grain size distribution of Teton Dam core material

Table 4.1 Particle size diameters corresponding to different size fractions for Teton Dam core material

Percent passing	Diameter (mm)
90	0.140
60	0.033
30	0.020
15	0.006
10	≈0.001

Based on the gradation curve of the Teton Dam core material, a range of acceptable filters, according to current USBR specifications, can be determined. A soil that plots within the boundaries shown on Figure 4.2 would meet the USBR specifications, provided that the soil contains non-plastic fines.

Atterberg limits (ASTM D4318) were determined for the Teton Dam core material. A Liquid Limit of 26.4%, a plastic limit of 24.1%, and a plasticity index of 2.3% were determined. These Atterberg limit results are shown plotted on a plasticity chart in Figure 4.3. Based on the gradation curve and the plasticity characteristics, the Teton Dam core material classifies as a sandy, inorganic silt of low plasticity (ML).

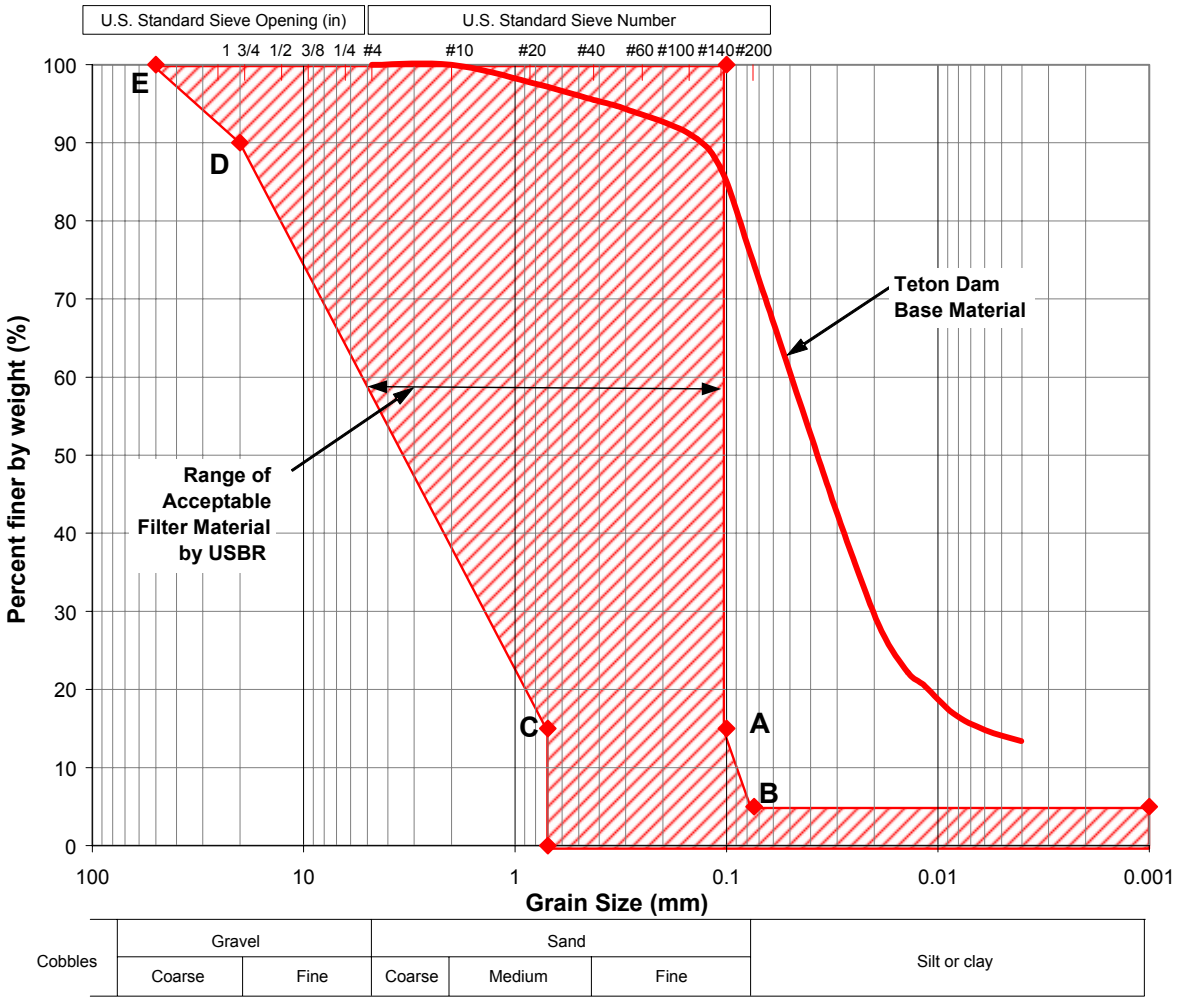

* Note:

A is minimum D_{15F} for permeability.

B is maximum 5% fines content limit.

C is maximum D_{15F} for restraint.

D is maximum D_{90F} for based on considerations of segregation.

E is maximum particle size of filter .

Figure 4.2 Range of gradations meeting USBR specifications for granular filters

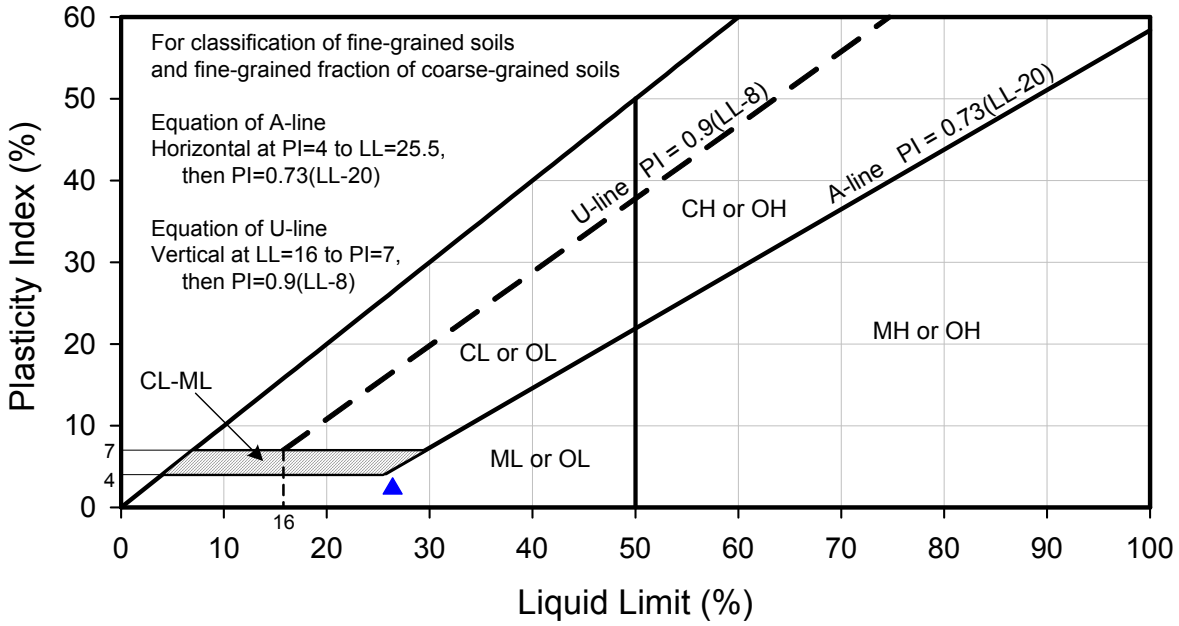

Figure 4.3 Plasticity chart showing Teton Dam core material (After ASTM D2487)

A standard Proctor (ASTM D698) compaction test was conducted on the Teton Dam core material. The compaction curve is shown in Figure 4.4. A maximum dry density of 106.8 pcf and an optimum water content of 16.1% were determined. Values of relative compaction and water contents relative to optimum in the subsequent parts of this report are referenced to these values.

Consolidated-Undrained triaxial tests were conducted on compacted specimens of the Teton Dam core material. The triaxial specimens were compacted to a relative compaction of 90% at water content near the optimum water contents using a Harvard miniature compaction apparatus. The test specimens had a nominal diameter of 1.38 inches and a height of 2.8 inches. The specimens were tested in an automated triaxial testing apparatus manufactured by the Geocomp Corporation of Boxborough, Mass. This device provides automatic back-pressure saturation, consolidation, and shearing. Four tests were conducted at consolidation pressures of 2.5, 5, 10, and 15 psi. The specimens were slightly anisotropically consolidated in order to maintain a compressive stress in the loading linkage of the testing apparatus.

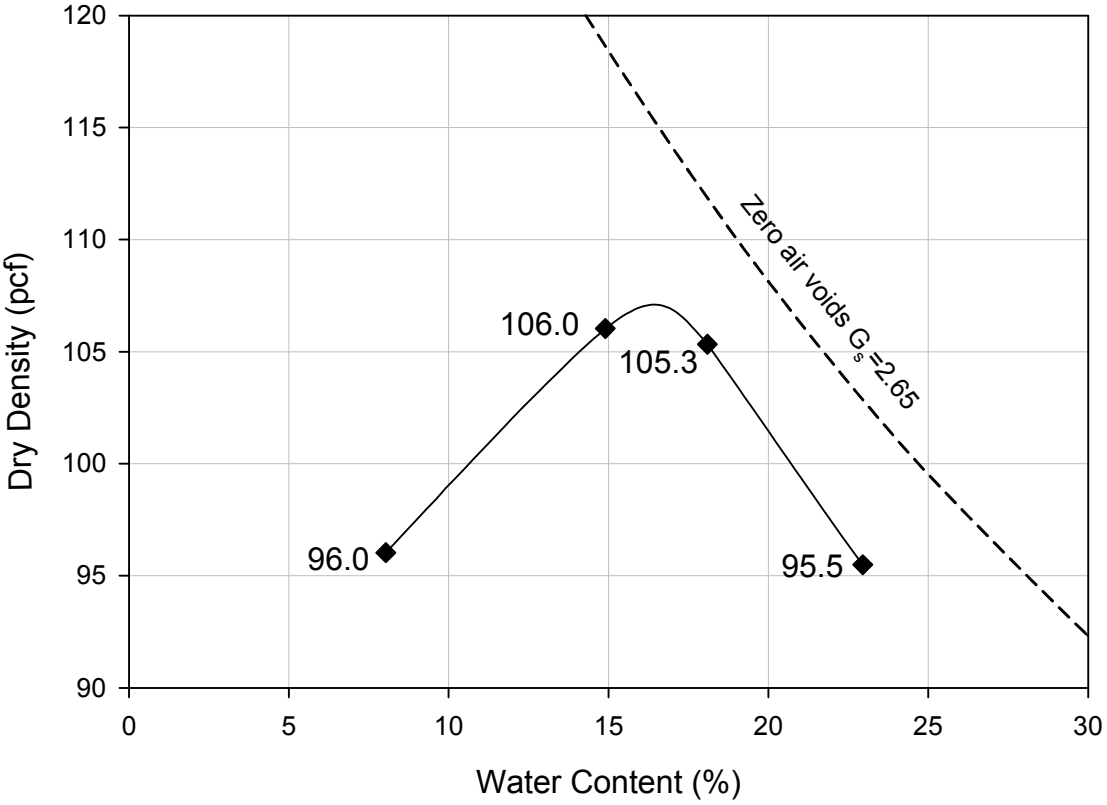

Figure 4.4 Standard Proctor compaction curve for Teton Dam core material

Figure 4.5 shows the effective stress paths measured for the CU triaxial tests. In this figure, $q = (\sigma_1 - \sigma_3)/2$ and $p' = (\sigma_1 + \sigma_3)/2$. The solid dark line shown on the figure is the K_f line derived from the test data. This line corresponds to $\phi' = 30$ degrees and $c' = 1.04$ psi.

A flexible wall permeability test (ASTM D5084) was conducted on a compacted test specimen of the Teton Dam core material. The test specimen was compacted in a

1/30ft^3 compaction mold at a relative compaction of 90% of the standard Proctor maximum dry density at the optimum water content. The test specimen was back-pressure saturated and then consolidated to an isotropic stress of 2.5 psi. The sample was permeated at a hydraulic gradient of about 5. From this test, the coefficient of permeability of the Teton Dam core material was found to be 1×10^{-6} to 1.5×10^{-6} cm/s.

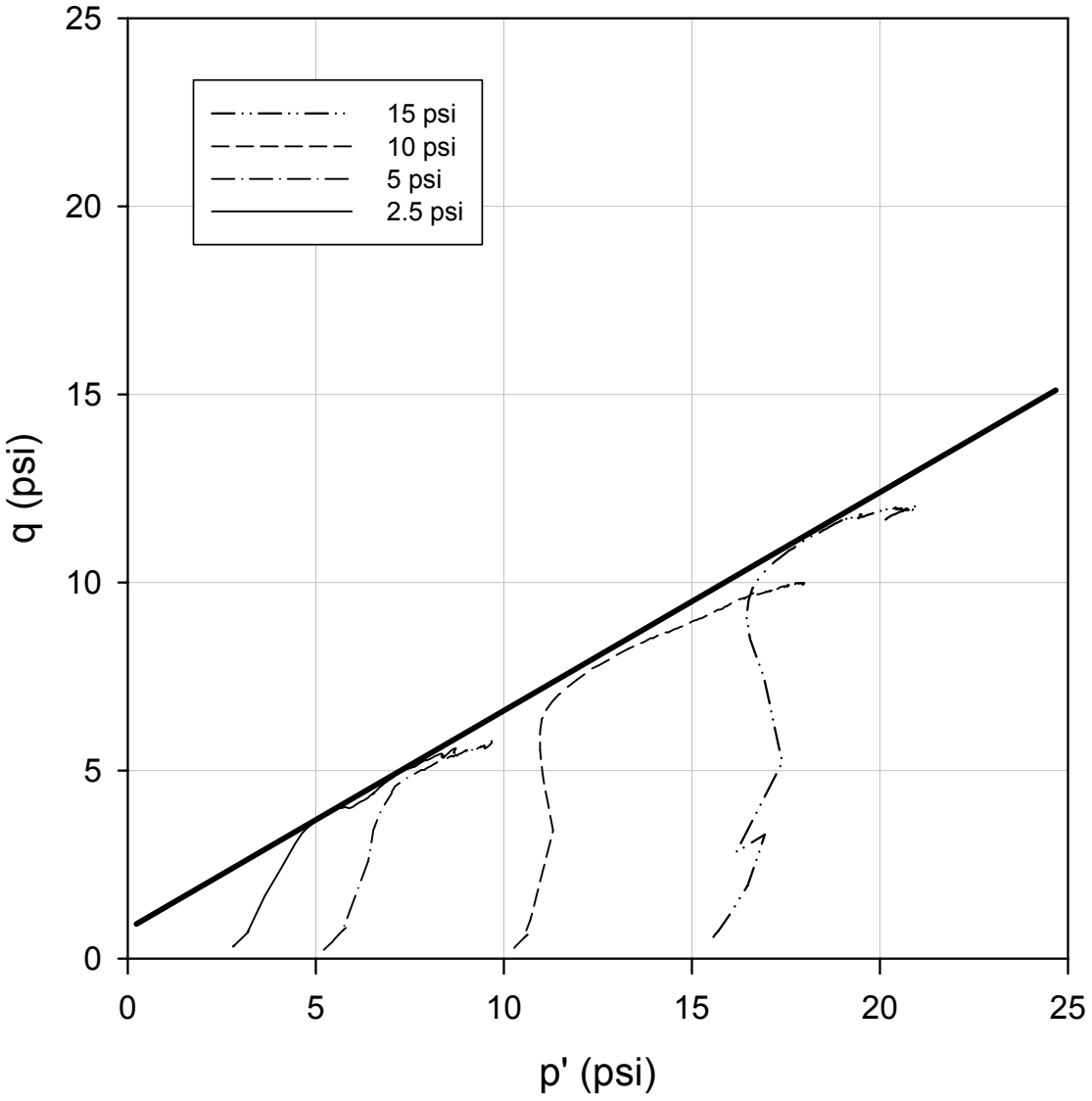

Figure 4.5 Effective stress paths for CU triaxial tests conducted on Teton Dam core material

4.3. Tests on Filter Material

Various filter materials were used in this research. The initial tests (Tests 1 through 5) used the filter soil from the Ochoco Dam that was provided by the USBR. Tests 7 and 8 used a filter material fabricated from commercially-available quartz sands. Tests 9 through 12 used the Ochoco filter material, and the remaining tests used the Horsetooth Dam filter material.

A sieve analysis was performed on the Ochoco Dam filter material and the gradation curve is shown in Figure 4.6. This material, in the as-delivered condition, would meet the USBR filter criteria for a filter for the Teton Dam core material, and was used for the first series of tests to troubleshoot the testing apparatus.

The production tests were conducted using the Horsetooth Dam filter material. A gradation curve for this filter is shown in Figure 4.7. As delivered, this soil contained 4% fines, and met the criteria for a filter material for the Teton Dam base material. The Horsetooth Dam filter soil was split on different size sieves, and recombined to form test specimens having 0%, 5%, and 15% fines. The gradation curves for these specimens are also shown in Figure 4.7. The plot shows both the as-delivered gradation curve, and the gradation curves of the recombined test specimens.

Maximum and minimum density tests (ASTM D4253 and ASTM D4254) were conducted on the Horsetooth Dam filter soil with different fines contents. The maximum and minimum densities that were measured are given in Table 4.2.

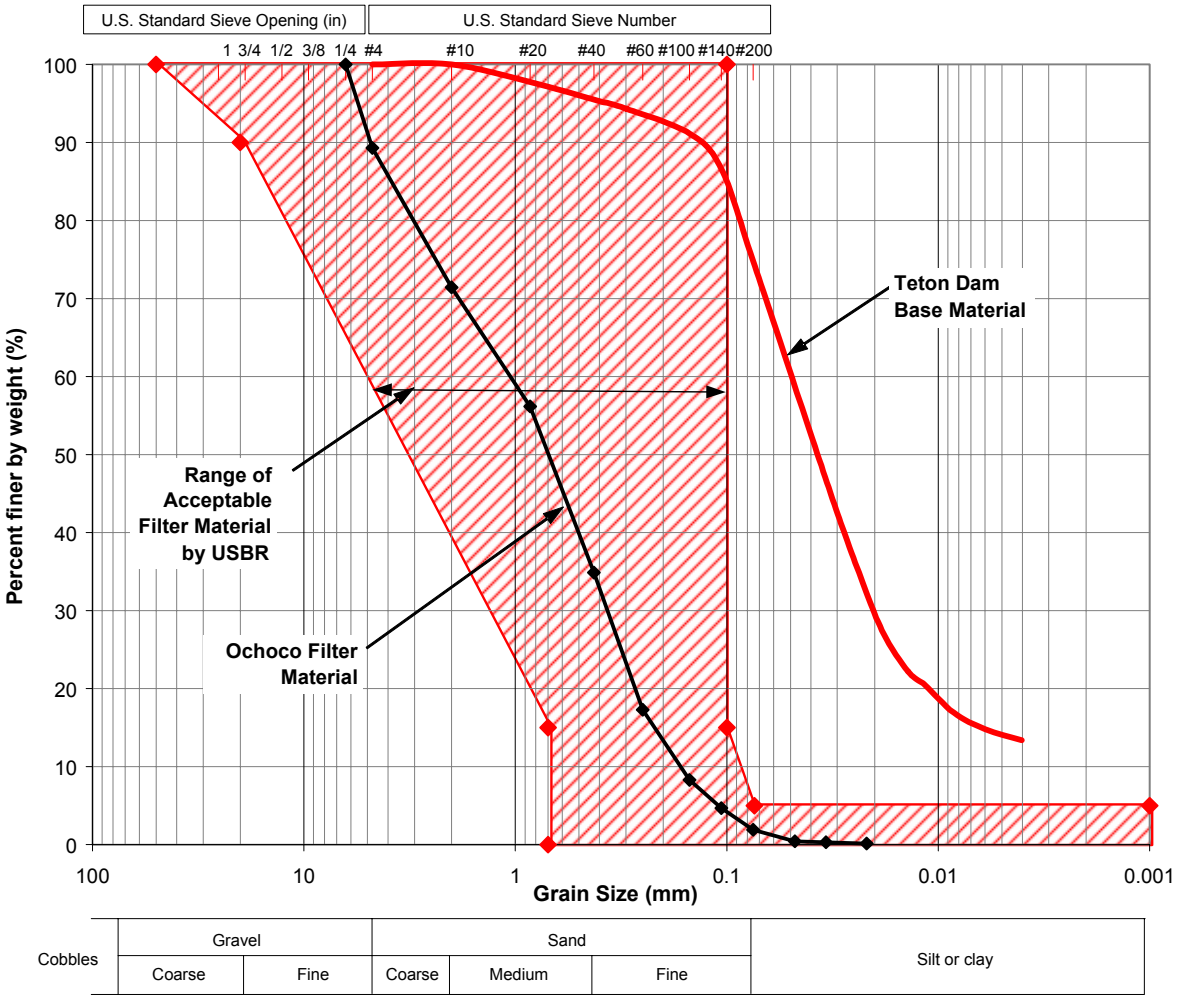

Figure 4.6 Gradation curve for Ochoco Dam filter material

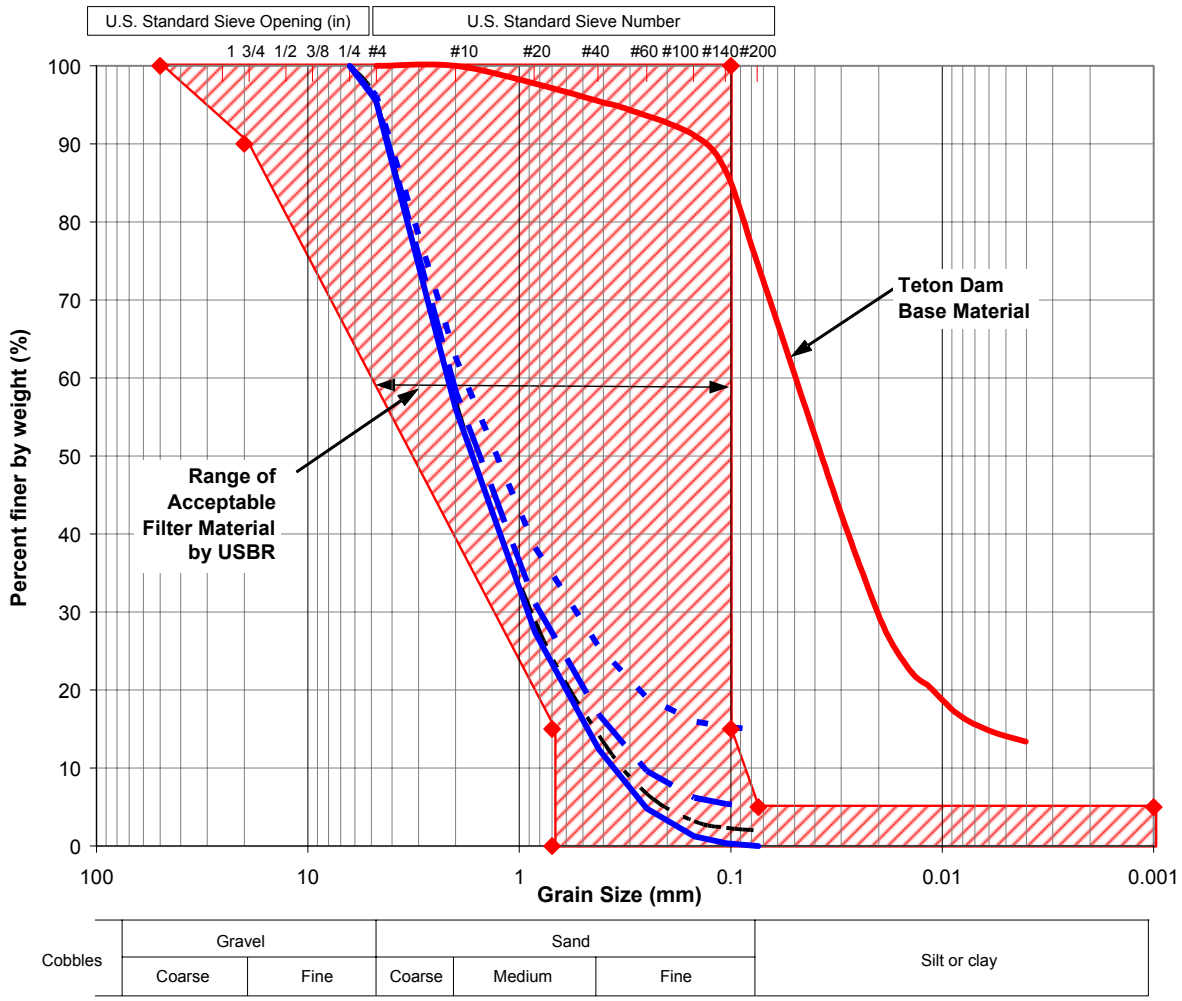

Figure 4.7 Gradation curves for Horsetooth Dam filter material

Table 4.2 Results of Maximum and Minimum density tests

% Fines	Maximum Density γ_{dmax} (pcf)	Minimum Density γ_{dmin} (pcf)
0	120.7	100.2
5	125.5	103.3
15	131.1	107.8

A standard Proctor compaction test (ASTM D698) was conducted on the Horsetooth material with 0% and 5% fines in order to compare relative compactions with relative densities. The compaction curves are shown in Figure 4.8. A maximum dry density of 115 pcf and an optimum water content of 13% were estimated from the curve for the soil having 0% fines. A maximum dry density of 121 pcf and an optimum water content of 12% were estimated from the curve for the soil having 5% fines.

Based on these data, the maximum dry density determined from a standard Proctor compaction test results in a relative density of 76% for the soil containing 0% fines and 83% for the soil containing 5% fines. In reporting the filter test results, relative density was used to characterize the filter materials.

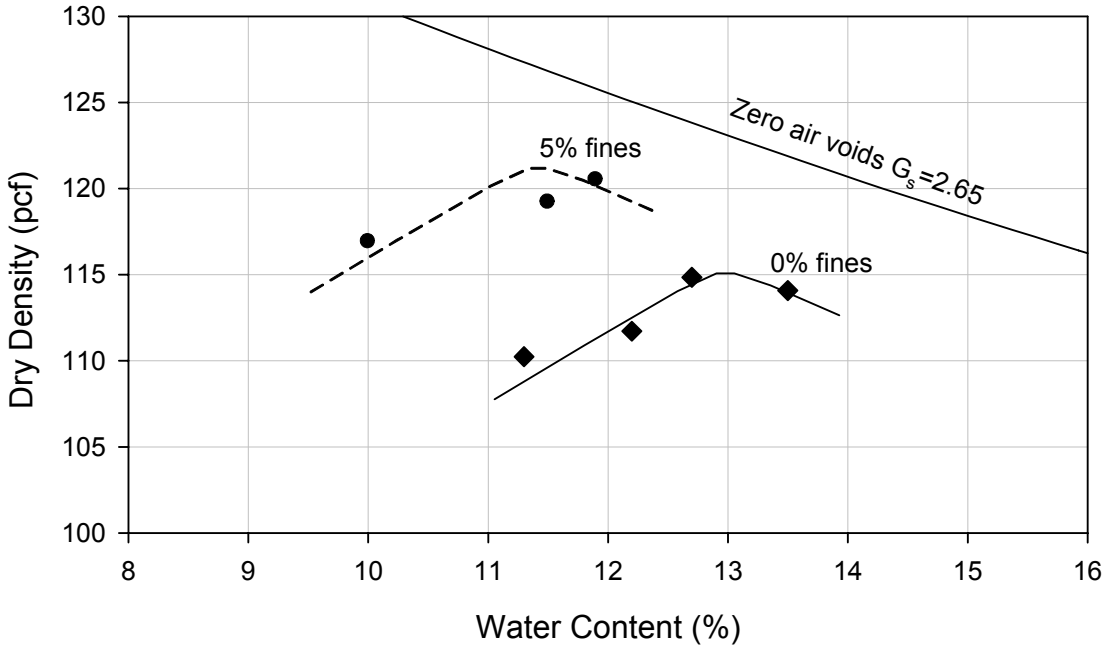

Figure 4.8 Standard Proctor compaction curves for Horsetooth Dam filter for 0% and 5% fines

Chapter 5. Tests Performed using 4-inch Diameter Filter Test Device

5.1. Introduction

A total of twenty-seven tests were conducted with the 4-inch diameter filter test device. The conditions examined in these tests are summarized in Table 5.1. Test 1 through Test 12 were pilot tests, conducted to determine the proper specimen fabrication techniques, to refine the instrumentation and data recording methods, and to examine the influence of the device orientation and flow direction on the test results.

The pilot tests were performed using the tap water in the laboratory as the source of water, controlling the pressure using a water pressure regulator. However, it proved not to be possible to maintain a constant pressure in this way. To overcome this difficulty a water tank pressurized with regulated air pressure was used as the source of water for subsequent tests. In all of the pilot tests, the crack width was 0.03 inches.

Table 5.1 Test summary of 4-inch filter test device

	Compaction Method	Crack width cw (inch)	Crack Oriendation / Flow Direction	Pressure Control	DAQ Measurement			Base Material	Filter Material	Filter Material Properties			
					Flow	Pressure	Video			fc (%)	w (%)	D_r (%)	γ_d (pcf)
Test 1	Standard Proctor Hammer	0.03	H / H	Direct Connection from Tap Water with Regulator	Not measured	Not measured	Not Monitored	Teton Dam Core	Ochoco Dam Filter	4	11.5	N/A	N/A
Test 2		0.03	H / H							4	11.5		
Test 3		0.03	V / H				Monitored			4	11.5		
Test 4		0.03	V / H							4	11.5		
Test 5		0.03	V / V							4	11.5		
Test 6		0.03	V / V						Pea Gravel	0	N/A		
Test 7		0.03	V / H			Measured			Fabricated Filter	0	5.6		111.4
Test 8		0.03	V / H							0	5.6		111.5
Test 9		0.03	V / V		Measured				Ochoco Dam Filter	0	12.3		109.9
Test 10		0.03	V / V							5	12.3		114.5
Test 11		0.03	V / V							10	12.3		110.1
Test 12		0.03	V / V							15	12.3		120.8
Test 13	Moist Tamping	0.03	V / V	Constant from Water Tank					Horsetooth Dam Filter	0	10	50	109.3
Test 14		0.06	V / V							0	10	50	109.3
Test 15		0.09	V / V							0	10	50	109.3
Test 16		0.03	V / V							0	10	70	113.7
Test 17		0.06	V / V							0	10	70	113.7
Test 18		0.09	V / V							0	10	70	113.7
Test 19		0.03	V / V							5	10	70	117.9
Test 20		0.06	V / V							5	10	70	117.9
Test 21		0.09	V / V							5	10	70	117.9
Test 22		0.03	V / V							15	10	70	123.2
Test 23		0.06	V / V							15	10	70	123.2
Test 24		0.09	V / V							15	10	70	123.2
Test 25		0.03	V / V							0	14	70	113.7
Test 26		0.09	V / V							15	14	46	123.2
Test 27		0.15	V / V							0	10	18	103.4

5.2. Sample Preparation

As mentioned earlier, the cross section of the 4-inch diameter filter test device is a truncated circle. The standard Proctor (ASTM D698) compaction hammer was used to compact the specimens in the filter test device. The segments of base and filter material were 3 inches high after compaction. The base material was compacted to 95% of the maximum density as determined by the standard proctor test, ASTM D698. The filter material was compacted to values of relative density varying from 18% to 70%. For density control, the thickness of every compaction lift was measured using the depth gauge shown in Figure 5.1.

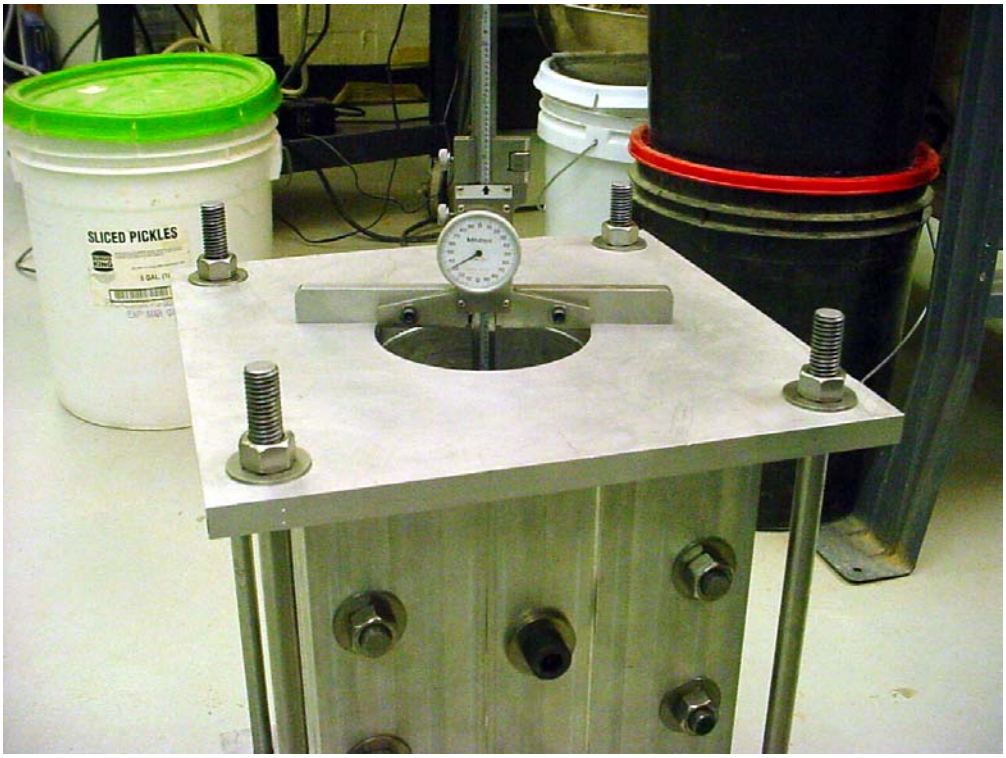

Figure 5.1 Measuring thickness of each layer by depth gauge

Figure 3.2(a) (in Chapter 3) shows a cross section through the 4-inch diameter filter test device. Compaction with void-forming plates inside the device produced samples with truncated circular shapes. The void-forming plates were removed after compaction. The void-forming plates extended over the filter and base material segments of the specimens. The closure plate was replaced by a clear plastic plate before testing so that particle movements could be observed during the tests. Figure 5.2 shows a perspective view of the 4-inch diameter filter test device. A longitudinal cross section through the device is shown in Figure 5.3. The detailed steps involved in assembly and preparation of a sample are explained in Appendix A.

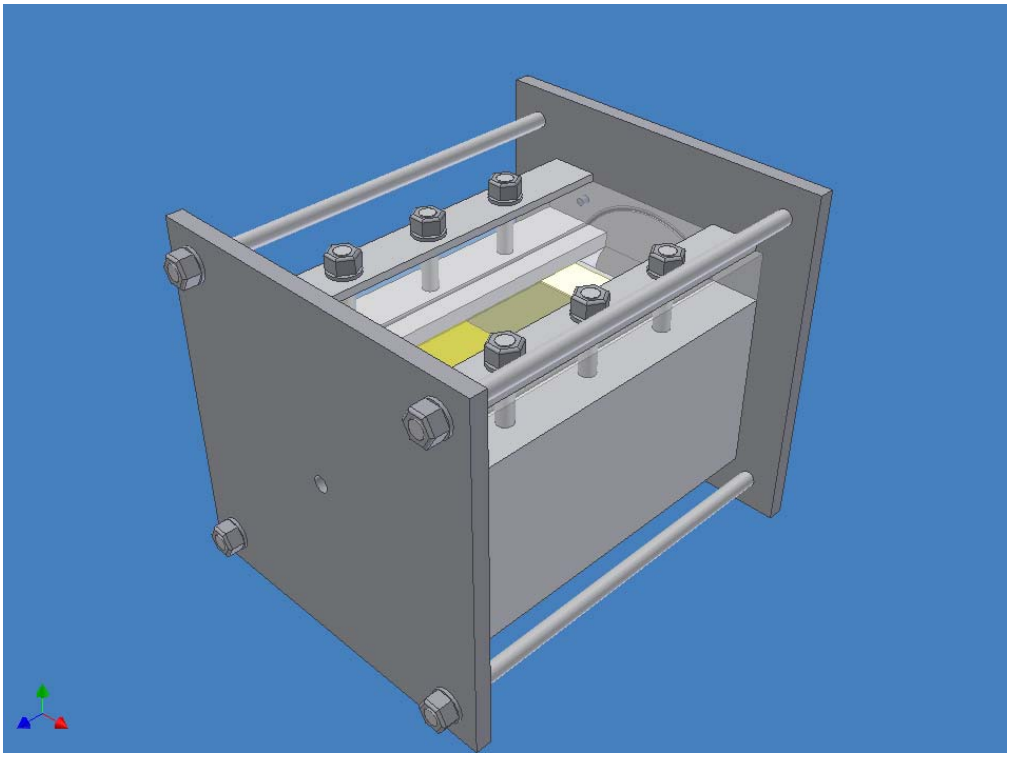

Figure 5.2 4-inch diameter filter test device

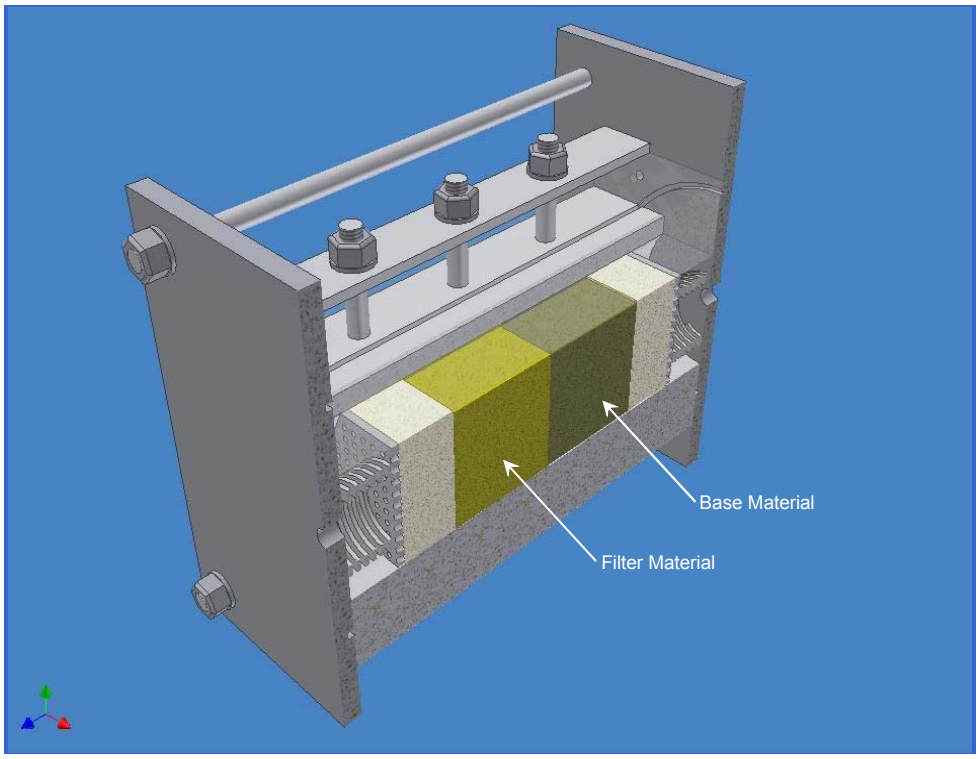

Figure 5.3 Longitudinal cross section through 4-inch diameter filter test device with compacted sample

5.3. Pilot Tests

5.3.1. Horizontal Crack Orientation and Horizontal Flow Direction

Tests 1 through 5 were conducted using the Teton Dam core material as the base material, and the Ochoco Dam filter material as the filter material. The Ochoco Dam filter material meets the USBR filter criteria for the Teton Dam core material.

In tests 1 and 2, the crack orientation was horizontal, and the flow direction was horizontal as shown in Figure 5.4. This condition is denoted here as HH. In this orientation, the filter material cannot close the crack by slumping, since gravitational forces tend to keep the crack open. Clogging is possible, however, as particle migration occurs due to flow of water through the specimen. Severe erosion was experienced in Test 1, and a continuous channel was eroded through the base and filter material. The effluent was visibly turbid throughout the test, and a stable condition was never reached.

Test 2 was conducted using the same conditions as Test 1, but the filter system successfully restrained the base material due to particle migration. Early in the test, particles of the base material covered the filter, and the filter and base then became "mixed." The mixed material was restrained by the pea gravel, as shown in Figure 5.5. The effluent was first turbid, and then quickly cleared as the test progressed.

These results showed that the HH condition, which does not permit slumping of the filter under the force of gravity, does not simulate the field conditions that are of interest for this study. Although testing with horizontal crack orientation offered some slight advantage with regard to test setup, it was decided that all subsequent tests should be performed with vertical crack orientations to better simulate field conditions.

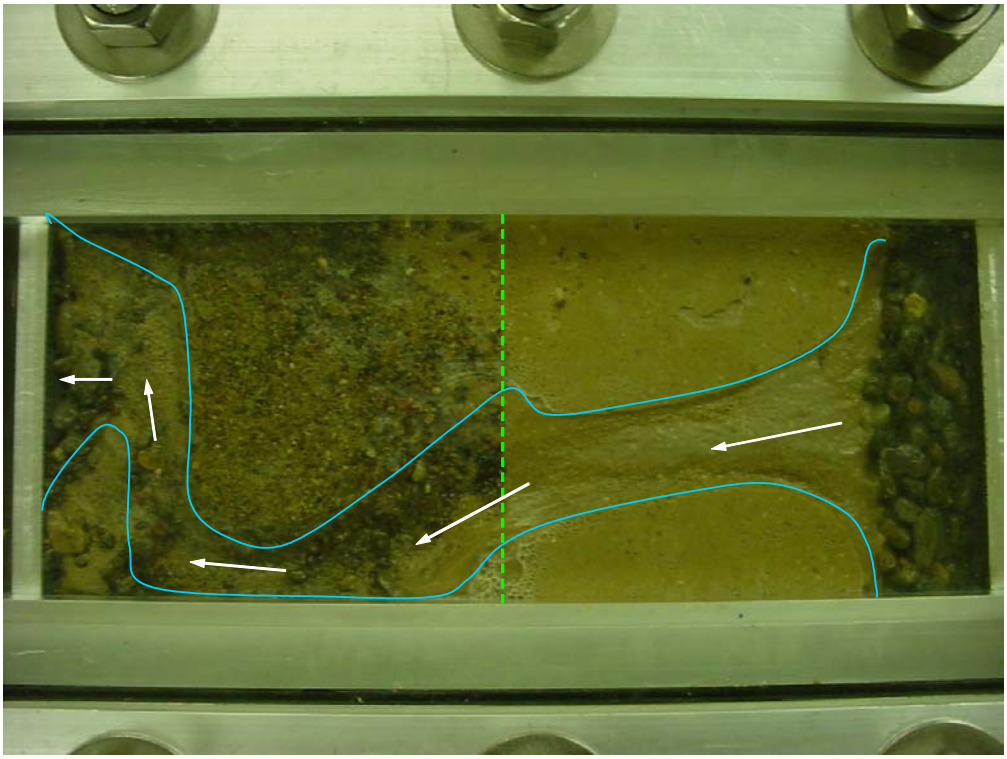

Figure 5.4 After Test 1 (HH condition)

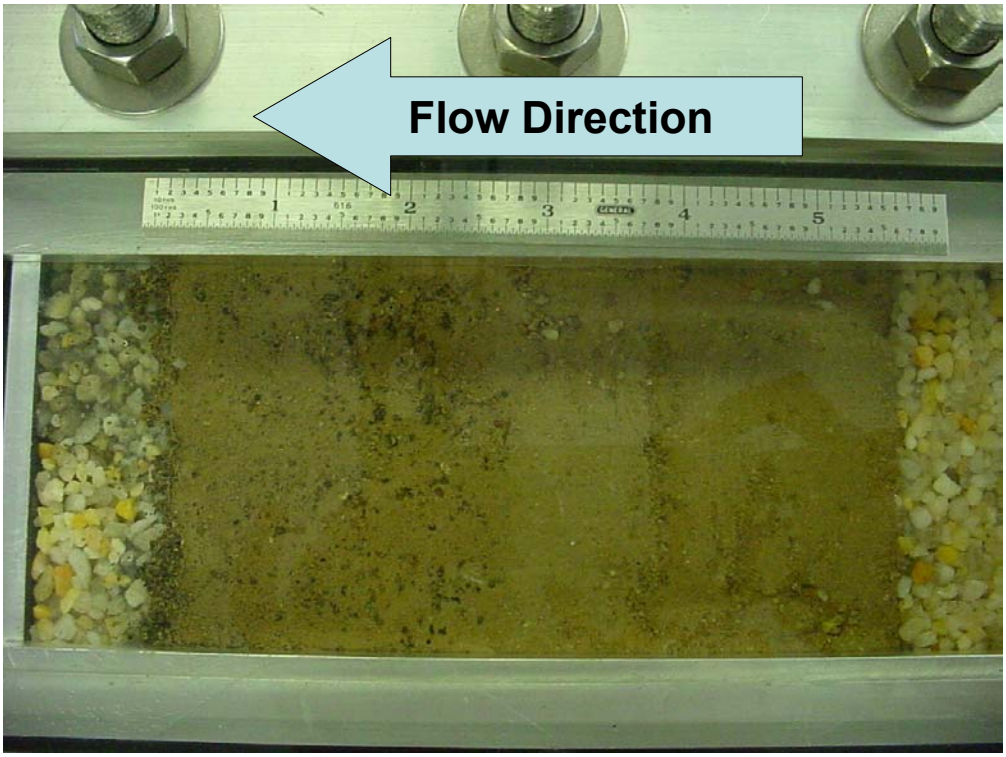

Figure 5.5 After Test 2 (HH condition)

5.3.2. Vertical Crack Orientation and Horizontal Flow Direction

Four tests (3, 4, 7, and 8) were performed with vertical crack orientation and horizontal flow, denoted here as condition VH.

Test 3 was performed using the Teton Dam core material and the Ochoco Dam filter material, with the filter test device rotated 90 degrees about its long axis, so that the plane of the crack was vertical. With flow in the horizontal direction, particles of the base material and the filter material migrated downstream and were restrained by the pea gravel as shown in Figure 5.6(a).

Test 4 (shown in Figure 5.6(b)) had the same conditions as Test 3, except that the section of the specimen comprised of base material was thicker, and a smaller hydraulic gradient was used. Although some base material was initially eroded, particles of the filter quickly migrated to collect on the pea gravel, and the effluent became clear.

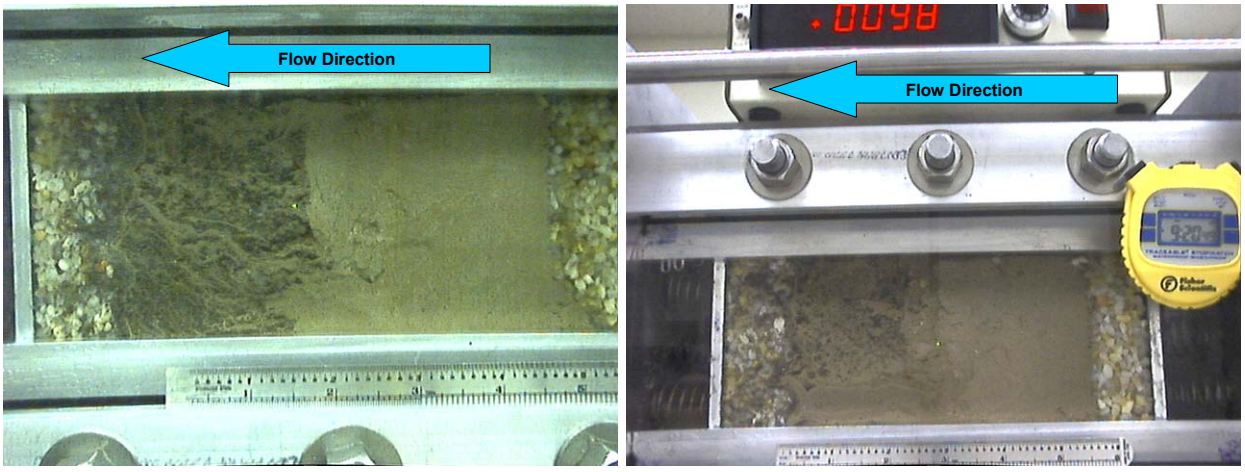

(a) After Test 3 **(b) After Test 4**

Figure 5.6 Tests 3 and 4 (VH condition)

Test 7 used the Teton Dam core material as the base soil, and the filter material was fabricated from quartz sand so that D_{15F}/D_{85B} ratio was equal to 6. This represents a filter that is slightly coarser than allowed by the current USBR criteria. The specimen was compacted about 24 hours prior to testing. During the time between compaction and testing, the base material swelled and partially filled the crack, within the area outlined by the dashed red line in Figure 5.7. When flow was started, particles of the filter migrated downstream and were restrained by the pea gravel, and the filter then successfully restrained the base material.

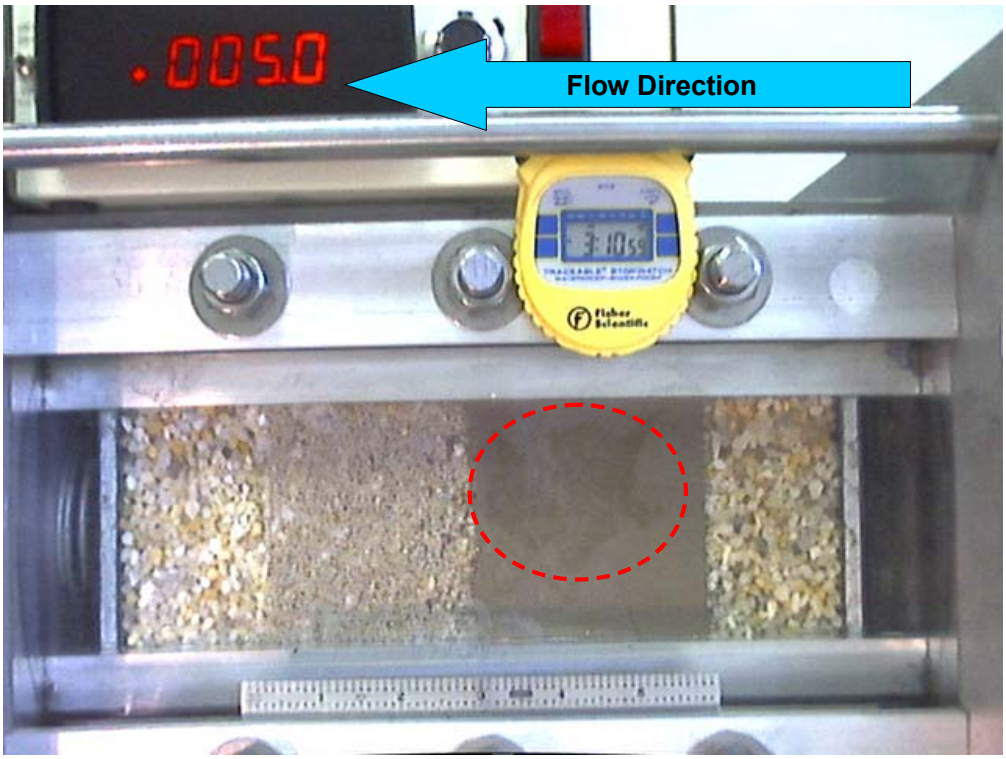

Figure 5.7 Before Test 7

Test 8 was conducted using the same conditions as Test 7, but the sample was tested soon after compaction. This test resulted in more base material being eroded, but the filter successfully restrained the base, as shown in Figure 5.8.

Test 7 and 8 were the first tests in which upstream pressures were measured. Figure 5.9 shows the variations of upstream water pressure with time measured in these tests. It may be

seen that the pressures dropped as soon as the valve was opened, and increased as clogging developed. Even though the filter successfully restrained the base material, the pressure did not return to the original value, as may be seen in Figure 5.9. Close examination of the specimens during these tests, showed that empty spaces remained at the top of the crack, and that there was free flow through these empty spaces.

(a) After Test 7 **(b) After Test 8**

Figure 5.8 Tests 7 and 8 (VH condition)

Tests with vertical crack orientation and horizontal flow direction modeled the desired field condition, but it resulted in empty spaces at the top of sample the crack. Because dams have freeboard, such spaces in the field would most likely be above water, and therefore not involved in flow through the crack, even if the upper part of the crack remained open. Therefore the VH condition in the 4-inch filter test device imposes a more severe condition than would be expected in the field.

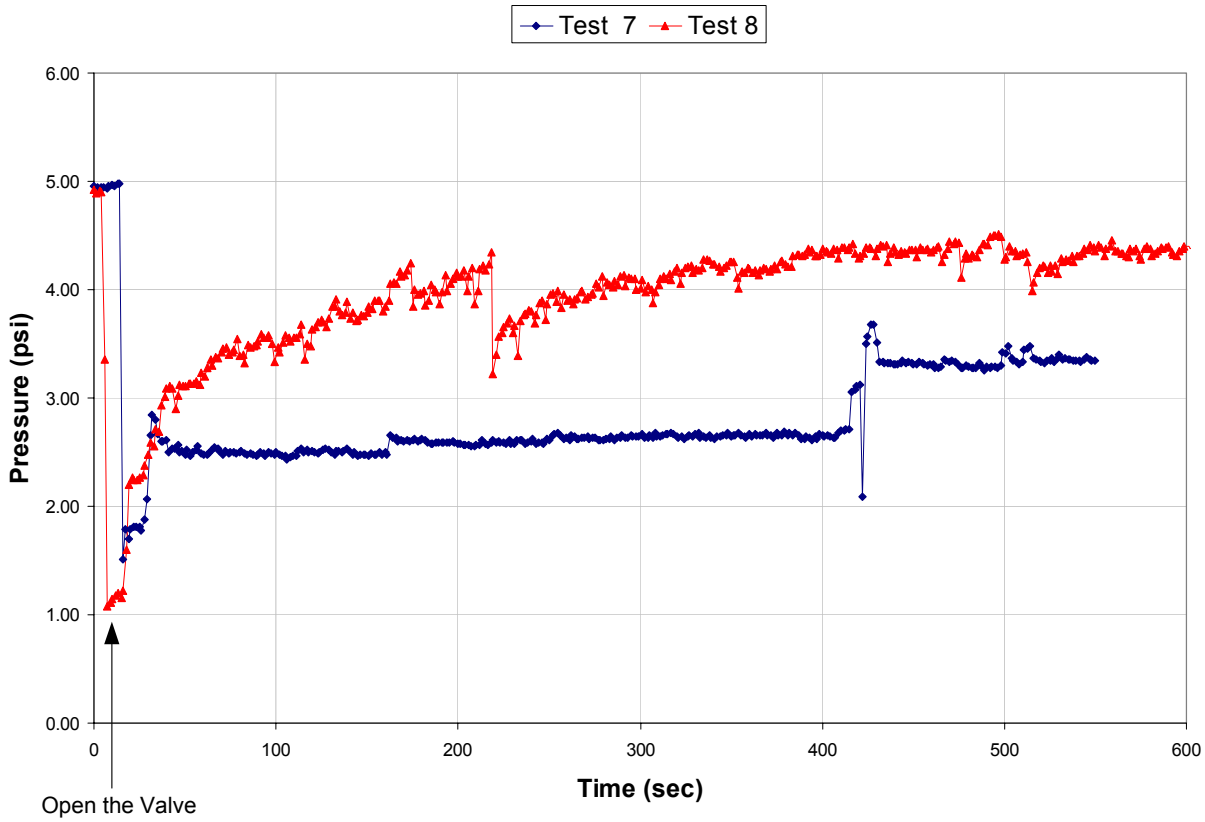

Figure 5.9 Pressure measurement of Test 7 and 8

5.3.3. Vertical Crack Orientation and Vertical Flow Direction

Tests 5 and 6 were conducted with the crack oriented vertically, and with the water flowing vertically downward through the crack. This condition is denoted here as VV.

Test 5 was conducted before the data acquisition (DAQ) system was built, so no continuous record of pressure variation was made. Figure 5.10(a) shows Test 5 before opening the valve. On the top left, the digital clock shows elapsed time (the reading shown is 11 hours, 47 minutes, and 24 seconds), and the digital display at the left shows a voltage that represents the

upstream pressure (0.0101 volts represent 5 psi pressure). As shown in Figure 5.10(b), the pressure immediately dropped by more than half (about 2 psi) after the valve was opened.

(a) Test 5 before opening the valve **(b) Test 5 immediately after opening the valve**

Figure 5.10 Early stage of Test 5 (VV condition)

As mentioned previously, the filter test device in this test (Test 5) was oriented vertically, with the base material above the filter material, and flow was downward. The average gradient used through the soil sample (i = 36) was slightly smaller than the values (i = 39 to 46) used in previous tests. During the test, the base material was first eroded and filled the crack, and then particles of the filter material also moved in to fill the crack, as shown in Figure 5.11(a). The effluent became clear very quickly. Figure 5.11(b) shows that the pressure returned almost to its initial value, and the filter material successfully restrained the base.

Figure 5.12 shows an enlarged view of Figure 5.11(b). It can be seen that a thin layer of the base material formed on top of the filter material that had slumped on top of the pea gravel. Subsequently, more filter material collapsed on top of the thin layer of base material. The condition shown in Figure 5.12 illustrates clogging mechanism described in Chapter 3, and shown by the sketch in Figure 3.5.

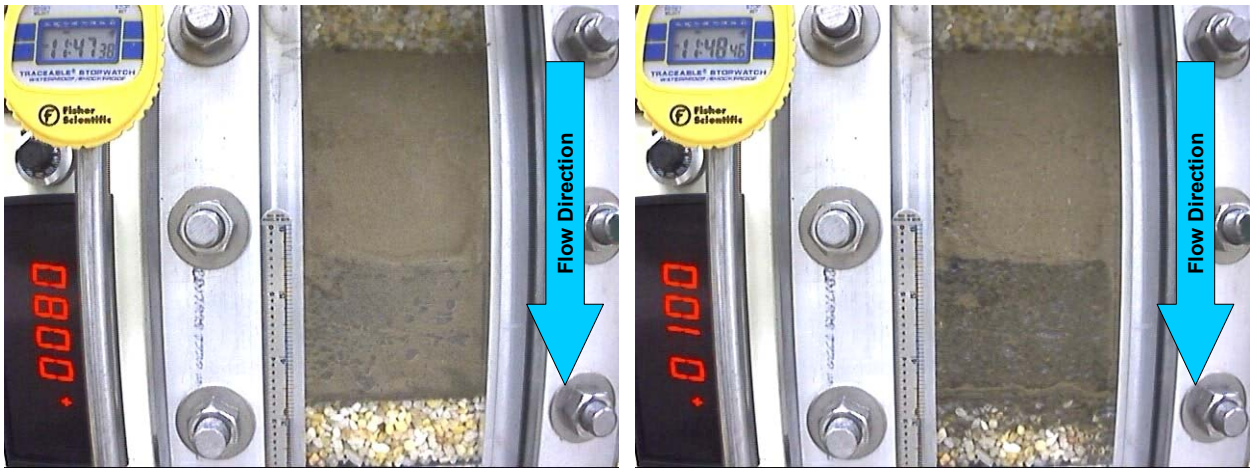

(a) Test 5 during the test **(b) Test 5 after the test**

Figure 5.11 Late stage of Test 5 (VV condition)

Figure 5.12 Clogging layer after Test 5

Test 6 was conducted to investigate whether the filter test device with vertical crack orientation was capable of showing filter failure for conditions under which filter failure should, in fact, occur. This test used pea gravel, which does not meet the USBR criteria for the Teton Dam core material, in place of the filter material. The ratio of the D_{15F} of the pea gravel divided by the D_{85B} of the Teton Dam core was equal to 25, far greater than the allowable value of five.

In this test, shown in Figure 5.13(b), most of the base material was washed through the pea gravel, and a stable condition was never reached. This result demonstrated that the successful performance of the filters in earlier were not an artifact of the test conditions, and were therefore indicative of the actual behavior of the filter materials tested.

5.4. Compaction Procedure and Water Supply

In Tests 9 through 12, as in Test 1 through 8 described previously, the specimens were compacted using the standard Proctor compaction hammer, and using water pressures controlled by a water pressure regulator attached to the laboratory water supply line. Tests 9 through 12 showed that this method of compaction and this method of controlling water pressures were not adequate to achieve consistent results for all of the tests.

Tests 9 through 12 were performed to investigate the effect of fines content on filter behavior, one of the major objectives of the study. These tests showed, as did later tests, which filters with as much as 15% non-plastic fines were able to collapse, fill an initial crack, and satisfactorily retain the base material. However, the results of these tests were not systematic with regard to the effects of the percentage of fines on the variation of flow with time during the tests.

It was surmised that these erratic results were due to variations in the dry densities achieved with the standard Proctor hammer and energy: It was decided that for subsequent tests the specimens would be compacted using a moist tamping procedure, with careful control of the density of each lift. As explained subsequently, consistent results were achieved when this was done.

It was also observed during Tests 9 through 12 that the water pressures varied erratically during the tests, and it was evident that the water pressure regulator was not able to control the water pressures with sufficient uniformity. It was found that much more uniform water pressures

could be achieved with a water supply tank using air pressures in the tank controlled by an air pressure regulator, and this system was used for all subsequent tests.

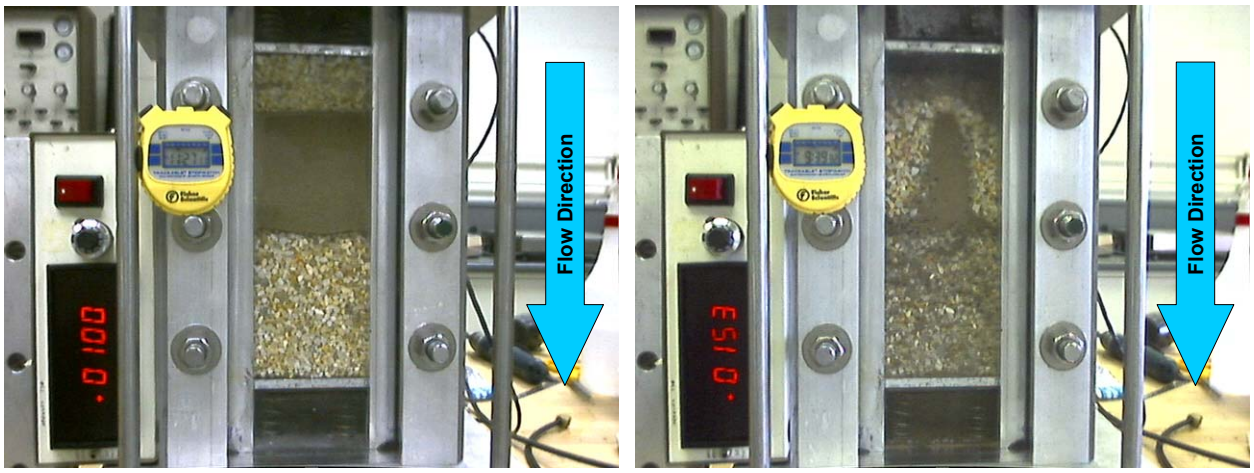

(a) Test 6 before opening the valve **(b) Test 6 after the test**

Figure 5.13 Test 6 (VV condition)

5.5. Major Test Results

5.5.1. Details for a Typical Test

As explained in previous sections, the apparatus and test procedures were developed as Test 1 through Test 12 were performed. Consequently, the procedures used for tests 9 through 12 were not standardized to the degree desired, and the results of these 12 tests are not reported in detail. Test 13 was the first in which the apparatus and test procedures were the same as used throughout the remainder of the tests.

The results of a typical test (Test 16) are shown in Figure 5.14, Figure 5.15, and Figure 5.16.

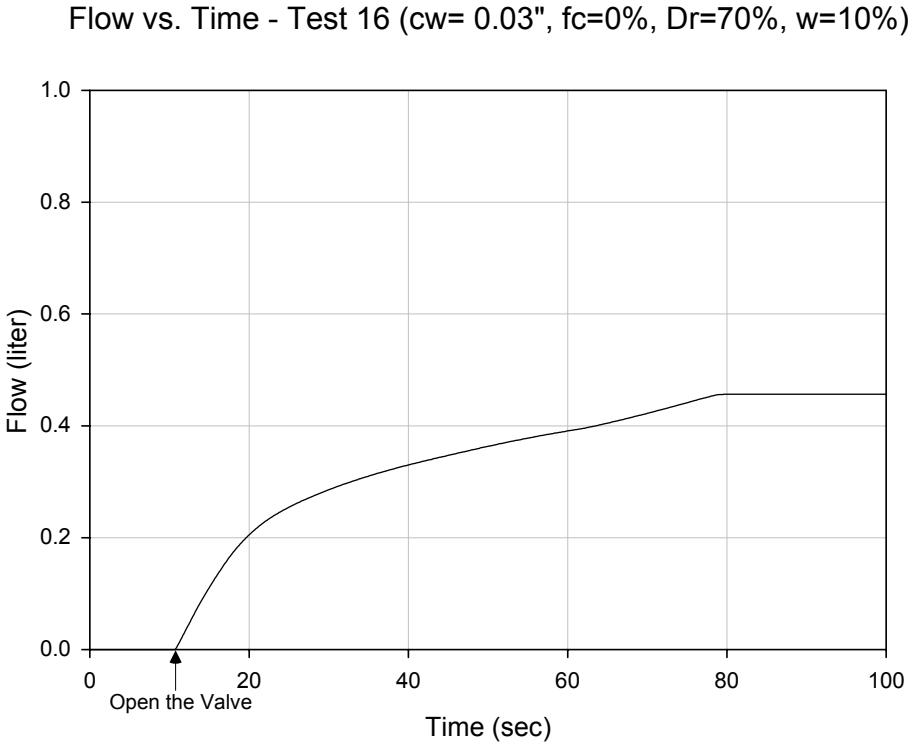

Figure 5.14 Flow vs. Time (Test 16)

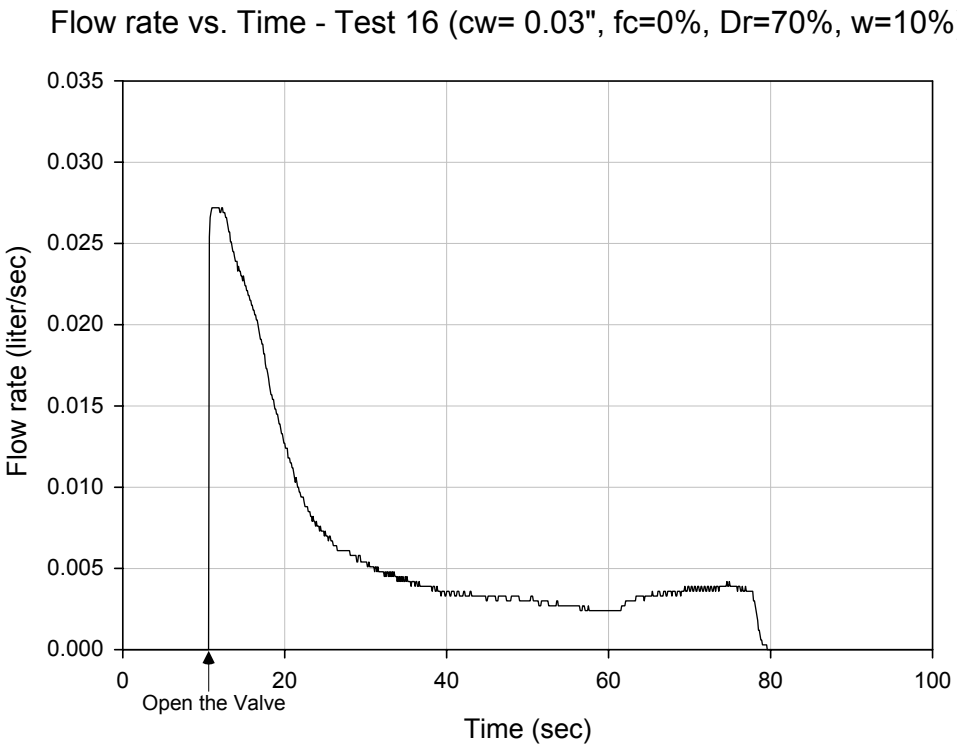

Figure 5.15 Flow Rate vs. Time (Test 16)

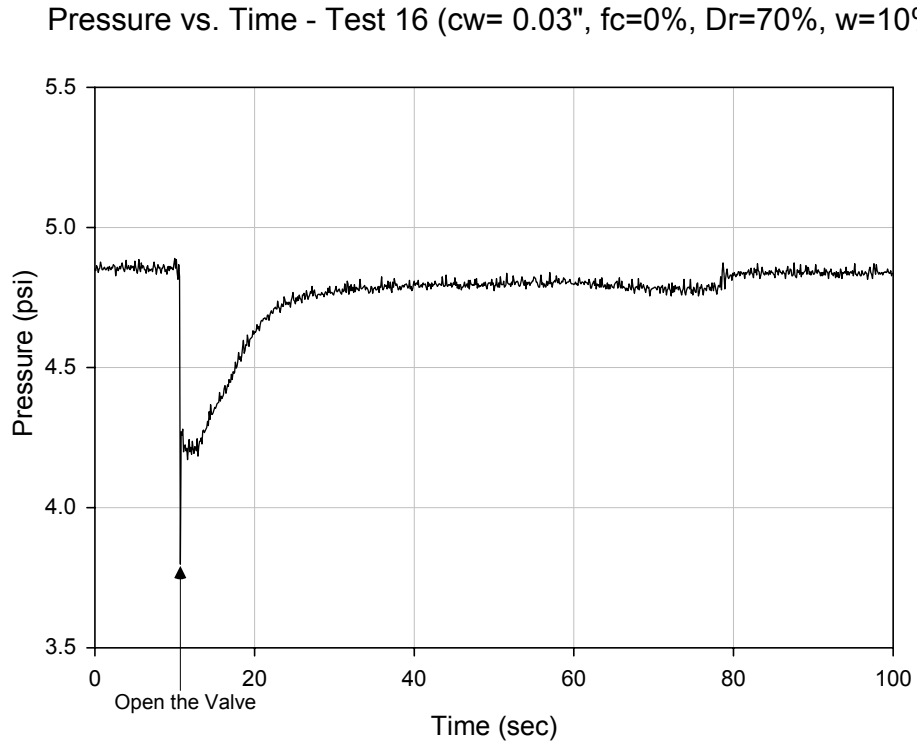

Figure 5.16 Pressure vs. Time (Test 16)

Figure 5.14 shows the variation of flow volume with time and Figure 5.15 shows the variation of flow rate with time. Flow through the test specimen began at t=10 seconds, when the flow control valve was opened. It can be seen that the flow rate was initially very rapid, and that it decreased essentially to zero in a period of about 80 seconds. At this stage in the test, the filter had collapsed and retained the eroding base material.

Figure 5.16 shows the recorded variation of pressure with time during the test. Immediately after opening the valve, the pressure dropped suddenly as the water flowed rapidly through the device. Within approximately 15 seconds the pressure had returned to near its initial value of about 4.7 psi.

It was found that the process of erosion and clogging during the tests often occurred episodically. As can be seen in Figure 5.15, there was evidence of a tendency for increased flow rate and subsequent rapid decrease in flow rate that is characteristic of these episodes of erosion, clogging and retention of the base materials by the filter. It is interesting to note, as can be seen in Figure 5.18, after the filter had reached an apparently stable condition there was a later episode of breakthrough and subsequent reestablishment of a stable condition in the period from about 350 to 400 seconds after the beginning of the test. The conditions remain stable throughout the remainder of the test, as can be seen in Figure 5.19. While the details of the tests vary somewhat from one test to the next, the characteristic behavior shown in Figure 5.14 through Figure 5.16 was consistent throughout Tests 13 through 27.

5.5.2. Effect of the Percent Fines

One of the primary objectives of this research program is to determine the effect of the fines content on the ability of a filter to collapse and fill a crack. Figure 5.17, 5.18, and Figure 5.19 show the results of Tests 16, 19, and 22. The only difference in the conditions for these tests was the percentage of fines in the filter material. In Test 16 the filter had no fines, in Test 19 the filter contained 5% fines and in Test 22 the filter contained 15% fines.

All three tests were conducted with an initial crack width of 0.03 inches, and with the filter compacted to a relative density of 70% at a water content of 10%. All three of these tests were successful, with the filter eventually collapsing and retaining the base material. After an initial reduction in pressure immediately after the valve was opened, the water pressures returned to their initial values very quickly, within about 20 seconds. It can be seen in Figure 5.17 that the flow rate diminished most quickly with the finest filter and most slowly with the coarsest filter.

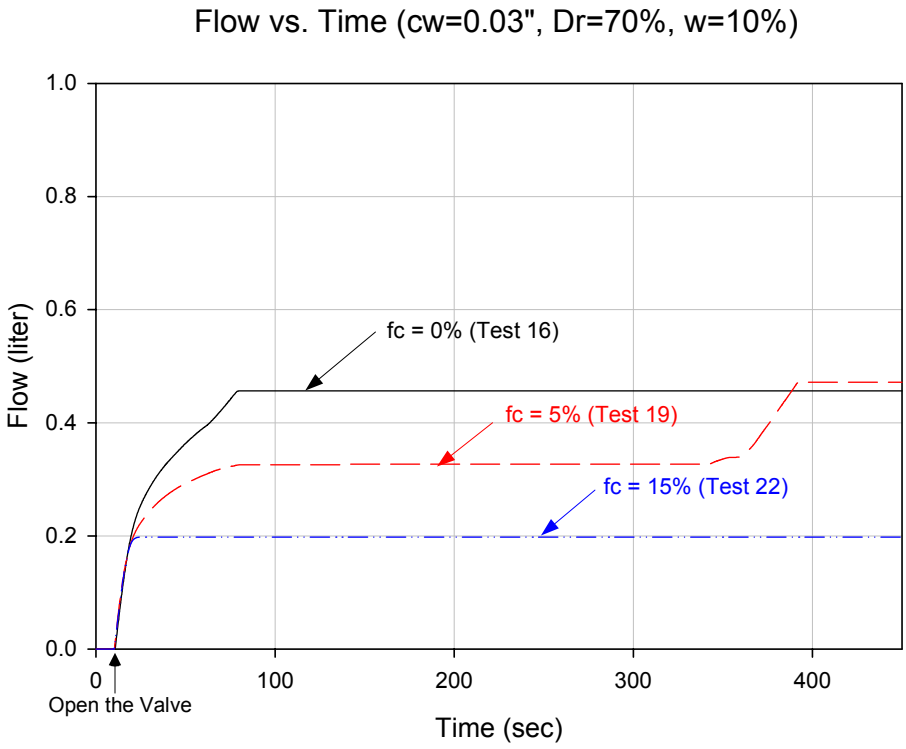

Figure 5.17 Flow vs. Time comparing Test 16, 19, and 22

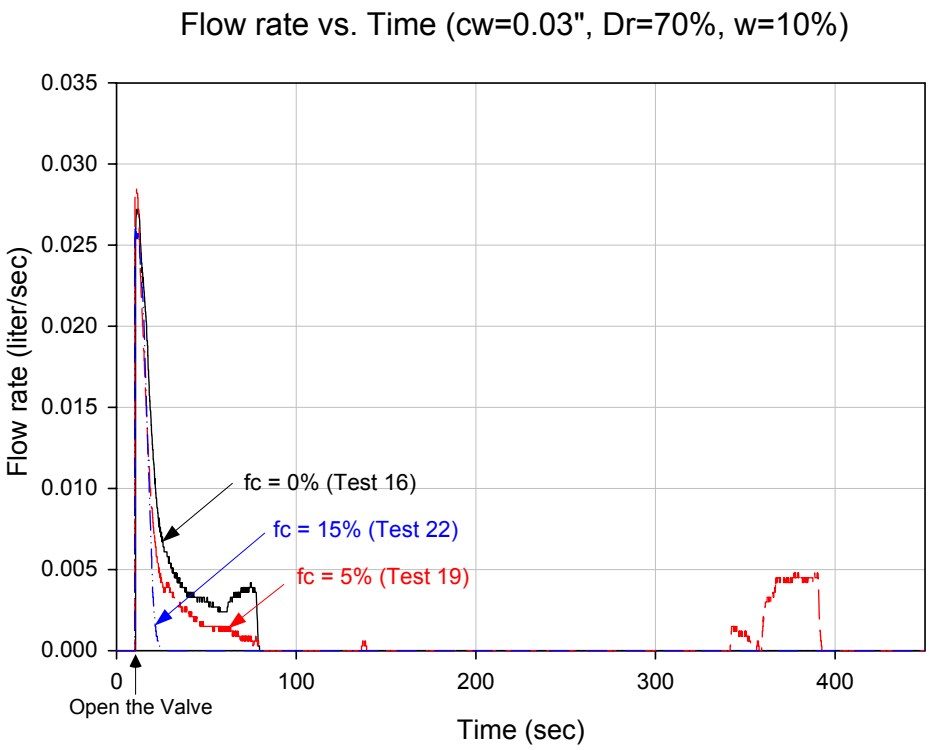

Figure 5.18 Flow Rate vs. Time comparing Test 16, 19, and 22

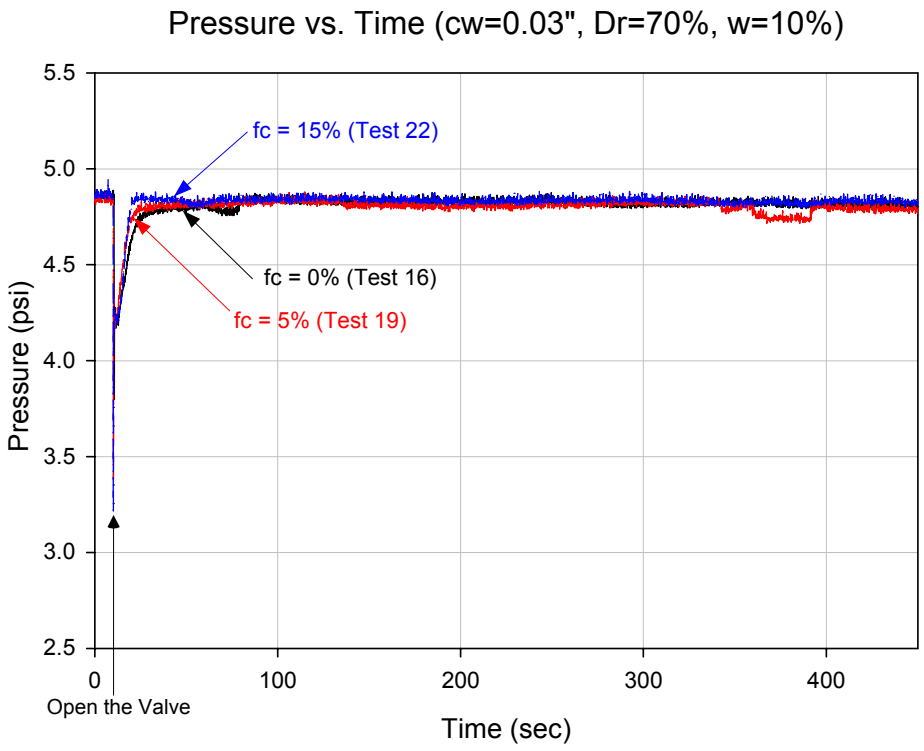

Figure 5.19 Pressure vs. Time comparing Test 16, 19, and 22

The conclusion based on the results of these three tests is that variation of the percentage of non-plastic fines from 0 to 15% does not change the ability of the filter to collapse, plug the crack, and prevent erosion of the base material.

5.5.3. Effect of Crack Width

It was considered important to investigate the width of the crack formed between the specimen and the wall of the filter test device, since this is an important boundary condition in the tests. The results shown in Figure 5.20, 5.21, and 5.22 indicate that variation of the crack width from 0.03 to 0.09 inches does not change the basic behavior of the specimens during the tests. Although there are some detailed differences in the test results, in all cases the filter was able to collapse and close the crack and retain the base soil, even with a crack width as large as 0.09 inches.

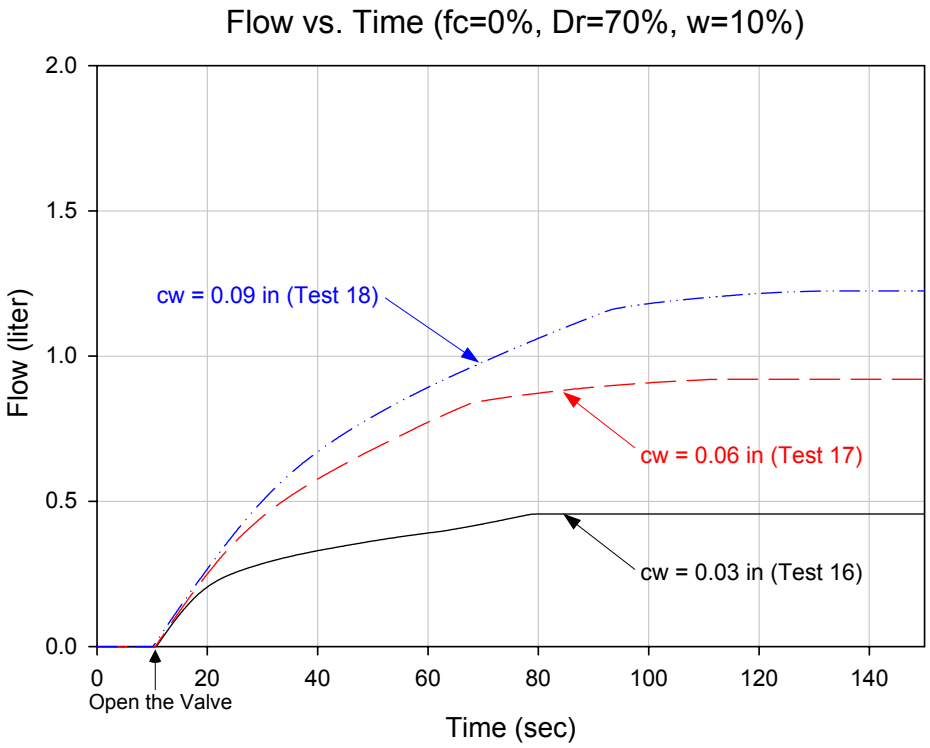

Figure 5.20 Flow vs. Time comparing Test 16, 17, and 18

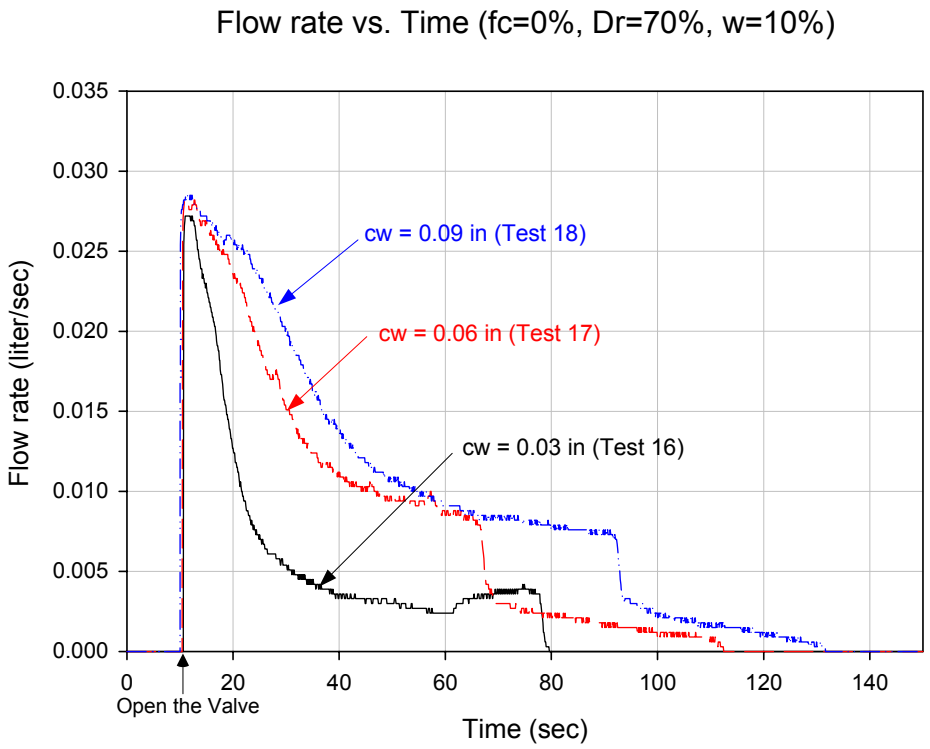

Figure 5.21 Flow Rate vs. Time comparing Test 16, 17, and 18

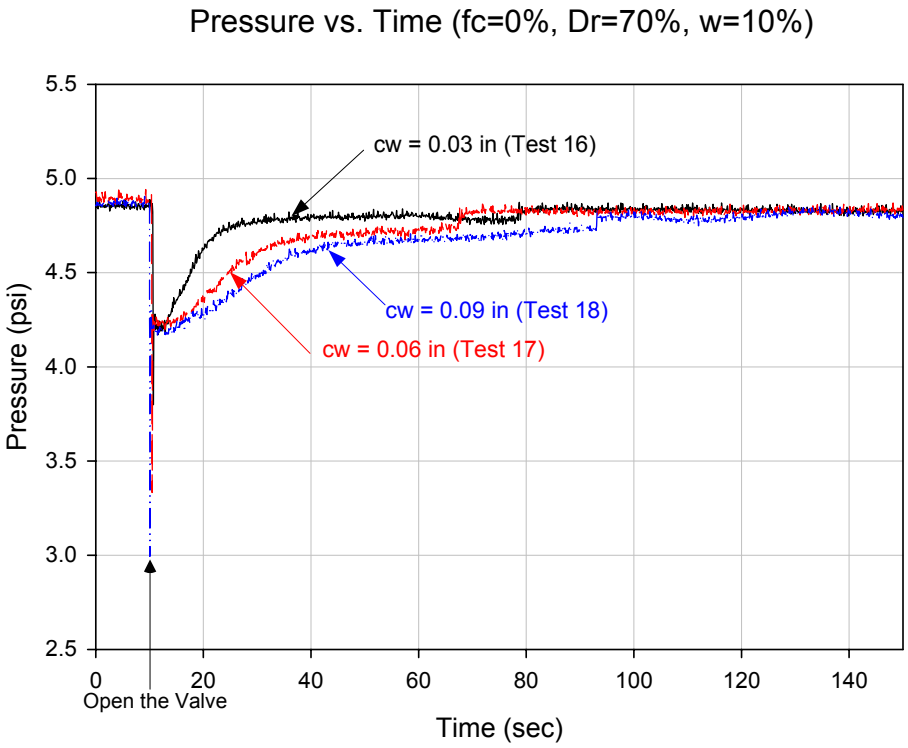

Figure 5.22 Pressure vs. Time comparing Test 16, 17, and 18

5.5.4. Effect of Density

The results of Test 13 and Test 16 are compared in Figure 5.23, 5.24, and 5.25. The relative density of the filter material in Test 13 was 50% and the relative density of the filter material in Test 16 was 70%. Although there are some differences in the rate at which the specimen reached a stable condition, both tests resulted in successful retention of the base by the filter. Test 13 is one of those in which there was a subsequent episode of collapse and reestablishment of a stable condition.

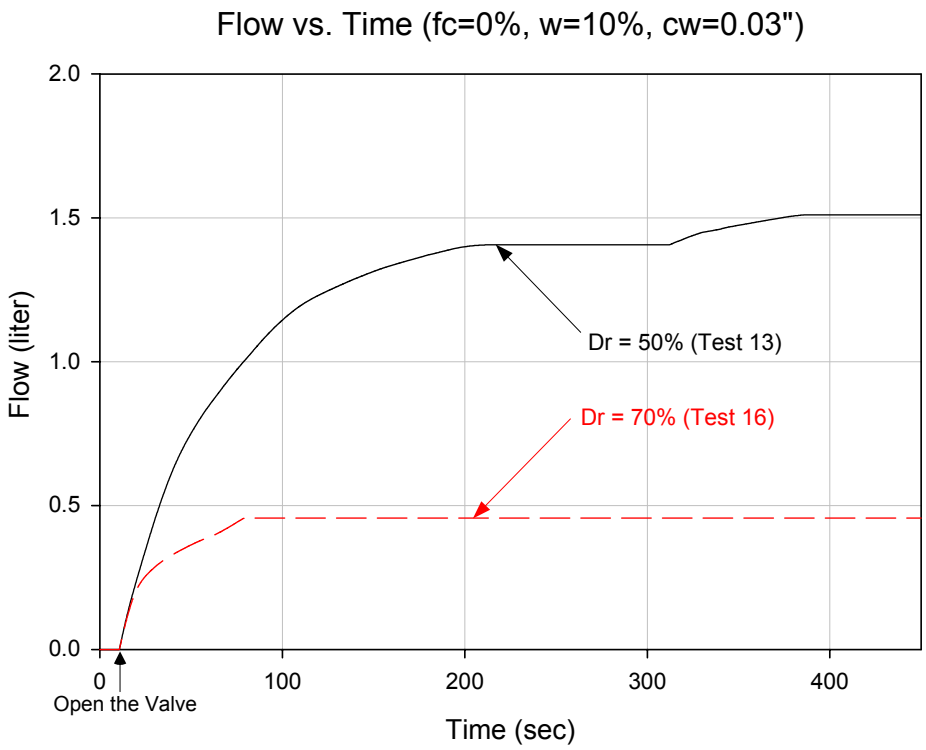

Figure 5.23 Flow vs. Time comparing Test 13 and 16

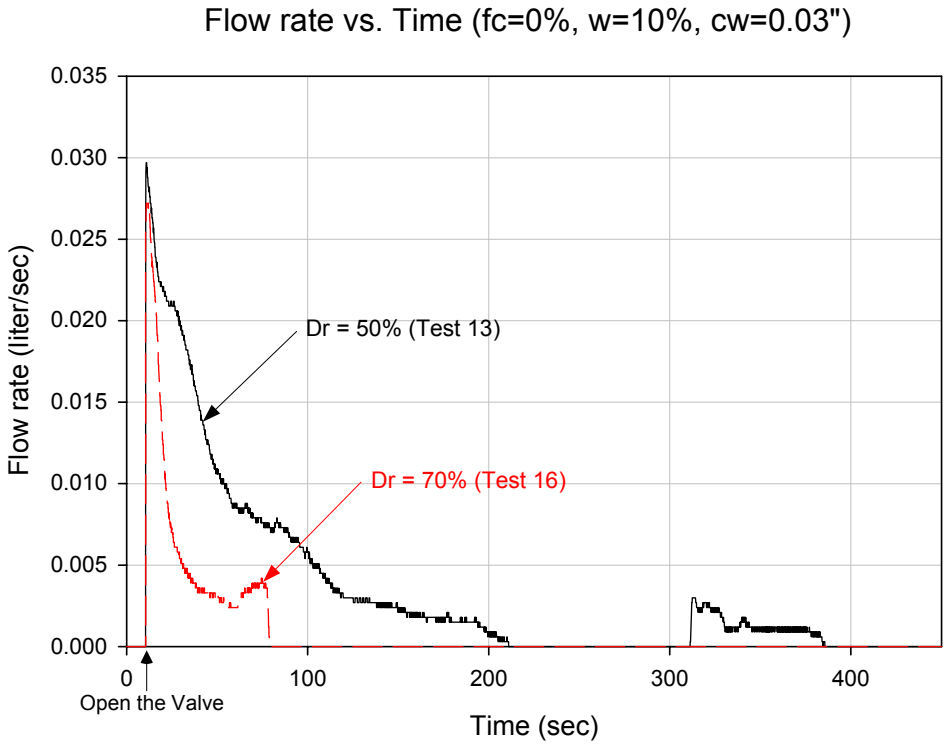

Figure 5.24 Flow Rate vs. Time comparing Test 13 and 16

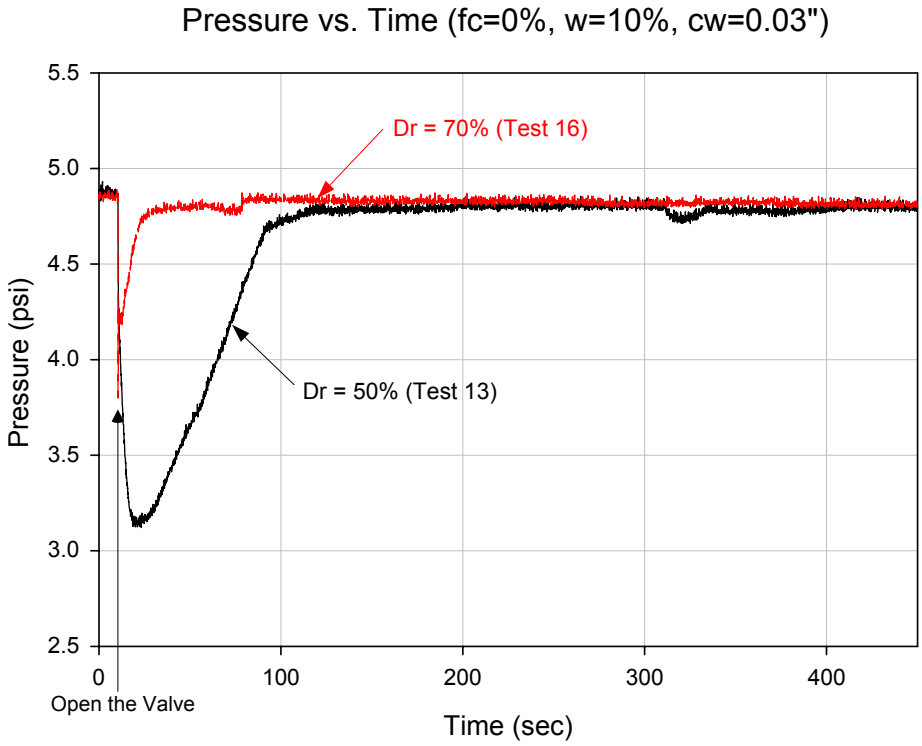

Figure 5.25 Pressure vs. Time comparing Test 13 and 16

5.5.5. Effect of Water Content

The effect of water content during compaction of the filter material can be seen by comparing the results of Test 16 and Test 25, which are plotted together in Figure 5.26, 5.27, and 5.28. These two tests had the same filter material, but different water contents. The results of these tests are nearly identical, with very similar flow rates versus time required to re-establish the initial pressure. This result might be expected, because the filter material is granular, and its compaction is not effected much by variation in compaction water content.

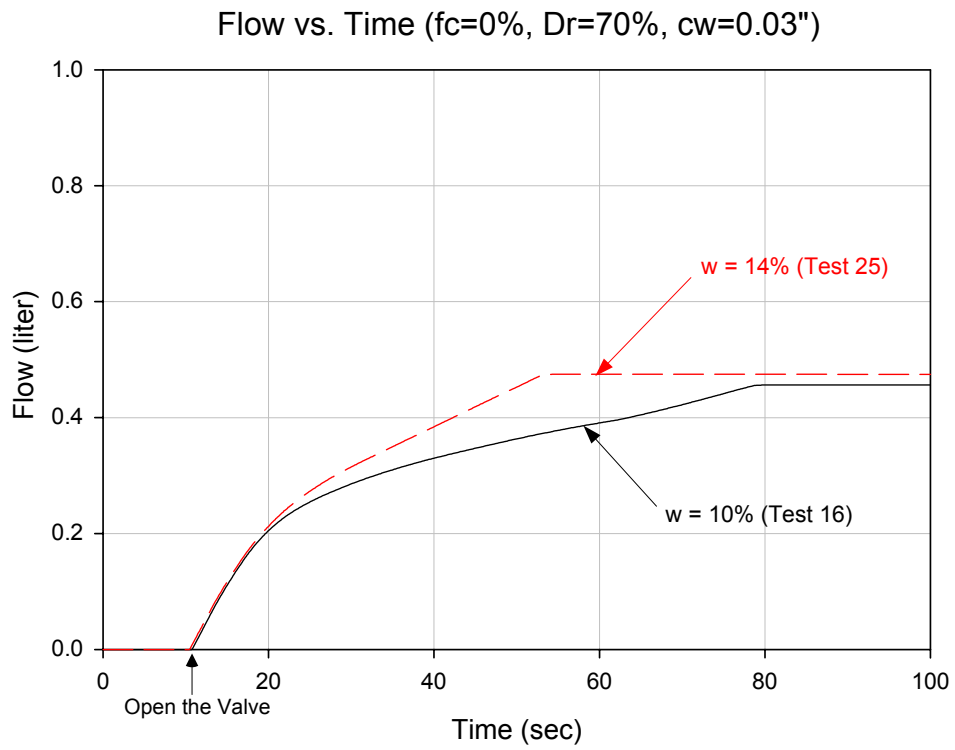

Figure 5.26 Flow vs. Time comparing Test 16 and 25

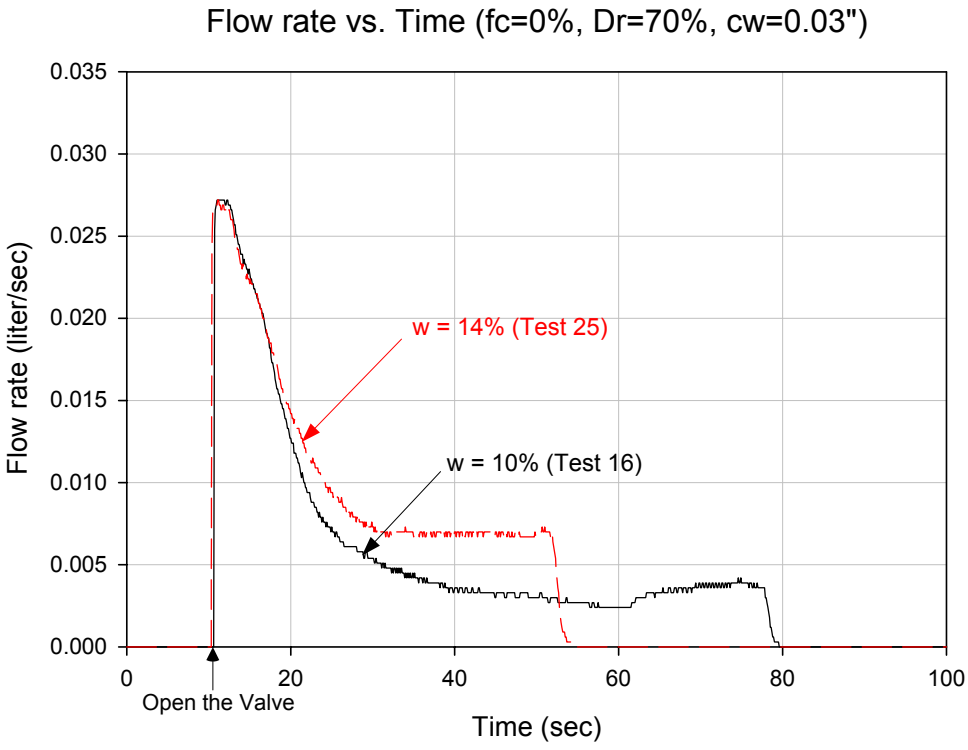

Figure 5.27 Flow Rate vs. Time comparing Test 16 and 25

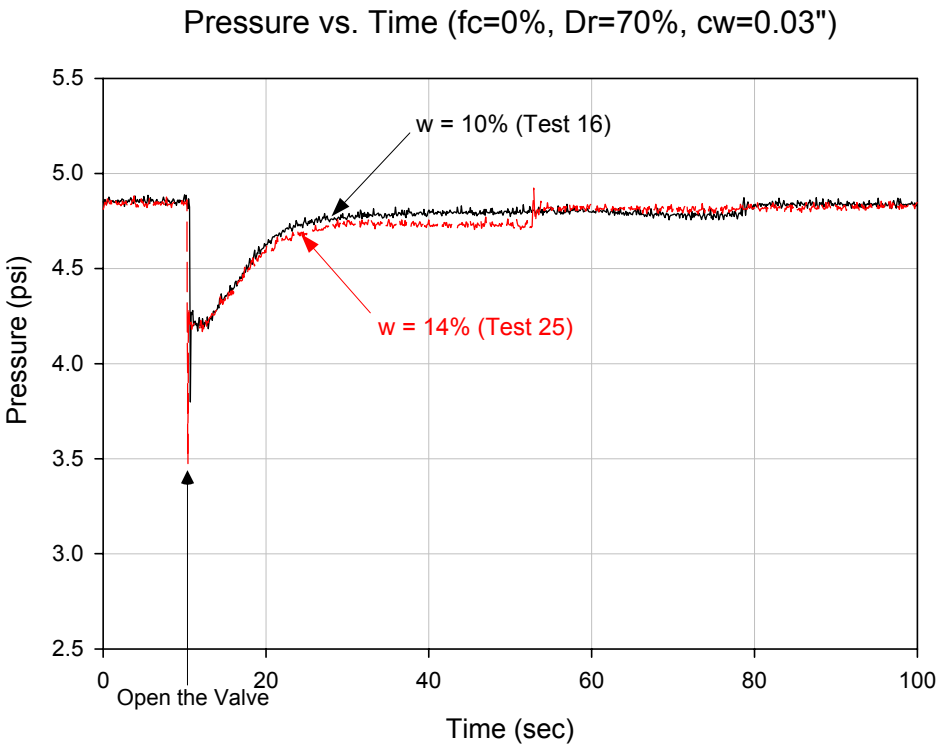

Figure 5.28 Pressure vs. Time comparing Test 16 and 25

Tests 24 and 26 were performed to determine if water content would have any effect on the behavior of filter materials containing fines. The results of these tests, conducted using filter material containing 15% fines, and compacted at water contents of 10% and 14%, are shown in Figure 5.29, 5.30, and 5.31. The results show that compaction water content did not have any significant effect on the results. Therefore, compaction water content does not appear to have any effect on the ability of the filter to collapse and block a crack, even if the filter material contains as much as 15% of non-plastic fine material.

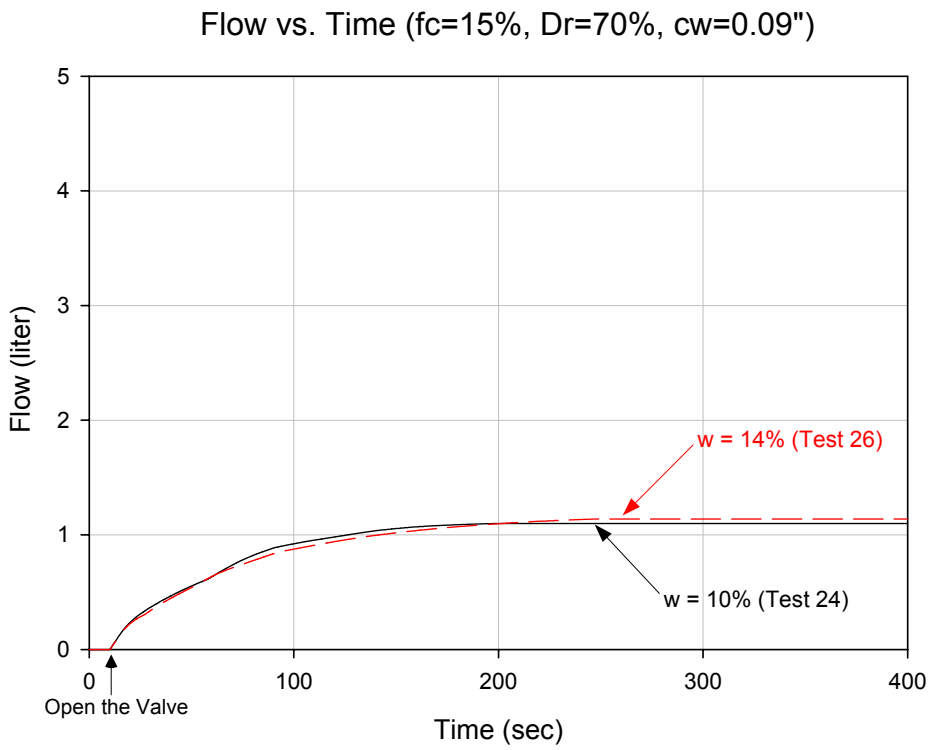

Figure 5.29 Flow vs. Time comparing Test 24 and 26

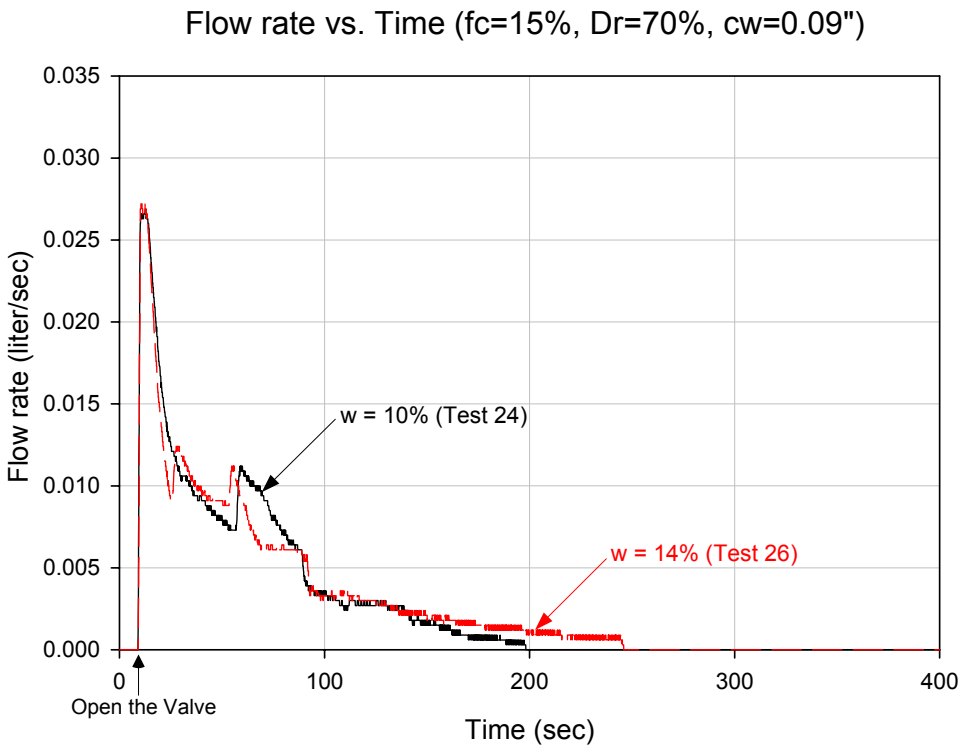

Figure 5.30 Flow Rate vs. Time comparing Test 24 and 26

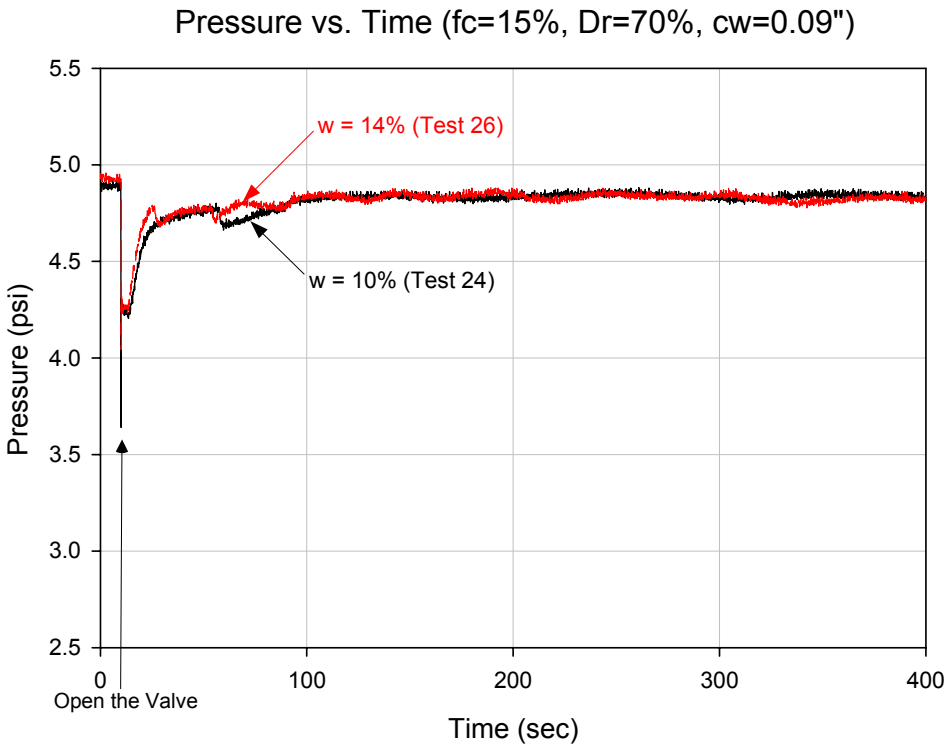

Figure 5.31 Pressure vs. Time comparing Test 24 and 26

5.6. Summary of Tests with 4-inch diameter Filter Test Device

The results obtained with the 4-inch diameter filter test device support these conclusions:

- An apparatus and test procedure has been developed that is capable of investigating the ability of filters to collapse and retain base materials that are initially cracked. The principal limitation is that the apparatus is only 4 inches in diameter, which only allows filter materials having maximum particle sizes of 0.25 inches.
- Tests have been performed to investigate the effects of the percentage of non-plastic fines in the filter (up to 15 percent), the effect of the crack widths (up to 0.09 inches), the effects of relative density in the range from 18% to 70%, and the effects of compaction water content in the filter ranging from 10% to 14 %. In all of the tests performed over

this range of variables the filter material successfully collapsed and retained the base material.

- The fact that the uniformly successful test results are not an artifact of the apparatus design is illustrated by the result of Test 6, in which the filter material was replaced by pea gravel too coarse to satisfy filter criteria. In this case, the base material was washed through the pea gravel continuously, and a stable condition was never reached during the test.
- A major finding of this research study is the fact that filters with as much as 15% of non-plastic fines are sufficiently cohesionless to collapse and retain the base material in an initially cracked specimen. Investigation of the effects of percent fines on the crack-stopping ability of filters was the major objective of this research.
- It should be noted that all of the filter materials used in these tests were composed of inert particles that exhibited no bonding or cementation during compaction. Bonding or cementation during compaction would be expected to have a major effect on the ability of filters to perform as crack stoppers.

Chapter 6. Tests Performed using the 12-inch Square Filter Test Device

6.1. Introduction

The 12-inch square filter test device was designed and constructed to make it possible to test larger filter materials and larger crack widths. The device, shown schematically in Figure 6.1, can be used to test filter materials with particles as large as 1.5 inches, and crack widths as large as 1.0 inches. Most of the tests performed using the 12-inch device were performed with a vertical crack and horizontal flow. The 4-inch diameter and 12-inch square filter test devices are shown side-by-side in Figure 6.2. Further appreciation for the scale of the larger tests is afforded by considering that the volume of a test specimen for the 12-inch device is about 30 times as large as the volume of a specimen for the 4-inch device. The time required for specimen preparation was considerably longer than for the smaller device. However, closer correspondence to real field conditions justified the larger-scale tests.

In addition to its larger size, the 12-inch device was constructed with a membrane (discussed in the subsequent section) that could be used to apply pressure to the top of the test specimen, simulating overburden pressure in the field. In the 4-inch diameter filter test device, the boundary conditions imposed on the test specimen did not allow for meaningful results to be obtained for a vertical crack orientation with horizontal flow, because a void formed at the top of the specimen when the filter slumped, and water continued to flow through this space even if the filter performed well. The membrane incorporated in the 12-inch device prevented formation of a void at the top of the specimen, and resulted in closer simulation of field conditions.

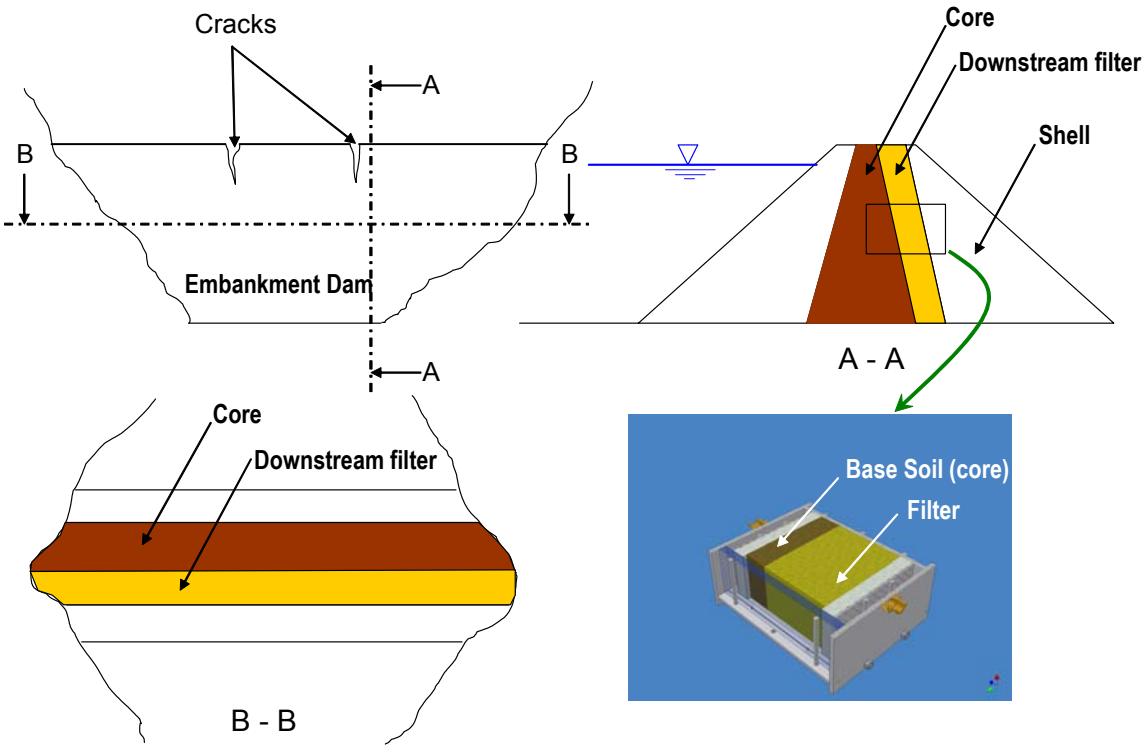

Figure 6.1 Relationship of tests to field conditions

Figure 6.2 Comparison of cross section of the two filter test device

Table 6.1 summarizes the results of the 11 tests performed using the 12-inch square filter test device. The base material used in all of the tests was the Teton Dam core material. Three different filter materials were used: Horsetooth Dam filter material, Horsetooth Dam filter material mixed with various amounts of highly plastic fines, and very coarsely graded marble chips.

Table 6.1 Summary of tests performed using 12-inch square filter test device

	Compaction Method	Crack width cw (inch)	Crack Oriendation / Flow Direction	Pressure Control	DAQ Measurement			Base Material	Filter Material	Filter Material Properties			
					Flow	Pressure	Video			fc (%)	w (%)	D_r (%)	γ_d (pcf)
Test 28	Standard Proctor Hammer	0.15	V / H	Constant from Water Tank	Measured	Measured	Monitored	Teton Dam Core	Horsetooth Dam Filter	0	10	70	109.5
Test 29		0.15	V / H							0	10	70	109.5
Test 30		0.50	V / H							0	10	70	113.7
Test 31		1.00	V / H							0	10	70	113.7
Test 32		1.00	V / V							0	10	70	113.7
Test 33		1.00	V / H						Horsetooth Dam Filter w/ HPF	5	10	70	112.7
Test 34		1.00	V / H							15	10	70	112.5
Test 35		1.00	V / H							10	10	70	113.8
Test 36		1.00	V / H						Fabricated Marble Chip	0	N/A	70	102.1
Test 37		1.00	V / H							0	N/A	70	111.1
Test 38		1.00	V / H							0	N/A	70	127.2

Note: HPF = highly plastic fines.

6.2. Pressure Membrane

As noted above, the 12-inch square filter test device was equipped with a flexible pressure membrane. The purpose of the membrane was to expand and fill the void that formed at the top of the specimen when the filter collapsed, and to prevent flow through this area. Figure 6.3 shows the orientation of the device for horizontal flow through a vertical crack. The flexible membrane is beneath the top panel. An exploded view of the membrane, and the panel to which it is attached, is shown in Figure 6.4. Figure 6.5 shows a cross section through the crack and the membrane, and indicates how the membrane expands to fill the void that forms as filter material slumps to fill the crack. Detailed drawings of the 12-inch square filter test device, the steps involved in sample fabrication, and assembly of the device for testing are shown in Appendix B.

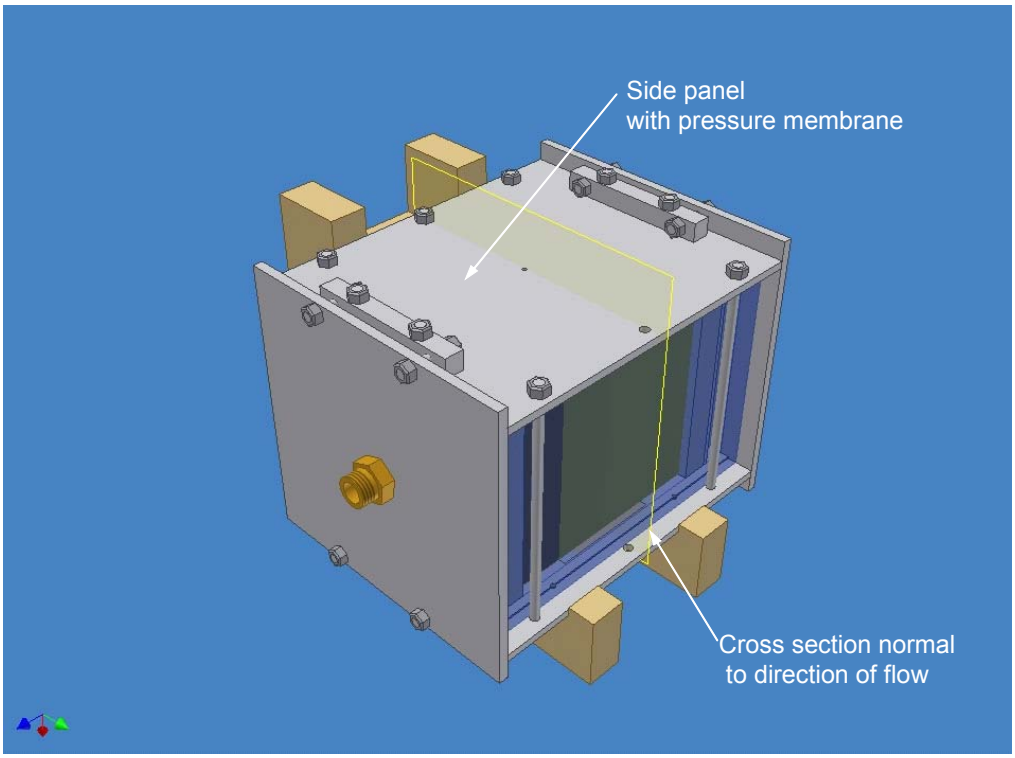

Figure 6.3 Permeameter orientation for vertical crack and horizontal flow

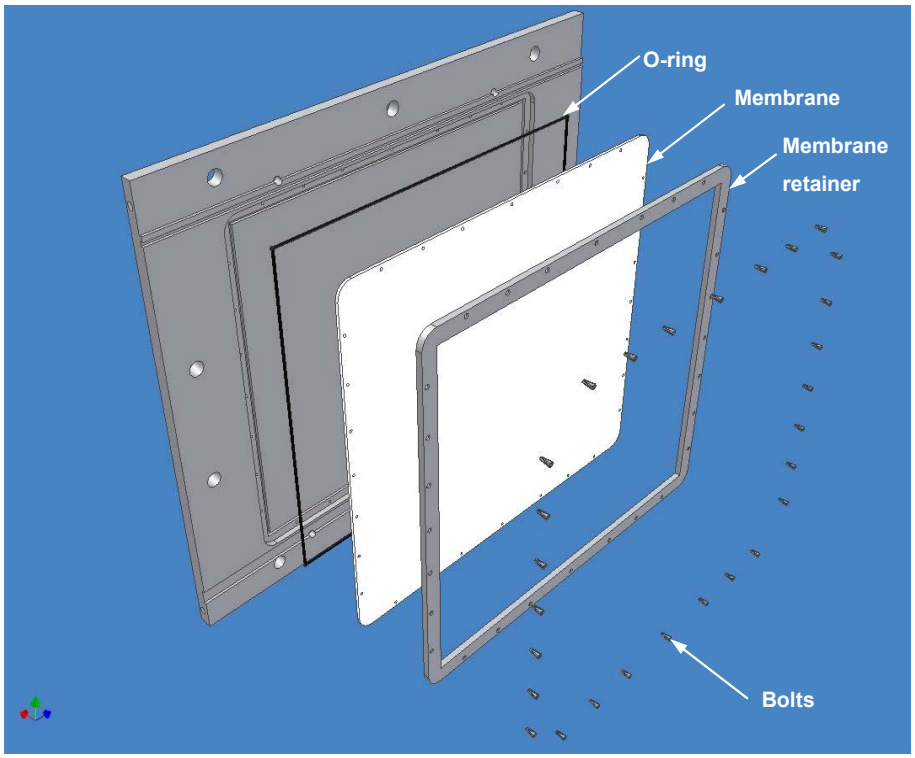

(a)

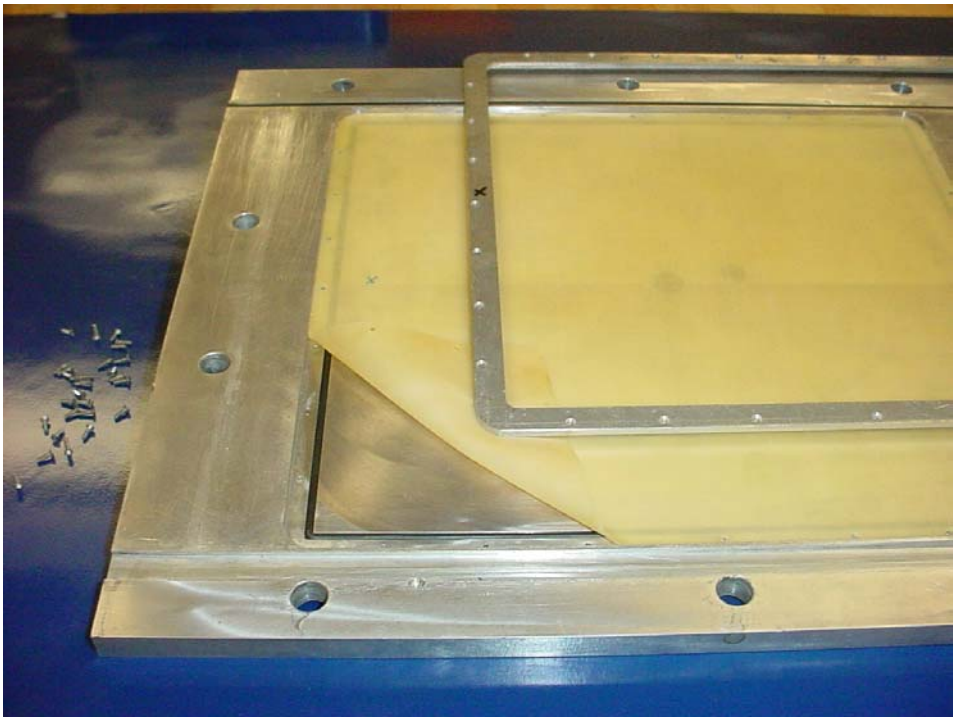

(b)

Figure 6.4 Exploded view of flexible membrane and backing panel

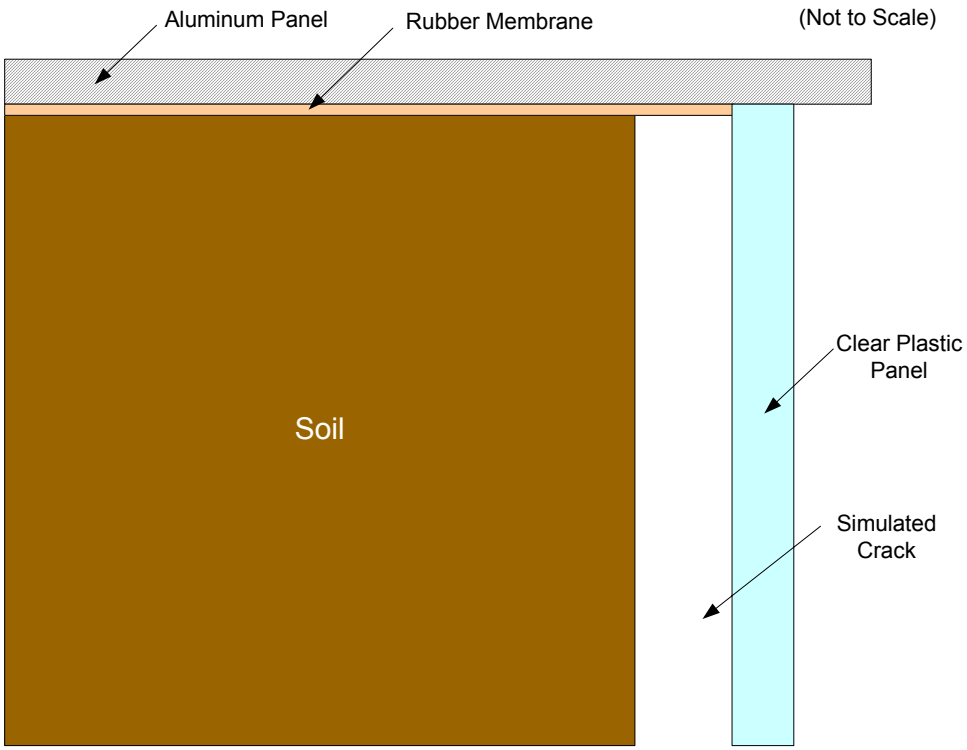

(a) Before the test

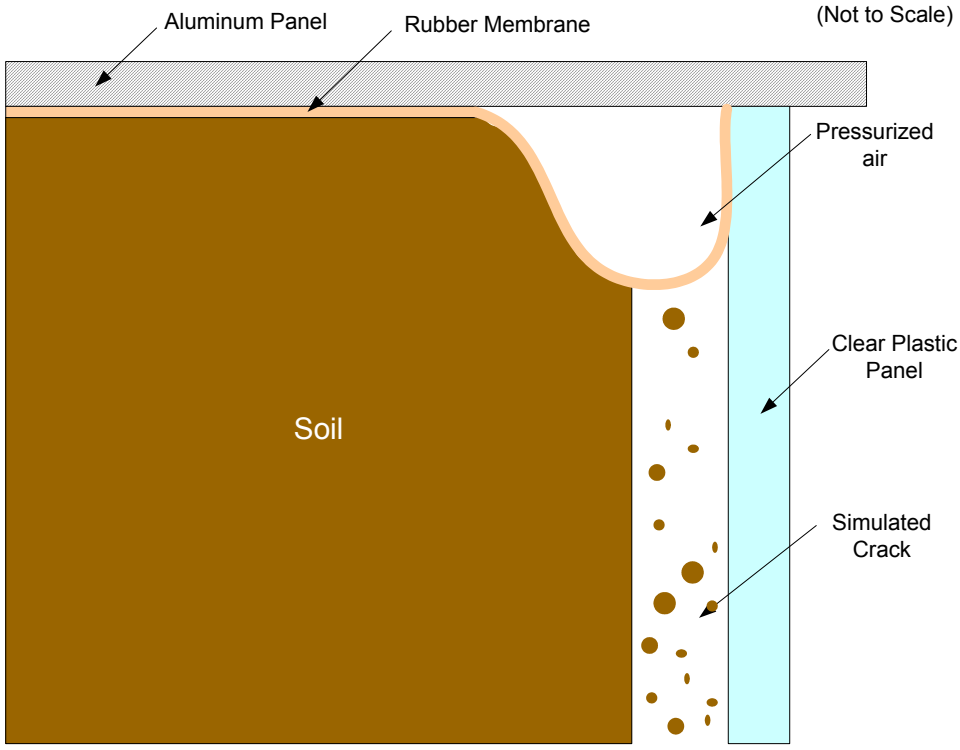

(b) During the test

Figure 6.5 Flexible membrane used to fill void at top of specimen

6.3. Test with Vertical Crack and Vertical Flow (VV test condition)

One test was performed using the same VV test condition used in the 4-inch diameter filter test device, to ensure that similar results were achieved for similar test conditions. The results of this test (Test 32) are shown in Figure 6.6. The gradations of the base and filter materials used in this test were the same as those used in Tests 16, 17, and 18. However, the gap width in Test 32 was 1.0 inch, as compared to gap widths varying from 0.03 inches to 0.09 inches in the earlier tests.

Figure 6.6(a) shows the specimen after it was tipped up into position for testing, and the filter material slumped to fill the bottom of the crack. Figure 6.6(b) shows the specimen at the end of the test, when base material had been retained on top of the filter material and conditions had stabilized.

Variations of flow rate and pressure with time during the test are shown in Figures 6.7 and 6.8. Immediately after the flow valve was opened, a spike in flow occurred, and the pressure dropped suddenly. As base material accumulated on the filter and blocked the flow path, the flow rate decreased and the pressure stabilized. It can be seen that the initial clogging event was followed by two smaller clogging events. This behavior was essentially the same as measured in similar tests with the 4-inch device using the same grain sizes in the base and filter materials, but smaller gap widths.

(a) Before the Test 32

(b) After the Test 32

Figure 6.6 Test 32 with 12-inch square filter test device (VV condition)

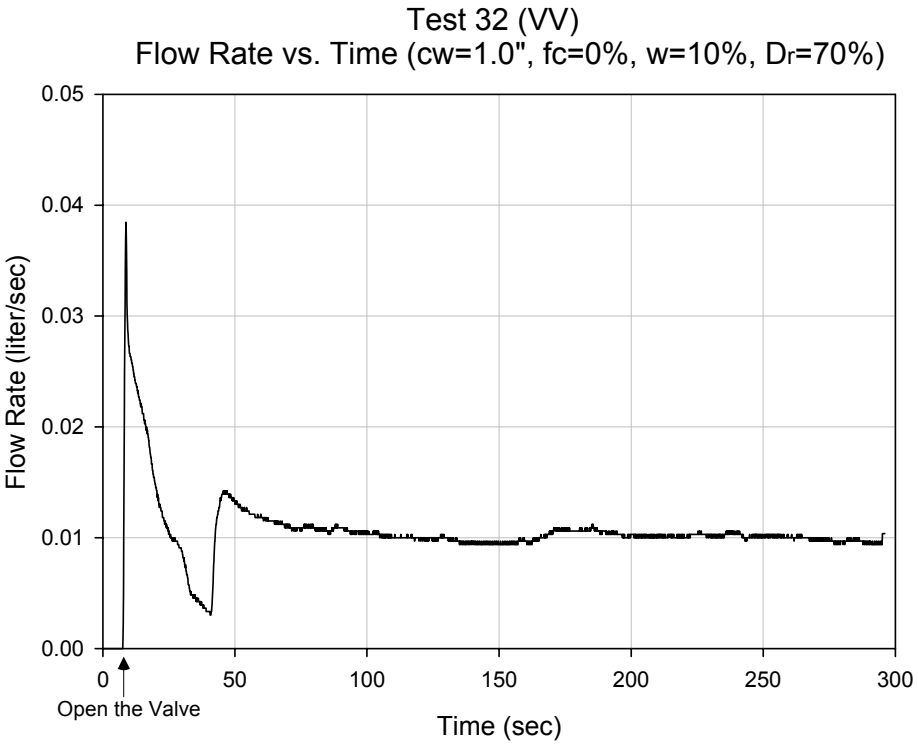

Figure 6.7 Flow rate vs. Time of Test 32

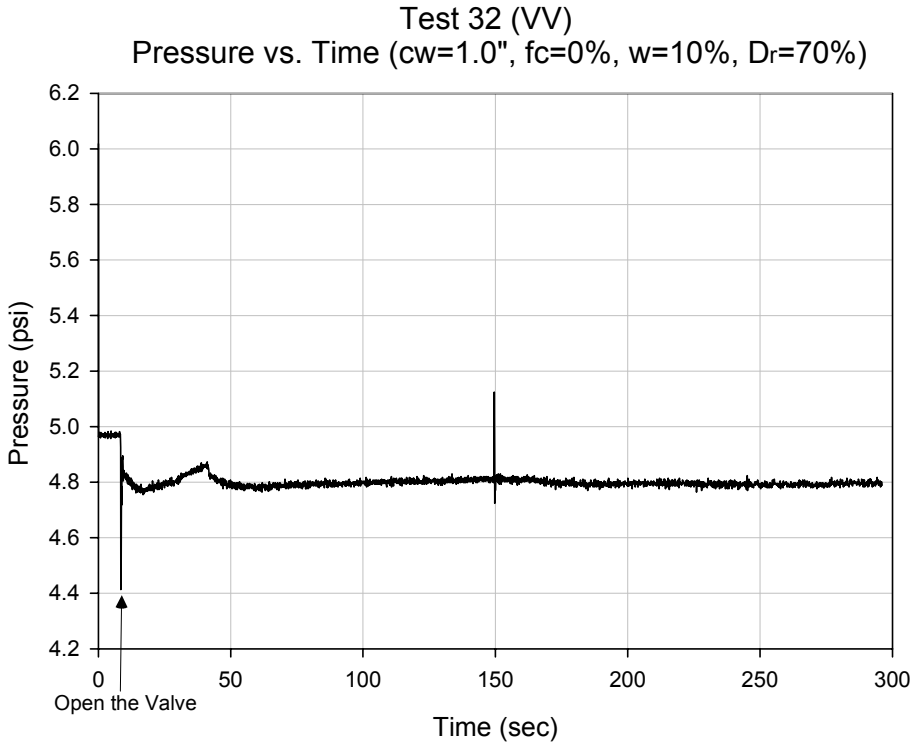

Figure 6.8 Pressure vs. Time of Test 32

6.4. Effect of Crack Width

Tests 29, 30, and 31 were performed using the Teton Dam base material and the Horse Tooth Dam filter material, with no fines. The crack widths used in the tests were 0.15 inches in Test 29, 0.5 inches in Test 30, and 1.0 inches in Test 31. The results of these tests are shown in Figures 6.9 and 6.10.

As shown in Figure 6.9, the measured flow rate increased with increasing crack width. Both the initial spike in flow rate, and the steady flow rate later in the test, were largest for Test 31 with a 1.0-inch crack width, and smallest for Test 29, with a 0.15-inch crack width. The measured pressures shown in Figure 6.10 also varied with crack width. Stabilized pressure after clogging was highest for Test 29, with the 0.15-inch crack, and smallest for Test 31, with the 1.0-inch crack.

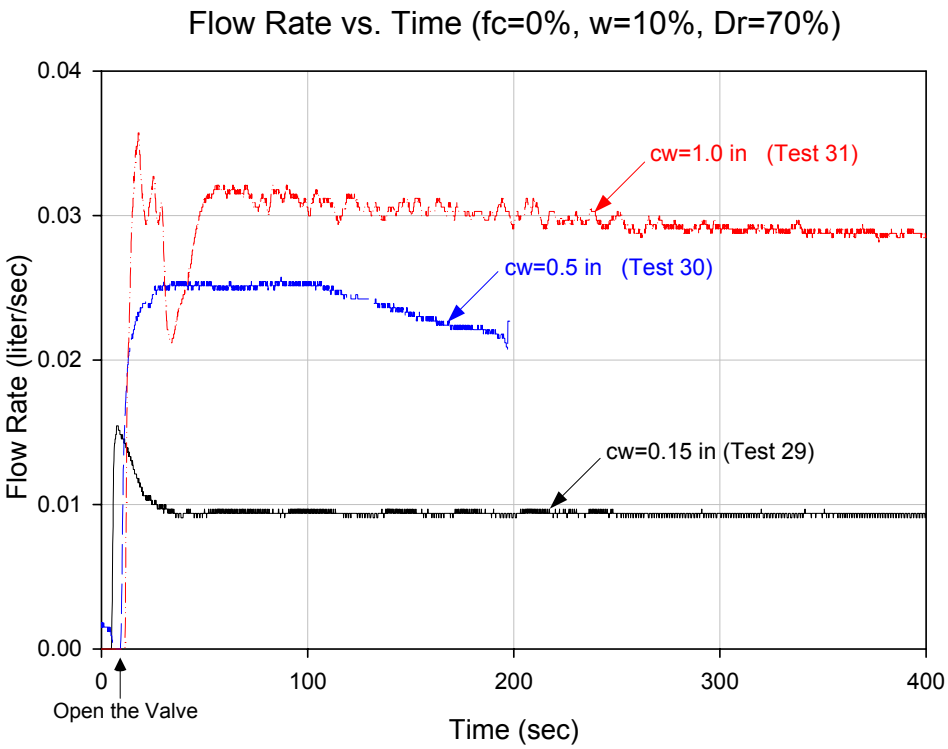

Figure 6.9 Flow rate vs. Time (Test 29, 30, and 31)

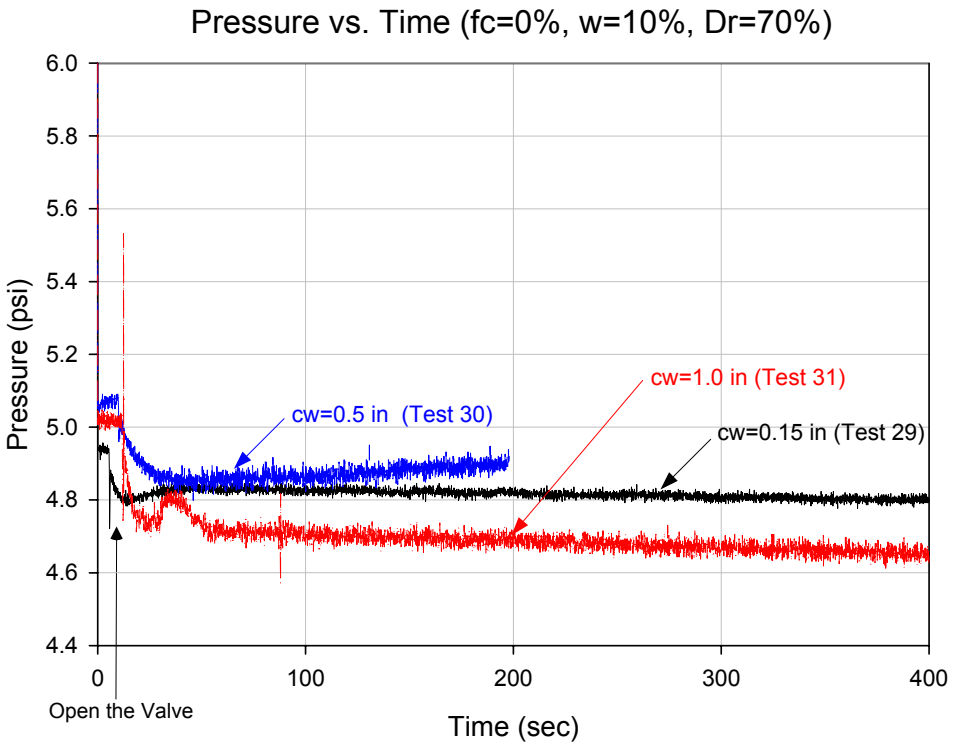

Figure 6.10 Pressure vs. Time (Test 29, 30, and 31)

6.5. Effect of Highly Plastic Fines Content

Three tests were conducted to investigate the effect of highly plastic fines on the ability of filters to collapse and fill cracks. Test 33 was performed on a specimen containing 5% of material with Liquid Limit = 72, and Plastic Limit = 32. Test 34 was performed on a specimen containing 15% of the same highly plastic material, and Test 35 was performed on a specimen with 10% of this material.

Figure 6.11 shows Test 33 (5% fines) before and during the test. In Figure 6.11(a), the test device has been rotated into position for testing, with the crack vertical. The filter and base materials have slumped, and fill the bottom part of the crack. Cloudy water fills the top of the crack. In Figure 6.11(b) the membrane has expanded to fill most of the void left by the collapsing filter material. Although a small void remained between the membrane and the soil beneath, the membrane did block most of the flow through the void, as would slumping soil in the field.

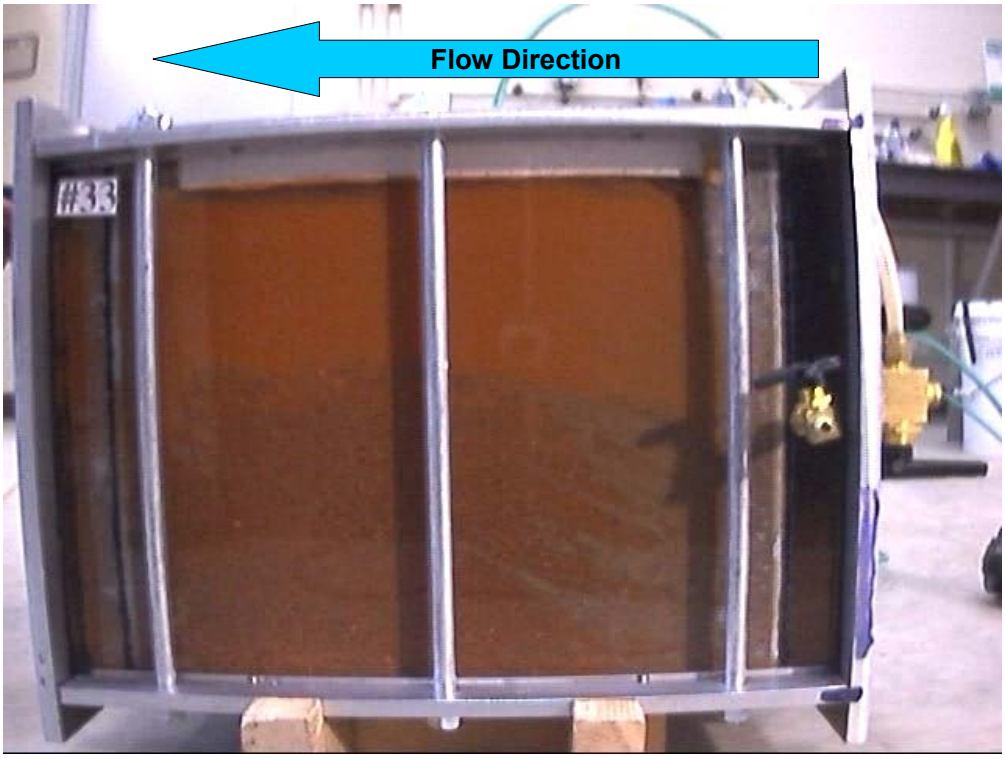

(a) Before the Test 33

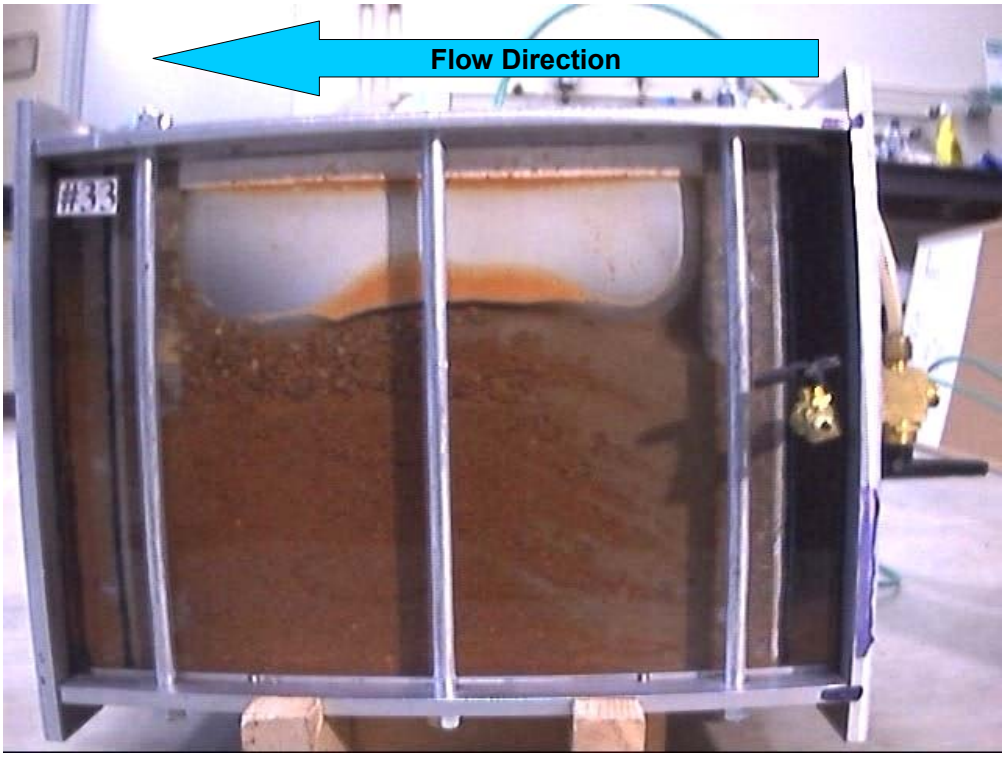

(b) During the Test 33

Figure 6.11 Test 33 (5% HPF)

Figure 6.12 shows Test 34 (15% fines) before and during the test. In Figure 6.12(a), the test device has been rotated into position for testing, with the crack vertical. Very little of the base material slumped to fill the crack when the device was rotated into position and most of the crack was filled with water. During the test, the membrane had to expand further than in Test 33. At a later stage of the test, the membrane burst, and useful results could not be obtained beyond that point. It may be noted that there is a void at about the lower third point across the specimen, between the darker material above (predominantly filter, with some base mixed in by particle migration) and the lighter material below (predominantly base, with particles of filter mixed in). Cloudy water flows through this void. This test, with the largest content of highly plastic fines, was the only test in which this phenomenon was observed.

The results of Tests 33, 34, and 35 are shown in Figures 6.13 and 6.14. As noted previously, the membrane burst during Test 34, and useful results were not obtained after about 220 seconds. In all three tests the flow rate increased with time and then stabilized at or near the maximum. The upstream pressures dropped immediately, and did not return close to their original values, as had pressures in tests on filters that did not contain highly plastic fines. These differences are qualitative indications that the highly plastic fines reduce the ability of the filter to slump and fill cracks.

In Test 33 (5% fines) and Test 35 (10% fines) a stable condition was achieved at the end of the tests, and the effluent was clear, indicating no continuing erosion of the base material. In Test 34, which had 15% fines, however, conditions did not stabilize. Cloudy effluent continued to flow from the specimen throughout the test, indicating that effective filter action was not established.

(a) Before the Test 34

(b) During the Test 34

Figure 6.12 Test 34 (15% HPF)

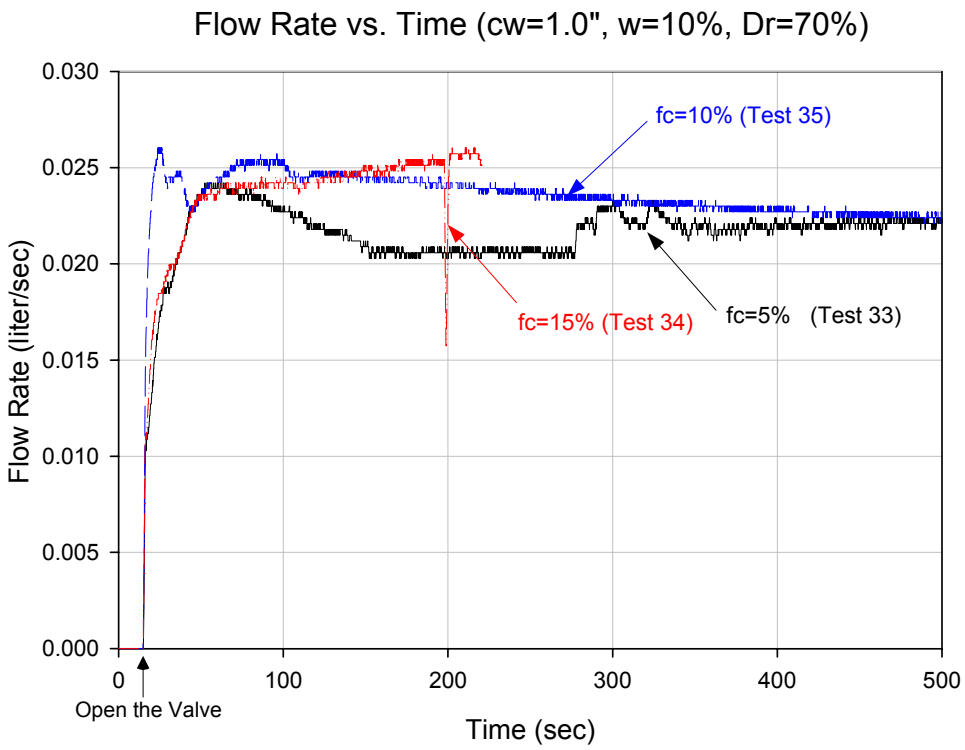

Figure 6.13 Flow rate vs. Time (Test 33, 34, and 35)

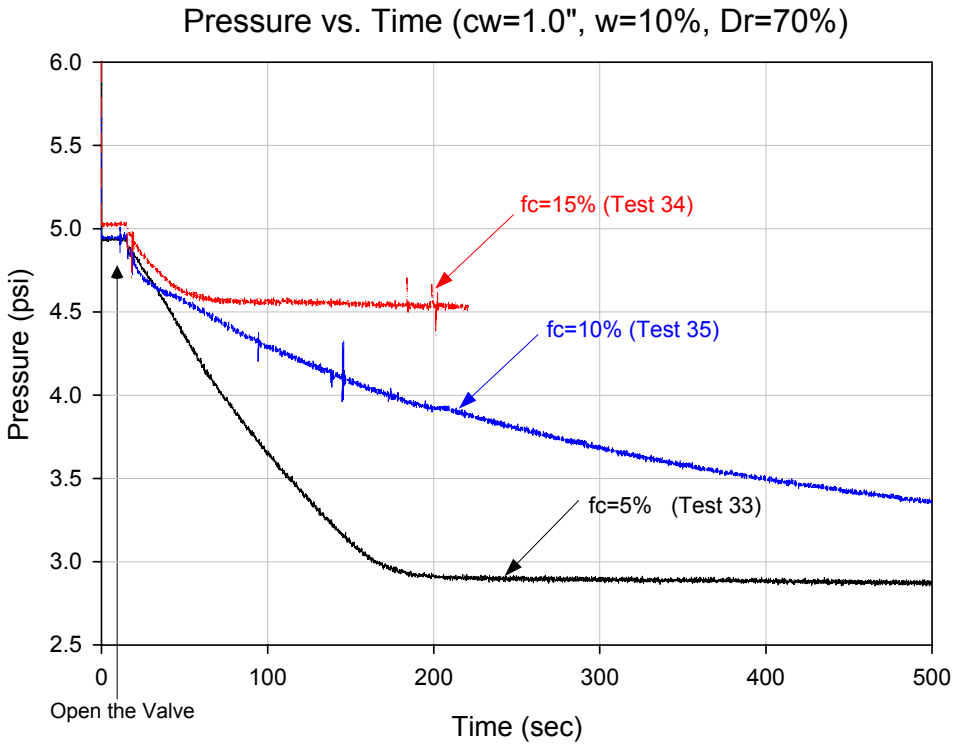

Figure 6.14 Pressure vs. Time (Test 33, 34, and 35)

6.6. Tests on Very Coarse Filters

Tests 36, 37 and 38 were performed on filters containing large particles. The gradations of these materials are shown in Figure 6.15. The materials used in Tests 36 and 37 were too coarse to satisfy Bureau of Reclamation filter criteria. The material used in Test 38 was at the coarsest boundary of Bureau filter criteria.

Figure 6.16 shows the Test 36 specimen before and during the test. The coarse material collapsed and filled the lower part of the crack when the filter test device was rotated into position for testing, and cloudy water filled the upper part of the crack. When the test was begun, the membrane expanded to fill most of the upper part of the crack. In Test 38 the membrane burst after about 200 seconds, and no more useful data could be obtained beyond that point in the test.

Although these coarse materials slumped and filled the crack, they all failed to perform as effective filters because of their excessively coarse gradations. The voids in these materials were so large that the Teton Dam base material was not restrained, and was washed through the voids of the "filter" materials. Even in Test 38, where the gradation was marginally acceptable, the effluent was cloudy throughout the test, and it appeared that erosion of the base continued at a steady rate until the test ended. The flow rates and pressure variations with time are shown in Figures 6.17 and 6.18. It can be seen that the results are very similar: The flow rates increase to maximum values and persisted, and the pressures dropped to nearly constant values.

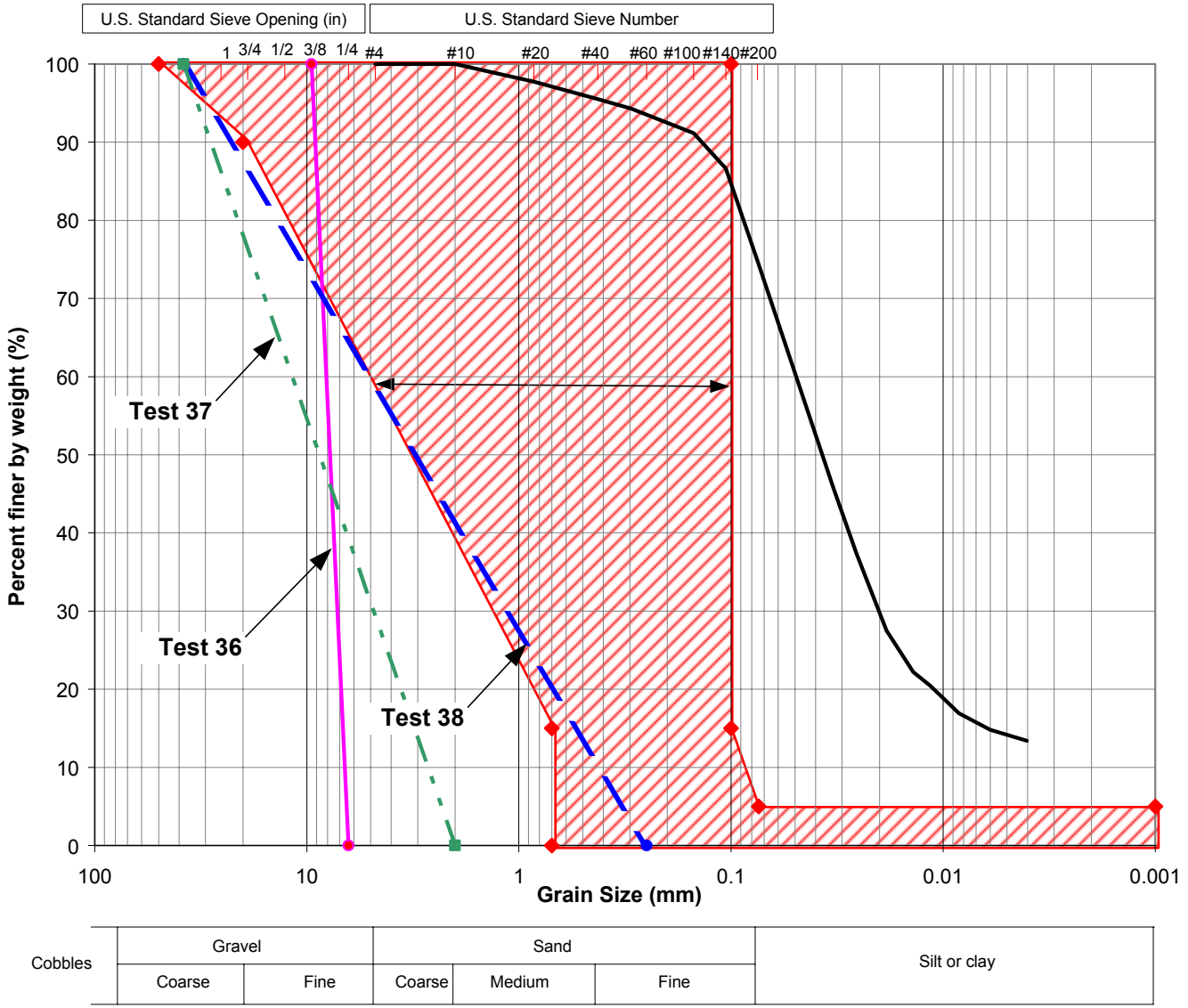

Figure 6.15 Gradation curves of Test 36, 37, and 38

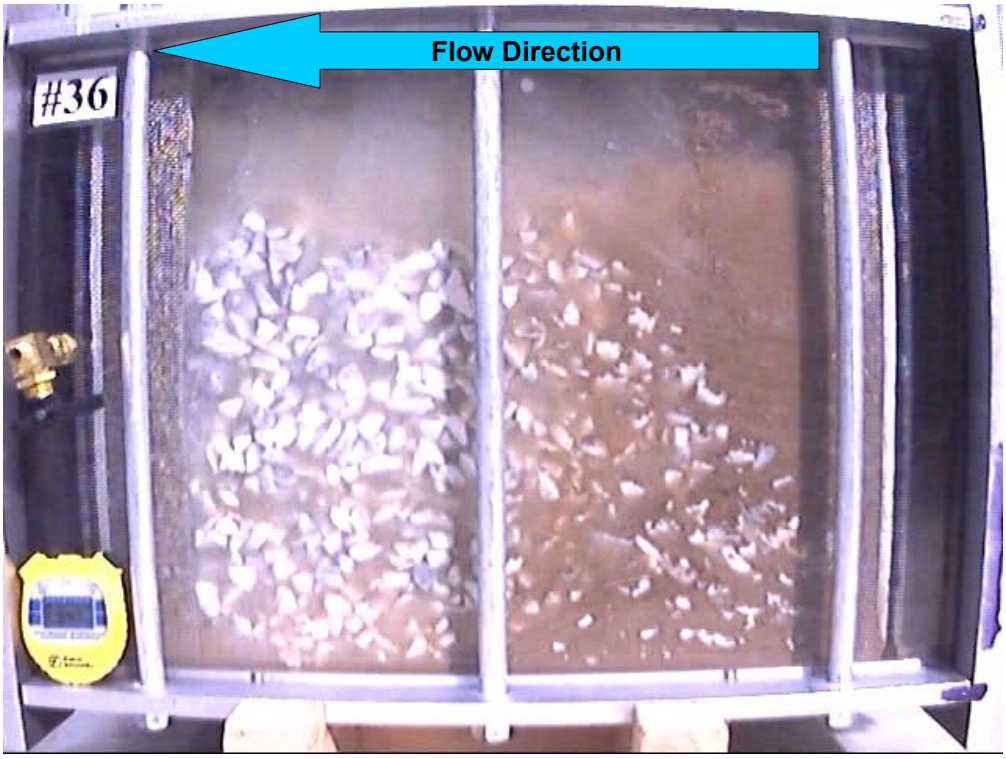

(a) Before the Test 36

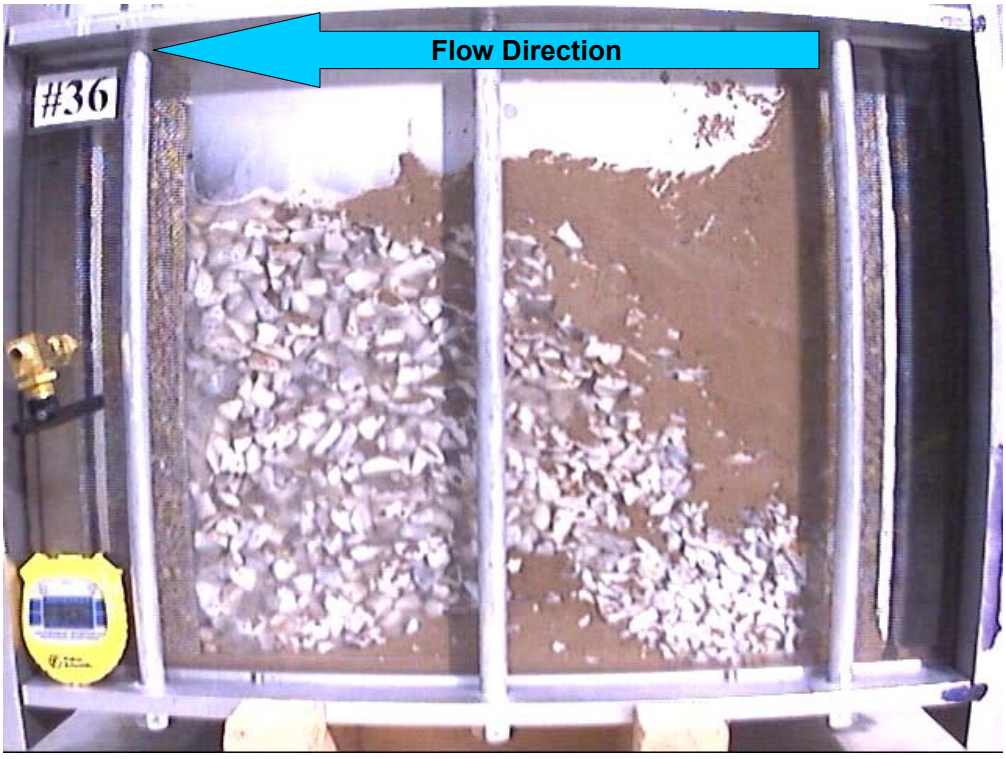

(a) During the Test 36

Figure 6.16 Test 36 (coarse filter material)

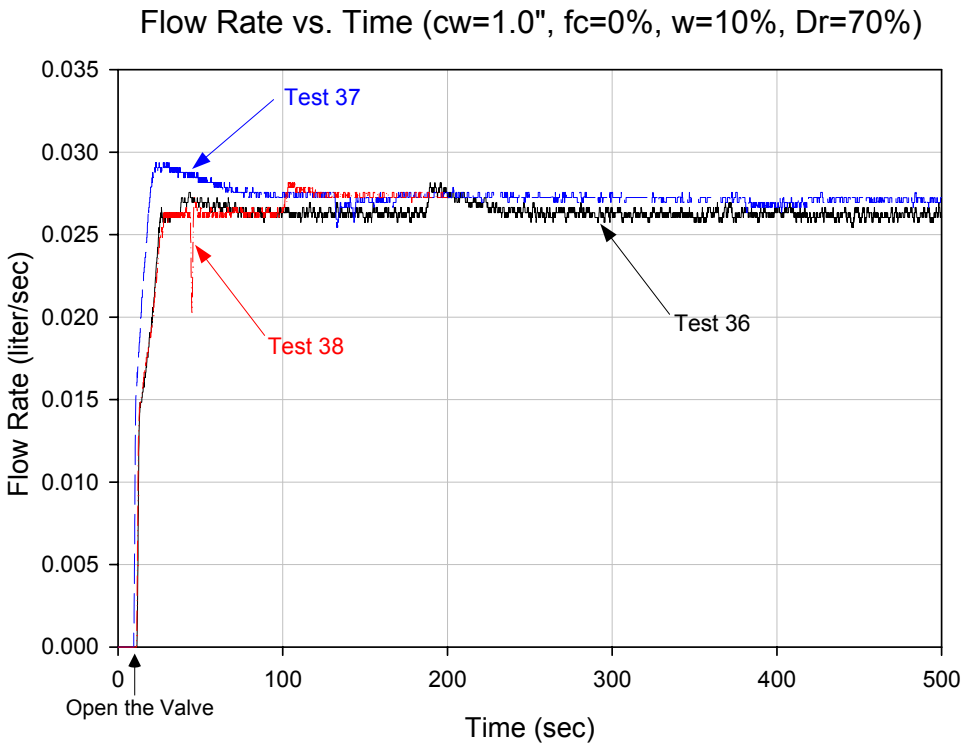

Figure 6.17 Flow rate vs. Time (Test 36, 37, and 38)

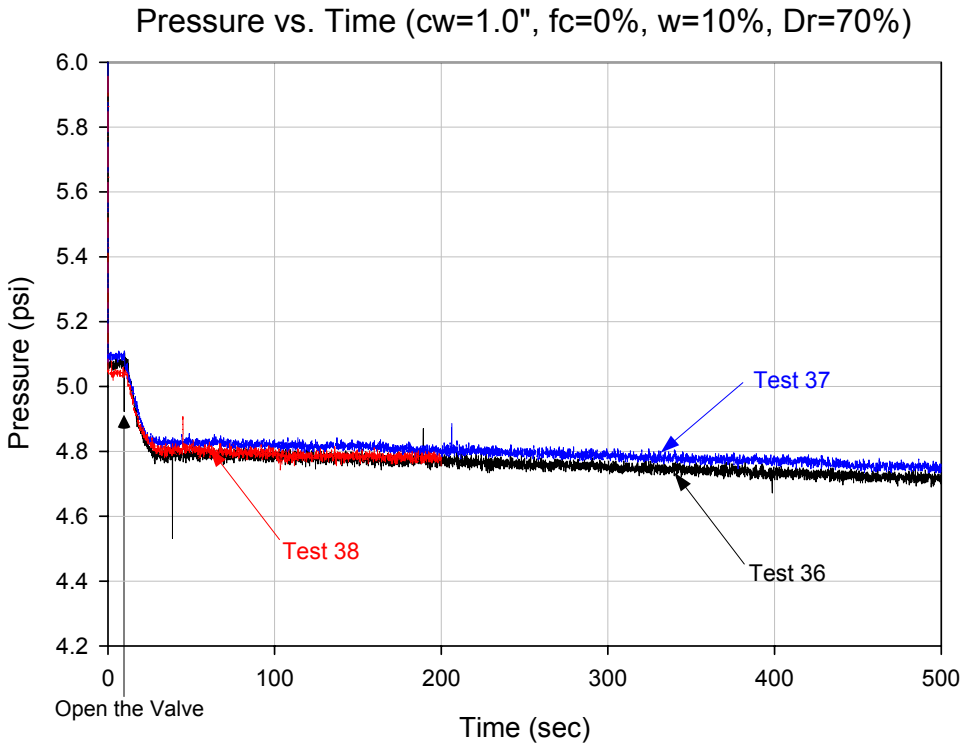

Figure 6.18 Pressure vs. Time (Test 36, 37, and 38)

6.7. Summary

The tests performed using the 12-inch square filter test device support these conclusions:

- The 12-inch device was found to be effective for testing specimens containing particles as large as 1.5 inches, with crack widths as large as 1.0 inch. The behavior observed in these tests was qualitatively the same as had been measured in the tests using the 4-inch diameter device, and showed that this behavior, involving collapse of the filter to fill cracks and clogging to stop erosion, applies to particle sizes and crack widths representative of field conditions.
- The pressure membrane incorporated in the 12-inch device was effective in simulating the effect of overburden pressure in the field, enhancing the tendency of the filter to collapse and fill the crack. Two tests on specimen with 1.0-inch cracks were terminated prematurely when the membranes burst. However, in other respects the membranes functioned as intended, and were effective in simulating the effect of overburden pressure in the field.
- A test performed in the 12-inch device using the VV condition (vertical crack, vertical flow), replicated the results achieved in the 4-inch device for this flow condition, demonstrating the fact that the results were not controlled by the size of the device, the particle size (for cohesionless materials), or the crack width.
- These tests were performed on specimens containing highly plastic fines (HPF) with the VH condition (vertical crack, horizontal flow). The crack widths in these tests were 1.0 inch, and the maximum particle size was 0.25 inches in all cases.

  The filter containing 5% HPF behaved the same as had filters with no fines – the filter collapsed (slumped) before flow was started, and clogging occurred quickly with clear effluent from the specimen.

  The filter containing 10% HPF did not collapse until flow began. Ultimately, however, collapse and clogging did occur, and the effluent became clear.

The filter containing 15% HPF also did not collapse until flow began. Even after collapse occurred, an un-collapsed flow channel remained which prevented clogging and effective filter action. The effluent never became clear, indicating that this material was not a reliable filter.

Chapter 7. Sand Castle Tests[3]

7.1. Background

To prevent continuous erosion through cracks, filter materials must satisfy two conditions. The first is that the gradation of the filter material falls within the proper gradation limits, detailed in previous chapters. The second is that the filter material must be capable of collapsing and filling a crack, should one develop. Vaughan and Soares (1982) noted that including fines in a filter to enable it to retain small clay particles may give it cohesion, thereby reducing its ability to collapse and fill cracks. They suggested a simple test to examine the ability of filter material & collapse using a compaction mold or a small bucket, like a child's toy used to build sand castle. The test is performed by placing a sample (the "sand castle") a shallow tray and the tray is flooded with water. A cohesionless material will collapse immediately, showing its ability to collapse and fill cracks. A sample with cohesion will not collapse, or will collapse only after a long period of time, indicating that it would not be suitable for use as a filter.

7.2. Description of device and test procedure

A sand castle test is performed by placing a compacted soil sample in water and observing it for some time. In the tests described in this chapter, the behavior of the samples was recorded using a digital camera. Figure 7.1 shows the test apparatus developed for the Sand Castle Tests described here. A plastic sheet was first inserted into a 261 ml plastic cup. The plastic sheet prevents the soil from adhering to the cup. The soil sample was then compacted in the cup using a hand compactor. The compacted sample was inverted over a wire mesh, and was lowered into a one gallon glass container filled with distilled water using the steel rod with hooks

[3] Sand Castle Test (SCT): The name of test was coined by Vaughan and Soares (1982)

at their ends. The condition of the sample was recorded using a digital camera, and a recording of the test was saved as a movie file. After the test, pictures at elapsed times of 0, 1, 2, 4, 8, 16, 32, and 64 minutes were extracted from the movie file for presentation.

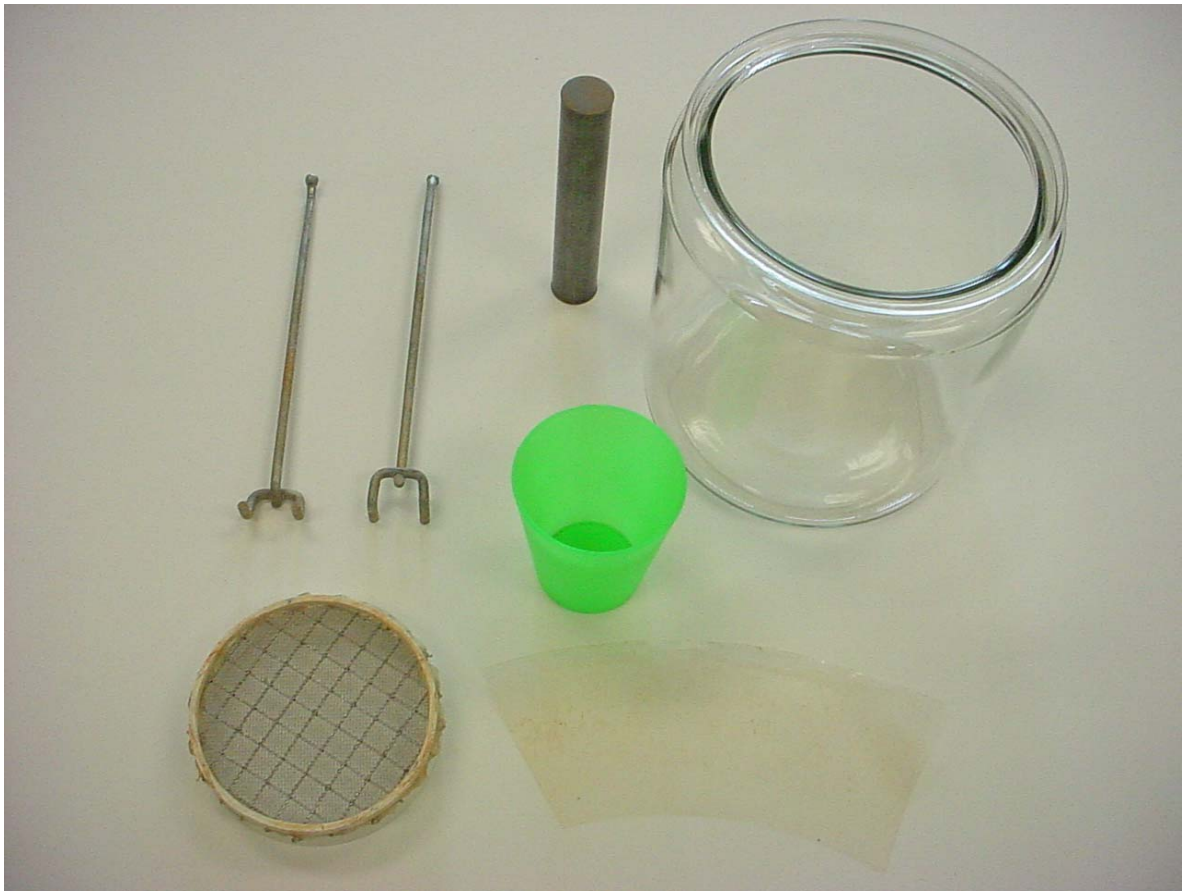

Figure 7.1 Devices for Sand Castle Test

Figure 7.2 shows the assembled apparatus ready for a sand castle test. White panels were placed behind the reservoir and in front of the camera to prevent glare during filming. The steel rod hooks were removed after the sample was placed under water. Time was measured by filming a digital clock. A description of the sample (test number, water content, fines content, types of fines, and sample weight) was posted on a card visible in the movie frame as shown in Figure 7.3.

Figure 7.2 Test configuration for Sand Castle Test

Figure 7.3 Front view of test setup

7.3. Test material

Sand castle tests were performed on the Horsetooth Dam filter material used in this research. The fine fraction of this material was separated from the coarse fraction by sieving through a #200 sieve. Samples were prepared for testing by mixing the coarse fraction of the Horsetooth Dam filter material with various percentages of highly plastic fines (HPF) or non-plastic fines (NPF). In this research, the plastic fines contents were 5%, 10% and 15%, and water contents were 5%, 7%, 10%, and 13%. All samples were stored for 24 hours in a plastic bag prior to testing. For highly plastic fines, CH material was used. The Liquid Limit was 72, the Plastic Limit was 32, resulting in a Plasticity Index of 40.

For tests with non-plastic fines, the original fines from the Horsetooth Dam filter material were remixed with the coarse fraction. This fine material cannot be rolled into a 1/8 inch thread at any water content; therefore it is classified as "non-plastic" by ASTM D2487. These non-plastic fines were combined with the coarse fraction to form test specimens having 15% fines.

Tests on samples containing highly plastic fines were conducted for various combinations of water and fines contents. Some samples containing non-plastic fines could not be tested because they slumped immediately after the samples were taken from mold, before immersion in water.

7.4. Test Results

As mentioned in the previous section, the Horsetooth Dam filter material was mixed to 5%, 10%, and 15% of HPF. For each fines content, water contents of 5%, 7%, 10%, and 13% were tested. Table 7.1 shows the results of tests at these four water contents with 5% HPF. The only test specimen which did not collapse completely in one minute or less was compacted at 13% water content.

Test results for the test specimens containing 10% HPF are shown in Table 7.2. The specimens formed at 5% and 7% water contents collapsed within 16 minutes. Test specimens compacted at higher water contents did not collapse in 64 minutes. This indicates that compaction water content is an important factor governing collapse behavior. This finding is substantiated by the results shown in Figure 7.4 and Figure 7.5.

Table 7.1 Sand Castle Test with 5% highly plastic fine

Time (min)	5% HPF, w=5%	5% HPF, w=7%	5% HPF, w=10%	5%HPF, w=13%
0				
1				
2	Complete collapse in 1 minute	Complete collapse in 1 minute	Complete collapse in 1 minute	
4				
8				
16				Complete collapse in 8 minute
32				
64				

Table 7.2 Sand Castle Test with 10% highly plastic fine

Time (min)	10% HPF, w=5%	10% HPF, w=7%	10% HPF, w=10%	10%HPF, w=13%
0				
1				
2	Complete collapse in 1 minute			
4				
8				
16				
32		Complete collapse in 16 minute		
64			Minor slumping after 64 minutes	Minor slumping after 64 minutes

Table 7.3 Sand Castle Test with 15% highly plastic fine

Time (min)	15% HPF, w=5%	15% HPF, w=7%	15% HPF, w=10%	15%HPF, w=13%
0				
1				
2	Complete collapse in 1 minute			
4				
8				
16		Complete collapse in 8 minute		
32				
64			Minor slumping after 64 minutes	Minor slumping after 64 minutes

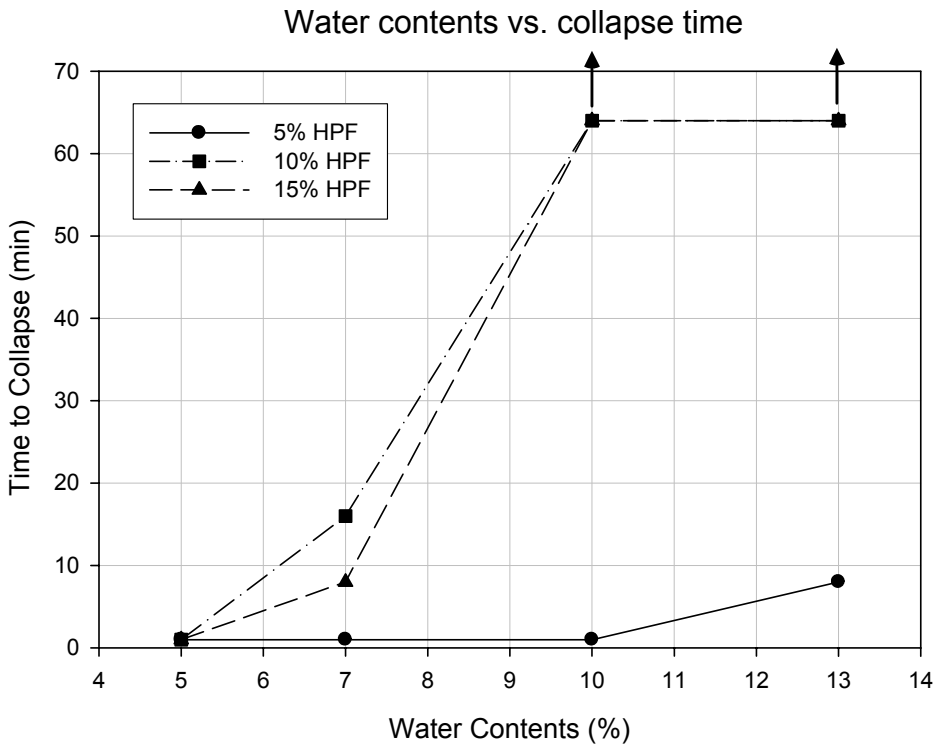

Figure 7.4 Water Contents vs. Time to Collapse from SCT

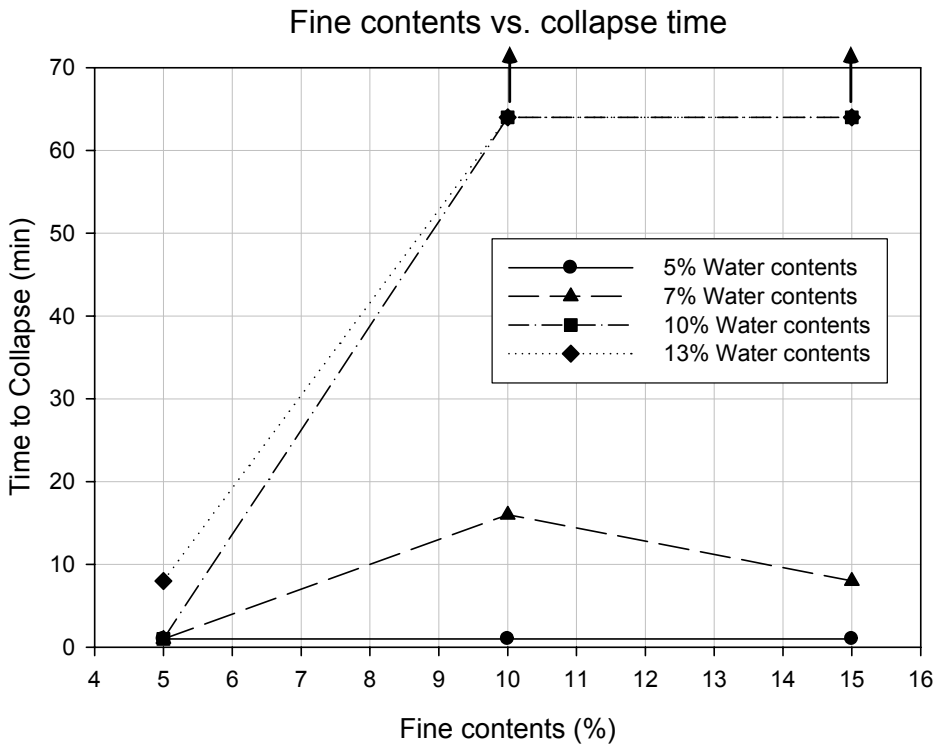

Figure 7.5 Fines Content vs. Time to Collapse from SCT

If a sample collapsed within one minute or less, it was described as "Collapsed Immediately." If sample collapsed after 1 to 64 minutes, it was described as "Collapsed in Time." If collapse did not occur within 64 minutes, "Did not collapse" was used to describe the result. Table 7.4 shows the results categorized in these terms.

All samples with non-plastic fines collapsed in less than one minute, even for 15% fines contents. Figure 7.6 shows the beginning of test 28. The sample has 15% NPF and 10% water content, as indicated by the test label. When the bottom of the sample touched the water, the clock indicated 3:53:26.

Figure 7.7 shows the test specimen 14 seconds later. The specimen immediately collapsed even before the sample base reached the bottom of tank. After 45 seconds, the sample was completely collapsed in Figure 7.8.

Since the test specimen with 15% NPF and 10% water content collapsed immediately, no more tests were performed on samples with non-plastic fines.

Table 7.4 Test results of HPF cases

		Water content (%)			
		5	7	10	13
Fine content (%)	5	Collapsed Immediately	Collapsed Immediately	Collapsed Immediately	Collapsed in Time
	10	Collapsed Immediately	Collapsed in Time	Did not collapse	Did not collapse
	15	Collapsed Immediately	Collapsed in Time	Did not collapse	Did not collapse

Figure 7.6 The beginning of Test 28 (w[4]=10%, fc[5]=15%, non-plastic fine)

Figure 7.7 Test 28 elapsed time of 14 seconds

[4] w: water content
[5] fc: fines content

Figure 7.8 Test 28 elapsed time of 45 seconds

7.5. Summary

The results of Sand Castle Tests are governed by:

- Plasticity of fines
- Fines content
- Compaction water content

Samples with non-plastic fines collapsed immediately, even when the fines content was as large as 15%. Some samples with highly plastic fines also collapsed immediately–samples with 5% HPF, and water contents less than 13% collapsed immediately.

All samples compacted at 5% water content also collapsed immediately, regardless of the percentage of highly plastic fines. Samples containing more than 5% highly plastic fines (which were compacted at water contents greater than 5%) did not collapse immediately.

Chapter 8. Summary, Conclusions and Recommendations for Further Research

8.1. Summary and Conclusions

This experimental study of the factors that control the behavior of filters in embankment dams involved development and use of three types of tests:

(1) Filter performance tests using a 4-inch diameter filter test device, with composite specimens containing a segment of base and a segment of filter. The specimens were formed with cracks as wide as 0.09 inches through both the base and the filter. The tests investigated the ability of the filter to slump, fill the crack, and prevent erosion of the base.

(2) Larger scale filter performance tests using a 12-inch square filter test device, also with composite specimens containing cracks. The cracks formed through the filter and the base in these specimens were as wide as 1.0 inch.

(3) "Sand Castle" tests, in which a compacted specimen of filter was immersed in water to investigate its tendency to slump when submerged successful filter must be capable of slumping and filling cracks to prevent erosion. These simple tests can be used to investigate this aspect of filter performance.

Tests were performed using the 4-inch diameter filter test devices to investigate the effects of the percentage of non-plastic fines in the filter (up to 15 percent), the effect of the crack widths (up to 0.09 inches), the effects of relative density in the range from 18% to 70%, and the effects of compaction water content in the filter ranging from 10% to 14%. In all of the tests performed over this range of variables the filter material successfully collapsed and retained the base material. Investigation of the effects of percent fines on the

crack- stopping ability of filters was the major objective of this research. A major finding of the tests performed using the 4-inch filter test device is the fact that filters with as much as 15% of non-plastic fines are sufficiently cohesionless to collapse and retain the base material in an initially cracked specimen.

The 12-inch device was found to be effective for testing specimens containing particles as large as 1.5 inches, with crack widths as large as 1.0 inch. The behavior observed in these tests was qualitatively the same as had been measured in the tests using the 4-inch diameter device, and showed that this behavior, involving collapse of the filter to fill cracks and clogging to stop erosion, applies to particle sizes and crack widths representative of field conditions. A pressure membrane incorporated in the 12-inch device was effective in simulating the effect of overburden pressure in the field, enhancing the tendency of a filter to collapse and fill a crack. Two tests on specimen with 1.0-inch cracks were terminated prematurely when the membranes burst. However, in other respects the membranes functioned as intended, and were effective in simulating the effect of overburden pressure in the field.

Tests in the 12-inch square filter test device were performed on specimens containing highly plastic fines (HPF). The crack widths in these tests were 1.0 inch, and the maximum particle size was 0.25 inches in all cases. The filter material with 5% HPF showed good filter performance, 10% showed marginal behavior, and 15% showed unacceptable results (the filter material could not stop continuous erosion). The limitation of 5% fines in current filter design criteria is appropriate, even if the fines are highly plastic.

The results of the Sand Castle tests were found to be governed by: percent fines, plasticity of fines, and compaction water content. Samples with non-plastic fines collapsed immediately, even when the fines content was as large as 15%. Samples containing more than 5% of highly plastic fines (which were compacted at water contents greater than 5%) did not collapse immediately. The Sand Castle tests proved to be useful for examining the collapse potential of candidate filters. The important factors that control the collapse potential of a filter can be varied, and a qualitative assessment of ability of the filter to collapse can be made quickly.

8.2. Recommendations for Further Research

The filter materials tested in this investigation contained inert particles that did not tend to cement or bond together when compacted. It would be of interest to continue these studies using materials such as limestone or dolomite, which may adhere during compaction, and thus be incapable of slumping to fill cracks.

Reference

Åberg, B. (1993). "Washout of Grains from Filtered Sand and Gravel Materials." Journal of Geotechnical Engineering, ASCE, Vol. 119, No. 1, 36–53.

Arulanandan, K. and Perry, E. B. (1983). "Erosion in Relation to Filter Design Criteria in Earth Dams." Journal of Geotechnical Engineering, ASCE, Vol. 109, No. 5, 682–698.

Arulanandan, K. (1978). "Erosion in Relation to Filter Design Criteria for Earth Dams." (Lecture Delivered at the Conference on "New Perspective on Dam Safety" Held at Stanford University, Aug. 29–31, 1978), University of California at Davis.

Arulanandan, K., Loganathan, P. and Krone, R. B. (1975). "Pore and Eroding Fluid Influences on Surface Erosion of Soil." Journal of Geotechnical Engineering Division, ASCE, Vol. 101, No. 1, 51–66.

American Society for Testing and Materials (ASTM). (1998). "Standard Test Method for Particle-Size Analysis of Soils." Annual Book of ASTM Standards, D422-63.

American Society for Testing and Materials (ASTM). (1998). "Standard Test Method for Laboratory Compaction Characteristics of Soils Using Standard Effort (12,400 ft-lbf/ft^3 (600 kN-m/m^3))." Annual Book of ASTM Standards, D698-91.

American Society for Testing and Materials (ASTM). (2002). "Standard Test Method for Specific Gravity of Soil Solids by Water Pycnometer." Annual Book of ASTM Standards, D854-02.

American Society for Testing and Materials (ASTM). (1998). "Standard Test Practice for Classification of Soils for Engineering Purpose (Unified Soil Classification System)." Annual Book of ASTM Standards, D2487-98.

American Society for Testing and Materials (ASTM). (2000). "Standard Test Method for Maximum Index Density and Unit Weight of Soils Using a Vibratory Table." Annual Book of ASTM Standards, D4253-00.

American Society for Testing and Materials (ASTM). (2000). "Standard Test Method for Minimum Index Density and Unit Weight of Soils and Calculation of Relative Density." Annual Book of ASTM Standards, D4254-00

American Society for Testing and Materials (ASTM). (2000). "Standard Test Method for Liquid Limit, Plastic Limit, and Plasticity Index of Soils." Annual Book of ASTM Standards, D4318-00.

American Society for Testing and Materials (ASTM). (1997). "Standard Test Method for Measurement of Hydraulic Conductivity of Saturated Porous Materials Using a Flexible Wall Permeameter." Annual Book of ASTM Standards, D5084-90.

Bertram, G. E. (1940). "An Experimental Investigation of Protective Filters." Harvard Soil Mechanics Series No. 7, Graduate School of Engineering Harvard University, Cambridge, MA.

Chapuis, R. P. (1992). "Similarity of Internal Stability Criteria for Granular Soils." Canadian Geotechnical Journal 29, 711–713.

Das Neves, E. M. (1989). "Analysis of Crack Erosion in Dam Cores: The Crack Erosion Test." De Mello Volume: a tribute to Prof. Dr. Victor F.B. de Mello, Sao Paulo, Brazil, 284–298.

Fenton, G. A., and Griffiths, D. V. (1997). "Extreme Hydraulic Gradient Statistics in Stochastic Earth Dam." Journal of Geotechnical and Geoenvironmental Engineering, ASCE, Vol. 123, No. 11, 995–1000.

Foster, M. and Fell, R. (2000). "Use of Event Trees to Estimate the Probability of Failure of Embankment Dams by Internal Erosion and Piping." Twentieth International Congress on Large Dams, 19-22 September 2000, Beijing-China, 237–258.

Foster, M. and Fell, R. (2001) "Assessing Embankment Dam Filters that Do Not Satisfy Design Criteria." Journal of Geotechnical and Geoenvironmental Engineering, Vol. 127, No. 5, 398–407.

Goldsworthy, M. H. (1990) "Filter Tests—Direct or Indirect?" Géotechnique 40, No. 2, 281–284.

Hillis, S. F. and Truscott, E. G. (1983). "Magat Dams: Design of Internal Filters and Drains." Canadian Geotechnical Journal 20, 491–501.

Honjo, Y. and Veneziano D. (1989) "Improved Filter Criterion for Cohesionless Soils." Journal of Geotechnical Engineering, Vol. 115, No. 1, 75–94.

Hsu, S.J.C. (1981) "Aspects of Piping Resistance to Seepage in Clayey Soils." International Conference on Soil Mechanics and Foundation Engineering, Stockholm, Vol. 10(1), 421–428.

Hurcomb, D. (2001). "Petrographic Examination of Exhumed Filter Sand – Horsetooth Dam Modifications – Colorado-Big Thompson Project." Colorado, U.S. Department of the Interior Bureau of Reclamation memorandum, Earth Sciences and Research Laboratory Referral No. 8340-01-36.

Hurley, H. W., and Newton, C. T. (1940). "An Investigation to Determine the Practical Application of Natural Bank Gravel as a Protective Filter." Massachusetts Institute of Technology.

Indraratna, B. and Radampola, S. (2002). "Analysis of Critical Hydraulic Gradient for Particle Movement in Filtration." Journal of Geotechnical and Geoenvironmental Engineering, Vol. 128, No. 4, 347–350.

Indraratna, B., Vafai, F., and Haque, M. A. (1996). "Laboratory and Analytical Modeling of granular filters." Australia - New Zealand Conference on Geomechanics, 7(1), 80–85.

Kenney, T. C., Chahal, R., Chiu, E., Ofoegbu, G. l., Omange, G. N., and Ume, C. A. (1985) "Controlling Constriction Sizes of Granular Filters." Canadian Geotechnical Journal 22, 32–34.

Kenney, T. C. and Lau D. (1985) "Internal Stability of Granular filters." Canadian Geotechnical Journal 22, 215–225.

Khor, C. H. and Woo, H. K. (1989) "Investigation of Crushed Rock Filters for Dam Embankment." Journal of Geotechnical Engineering, ASCE, Vol. 115, No. 3, 399–412.

Lafleur, J. (1984). "Filter Testing of Broadly Graded Cohesionless Tills." Canadian Geotechnical Journal 21, 634–643.

Leonards, G. A., Huang, A. B., and Ramos, J. (1991) "Piping and Erosion Tests at Conner Run Dam." Journal of Geotechnical Engineering, ASCE, Vol. 117, No. 1, 108–117.

Locke, M. & Indraratna, B., and Adikari, G. (2000) "Erosion and Filtration of Cohesive Soils." Filters and Drainage in Geotechnical and Environmental Engineering (ISBN: 90 5809 146 5) / GeoFilters 2000, 175–182.

Low III, J. (1988) "Seepage Analysis, Advanced Dam Engineering for Design, Construction, and Rehabilitation." Edited by Jansen, R. B., New York: Van Nostrand Reinhold, 217–275.

McCook, D. K., and Talbot, J. (1995) "NRCS Filter Design Criteria – A Step by Step Approach." Association of State Dam Safety Officials Conference (12th, 1995; Atlanta, GA.), 49–58.

Ramos, F. D. and Locke, M. (2000) "Design of Granular Filters: Guidelines and Recommendations for Laboratory Testing." Filters and Drainage in Geotechnical and Environmental Engineering (ISBN: 90 5809 146 5) / GeoFilters 2000, 115–122.

Reddi, L. N., Ming, X., Hajra, M. G., and Lee I. M. (2000) "Permeability Reduction of Soil Filters Due to Physical Clogging." Journal of Geotechnical and Geoenvironmental Engineering, ASCE, Vol. 126, No. 3, 236–246.

Pinto, P.S.SÊCO E., and Santana, T. (1989) "Filters for Clay Cores of Embankment Dams." International Conference on Soil Mechanics and Foundation Engineering, Vol. 12(3), 1689–1692.

Sherard, J. L. (1979) "Sinkholes in Dams of Coarse, Broadly Graded Soils." Thirteenth International Congress on Large Dams, New Delhi, Vol. 2, 25–35.

Sherard, J. L. (1984) "Trends and Debatable Aspects in Embankment Dam Engineering." Water Power and Dam Construction, Vol. 36, No. 12, 26–32.

Sherard, J. L., Dunnigan, L. P., and Talbot, J. R. (1984a) "Basic Properties of Sand and Gravel Filters." Journal of Geotechnical Engineering, ASCE, Vol. 110, No. 6, 684–700.

Sherard, J. L., Dunnigan, L. P., and Talbot, J. R. (1984b) "Filters for Silts and Clays." Journal of Geotechnical Engineering., ASCE, Vol. 110, No. 6, 701–718.

Sherard, J. L. and Dunnigan, L. P. (1985) "Filters and Leakage Control in Embankment Dams." Proceedings, Symposium on Seepage and Leakage from Dams and Impoundments, Edit by Volpe, R. L. and Kelly, W. E., ASCE, 1–30.

Sherard, J. L. and Dunnigan, L. P. (1989) "Critical Filters for Impervious Soils." Journal of Geotechnical Engineering., ASCE, Vol. 115, No. 7, 546–566.

Talbot, J. R. and Deal, C. E. (1993) "Rehabilitation of Cracked Embankment Dams." Geotechnical Special Publication 35, ASCE, 267–283.

Terzaghi, K. (1922). "Der Grundguch an Stauwerken und seine Verhütung." (The failure of dams by piping and its prevention.), Die Wasserkraft, Vol. 17, 445–449

Terzaghi, K., Peck, R.B., and Mesri, G. (1996) "Soil Mechanics in Engineering Practice." 3rd Edition, Wiley, New York.

Townsend, F. C., Shiau, J. M., and Pietrus, T. J. (1987) "Piping Susceptibility and Filter Criteria for Sand." Engineering Aspects of Soil Erosion, Dispersive Clays and Loess, Geotechnical Special Publication 10, ASCE, 46–66.

U.S. Army Corps of Engineers. (1996). "Engineering and Design: Seepage Analysis and Control for Dams." EM 1110-2-1901, Department of the Army, Corps of Engineers, Office of the Chief of Engineers, Washington, D.C.

U.S. Army Corps of Engineers, WES. (1953). "Filter Experiments and Design Criteria." Technical Memo No. 3-360, Vicksburg, MS.

U. S. Department of the Interior Bureau of Reclamation. (1994). "Design Standards No. 13: Embankment Dams." Chapter 5 – Protective Filters, United States Department of the Interior Bureau of Reclamation, Technical Service Center, Denver, CO.

U. S. Department of the Interior Bureau of Reclamation. (1998). "Earth Manual – Part 1, 3rd edition." Earth Science and Research Laboratory Geotechnical Research, U.S. Department of the Interior Bureau of Reclamation, Denver, CO.

USCOLD. (1992). "Observed Performance of Dams during Earthquakes." Prepared by USCOLD Committee on Earthquakes, U. S. Committee on Large Dams, Denver, July, 1992.

Vaughan, P. R. and Soares, H. F. (1982) "Design of Filters for Clay Cores of Dams." Journal of Geotechnical Engineering Division, ASCE, Vol. 108, No. 1, 17–31.

Vaughan, P. R. (1978) "Design of Filters for the Protection of Cracked Dam Cores against Internal Erosion." ASCE Convention & Exposition (Chicago, Oct. 16–20, 1978).

Appendix A. The 4-inch Filter Test Device

A.1.Device Assembly and Sample Preparations

The procedure used to assemble the device and prepare the specimen for testing is shown in this appendix. The figure labeled Step 1 shows the aluminum base that forms the shell of the first filter device. Step 2 shows the shell with threaded rods inserted, and Step 3 shows the side panel bolted to the aluminum base to complete the first filter device. The void forming plate is attached to the aluminum side panel but is inside and not visible in Step 3. Step 4 shows addition of the compaction spacer to the end of the first filter device. Step 5 shows the bottom plate in place. Step 6 shows the assembly rods which will secure the top plate to the first filter device during compaction. Step 7 shows the location pins used to position the top plate, and Step 8 shows the top plate bolted in place. Step 9 shows the assembly rotated upright and ready to receive the specimen for compaction. Step 10 shows a cross section through the device ready for compaction.

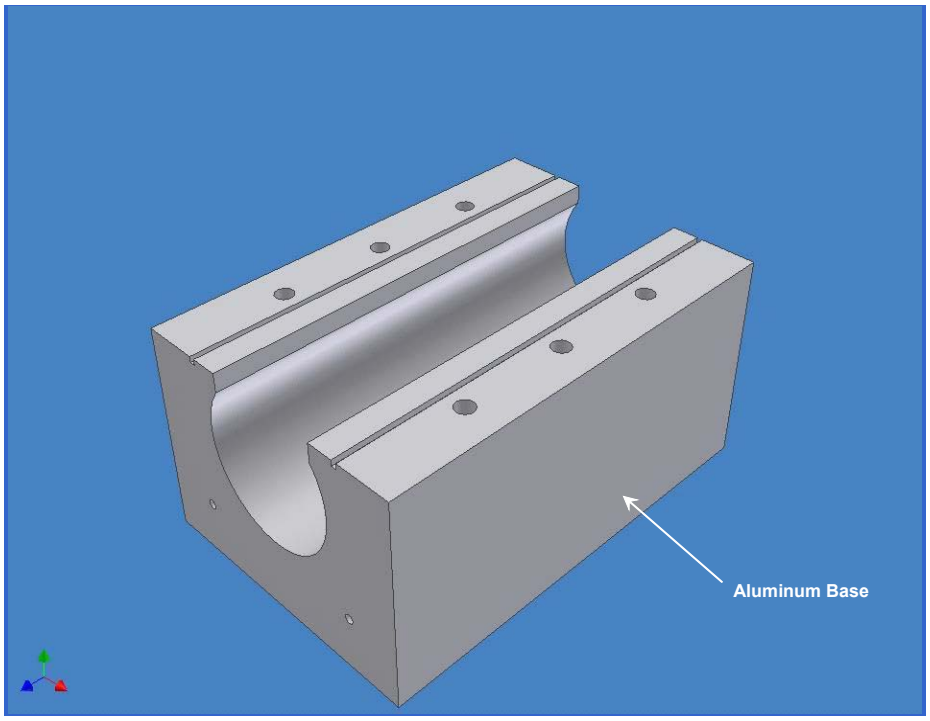

Figure A.1 Step 1 (aluminum base)

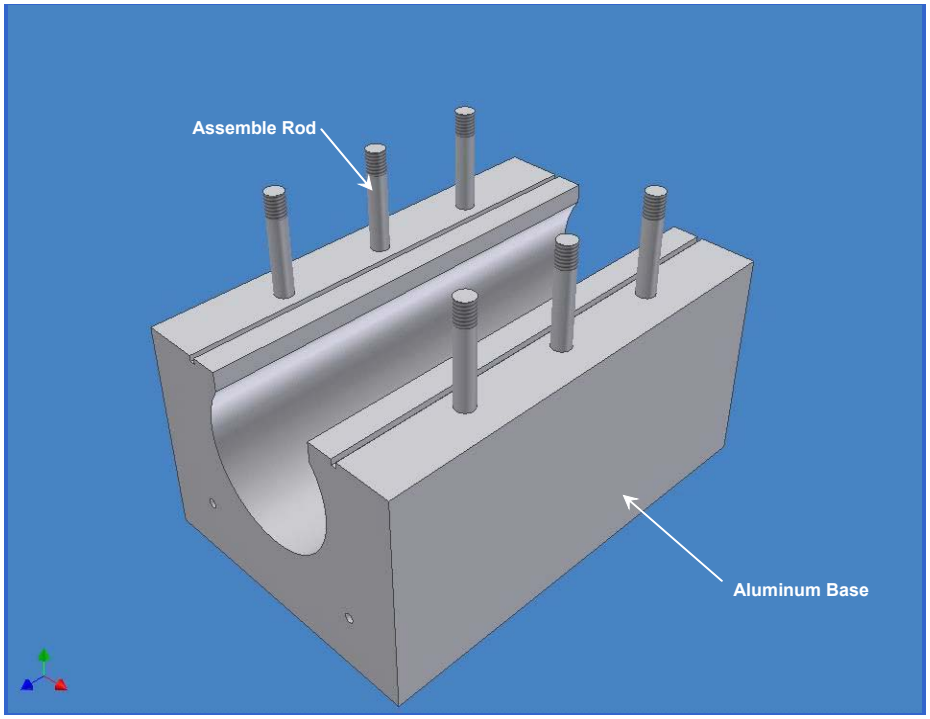

Figure A.2 Step 2 (install assembly rods)

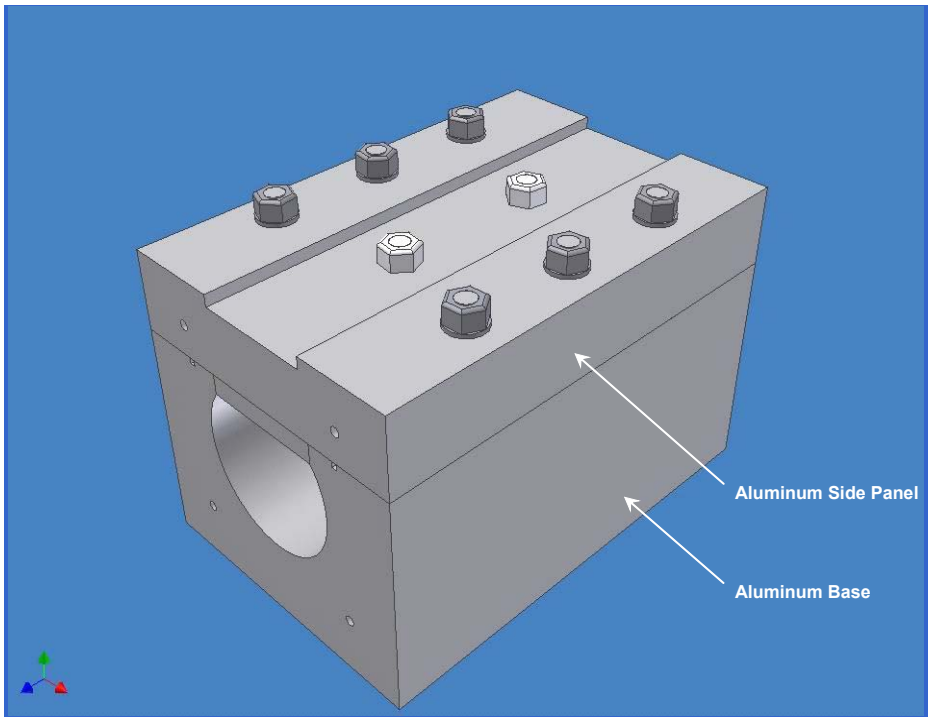

Figure A.3 Step 3 (install aluminum side compaction panel)

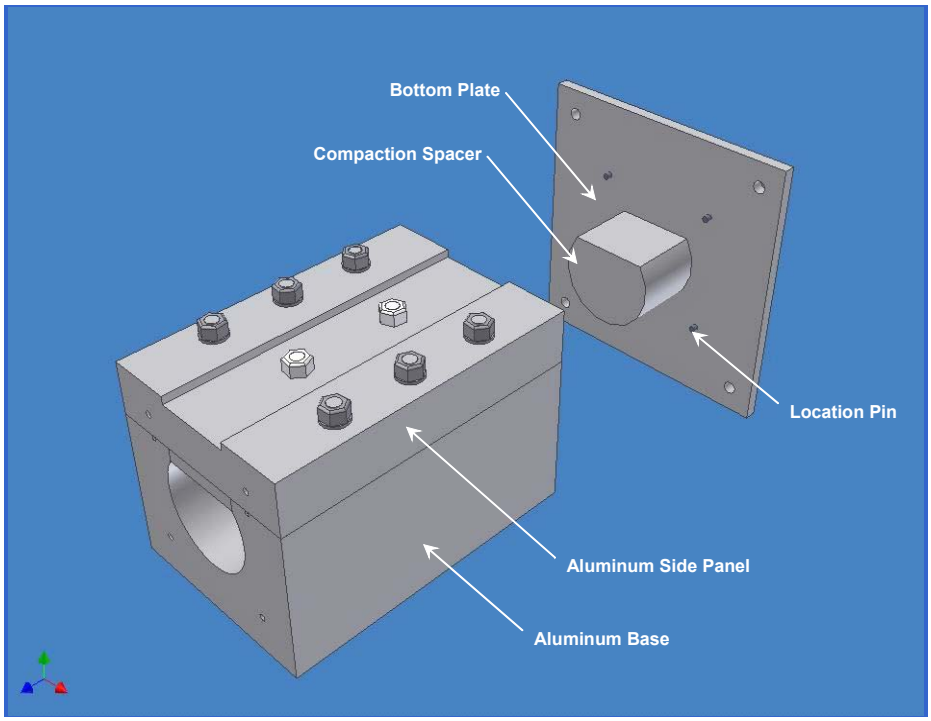

Figure A.4 Step 4 (place the compaction spacer and bottom plate)

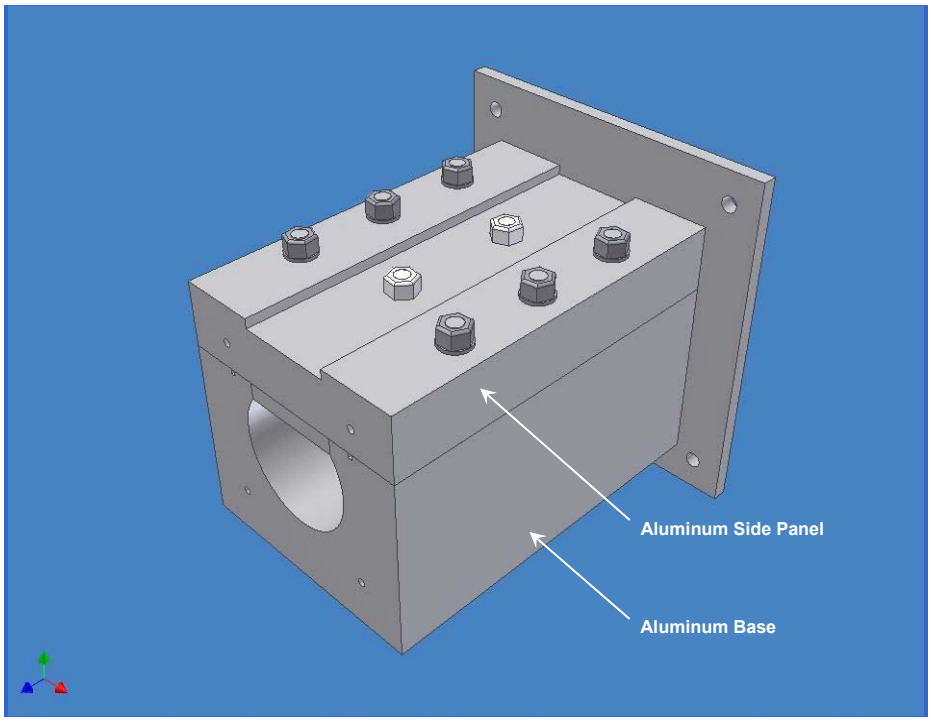

Figure A.5 Step 5 (locate the bottom panel)

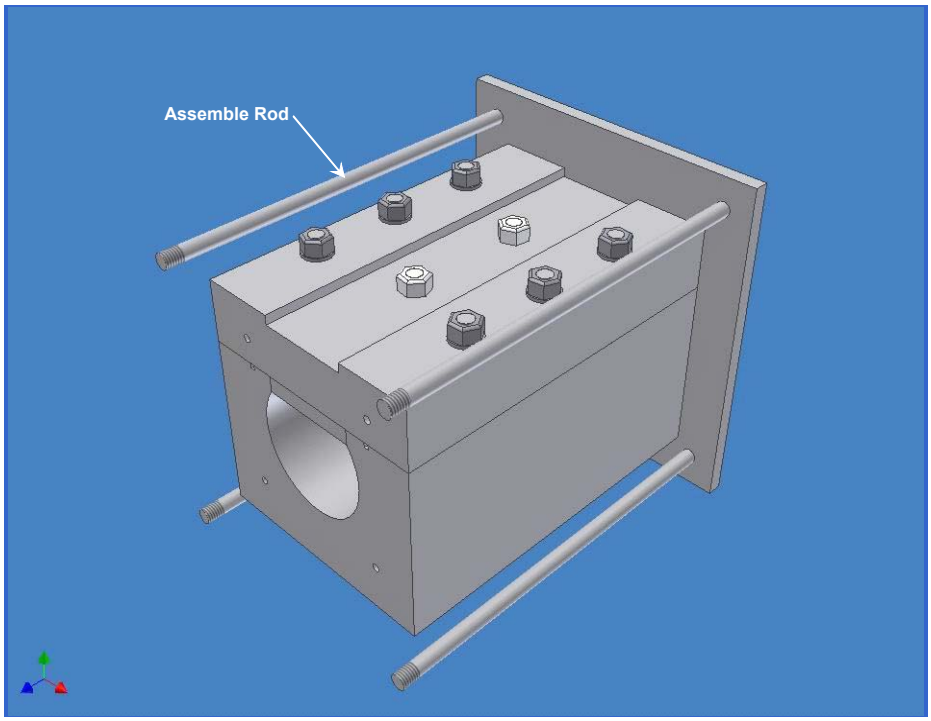

Figure A.6 Step 6 (install assembly rods)

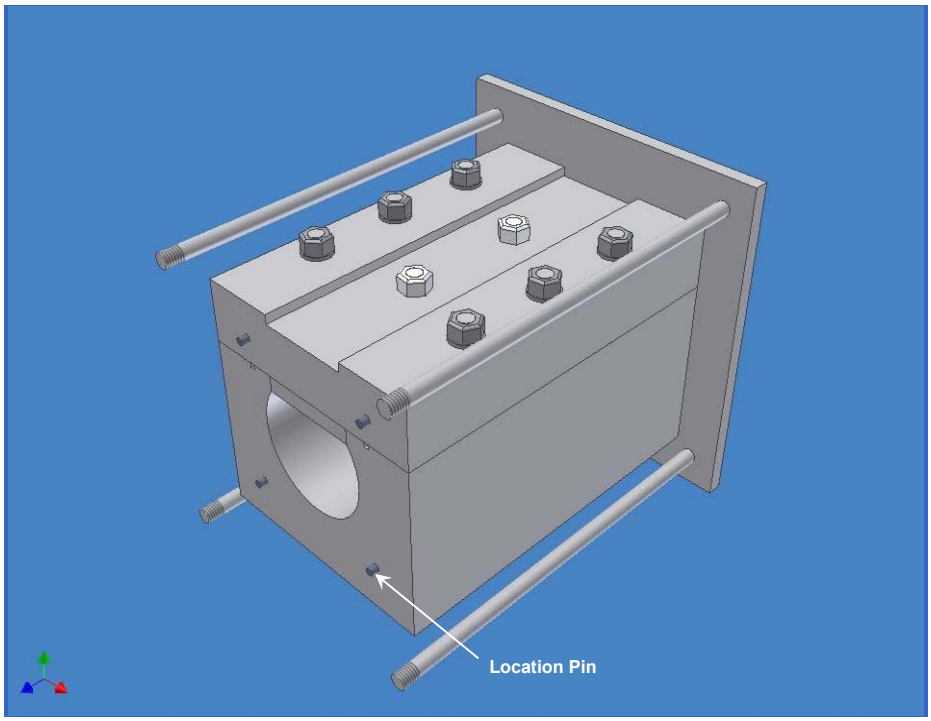

Figure A.7 Step 7 (install the location pins)

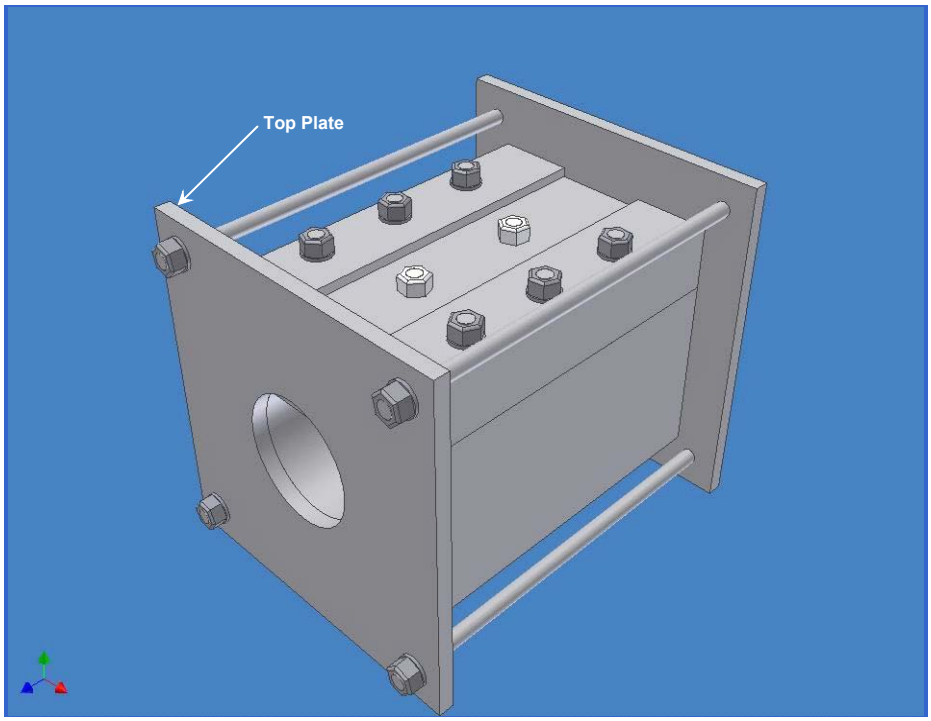

Figure A.8 Step 8 (install the top plate)

Figure A.9 Step 9 (ready to compact)

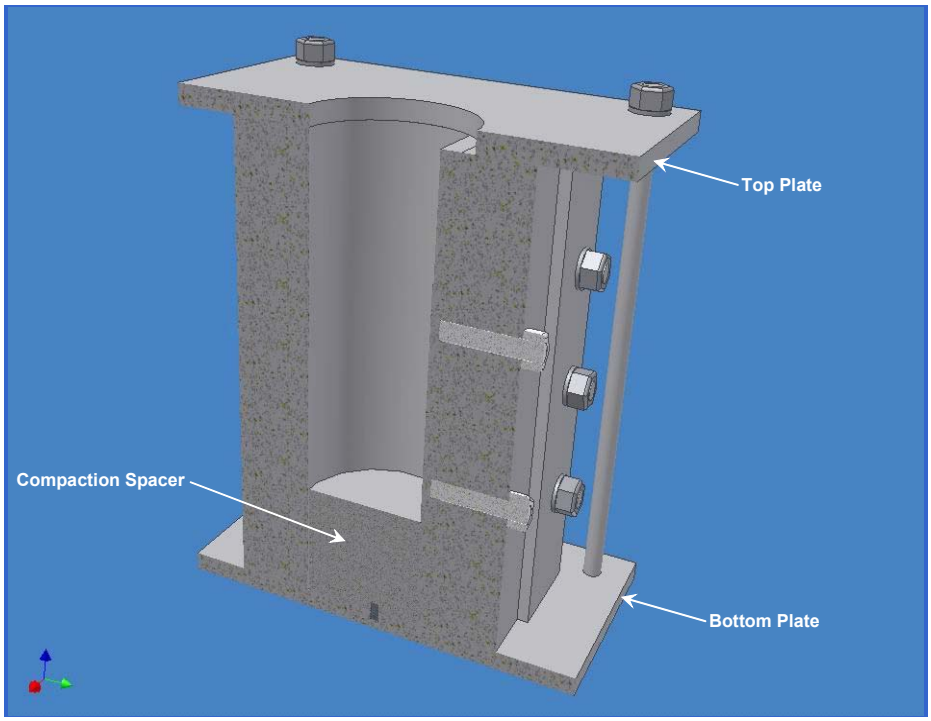

Figure A.10 Step 10 (cross section to compact)

Step 11 shows a photograph of a specimen being compacted in the device using the Standard Proctor compaction hammer. Step 12 shows a cross section through the device with the base material having been compacted on the compaction spacer, and Step 13 shows the filter material compacted on top of the base. Step 14 shows the pea gravel compacted on top of the filter material and step 15 shows the addition of the porous plate that retains the pea gravel. Step 16 shows the spring that was used to apply pressure to the porous plate and keep it snug against the pea gravel.

In Step 17, the top plate used during compaction is removed and replaced, as shown in Step 18, with a different top plate used during testing. This top plate has a smaller hole for attachment of the tubing used to flow water through the specimen. Step 19 shows the apparatus and the specimen rotated 180 degrees, upside down from the previous picture, and ready for assembly of the remainder of the specimen.

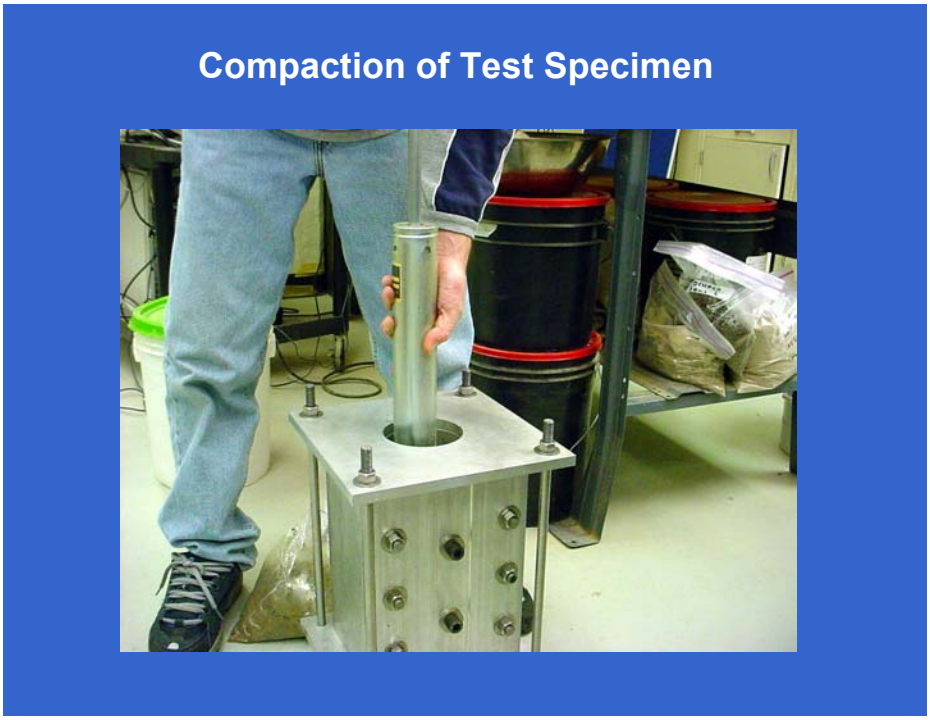

Figure A.11 Step 11 (compaction of test specimen)

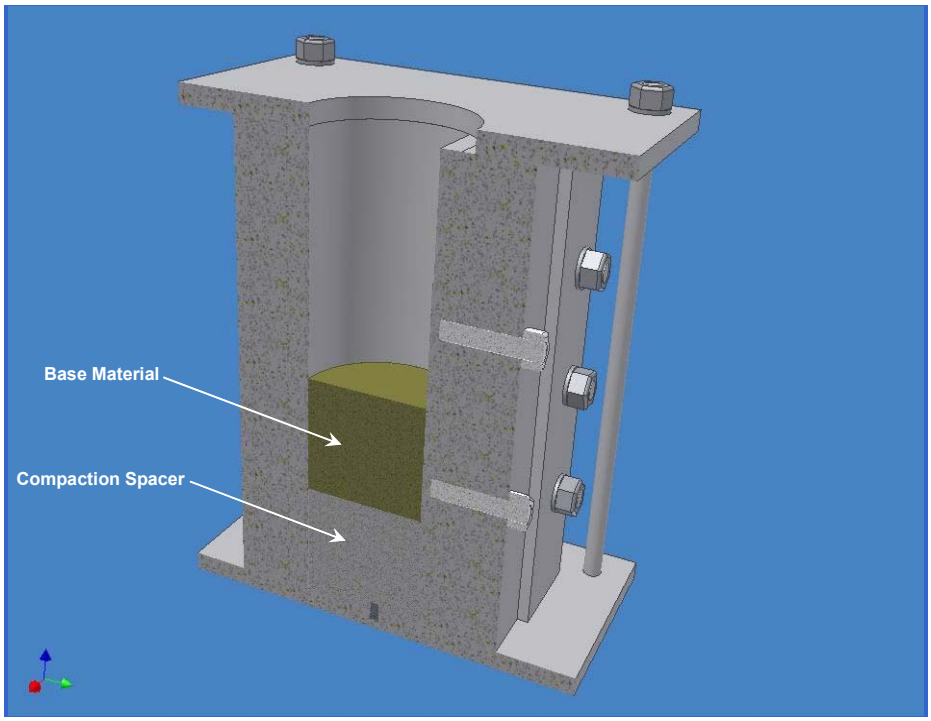

Figure A.12 Step 12 (compact base material)

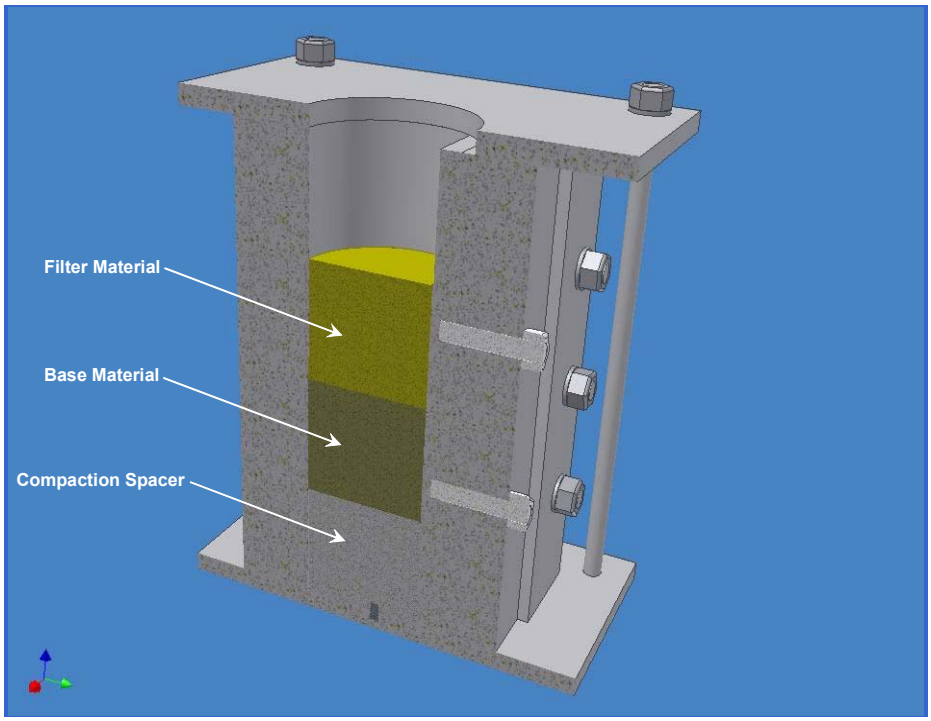

Figure A.13 Step 13 (compact filter material)

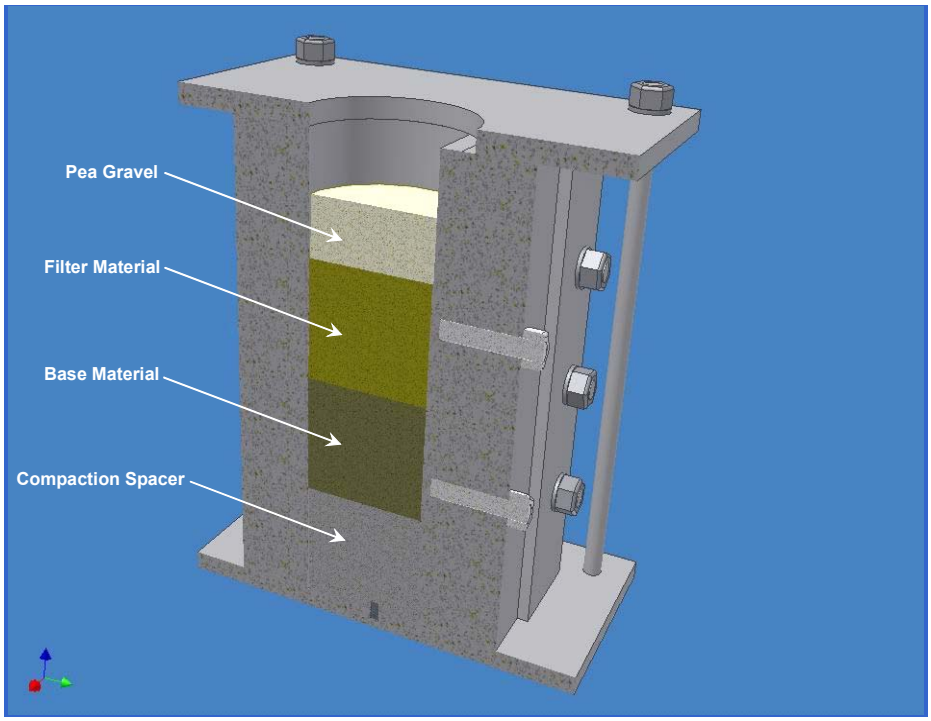

Figure A.14 Step 14 (compact pea gravel)

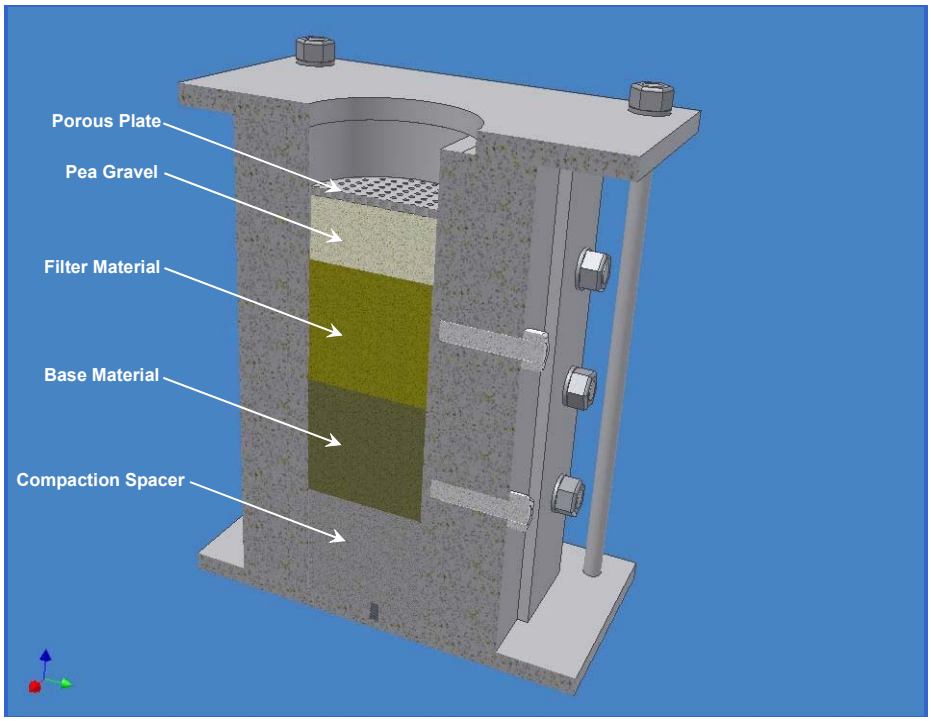

Figure A.15 Step 15 (install porous plate)

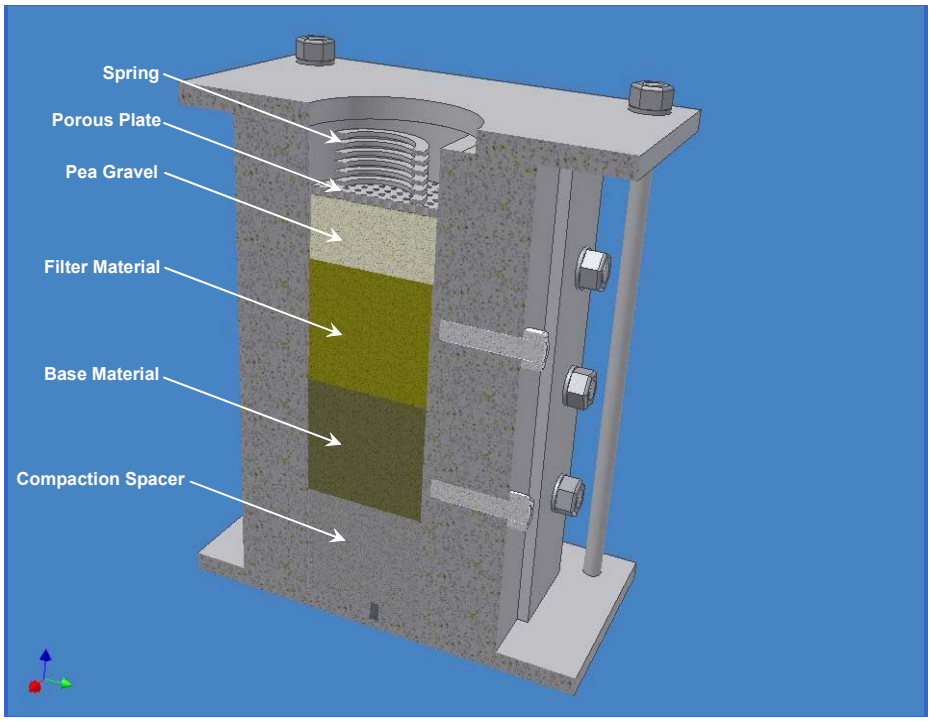

Figure A.16 Step 16 (install spring)

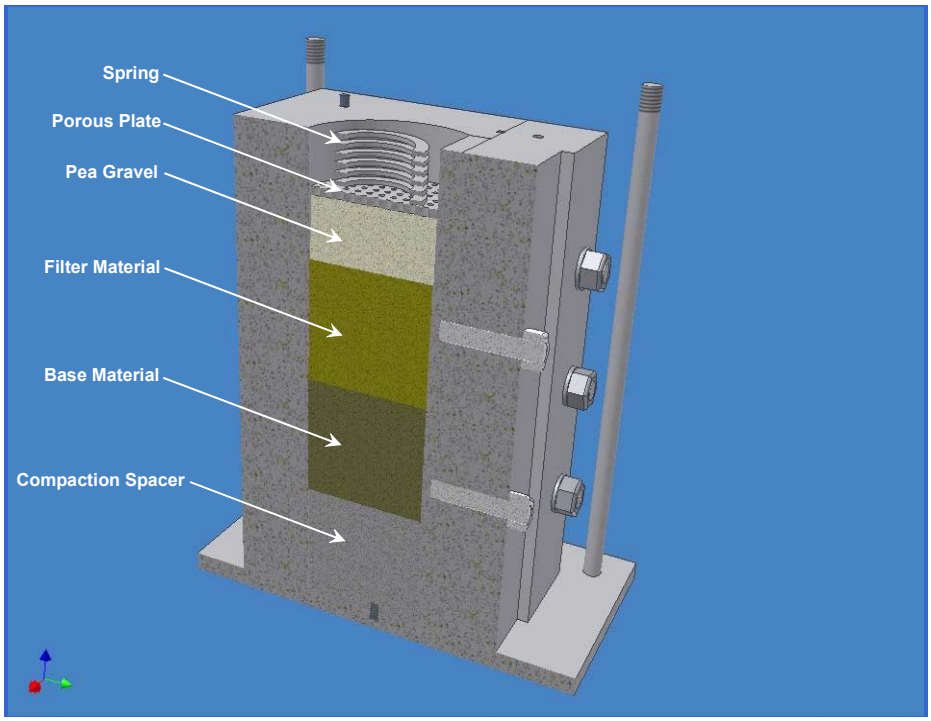

Figure A.17 Step 17 (remove the top plate)

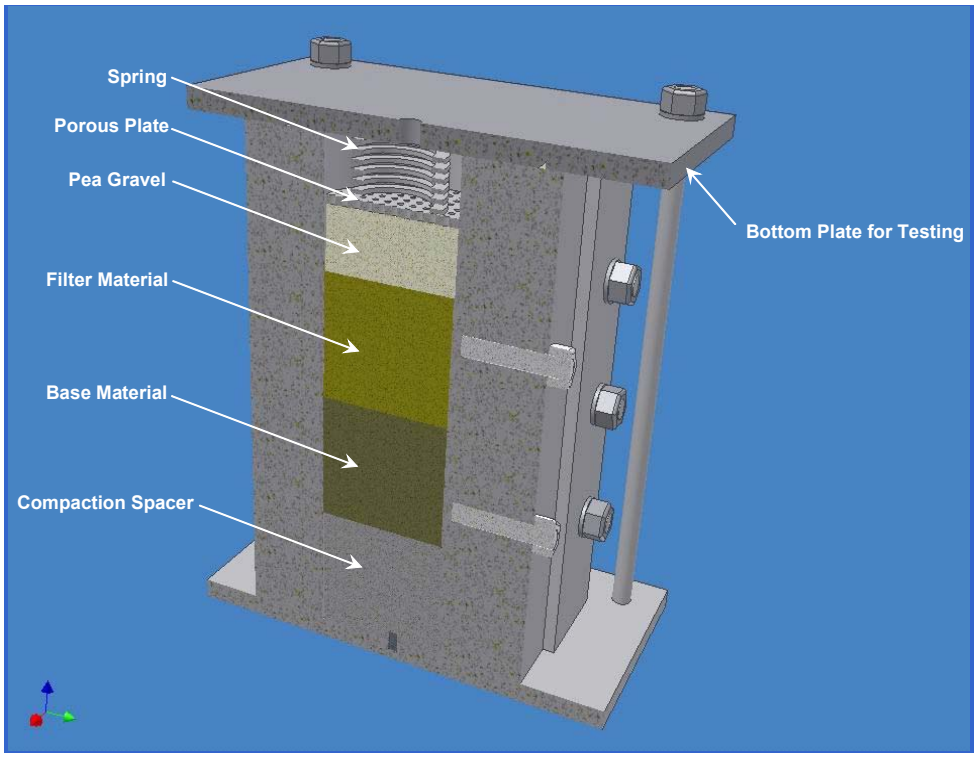

Figure A.18 Step 18 (assemble the bottom plate for testing)

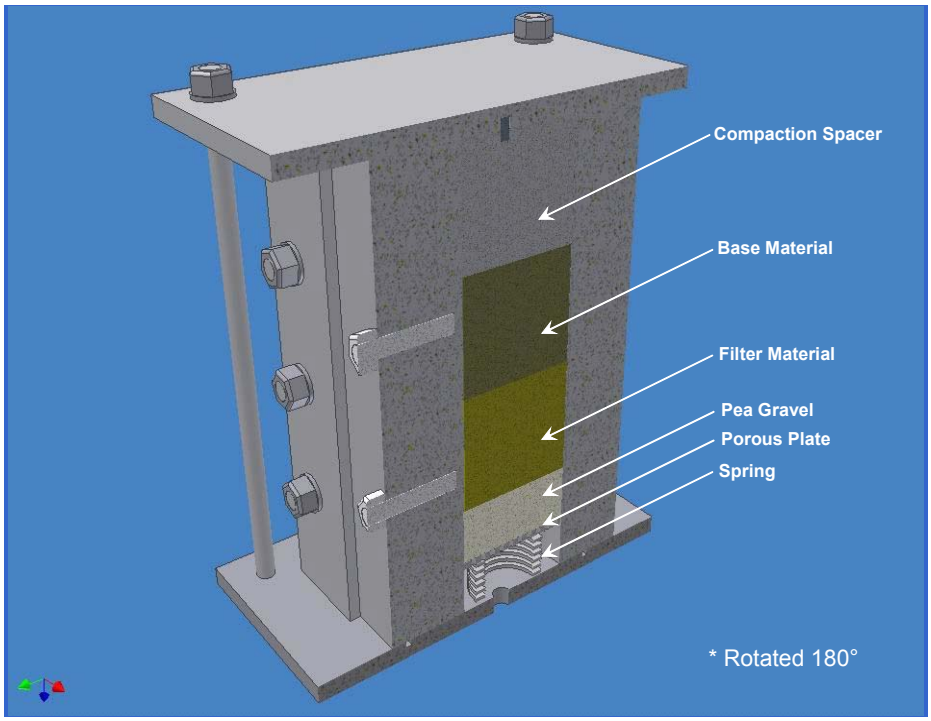

Figure A.19 Step 19 (rotate 180 degree)

Step 20 shows the plate removed from what is now the upper end of the specimen and the compaction spacer still in place. In Step 21 the compaction spacer has been removed and in Step 22 pea gravel has been compacted against the base coarse material. In Step 23, a porous plate has been placed on top of the compacted pea gravel, and in Step 24 a spring has been placed on top of the porous plate to keep it in snug contact with the underlying pea gravel.

In Step 25, an end plate called the top plate for testing has been bolted onto the device using the tie rods. Step 26 shows the apparatus rotated through 90 degrees and Step 27 shows the side plate used during compaction having been removed. The void that was formed by the spacer plate during compaction is revealed when this side plate is removed. In Step 28 the side plate used during compaction has been replaced by a Lucite side panel. The purpose of this Lucite panel is to make it possible to monitor the progress of erosion and clogging during the test. Step shows the Lucite panel bolted into place and ready for testing. Step 30 shows the composite specimen after compaction and assembly, with the specimen rotated so that the crack plane (void plane) is vertical.

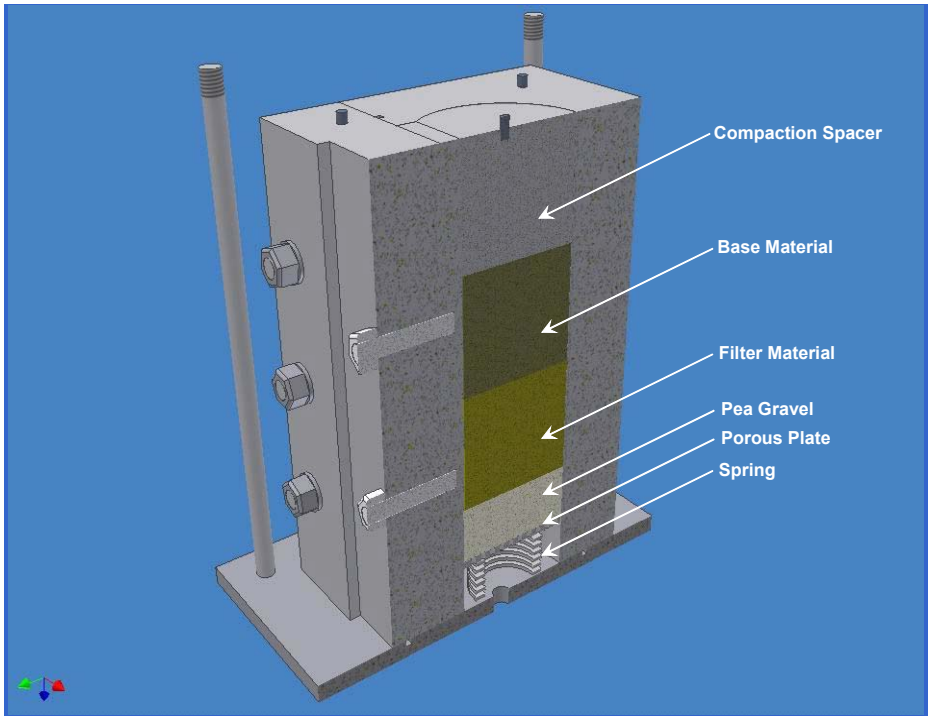

Figure A.20 Step 20 (remove the bottom plate)

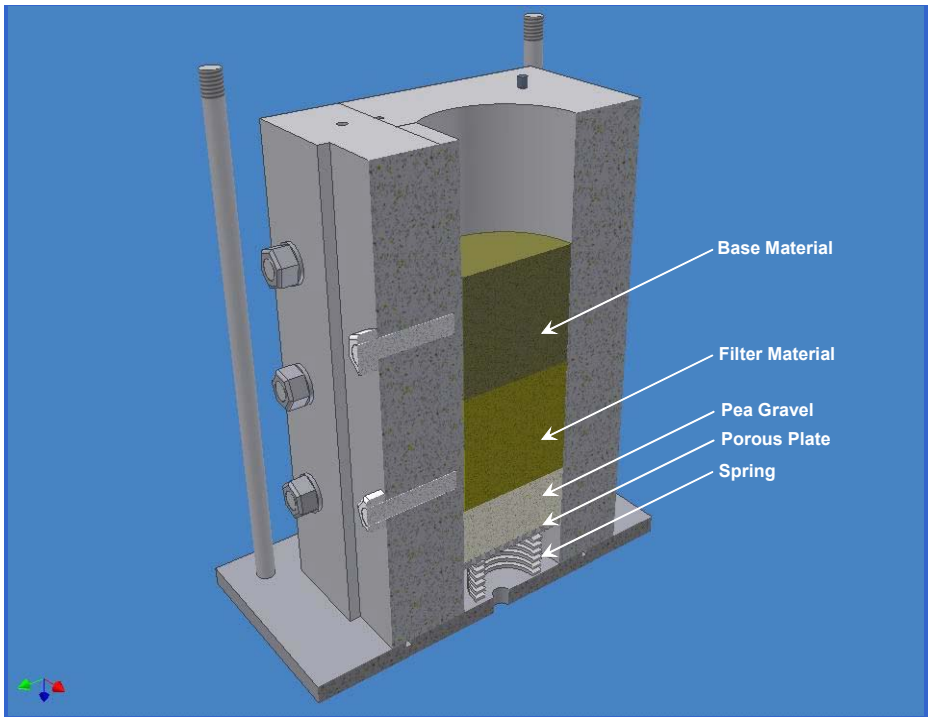

Figure A.21 Step 21 (remove the compaction spacer)

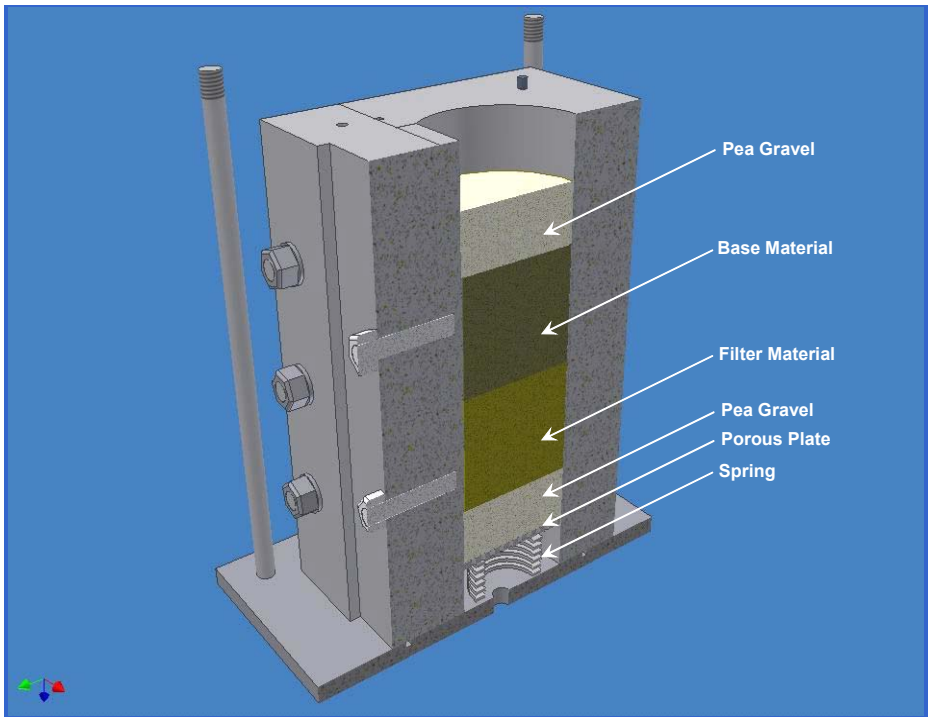

Figure A.22 Step 22 (install pea gravel)

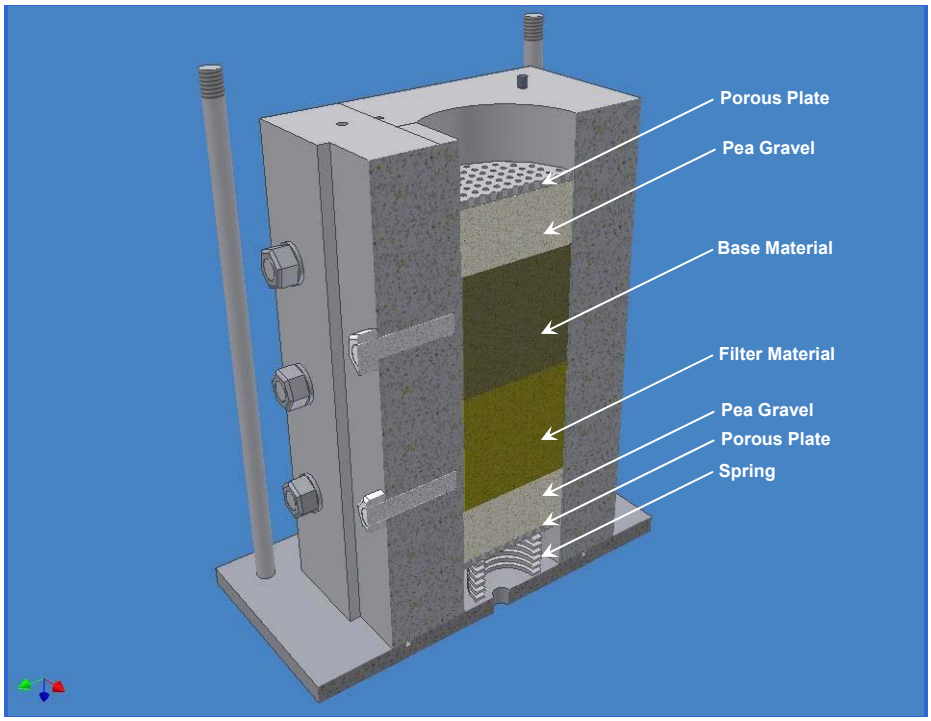

Figure A.23 Step 23 (install the porous plate)

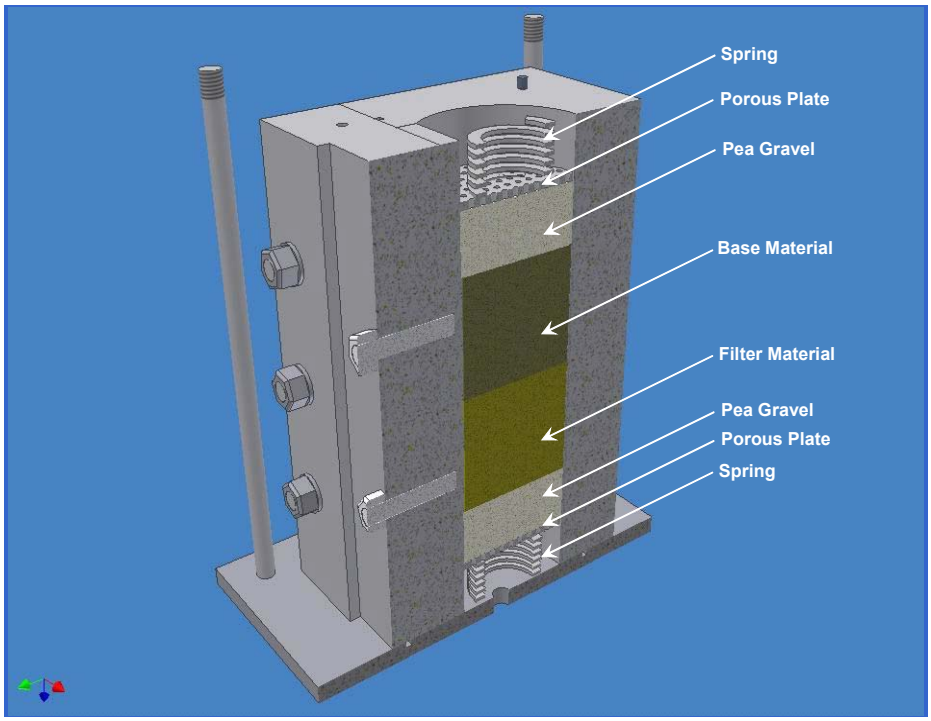

Figure A.24 Step 24 (install the spring)

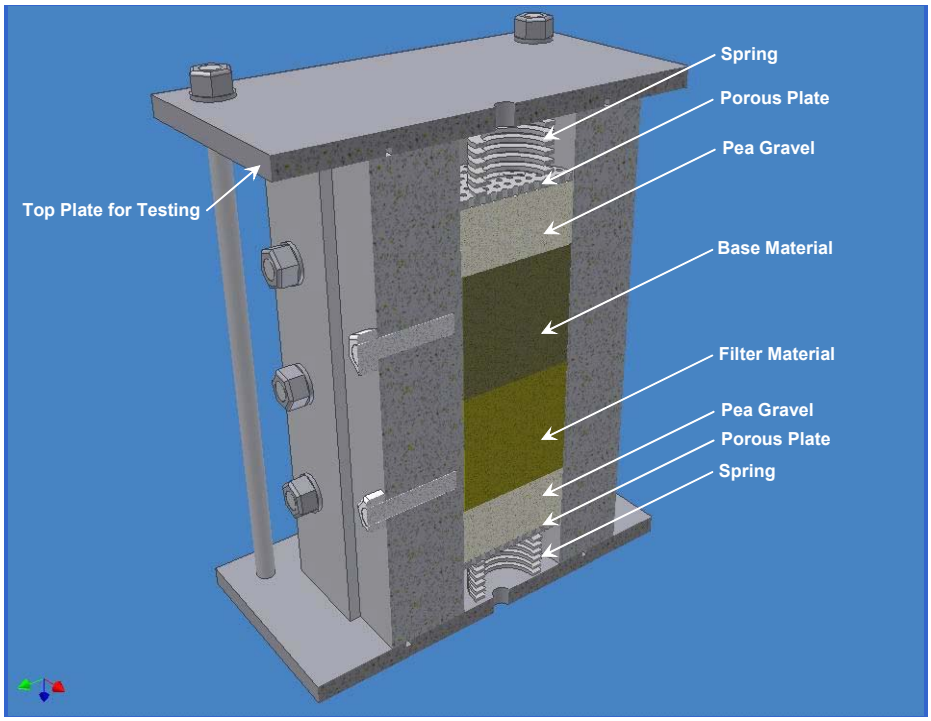

Figure A.25 Step 25 (install the top plate for testing)

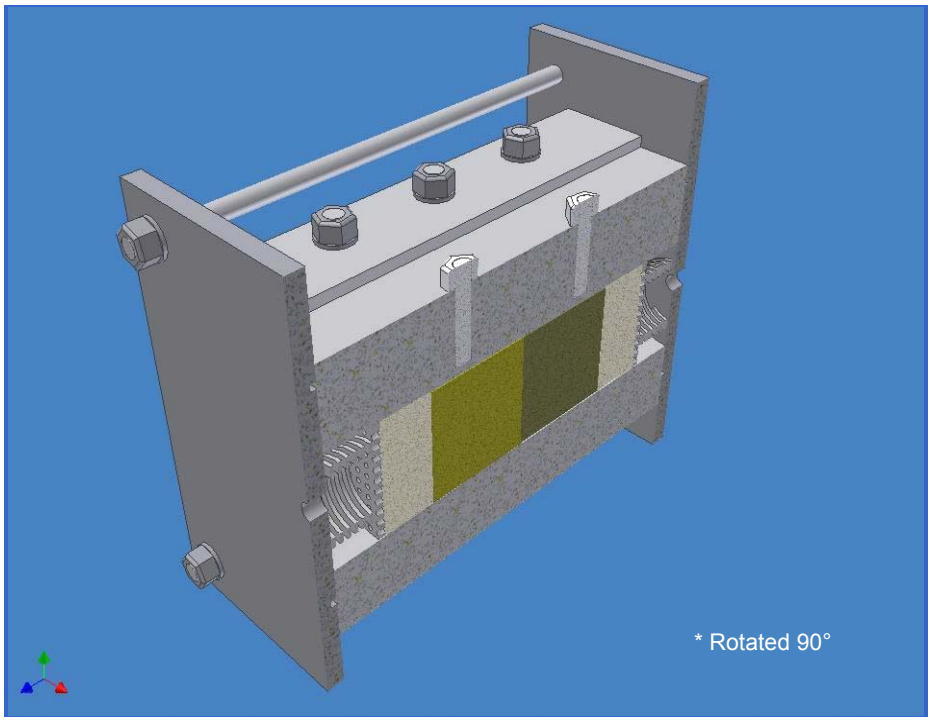

Figure A.26 Test 26 (rotate 90 degree)

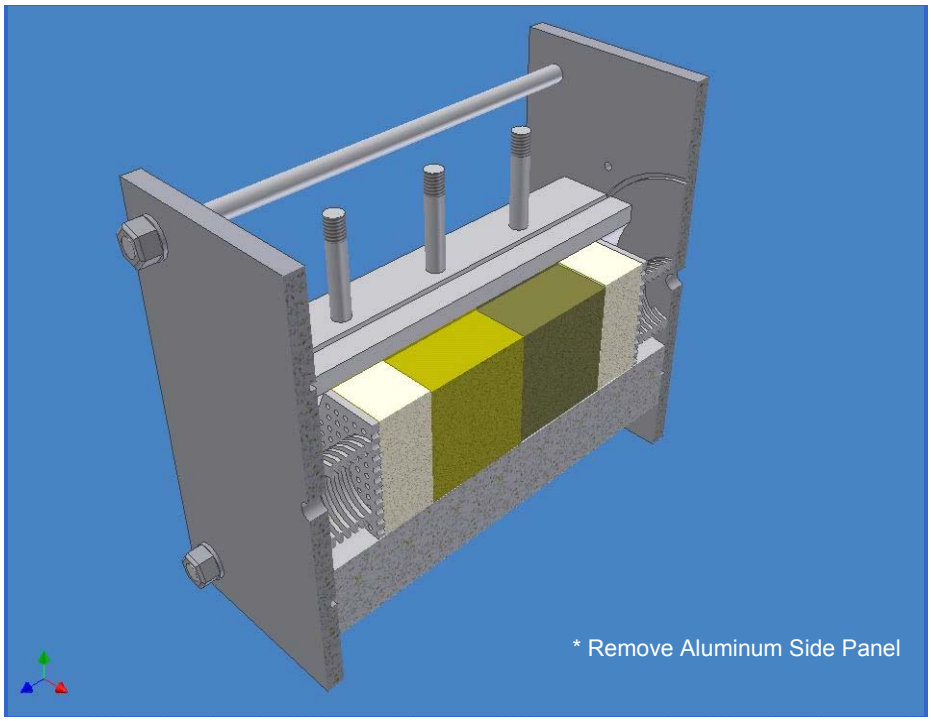

Figure A.27 Step 27 (remove the aluminum side panel)

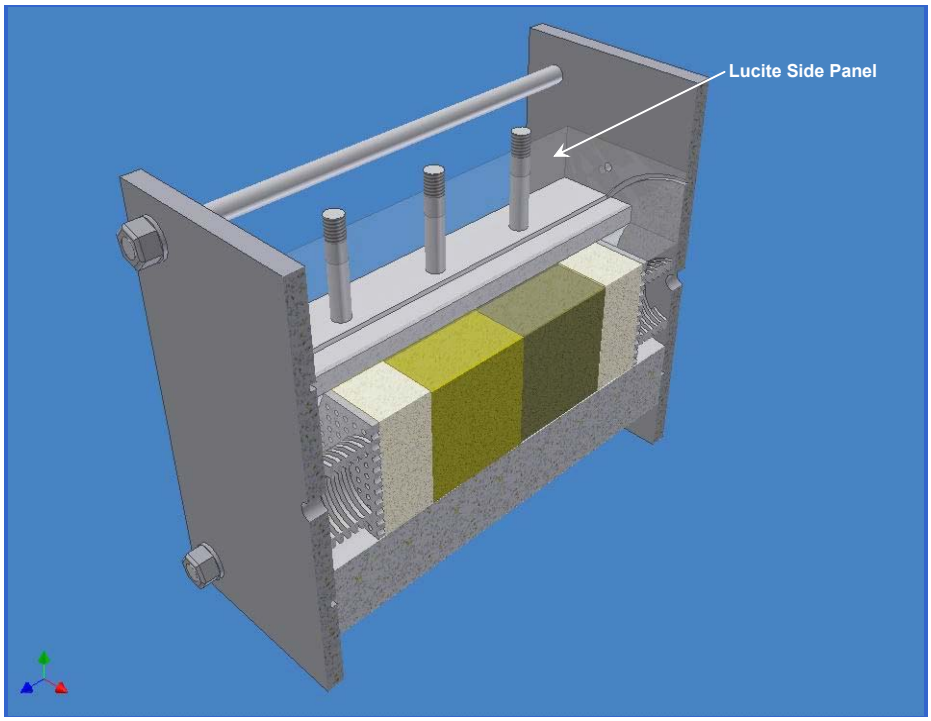

Figure A.28 Step 28 (place the Lucite side panel)

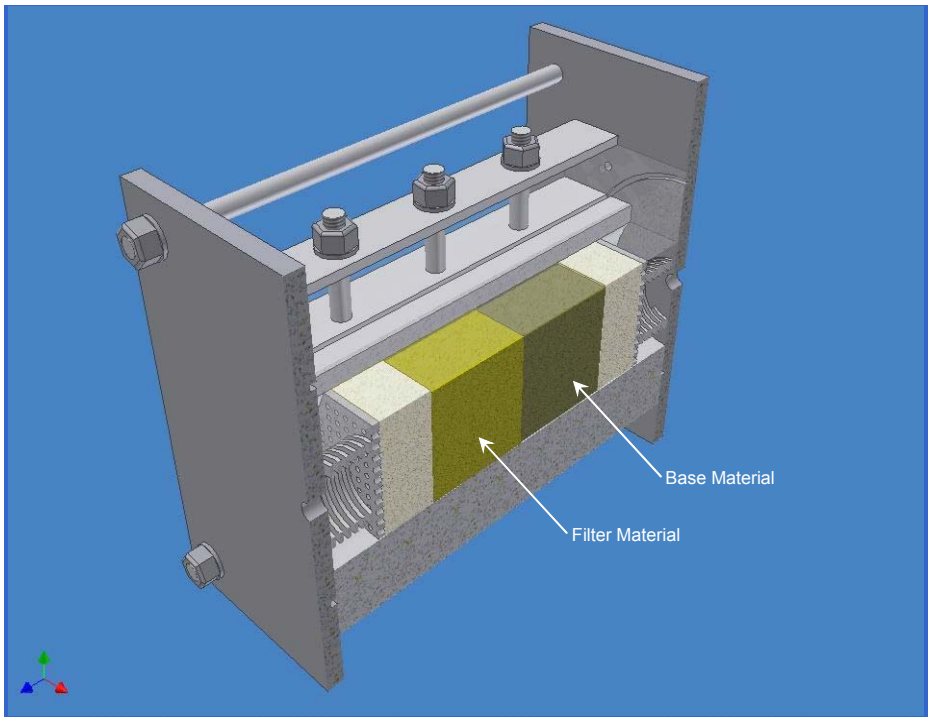

Figure A.29 Step 29 (secure the Lucite side panel)

A.2. Shop Drawings for the 4-inch diameter filter test device

The shop drawings for the 4-inch diameter filter test device are shown in Figure A.30 through Figure A.38. All of parts were aluminum except for the Lucite side panel shown in Figure A.33.

Aluminum Base

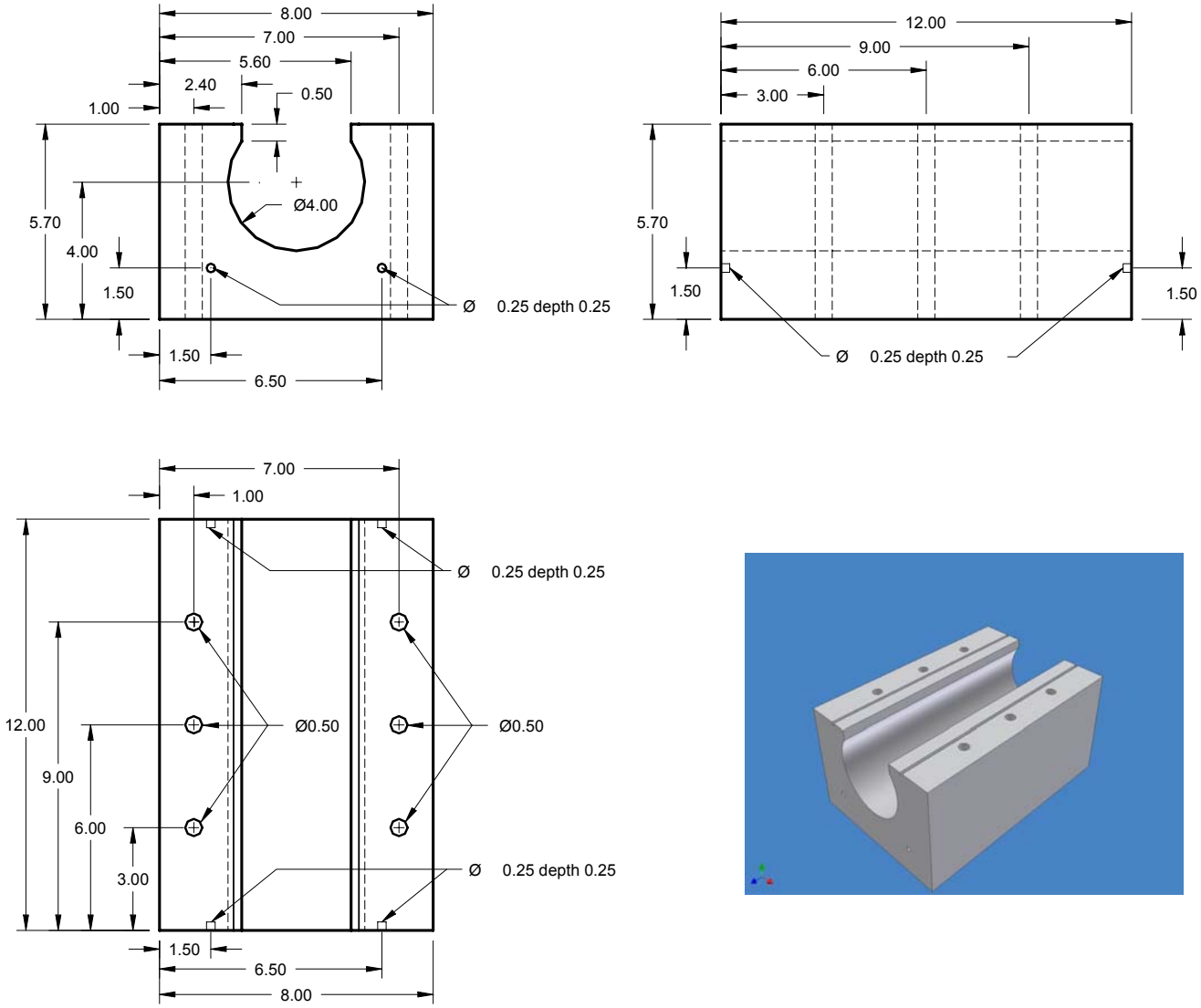

Figure A.30 Aluminum base

Aluminum Side Panel (for Compaction)

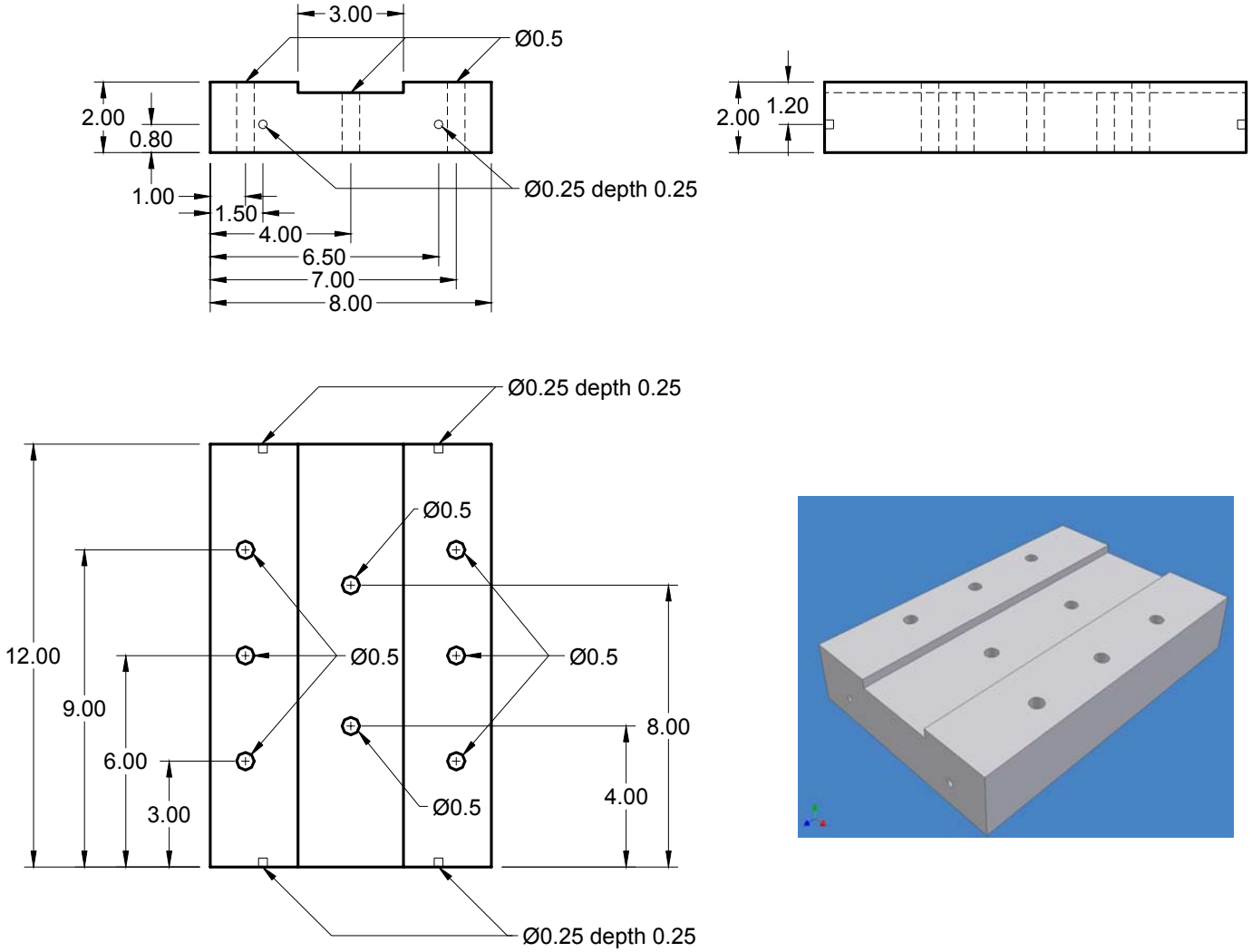

Figure A.31 Aluminum side panel for compaction

Void-forming Plate

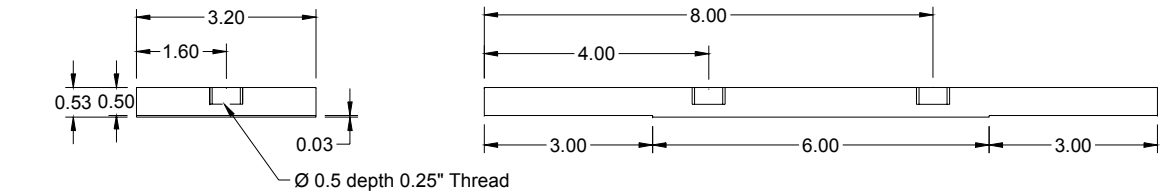

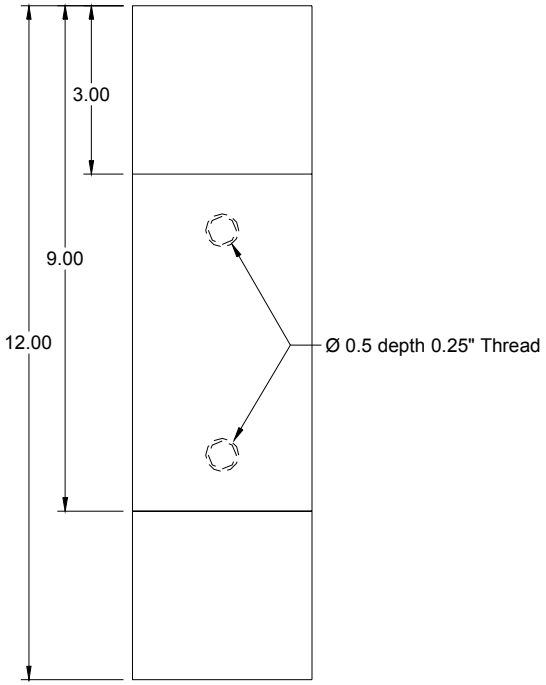

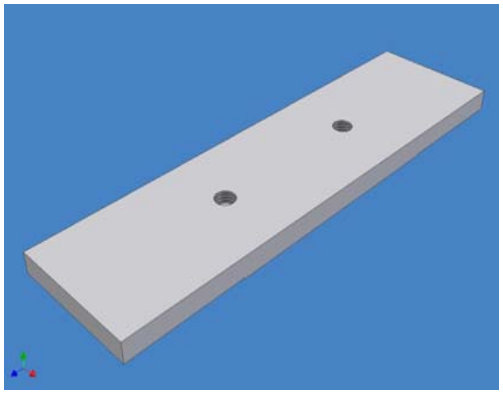

Figure A.32 Void-forming plate

Lucite Side Panel

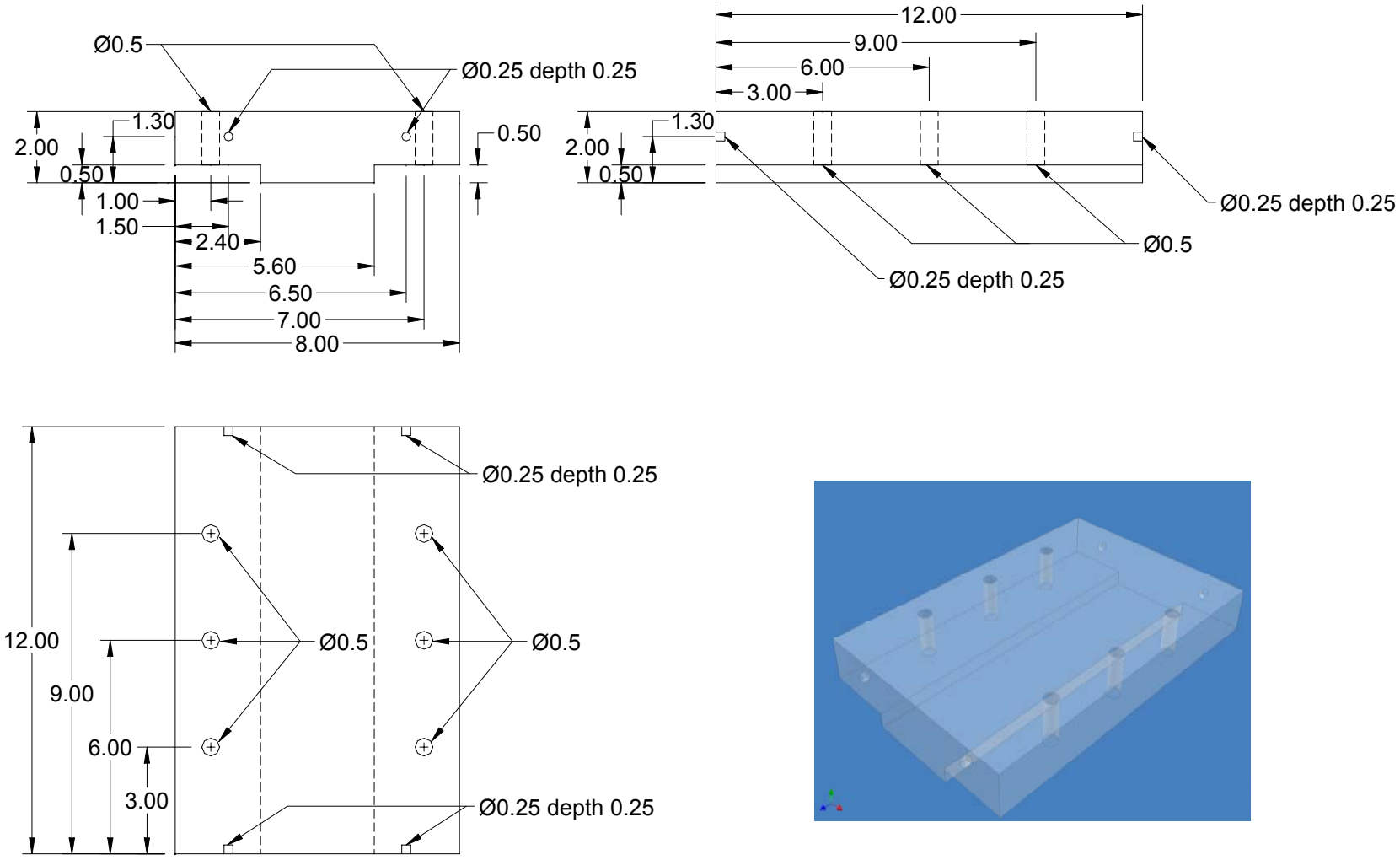

Figure A.33 Lucite side panel

Compaction Spacer

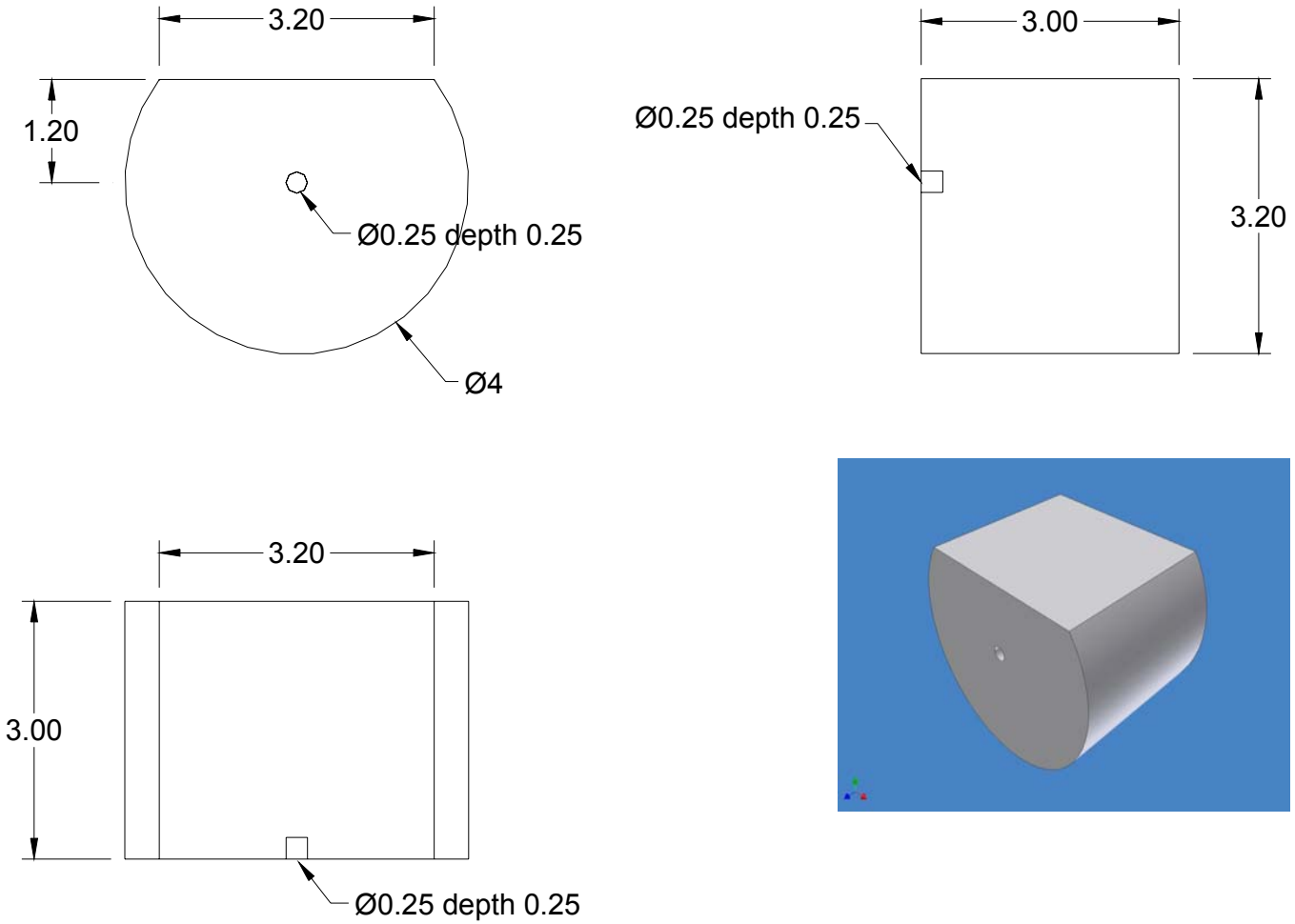

Figure A.34 Compaction spacer

Bottom Plate for Compaction

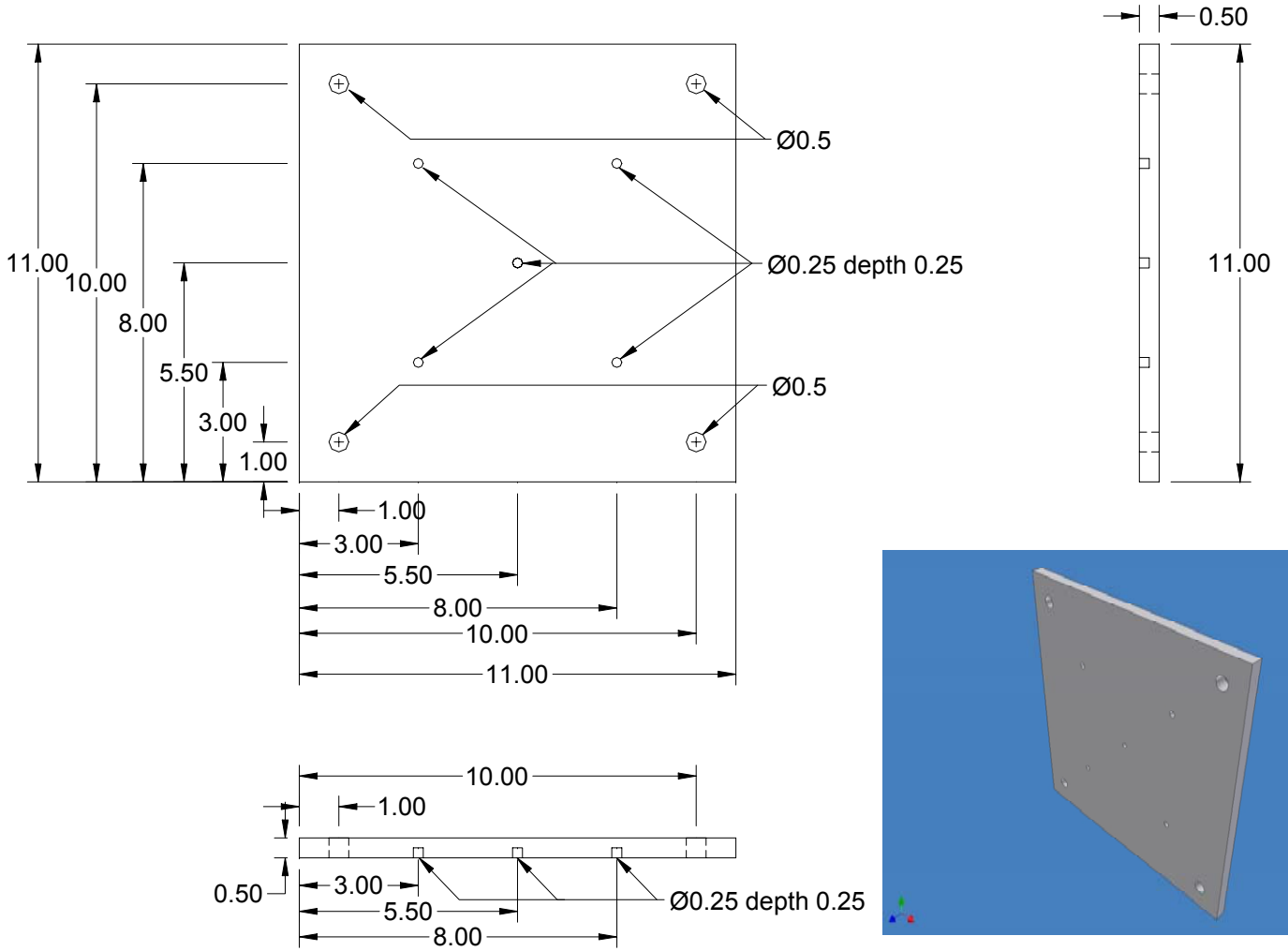

Figure A.35 Bottom plate for compaction

Top Plate for Compaction

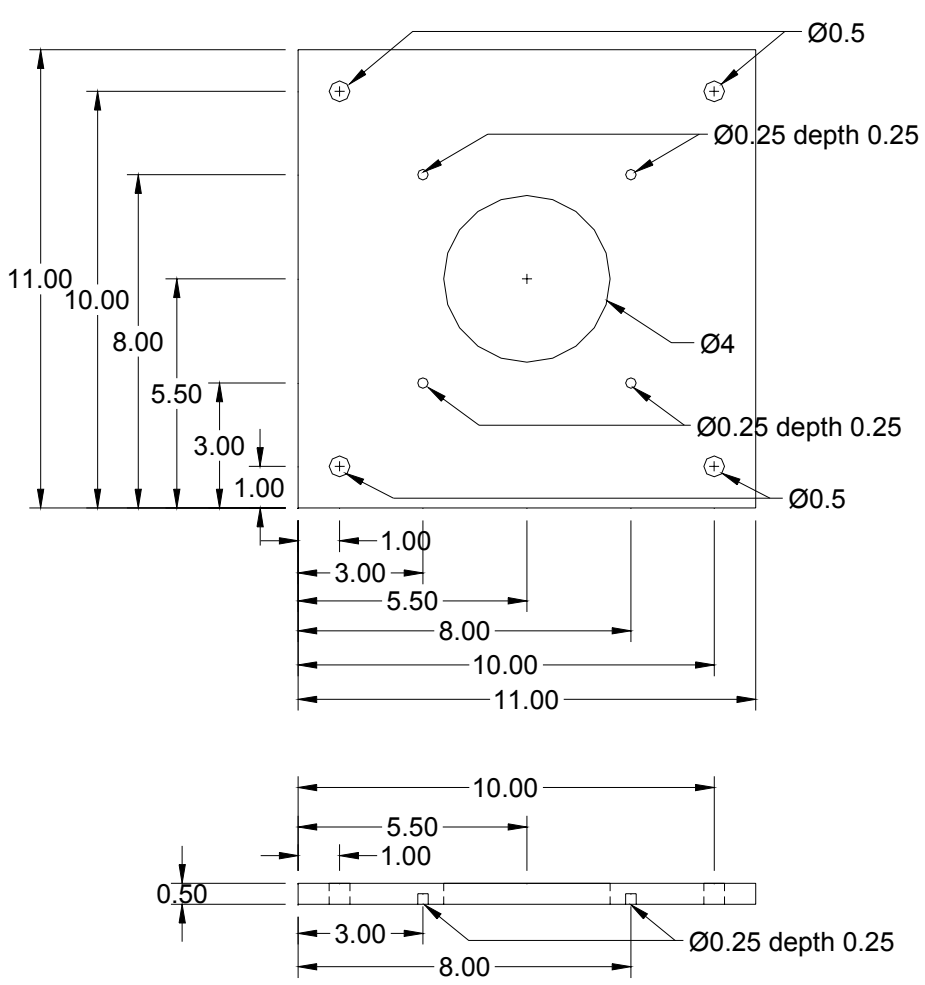

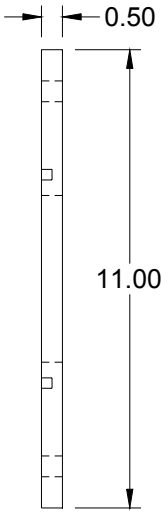

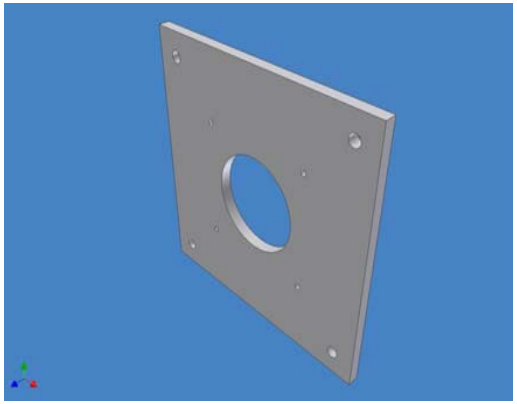

Figure A.36 Top plate for compaction

Top and Bottom Plate for Testing

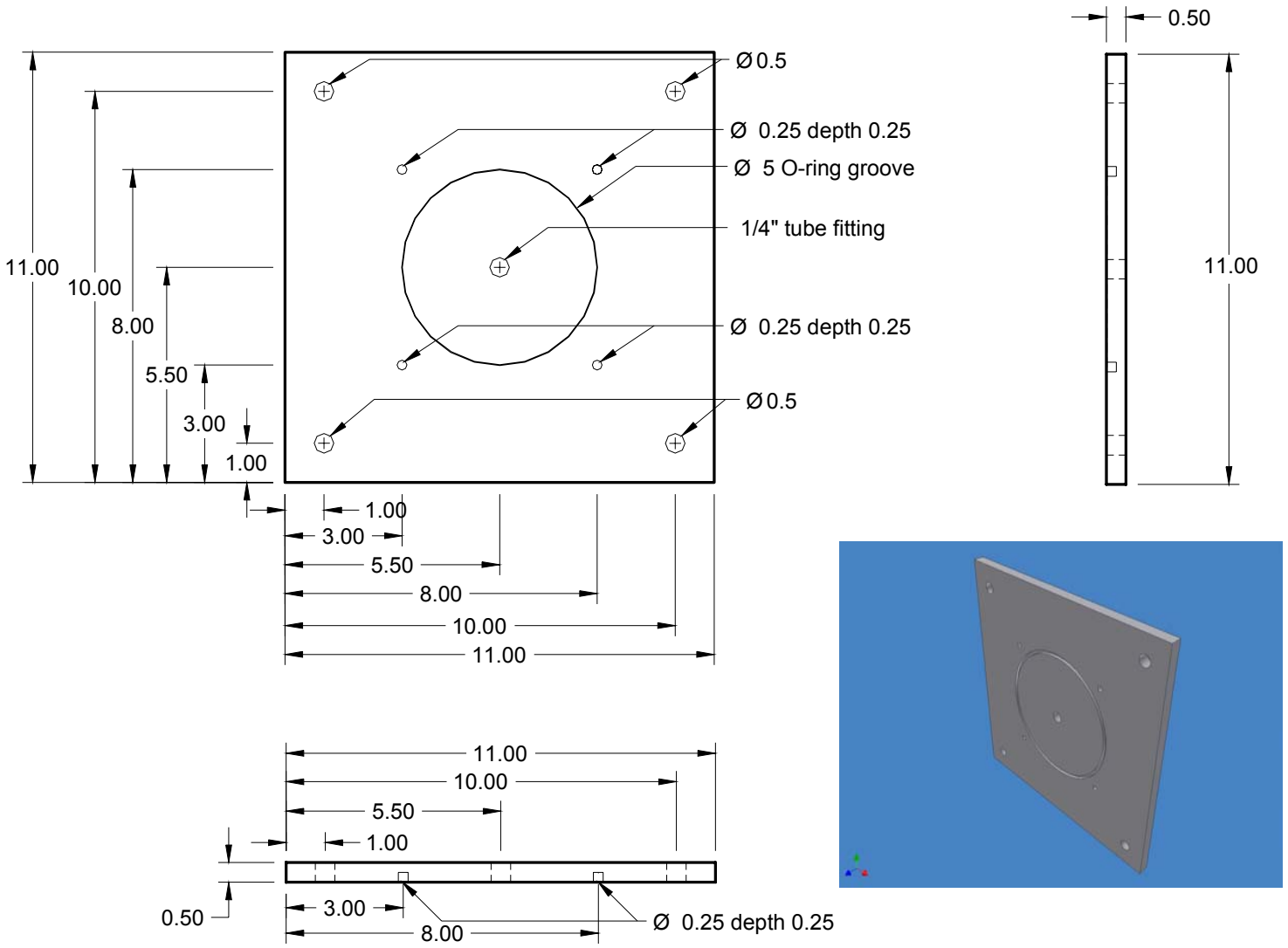

Figure A.37 Top and bottom plate for testing

Porous Plate

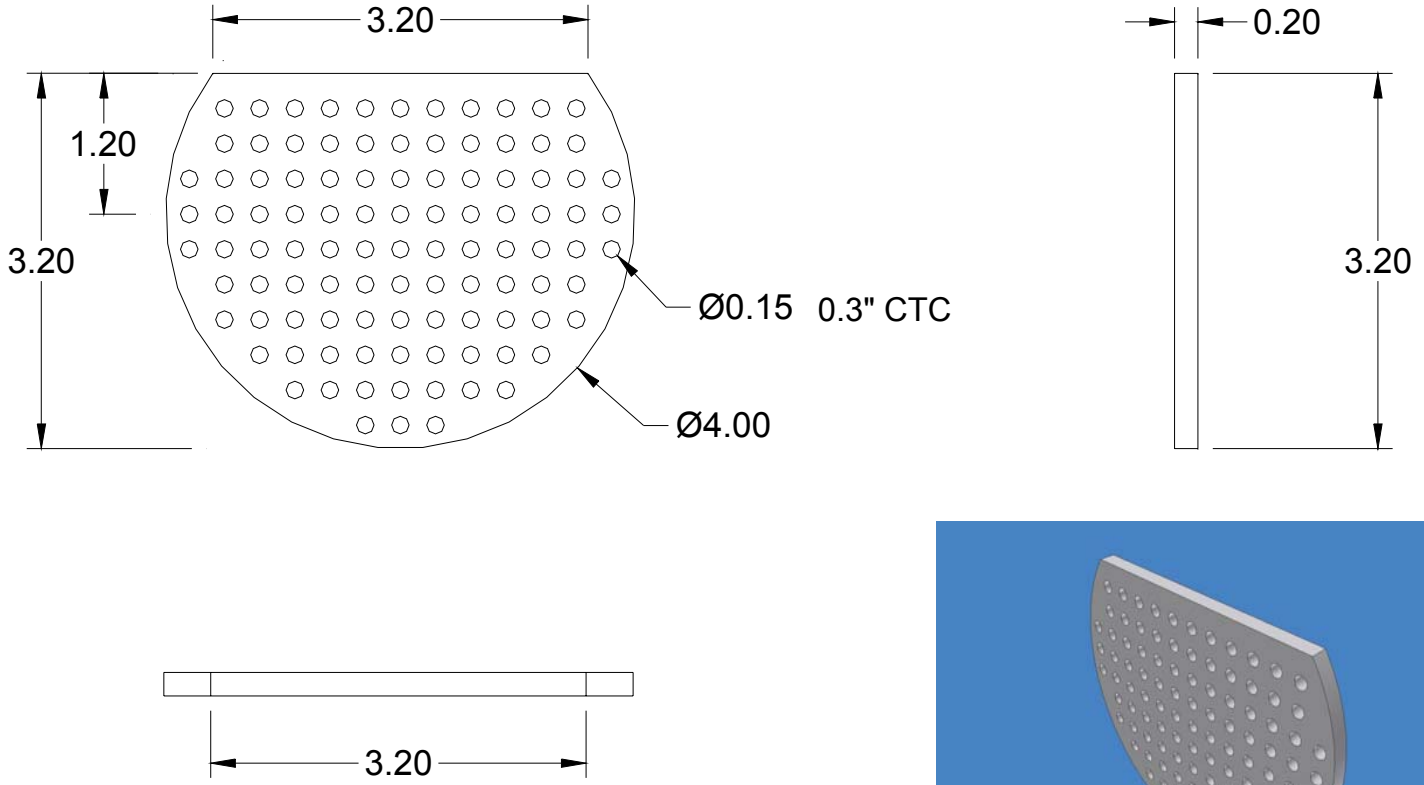

Figure A.38 Porous plate

Appendix B. The 12-inch Square Filter Test Device

B.1. Device Assembly and Sample Preparations

In this appendix, the assembly of the 12-inch square filter test device is shown step-by-step in Figure B.1 through Figure B.56. Steps 1 through 13 show the assembly of the 12-inch filter test device before the compaction. Steps 14 through 36 show the compaction procedure to prepare the specimen. As mentioned in Chapter 6, the assembly of the pressure membrane panel is shown in Steps 37 through 49.

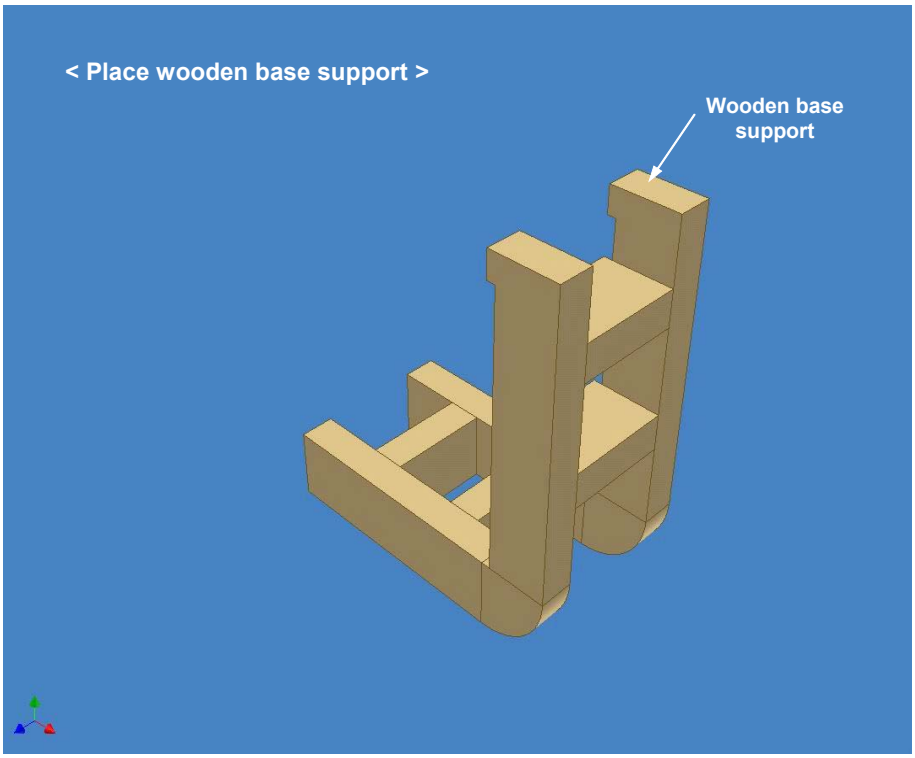

Figure B.1 Step 1 (place wooden base support)

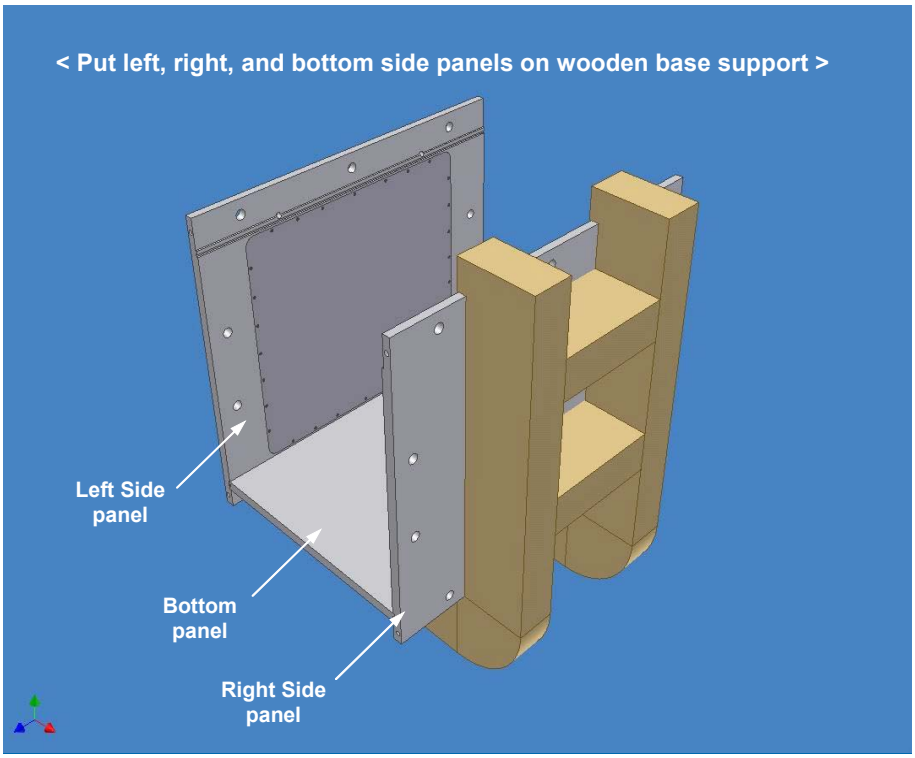

Figure B.2 Step 2 (install left, right, and bottom side panels on wooden base support)

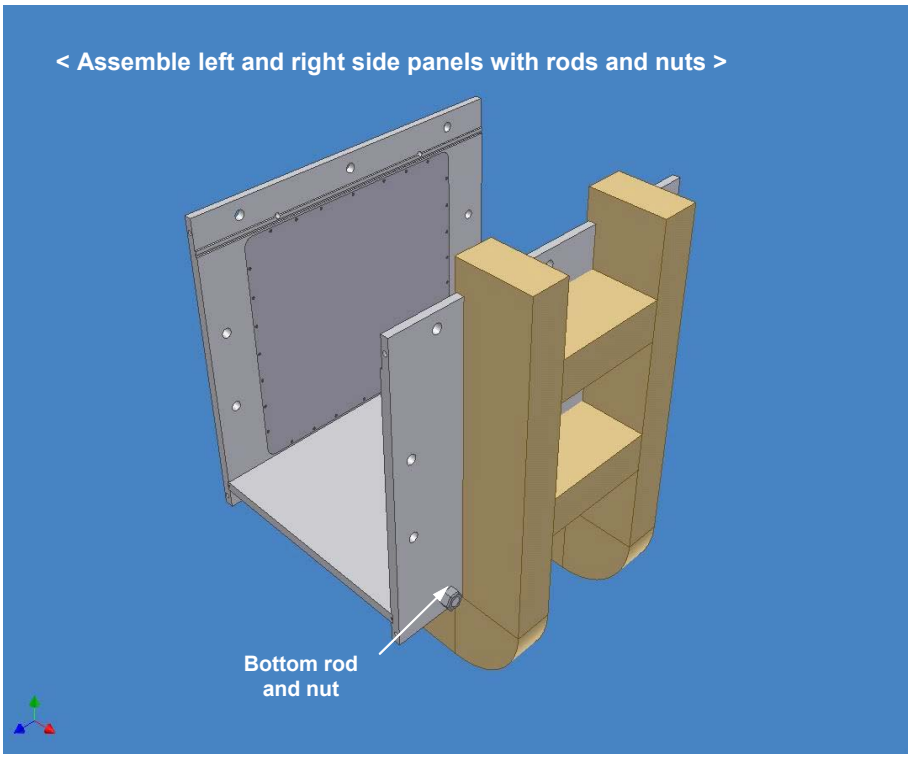

Figure B.3 Step 3 (assemble left and right side panels with rods and nuts)

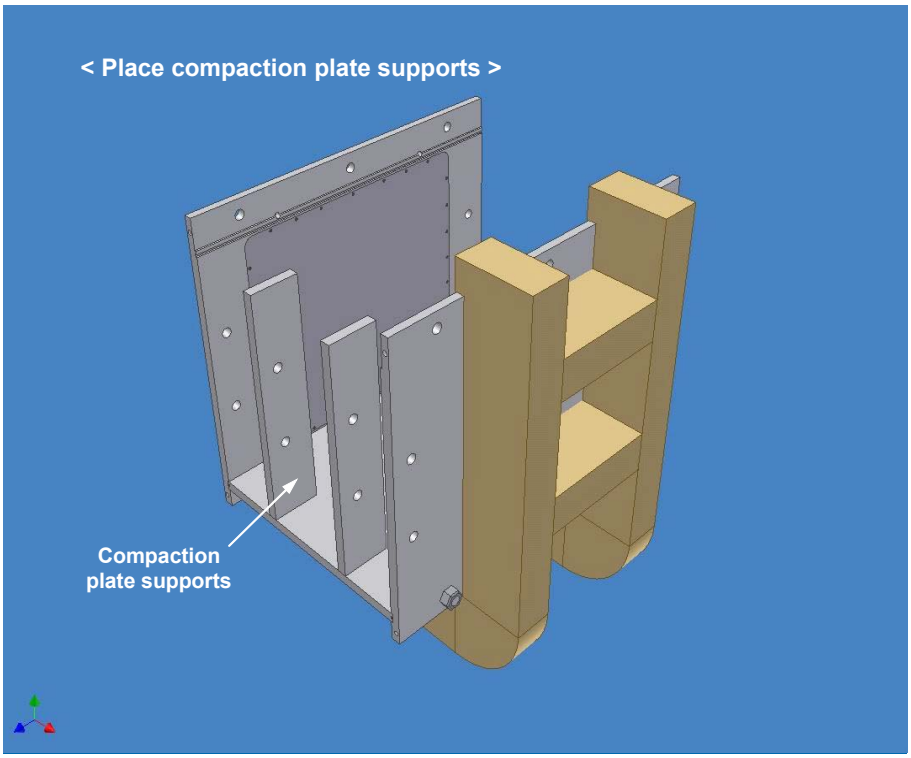

Figure B.4 Step 4 (place compaction plate supports)

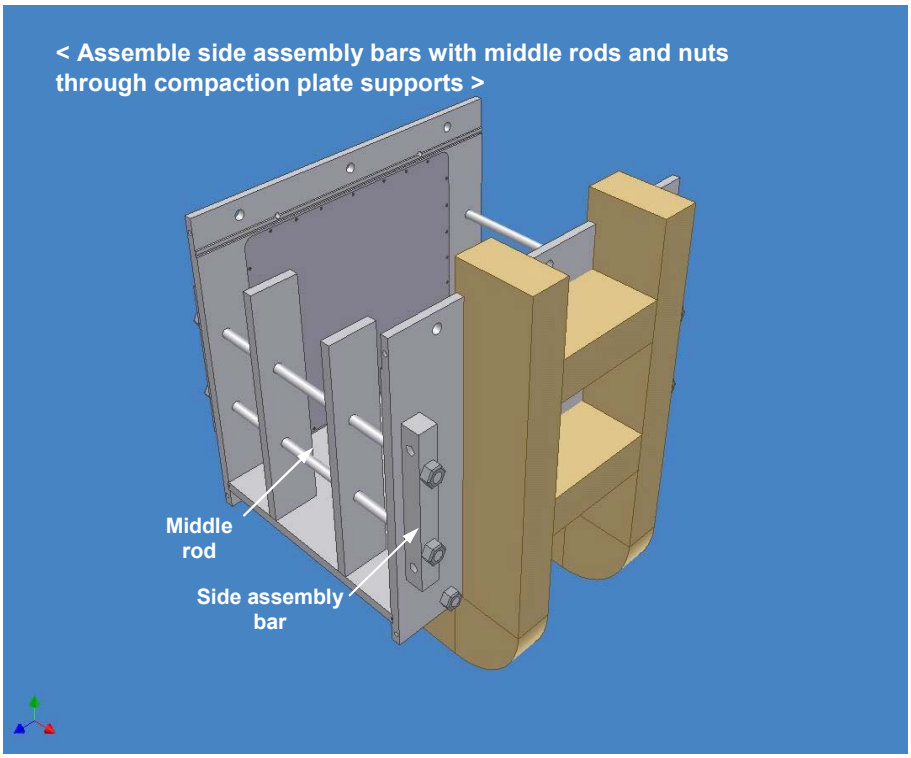

Figure B.5 Step 5 (assemble side assembly bars with middle rods and nuts)

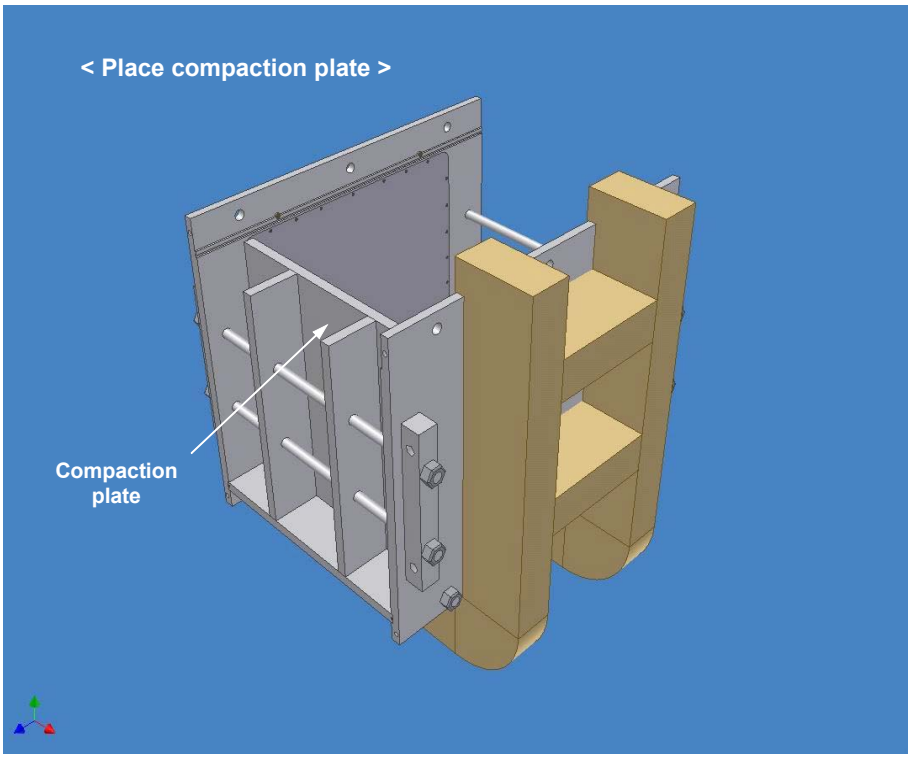

Figure B.6 Step 6 (place compaction plate)

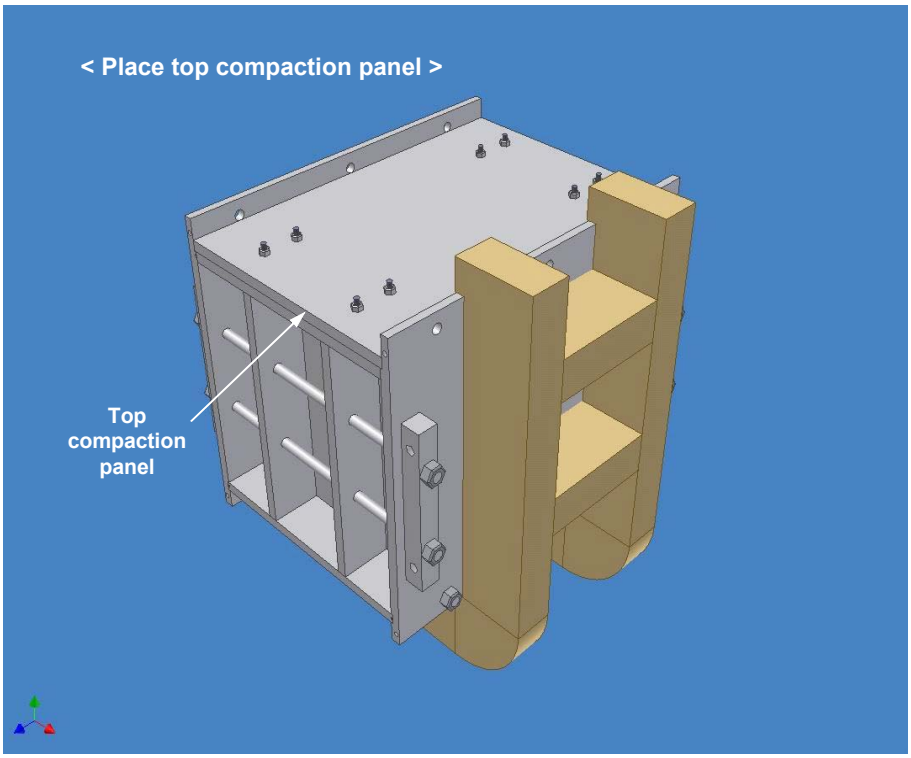

Figure B.7 Step 7 (place top compaction panel)

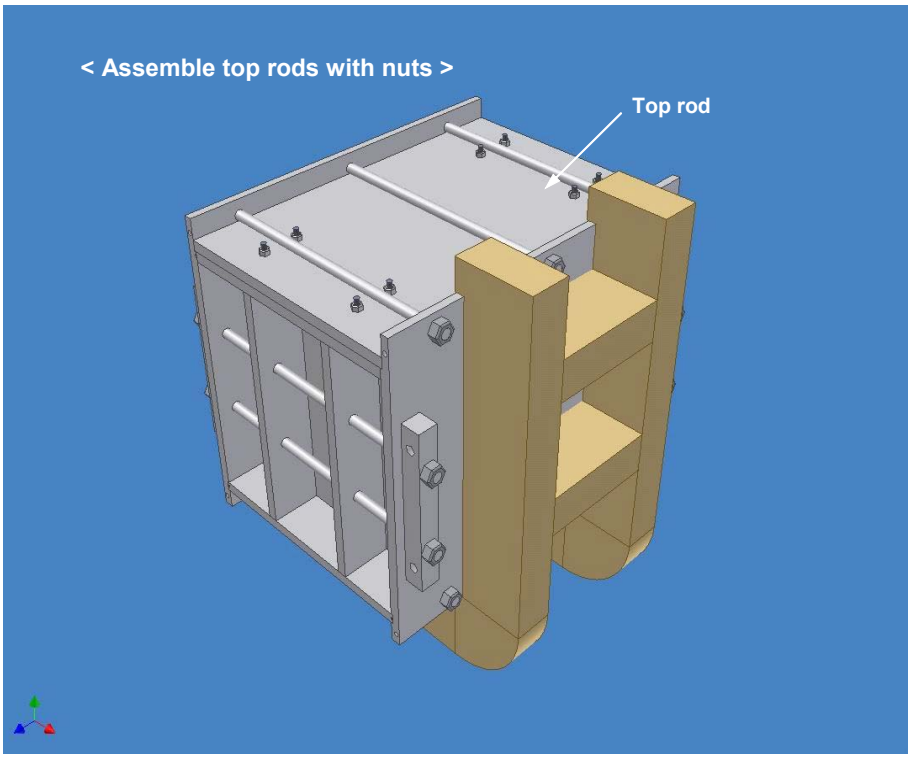

Figure B.8 Step 8 (assemble top rods with nuts)

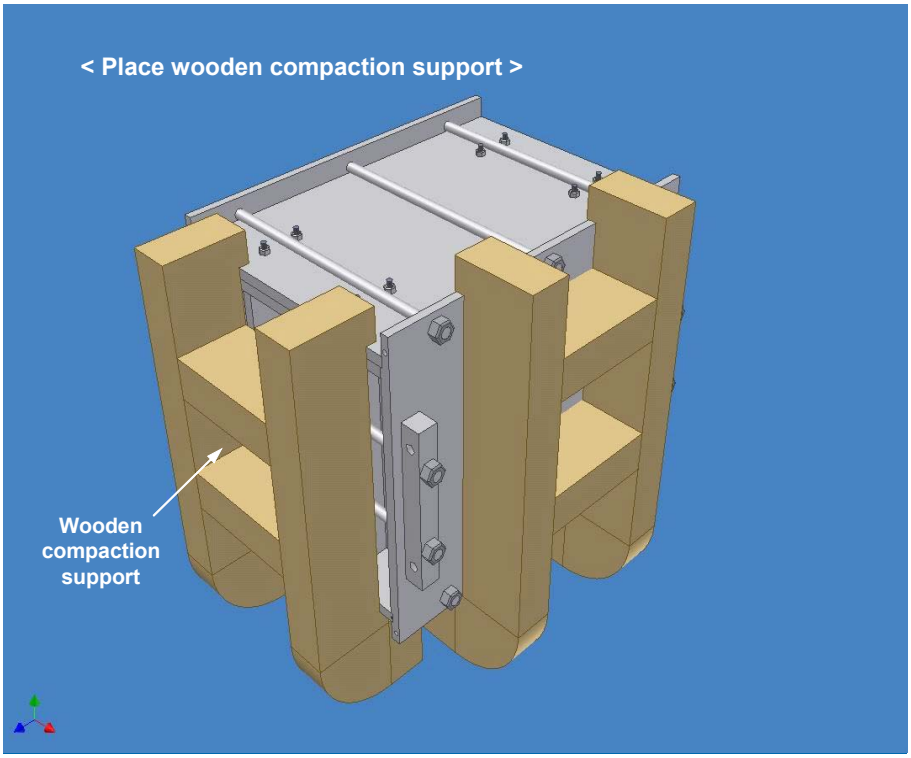

Figure B.9 Step 9 (place wooden compaction support)

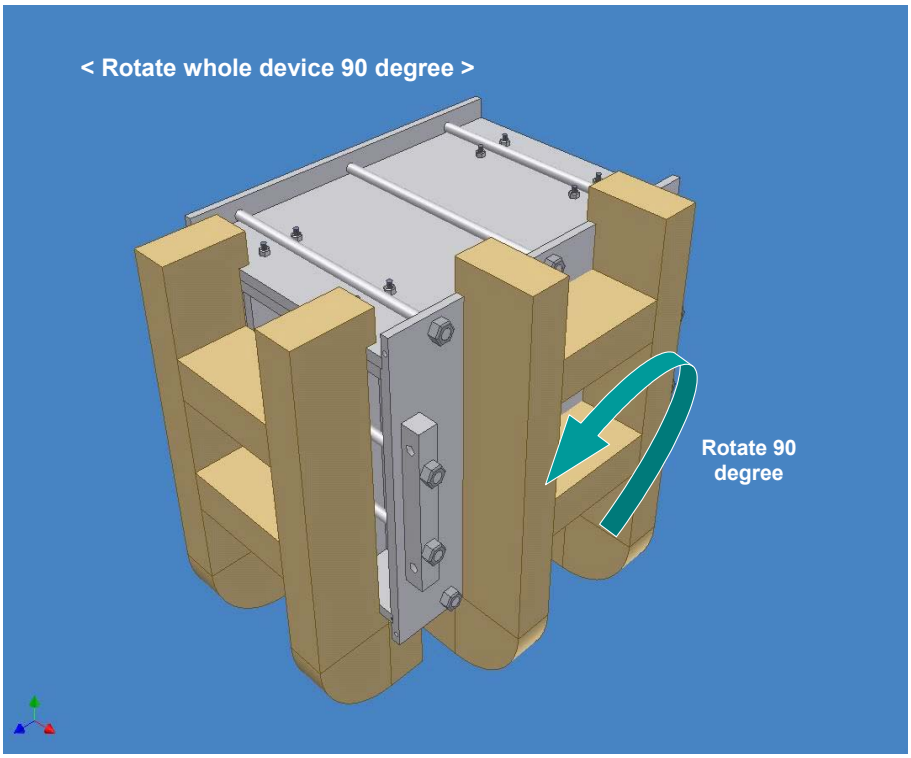

Figure B.10 Step 10 (rotate whole device 90 degree)

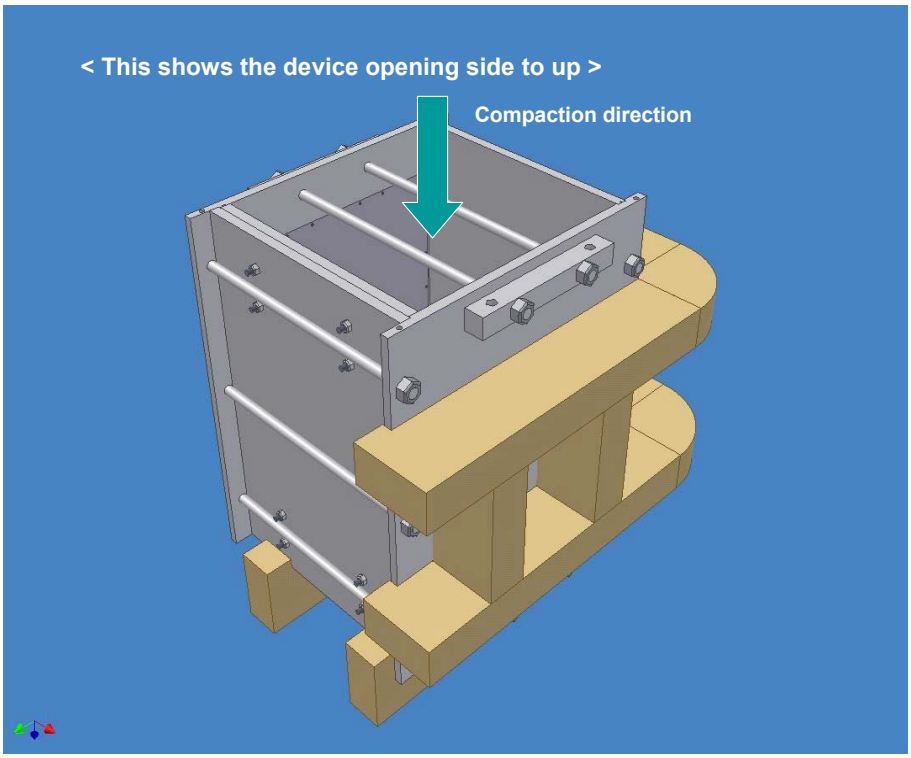

Figure B.11 Step 11 (the device opening side to up)

Figure B.12 Step 12 (remove wooden base support)

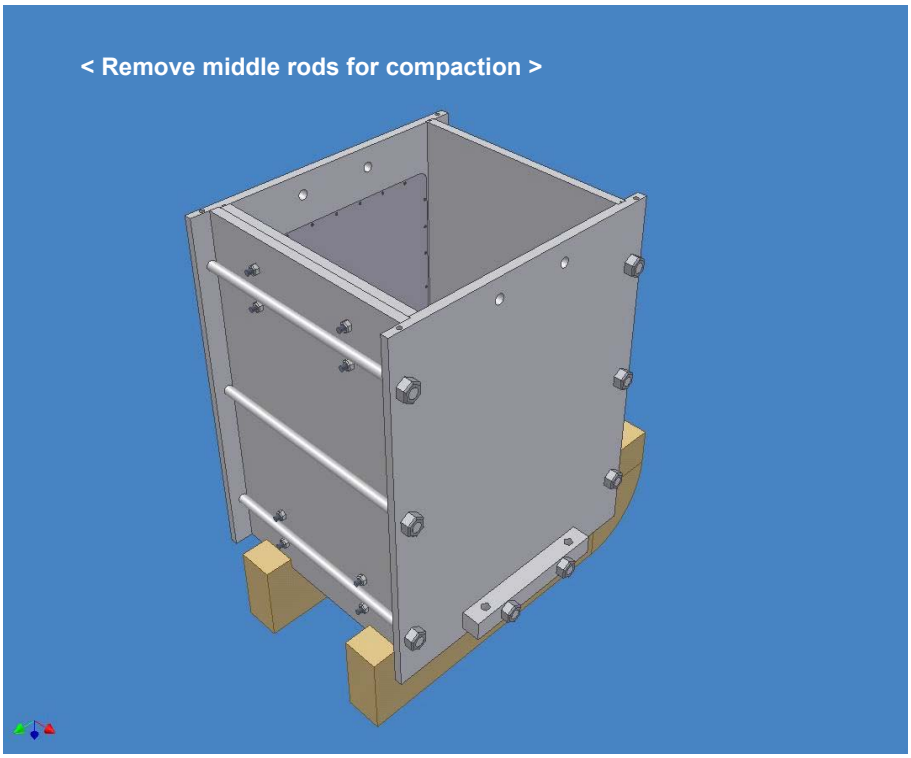

Figure B.13 Step 13 (remove middle rods for compaction)

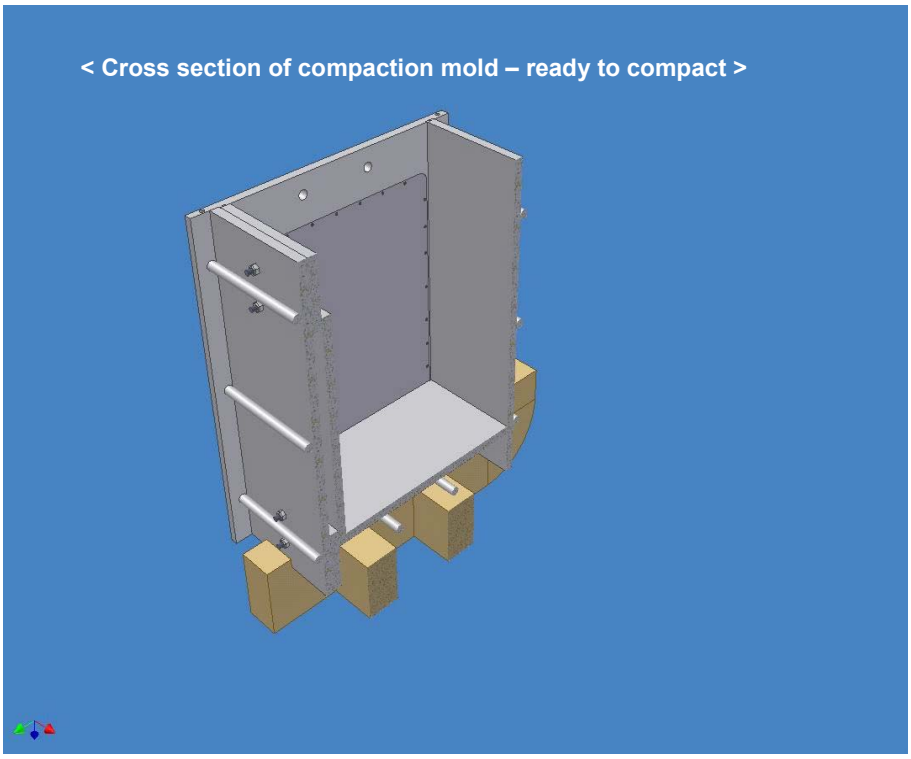

Figure B.14 Step 14 (cross section of compaction mold)

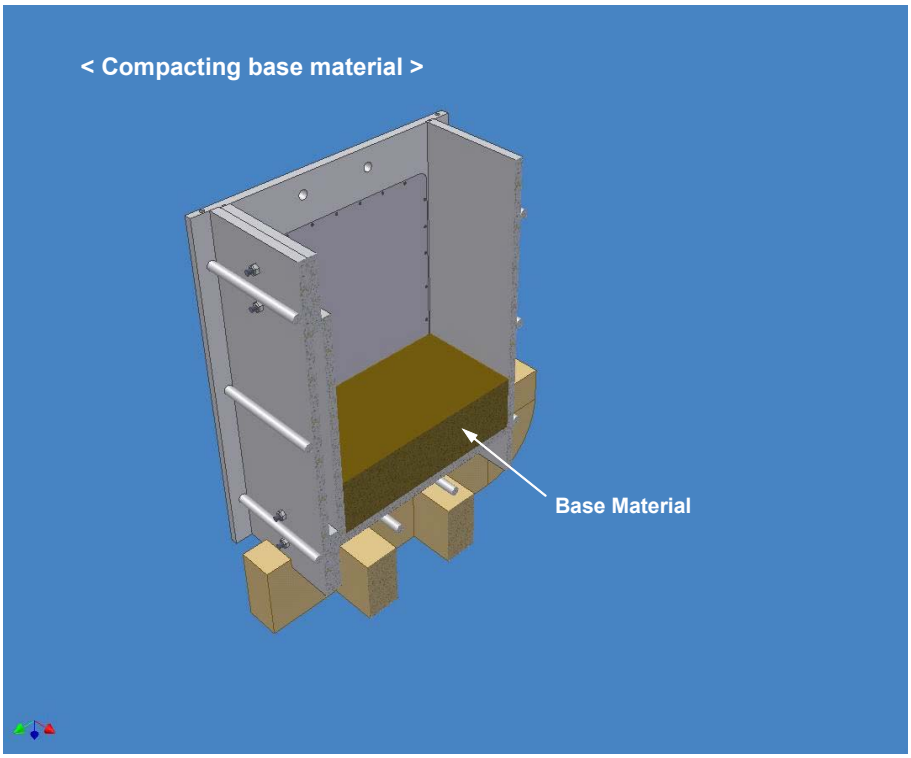

Figure B.15 Step 15 (compacting base material)

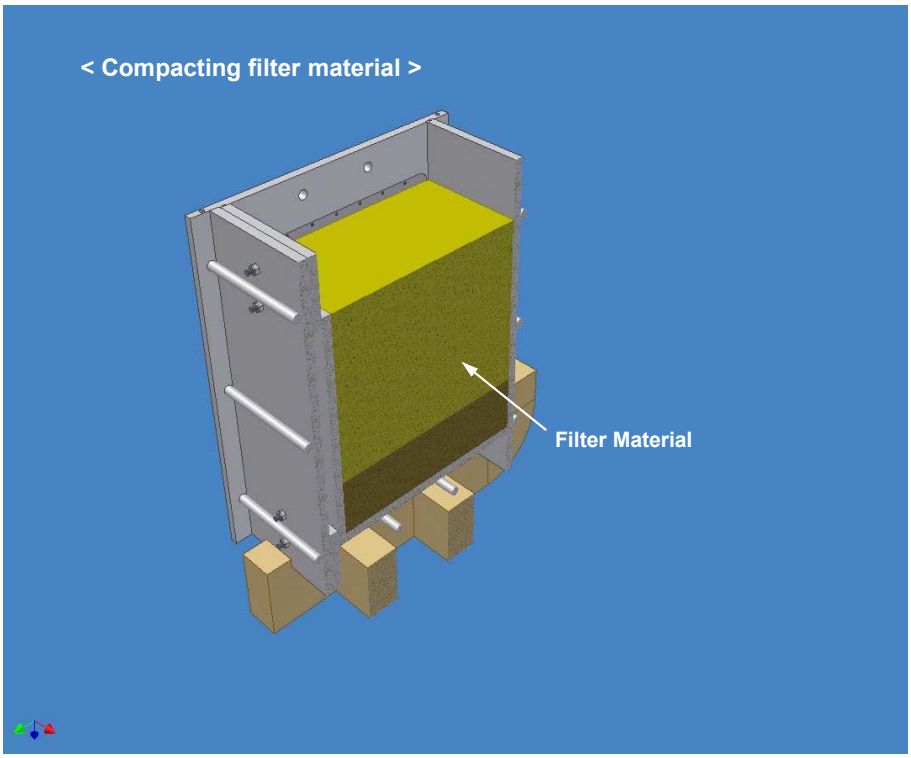

Figure B.16 Step 16 (compacting filter material)

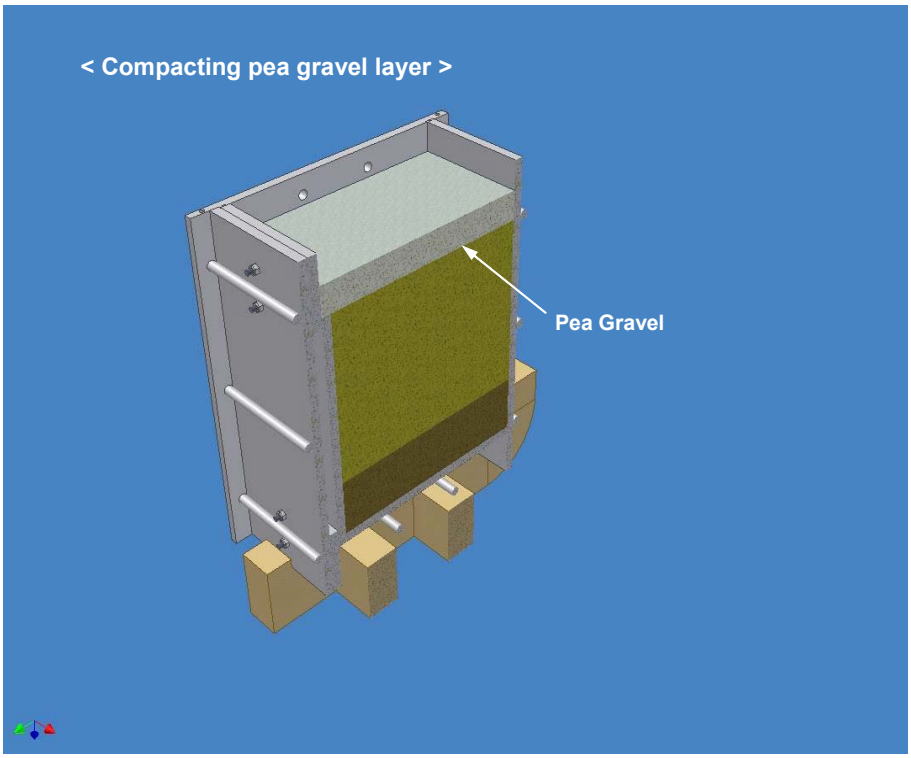

Figure B.17 Step 17 (compacting pea gravel layer)

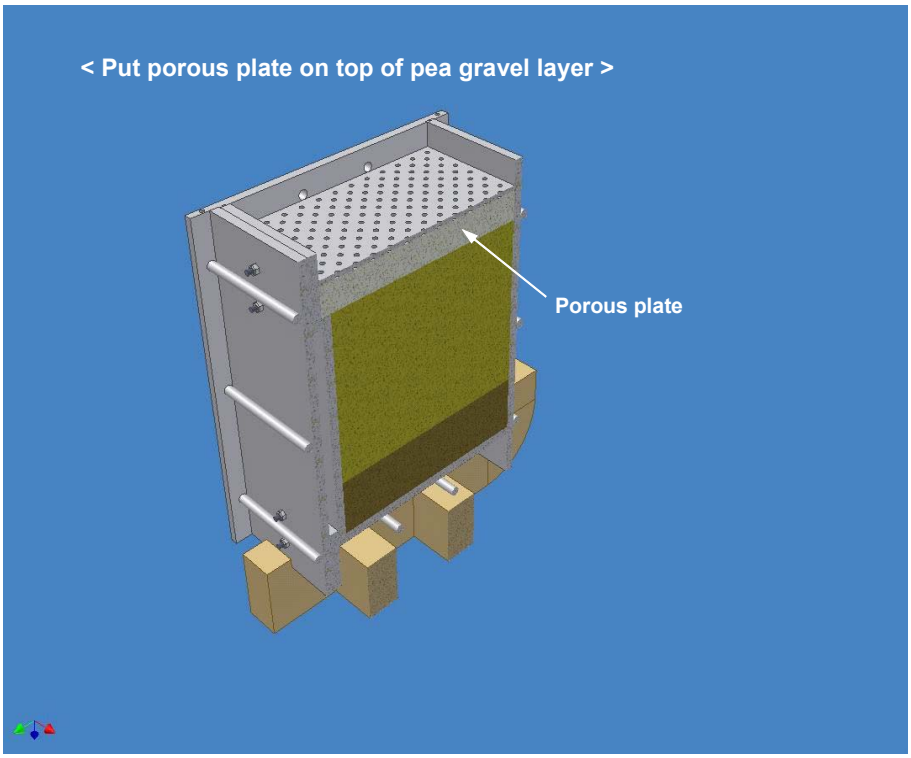

Figure B.18 Step 18 (install porous plate)

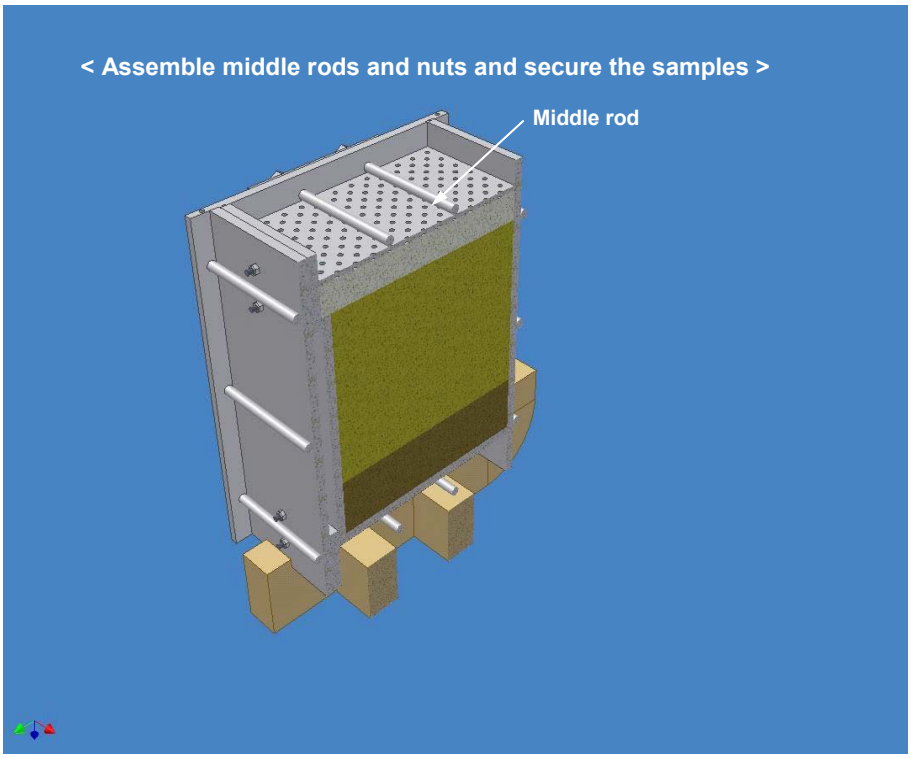

Figure B.19 Step 19 (assemble middle rods and nuts)

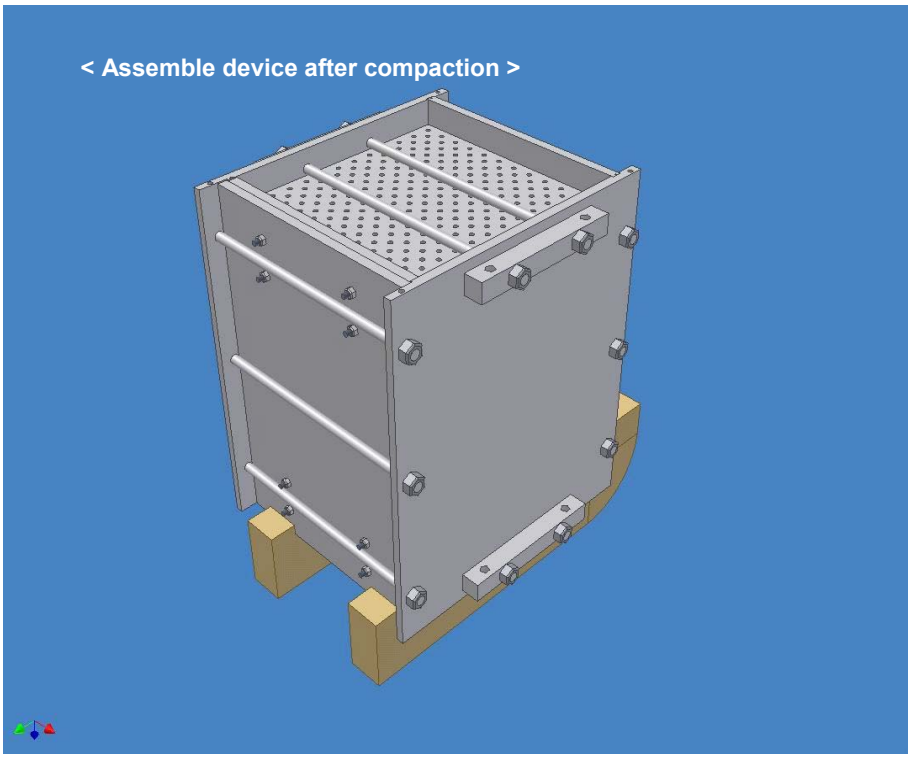

Figure B.20 Step 20 (assemble device after compaction)

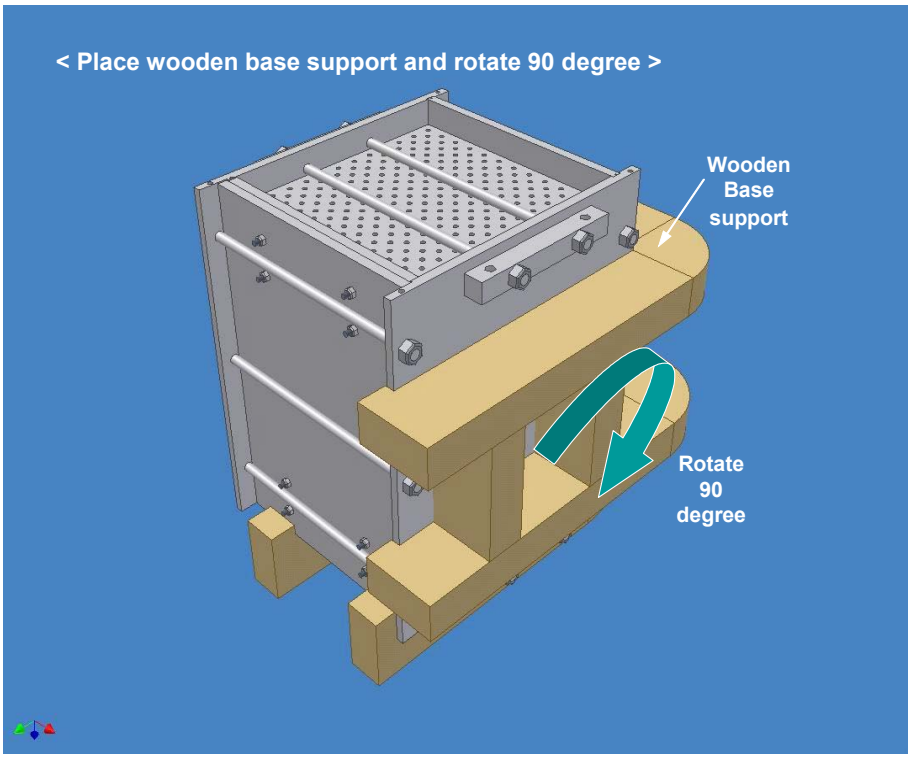

Figure B.21 Step 21 (place wooden base support and rotate 90 degree)

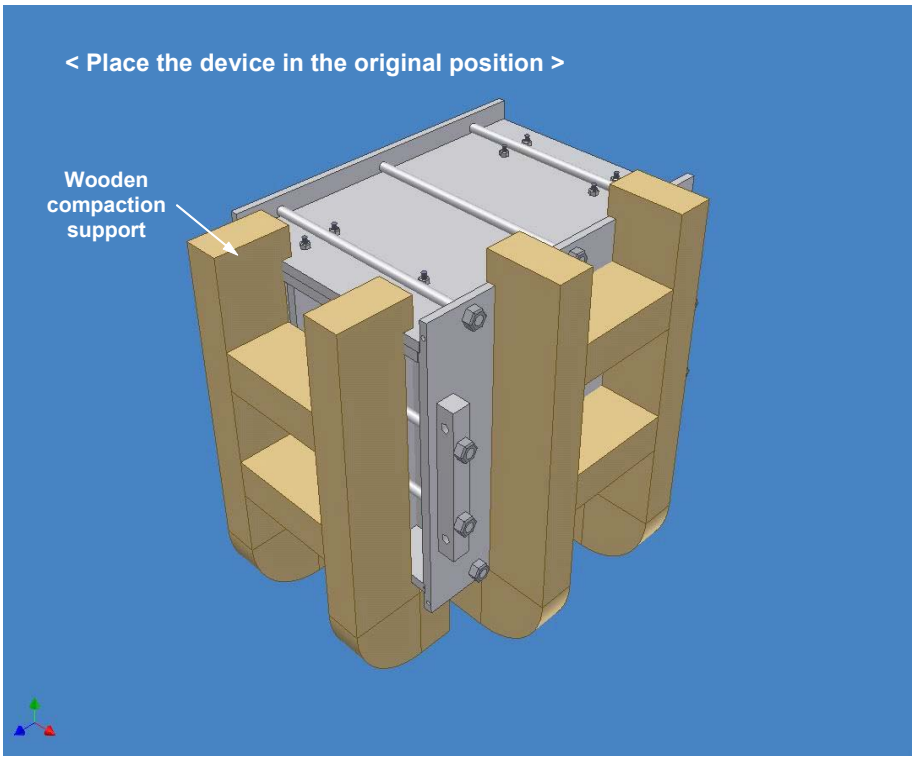

Figure B.22 Step 22 (place the device in the original position)

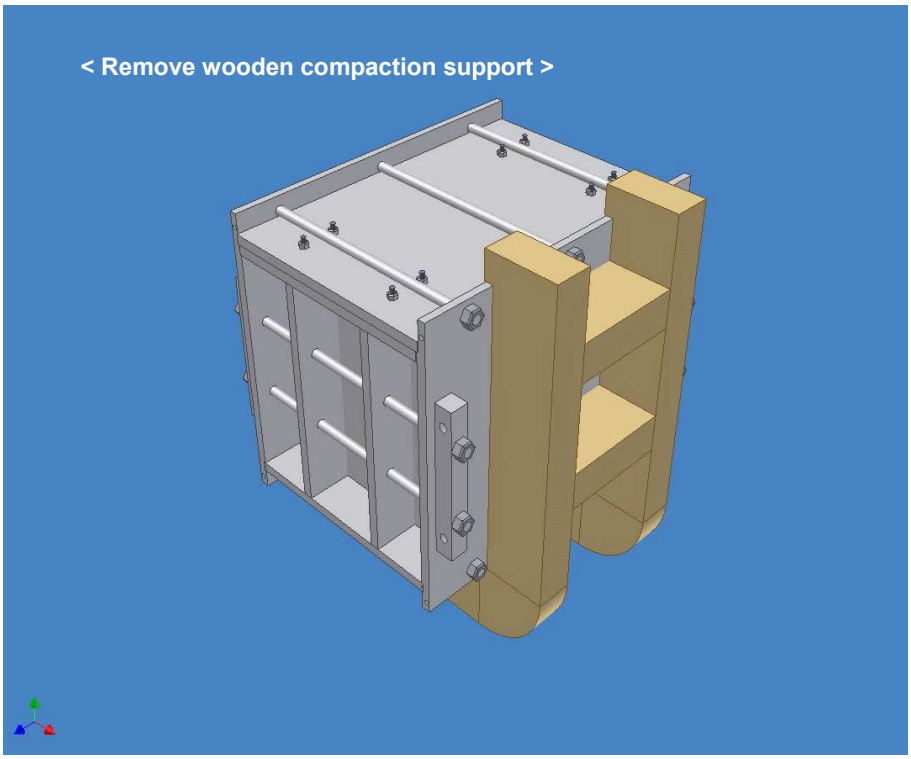

Figure B.23 Step 23 (remove wooden compaction support)

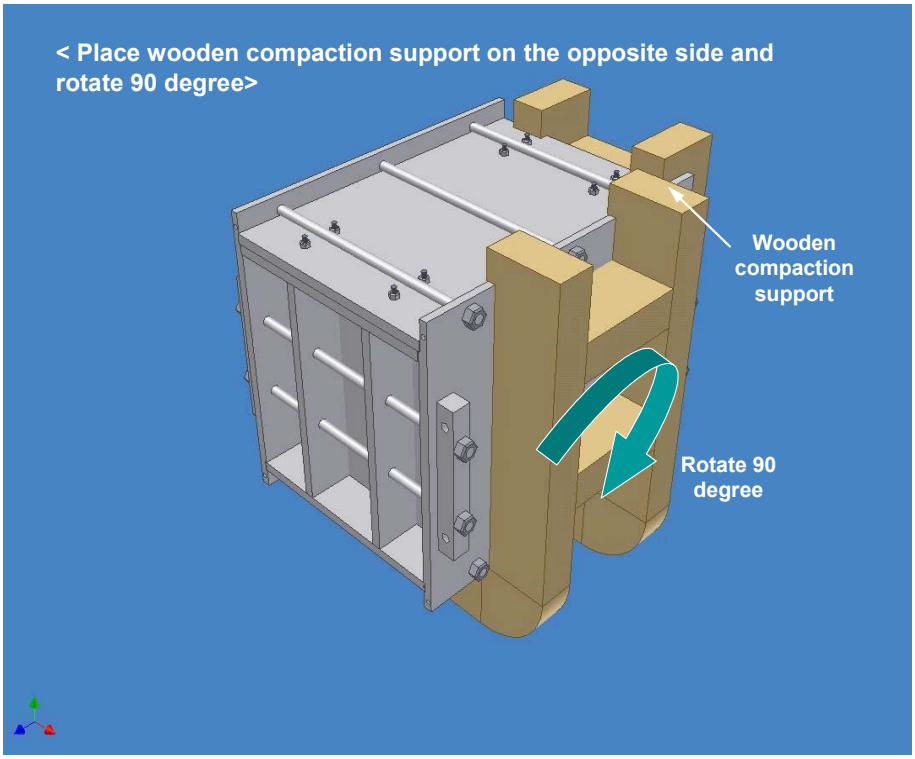

Figure B.24 Step 24 (place wooden compaction support on the opposite side and rotate 90 degree)

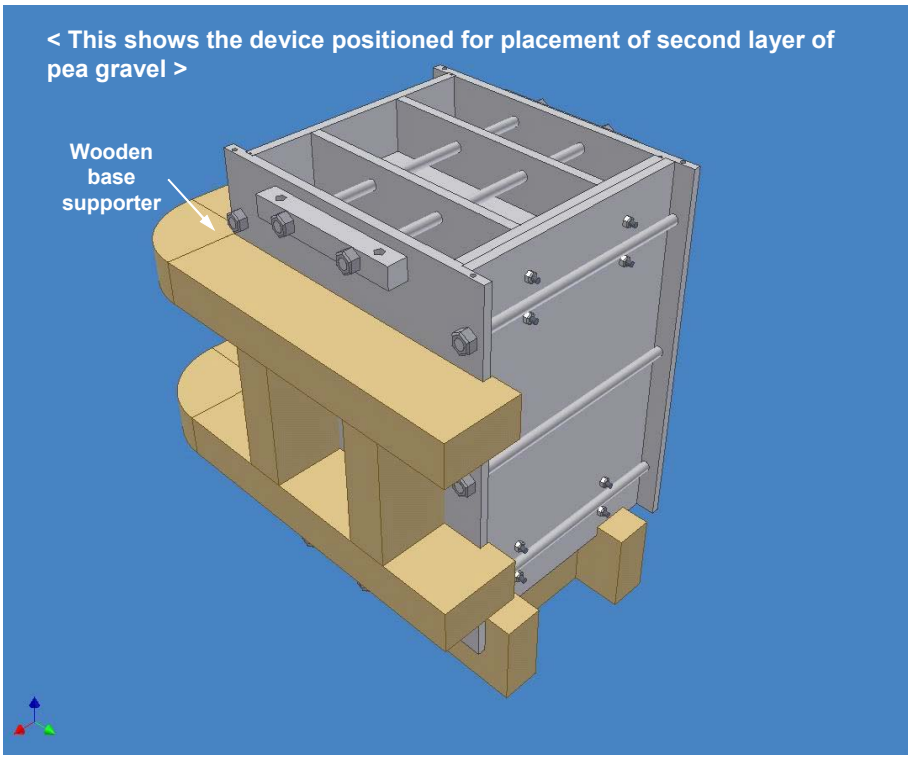

Figure B.25 Step 25 (the device positioned for placement of second layer of pea gravel)

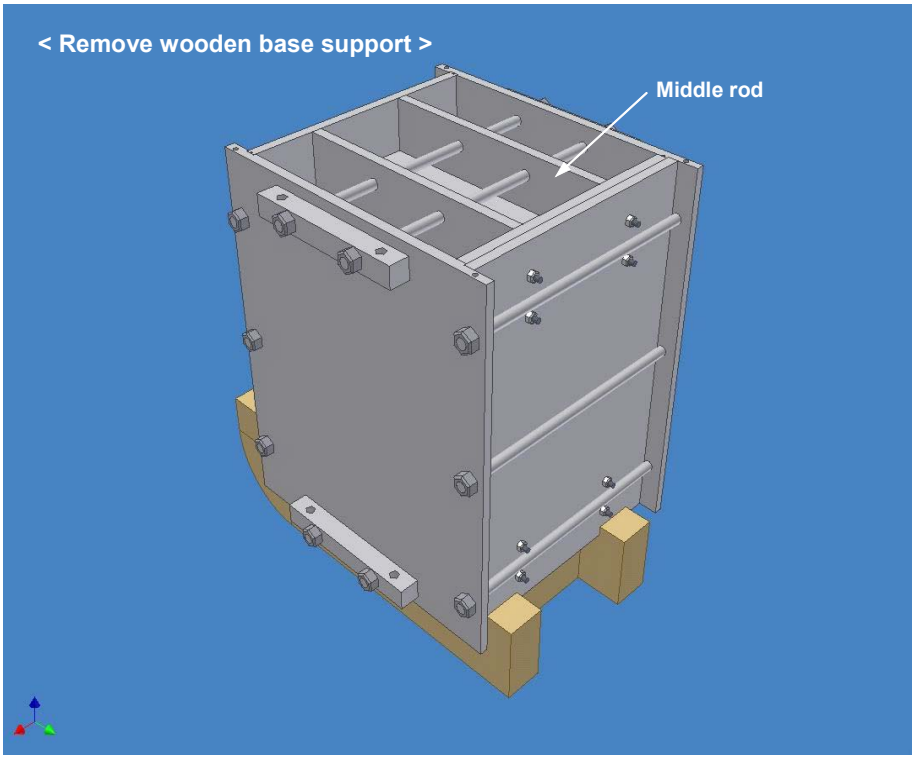

Figure B.26 Step 26 (remove wooden base support)

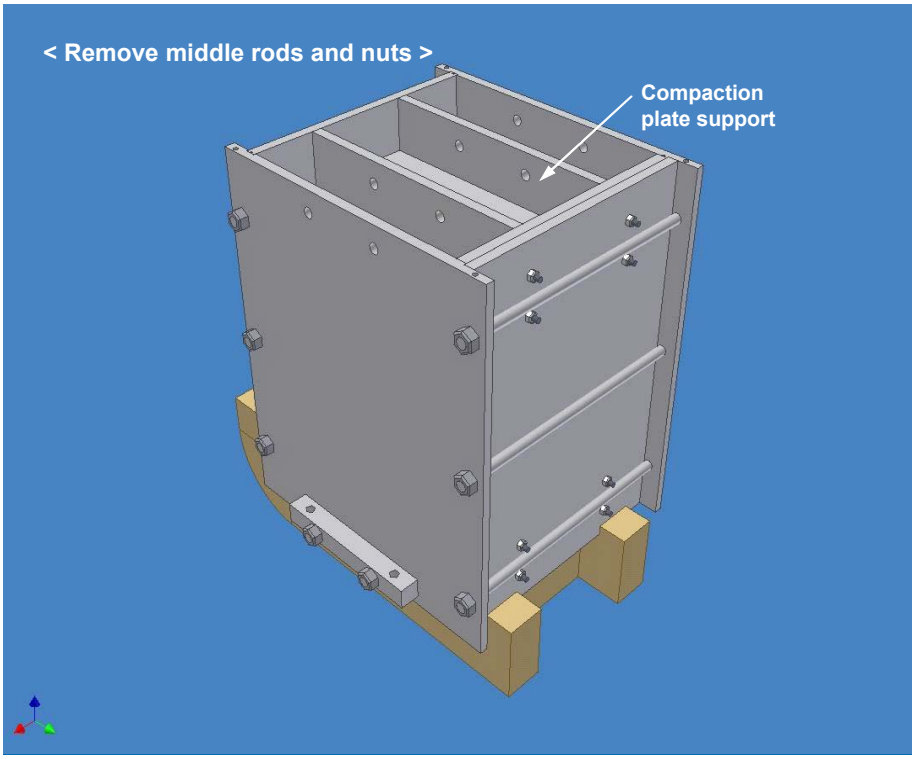

Figure B.27 Step 27 (remove middle rods and nuts)

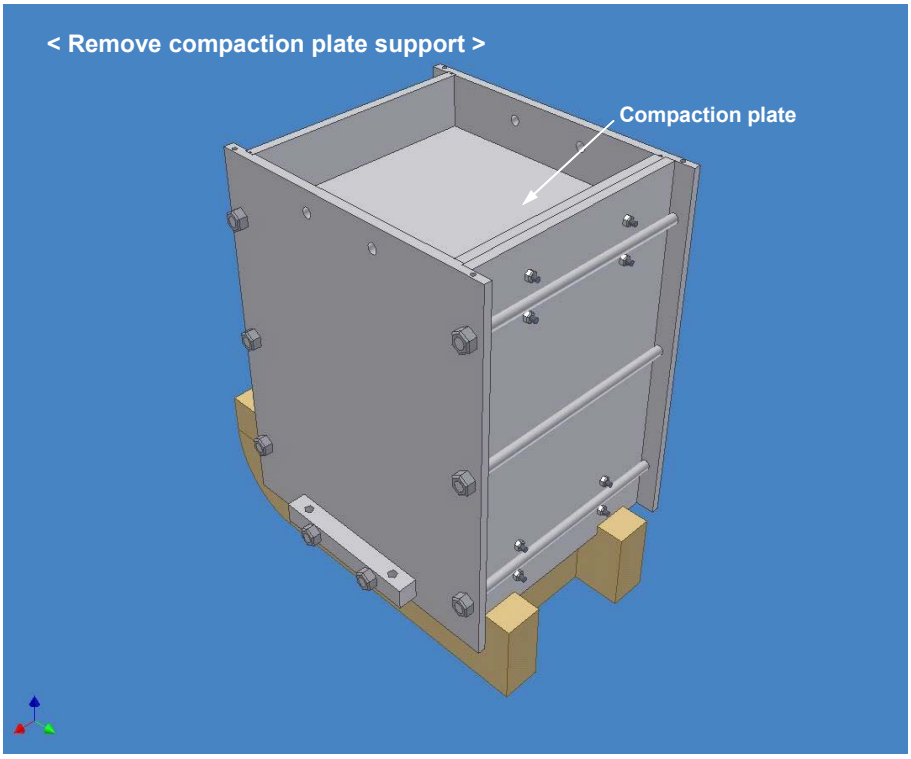

Figure B.28 Step 28 (remove compaction plate support)

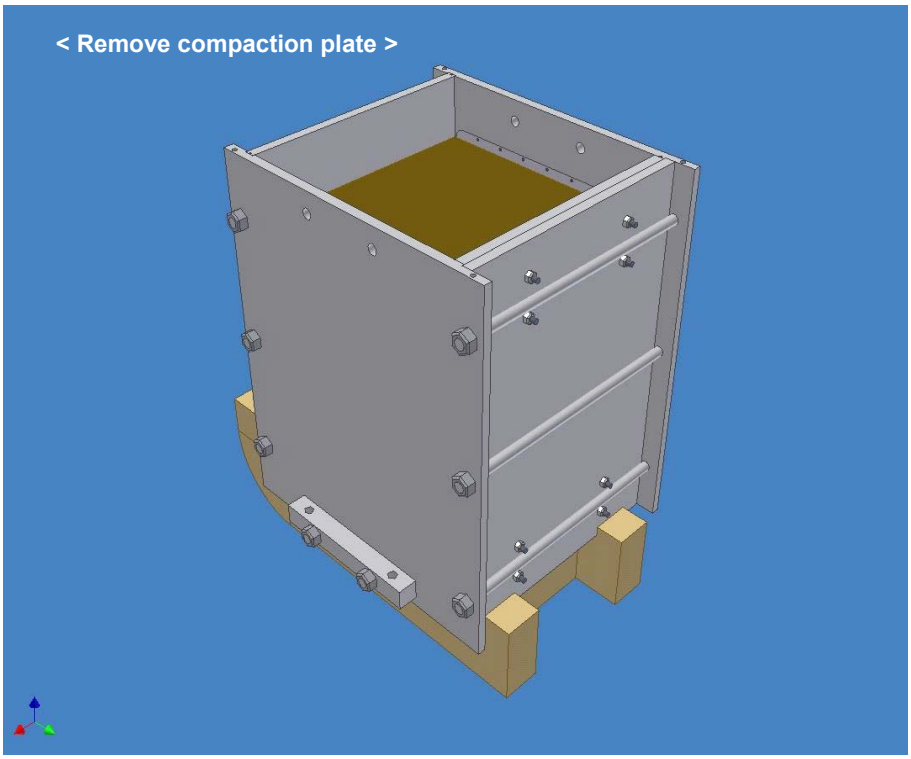

Figure B.29 Step 29 (remove compaction plate)

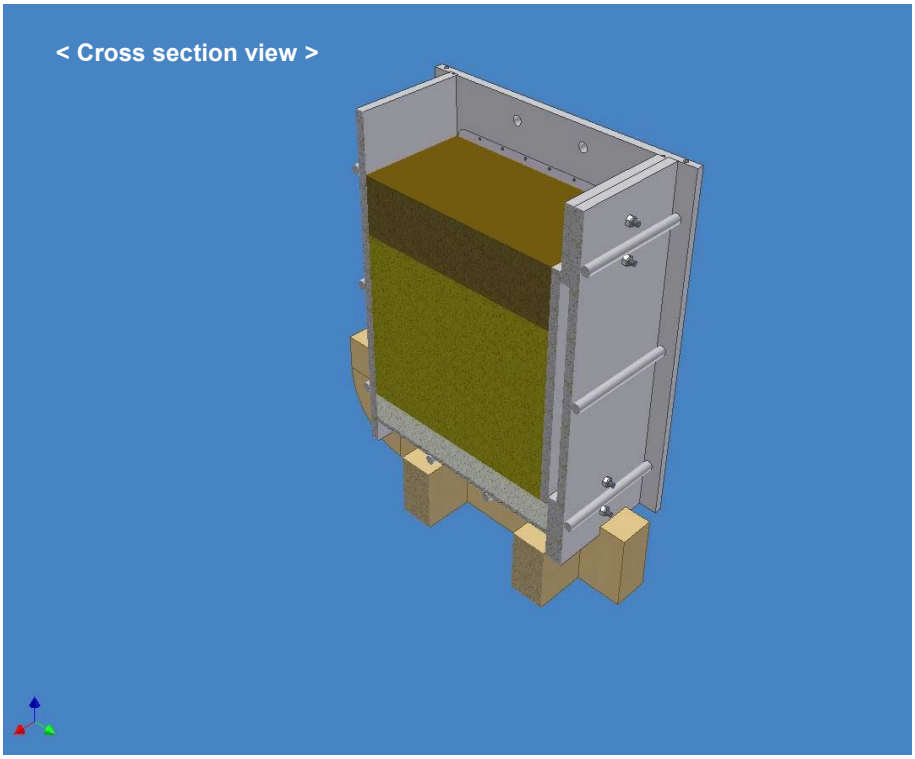

Figure B.30 Step 30 (cross section view)

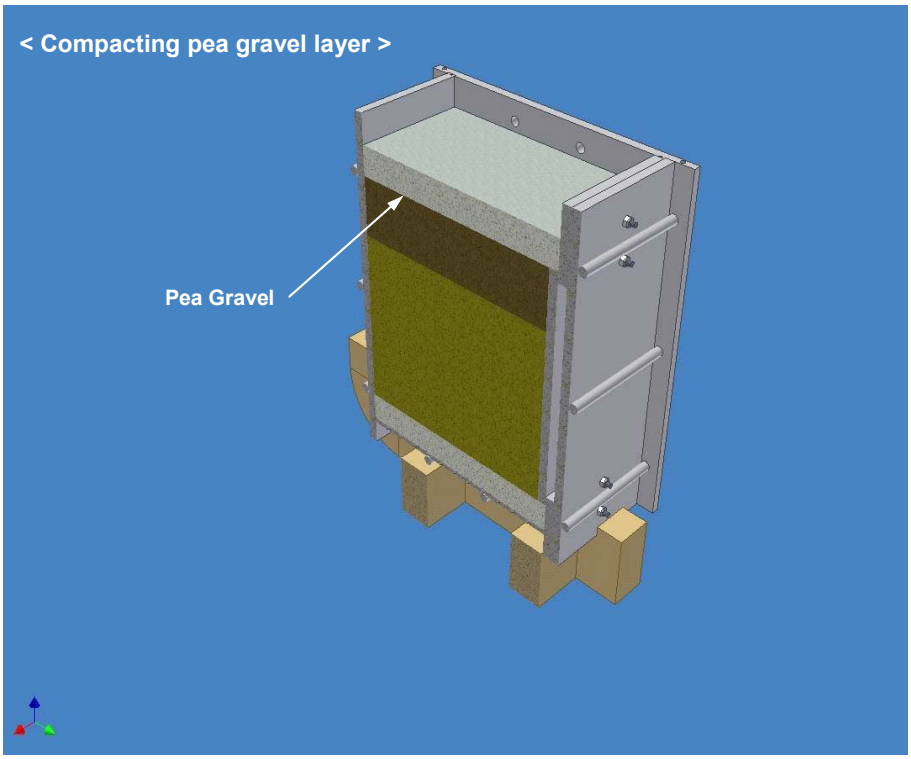

Figure B.31 Step 31 (compacting pea gravel layer)

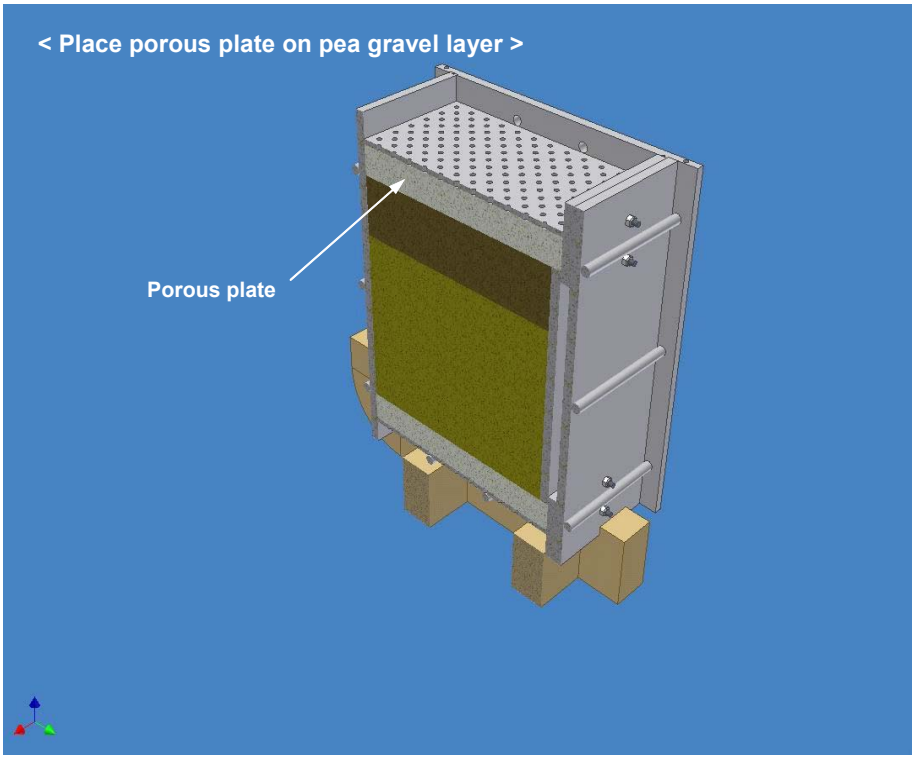

Figure B.32 Step 32 (place porous plate)

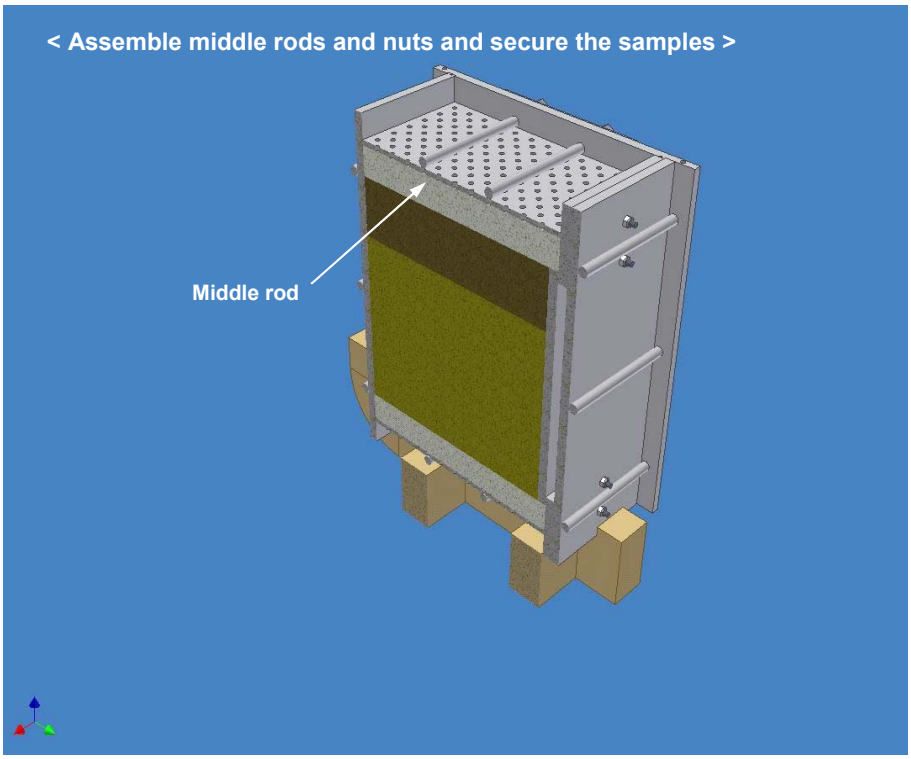

Figure B.33 Step 33 (assemble middle rods and nuts)

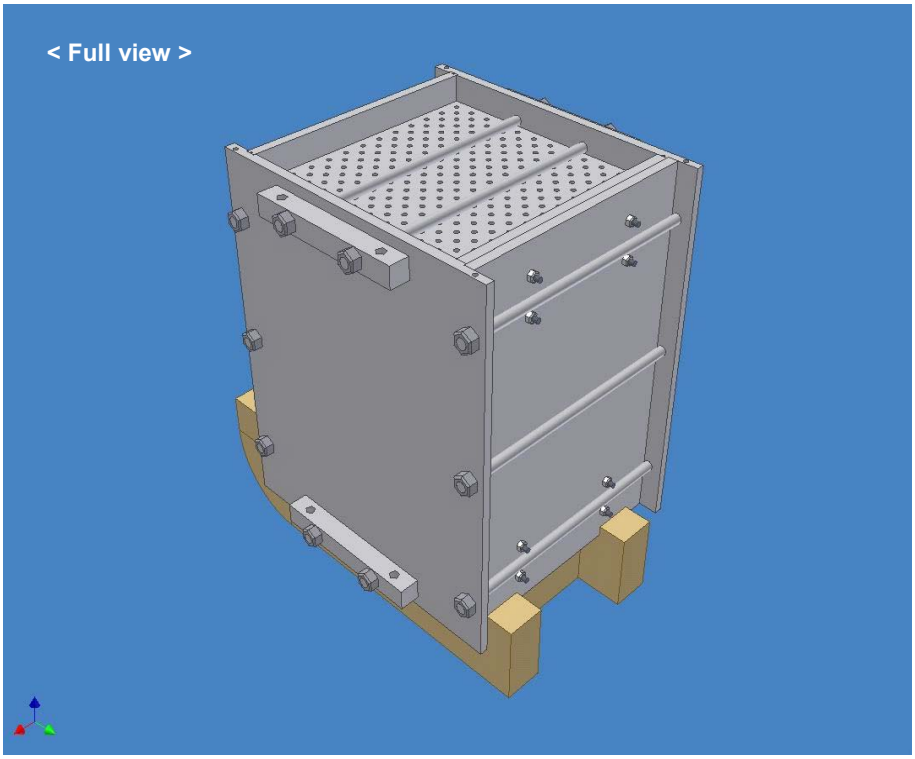

Figure B.34 Step 34 (full view)

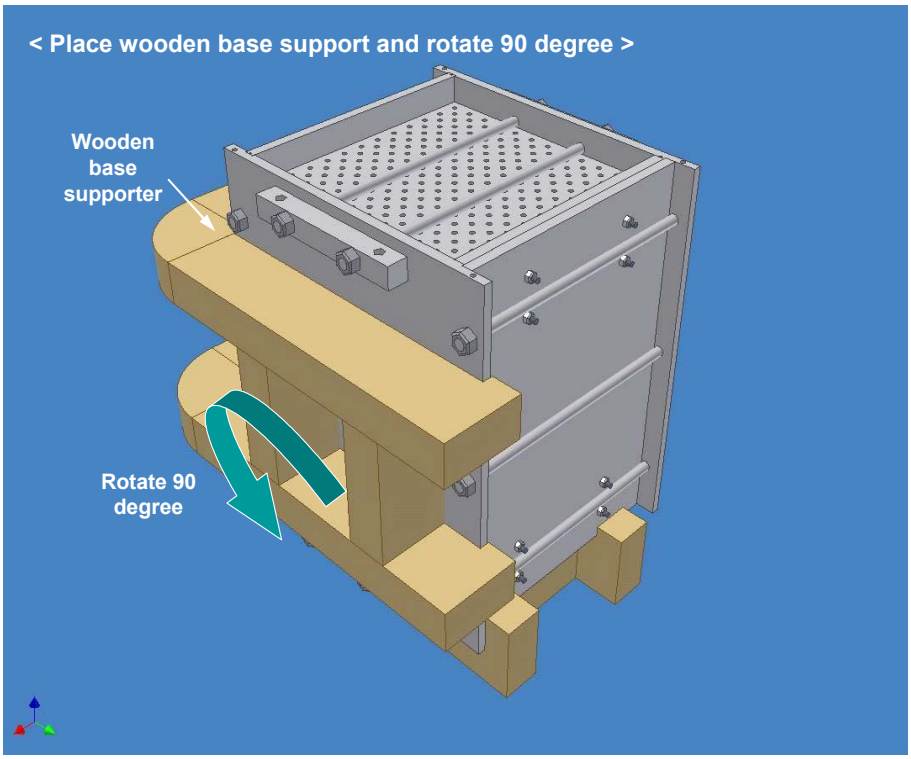

Figure B.35 Step 35 (place wooden base support and rotate 90 degree)

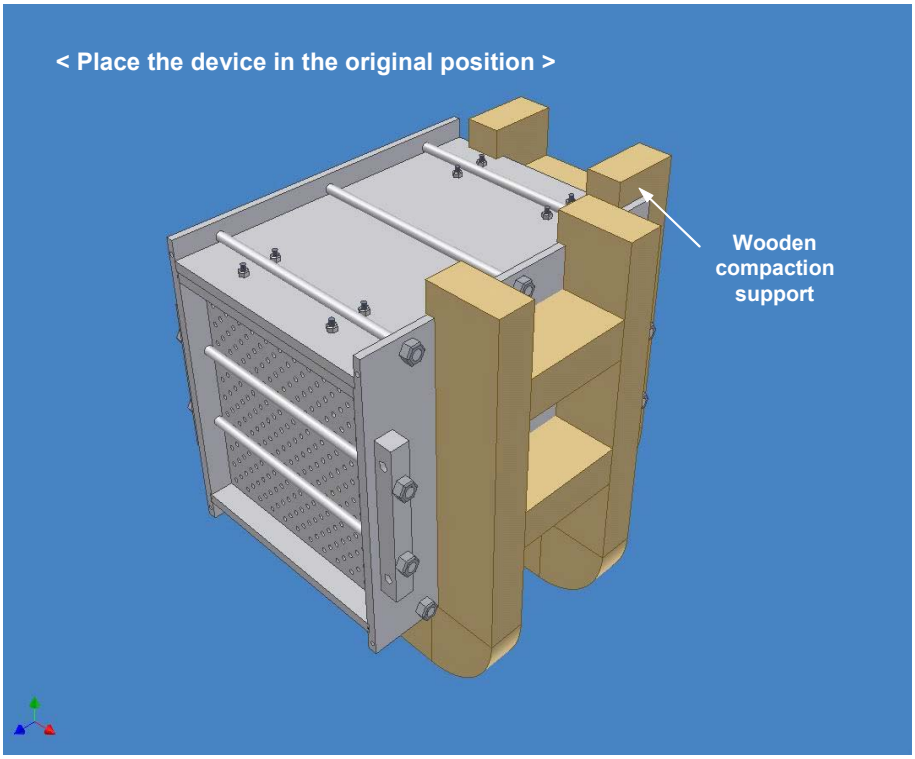

Figure B.36 Step 36 (place the device in the original position)

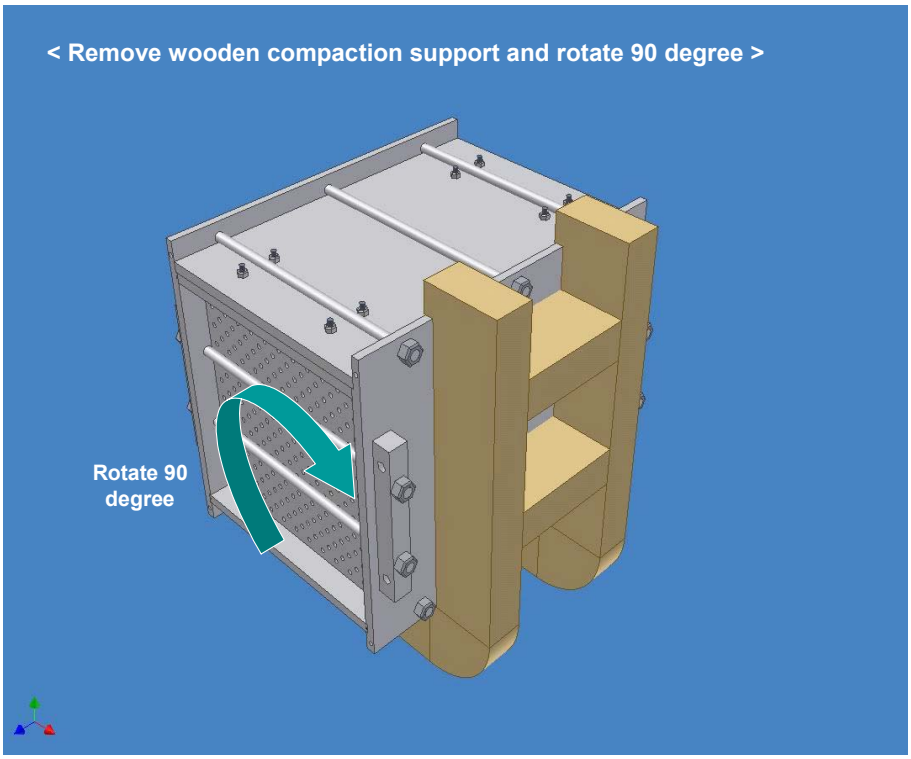

Figure B.37 Step 37 (remove wooden compaction support and rotate 90 degree)

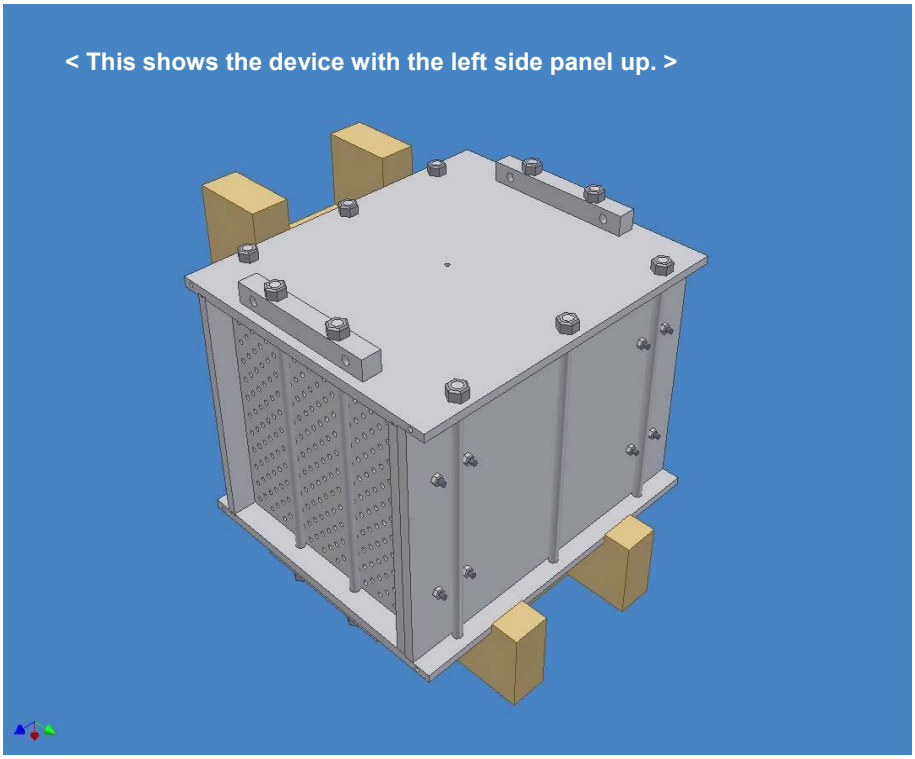

Figure B.38 Step 38 (the device with left side panel to up)

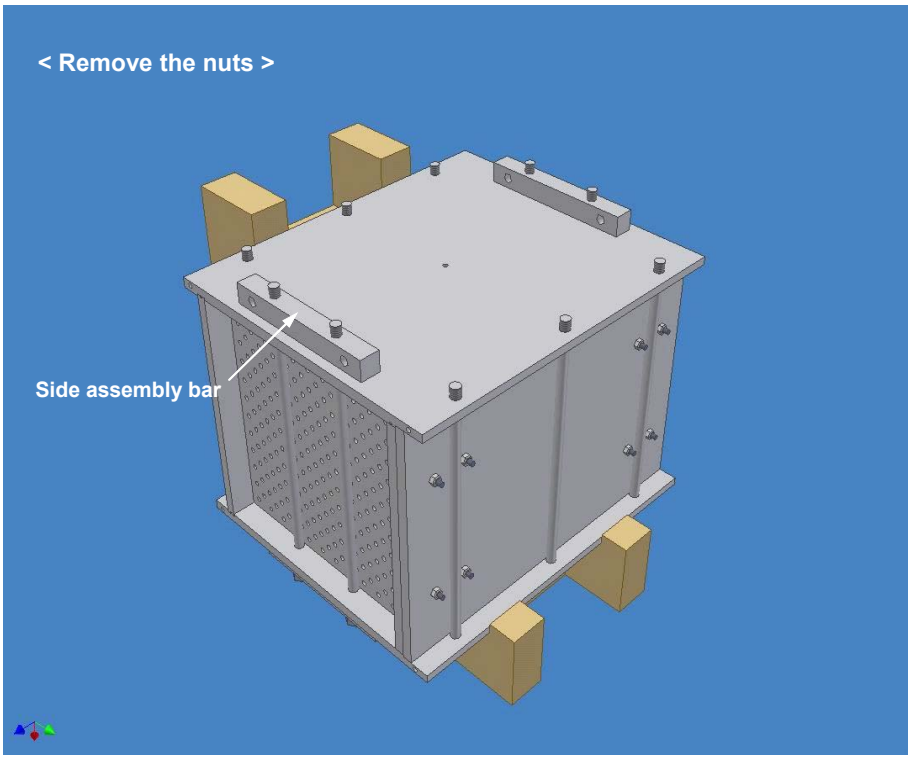

Figure B.39 Step 39 (remove the nuts)

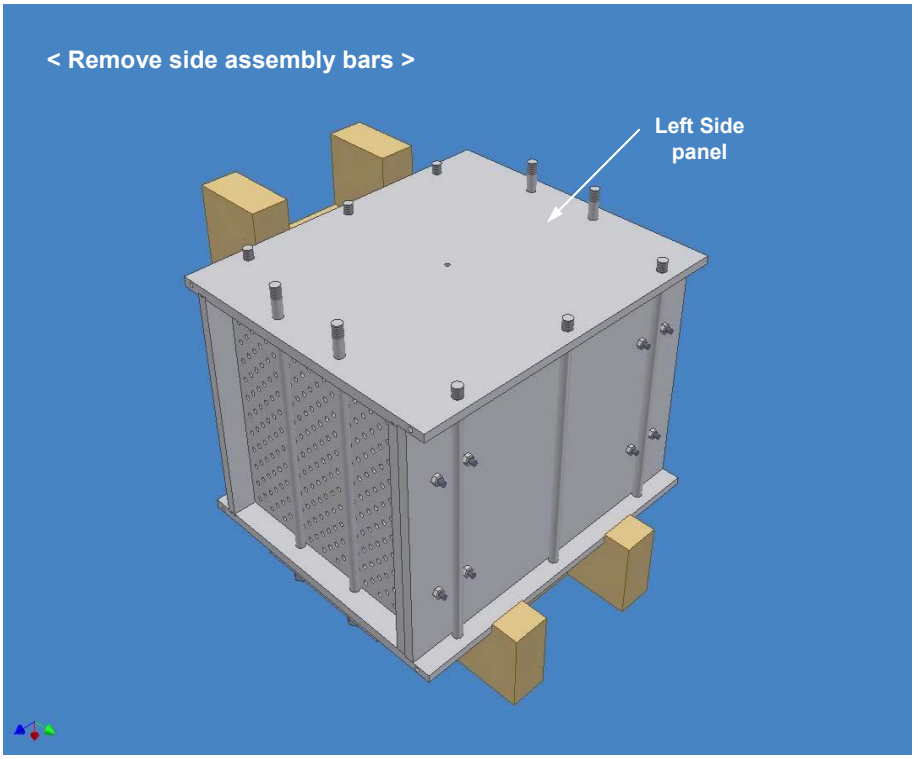

Figure B.40 Step 40 (remove side assembly bars)

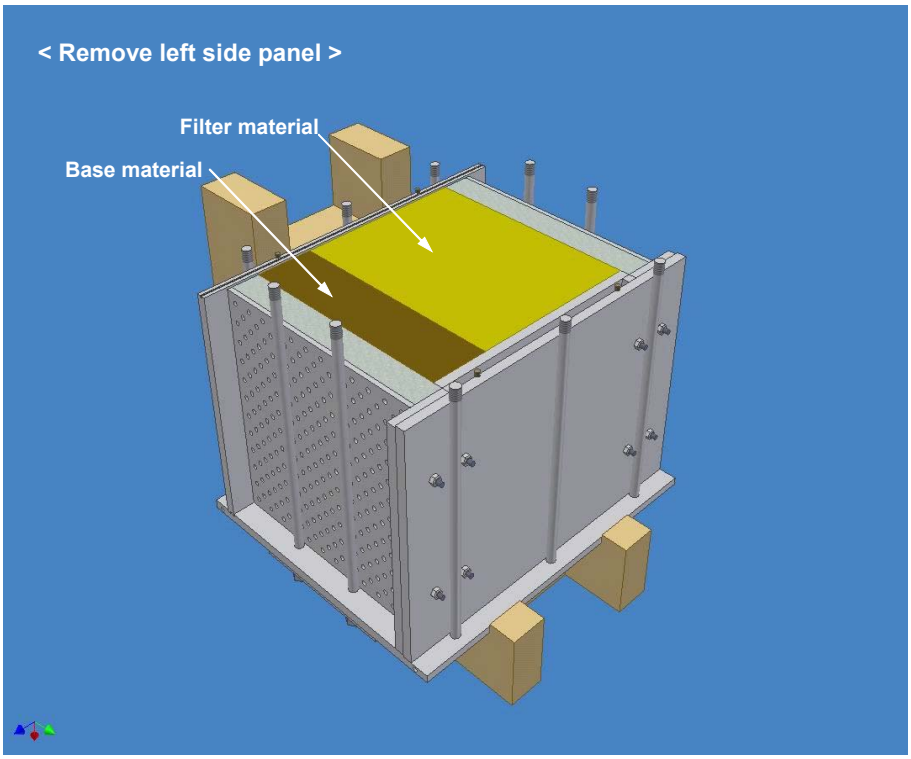

Figure B.41 Step 41 (remove left side panel)

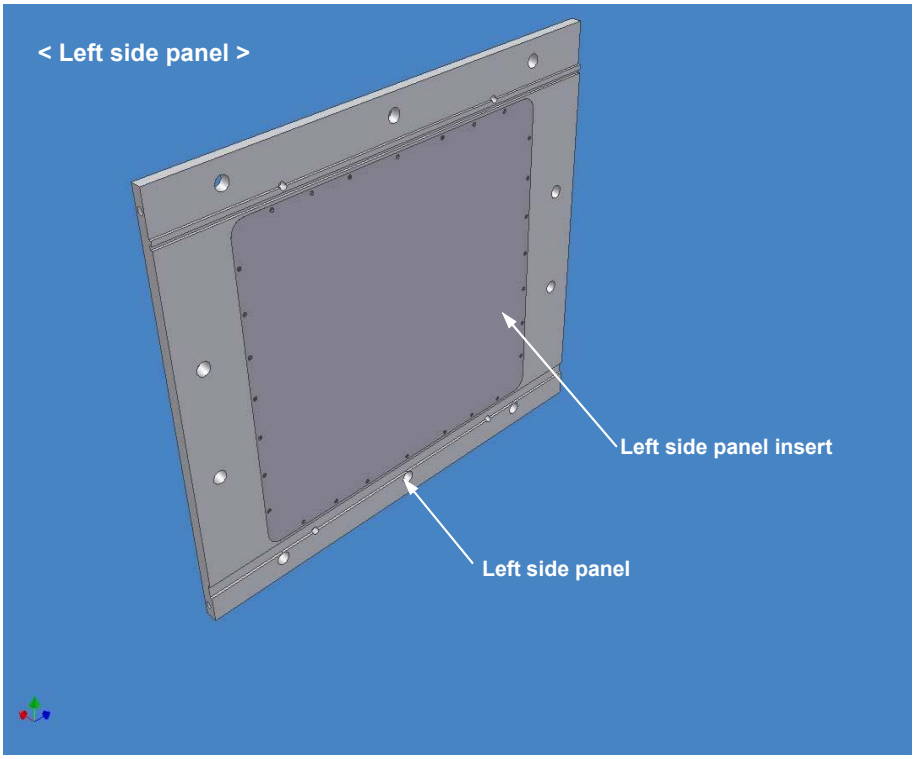

Figure B.42 Step 42 (left side panel)

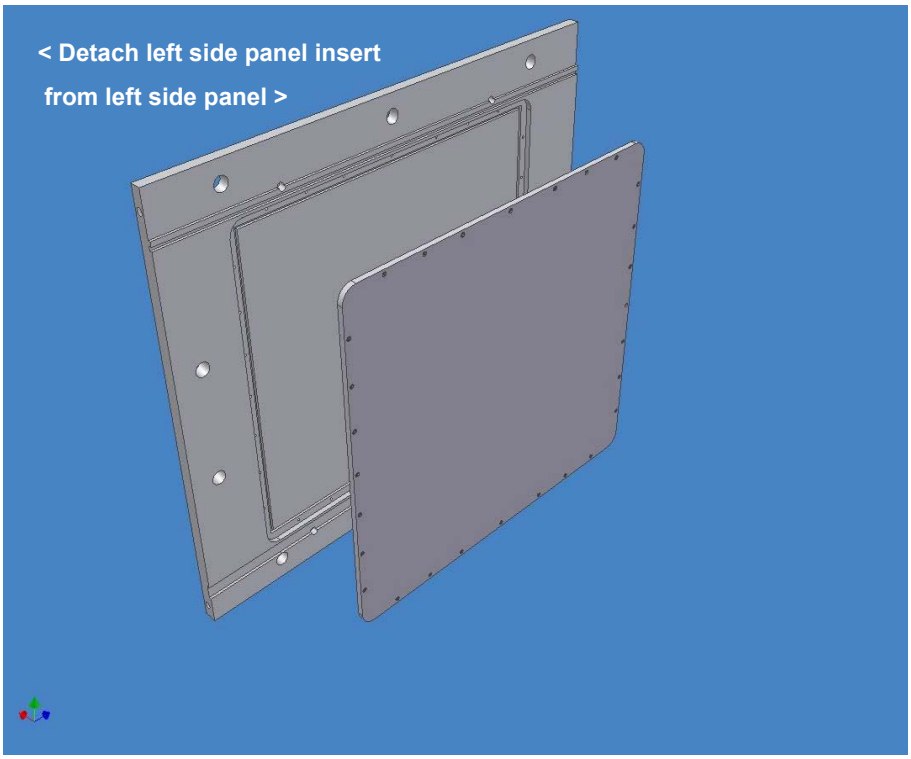

Figure B.43 Step 43 (detach left side panel insert)

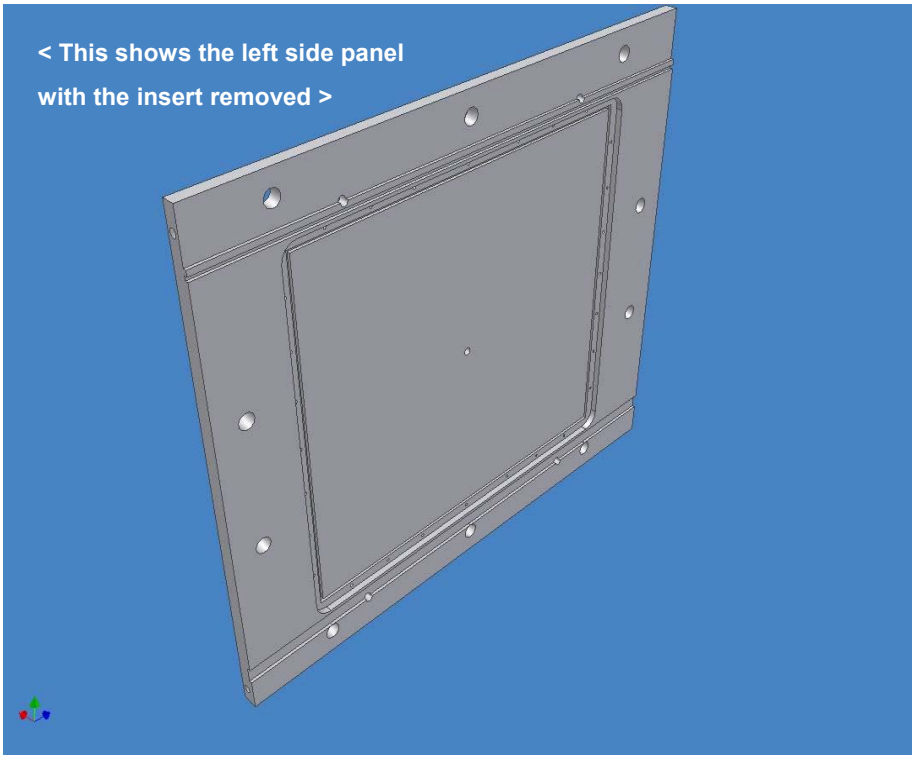

Figure B.44 Step 44 (the left side panel with the insert removed)

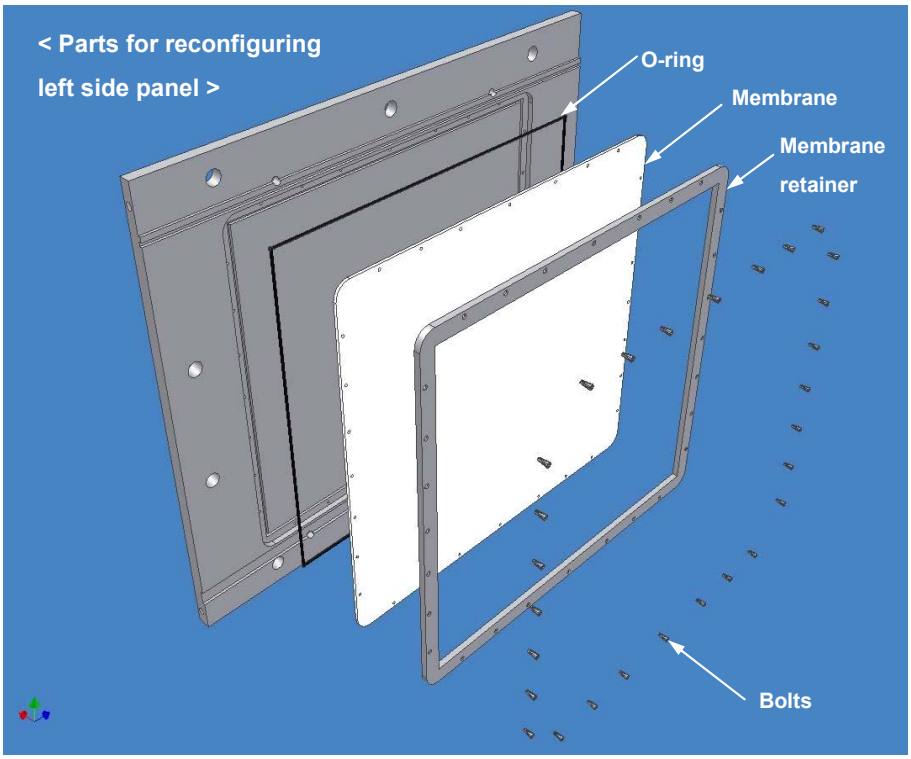

Figure B.45 Step 45 (parts for reconfiguring left side panel)

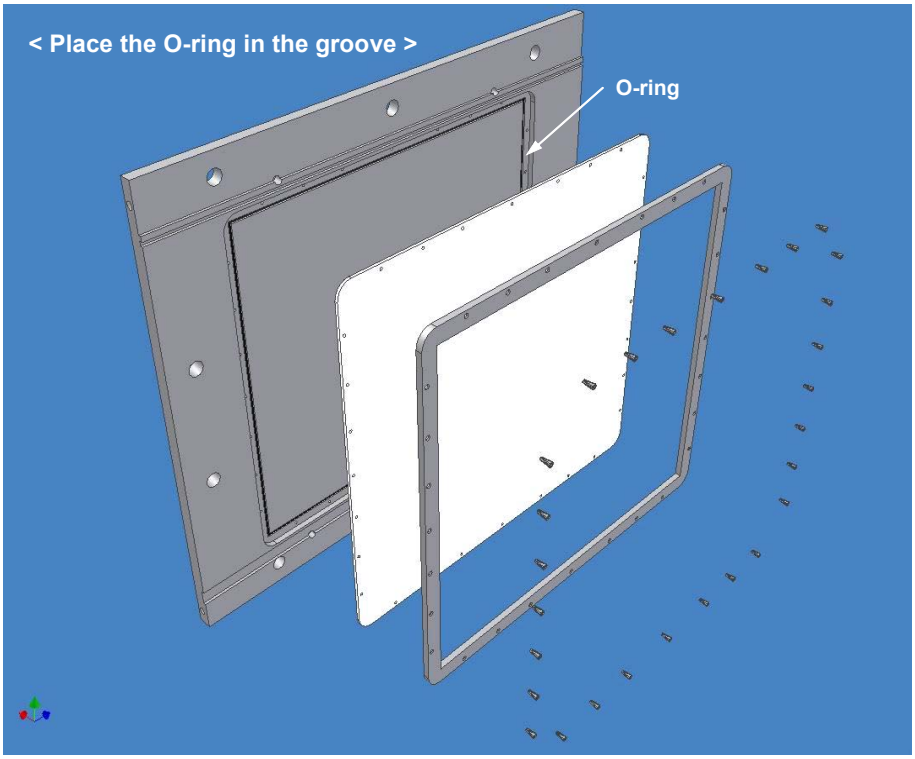

Figure B.46 Step 46 (place O-ring in the groove)

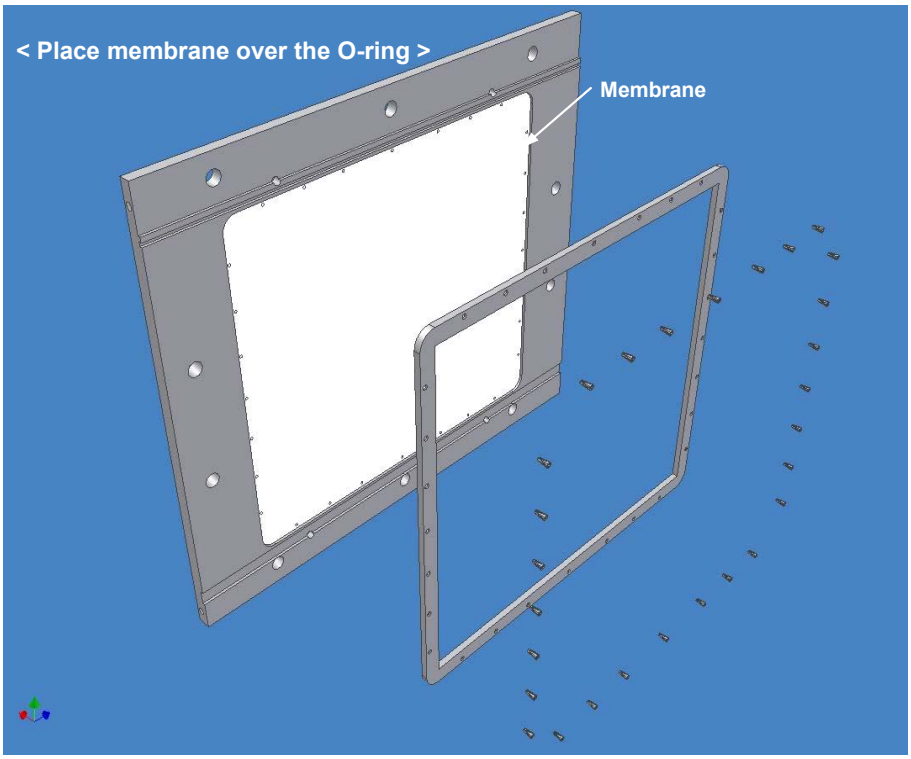

Figure B.47 Step 47 (place membrane over the O-ring)

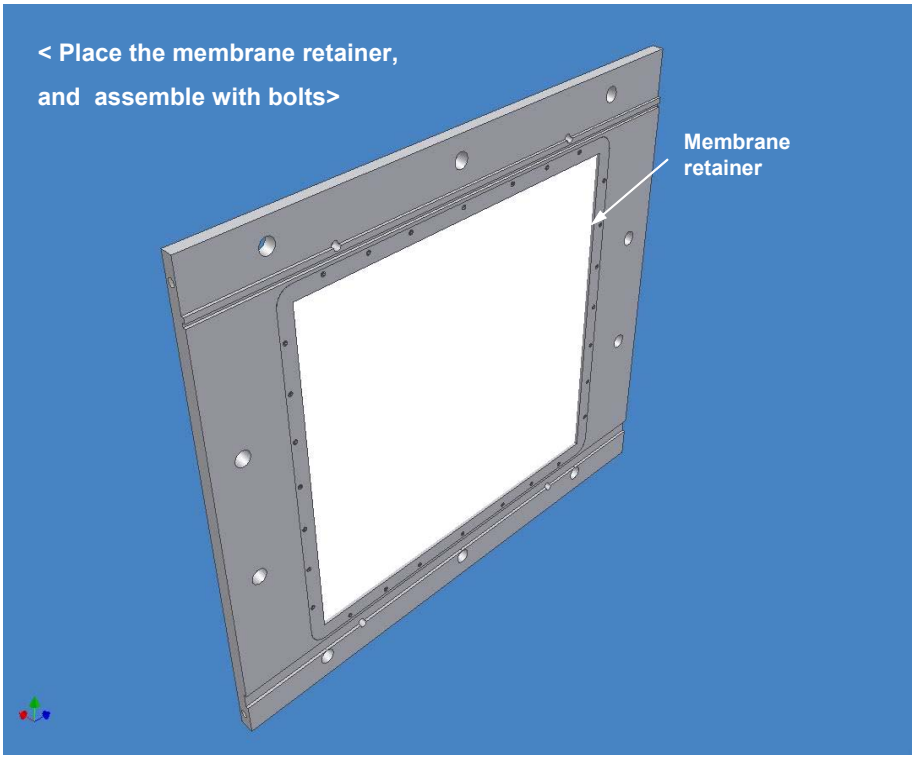

Figure B.48 Step 48 (place the membrane retainer, and assemble with bolts)

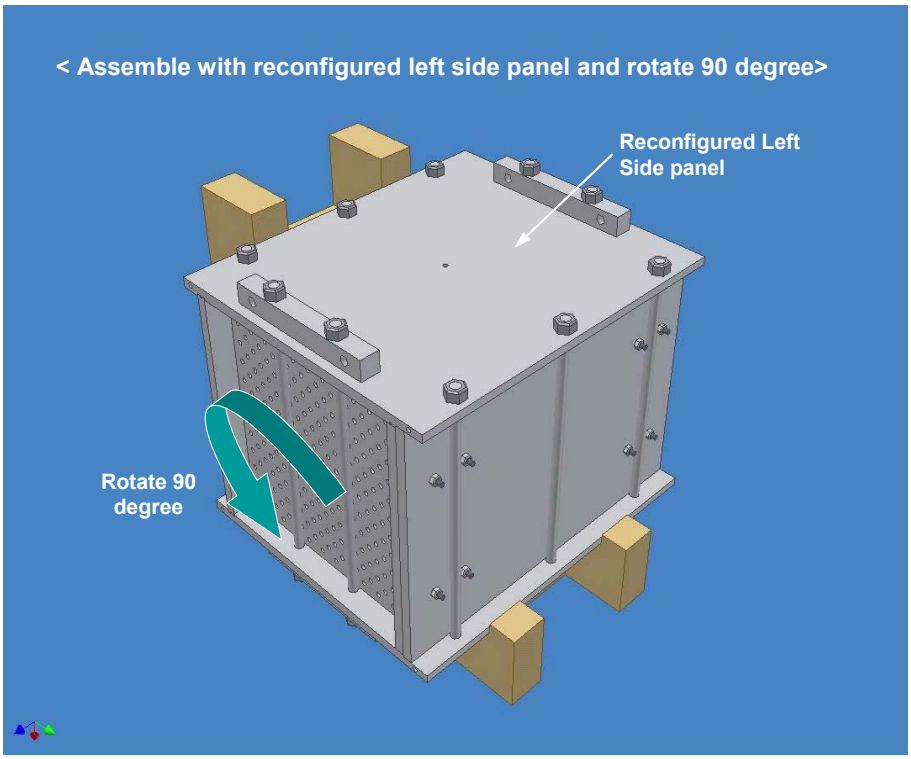

Figure B.49 Step 49 (assemble with re-configured left side panel and rotate 90 degree)

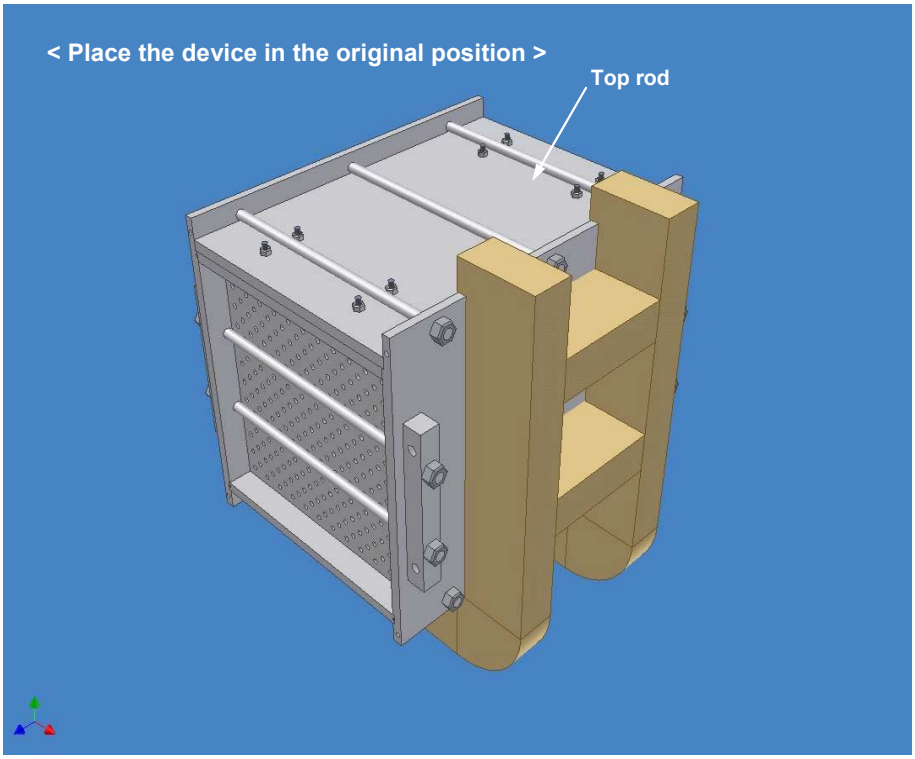

Figure B.50 Step 50 (place the device in the original position)

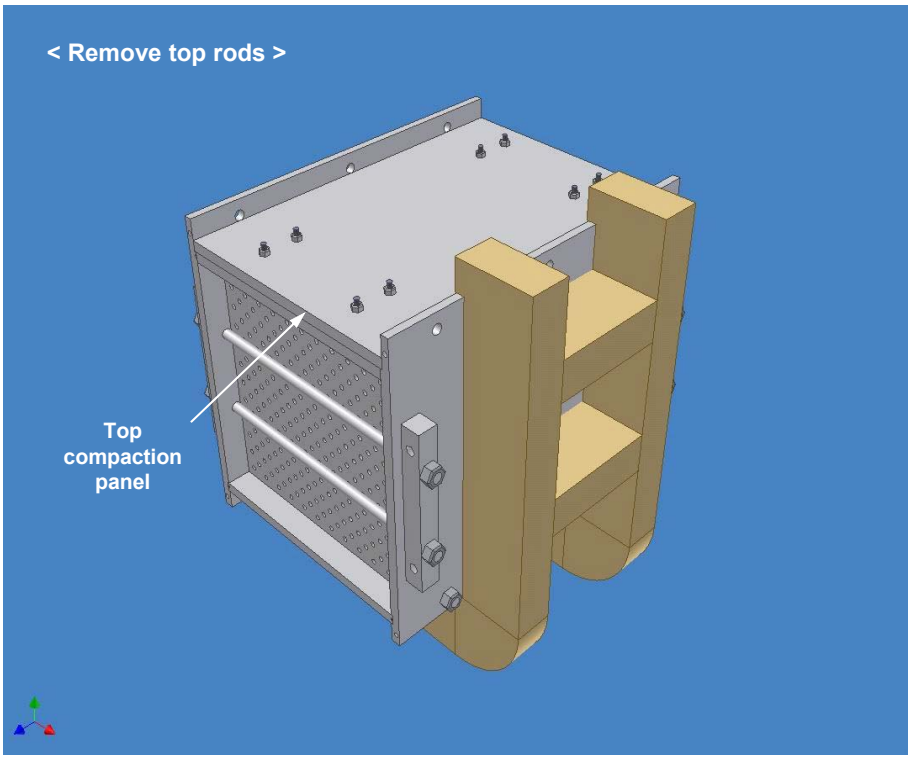

Figure B.51 Step 51 (remove top rods)

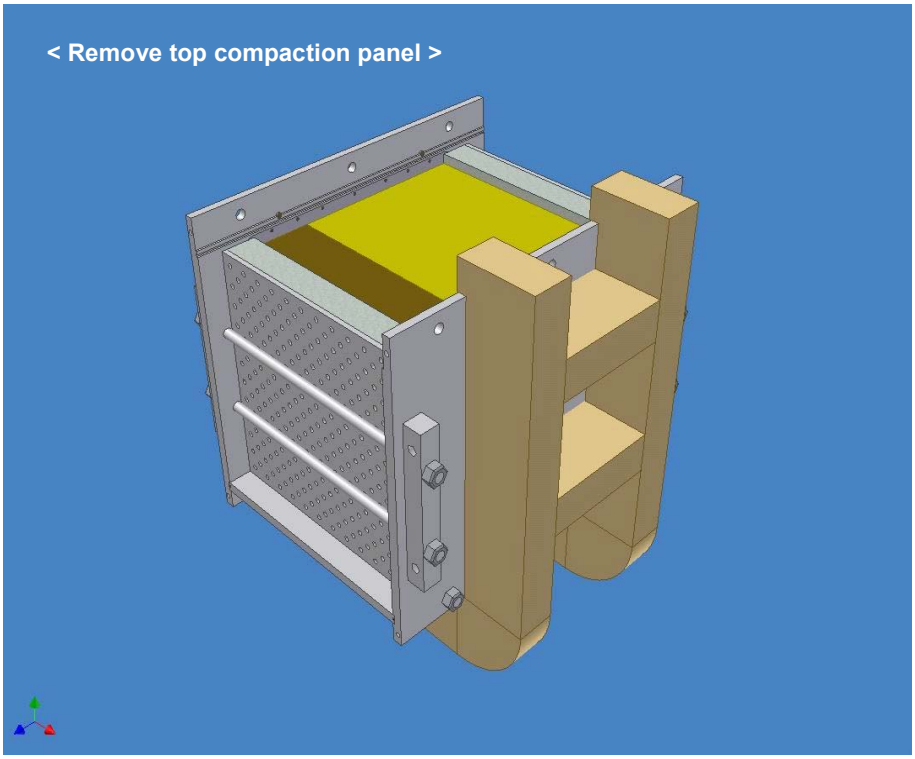

Figure B.52 Step 52 (remove top compaction panel)

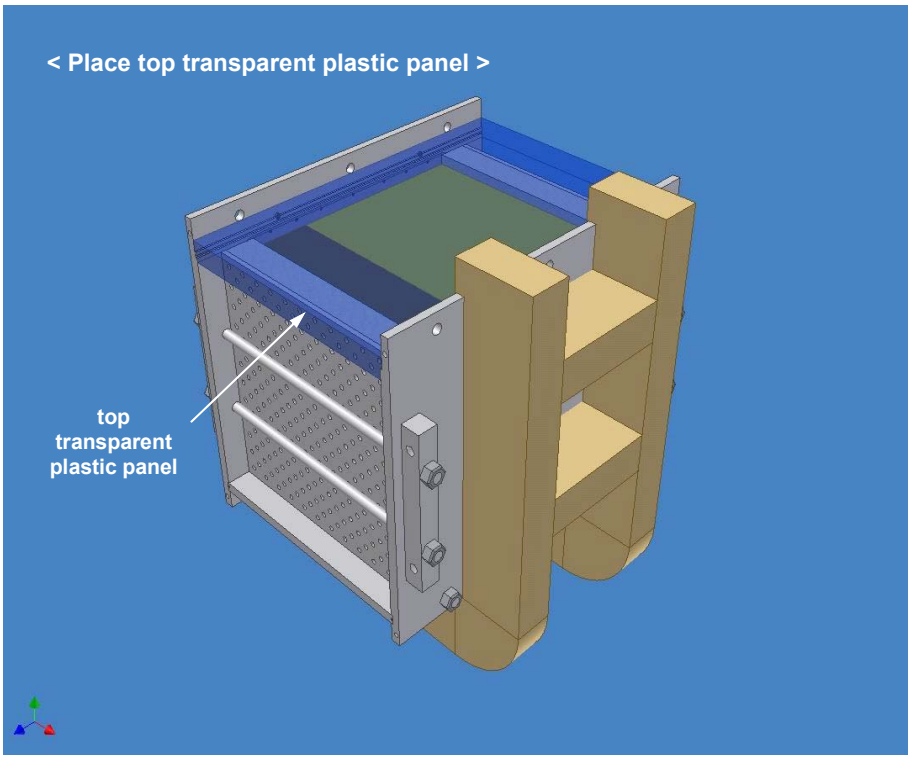

Figure B.53 Step 53 (place top transparent plastic panel)

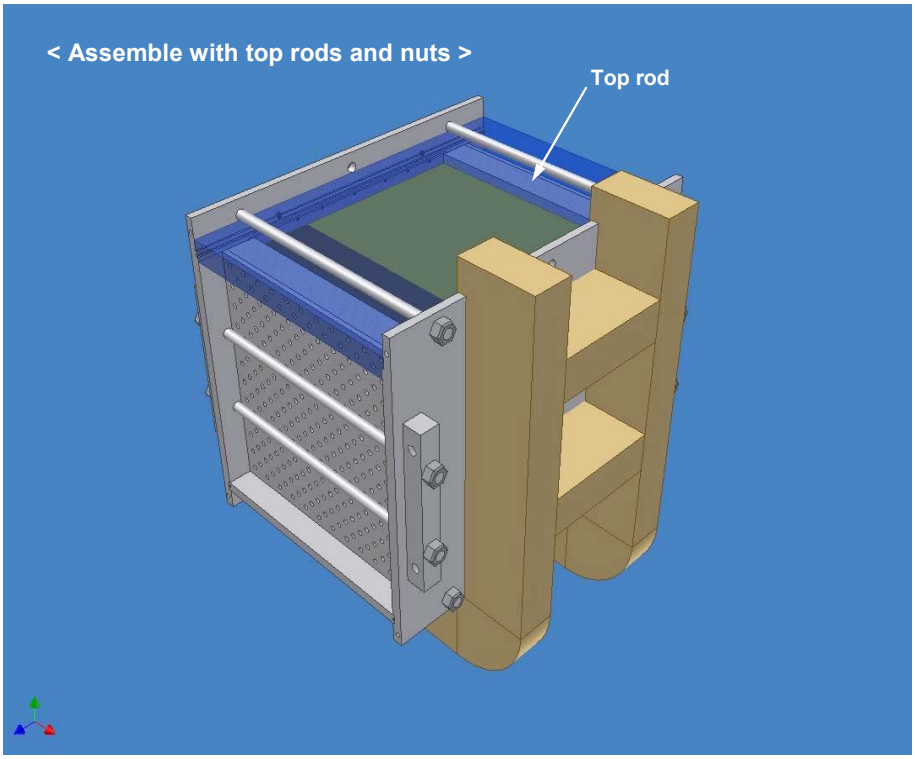

Figure B.54 Step 54 (assemble with top rods and nuts)

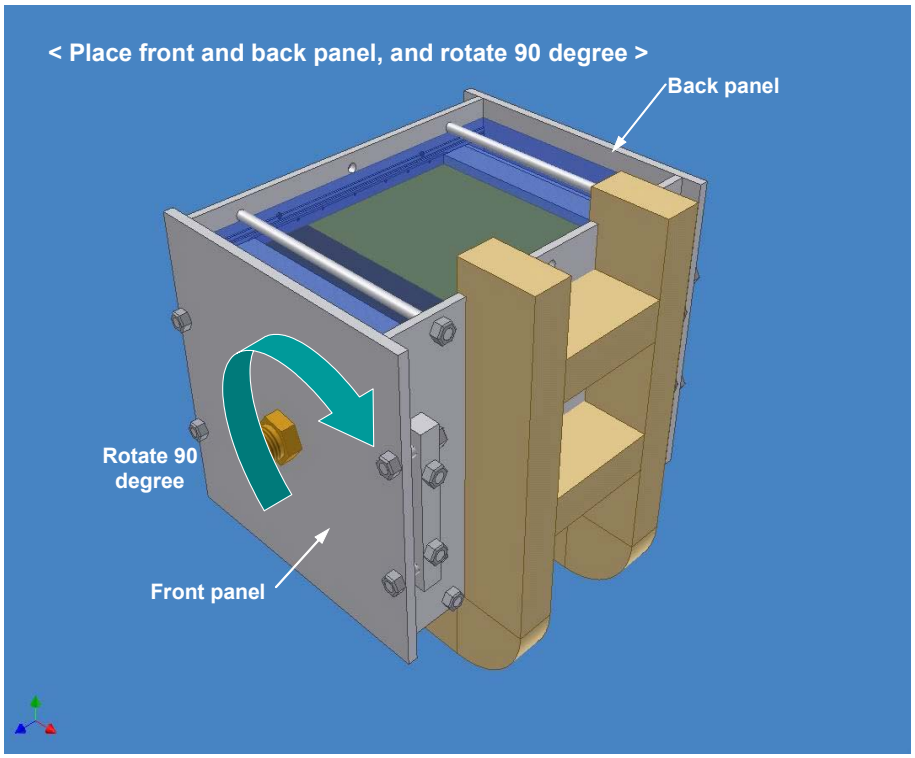

Figure B.55 Step 55 (place front and back panel and rotate 90 degree)

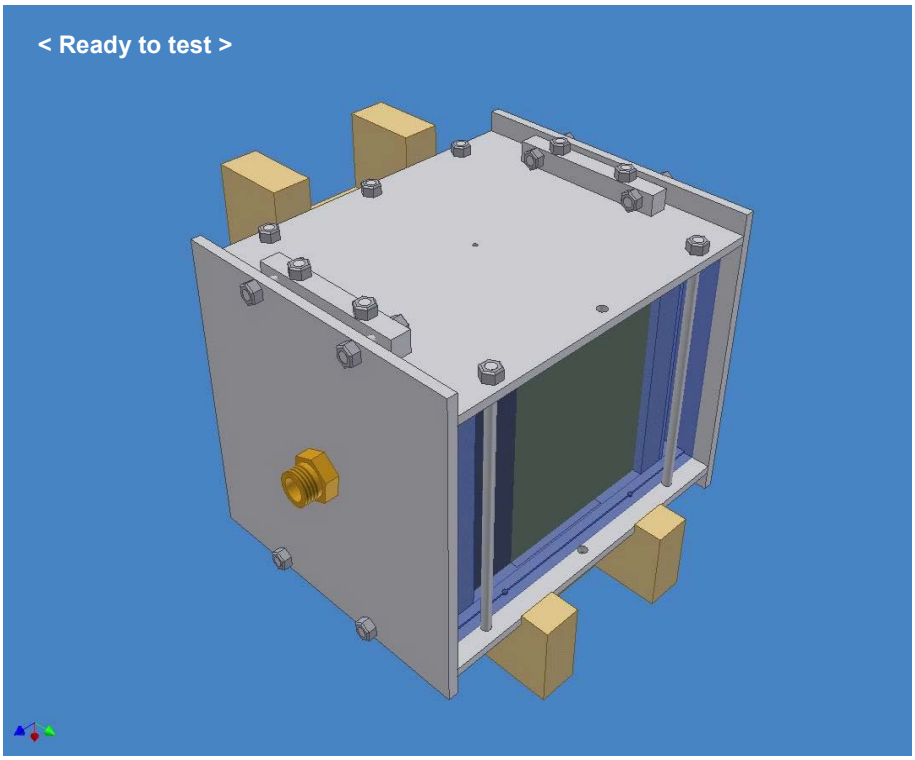

Figure B.56 Step 56 (ready to test)

B.2. Shop Drawings for the 12-inch Square Filter Test Device

The shop drawings for the 12-inch diameter filter test device are shown in Figure B.57 through Figure B.72. All of parts were aluminum, except for the transparent plastic panel shown in Figure B.72.

Bottom Panel

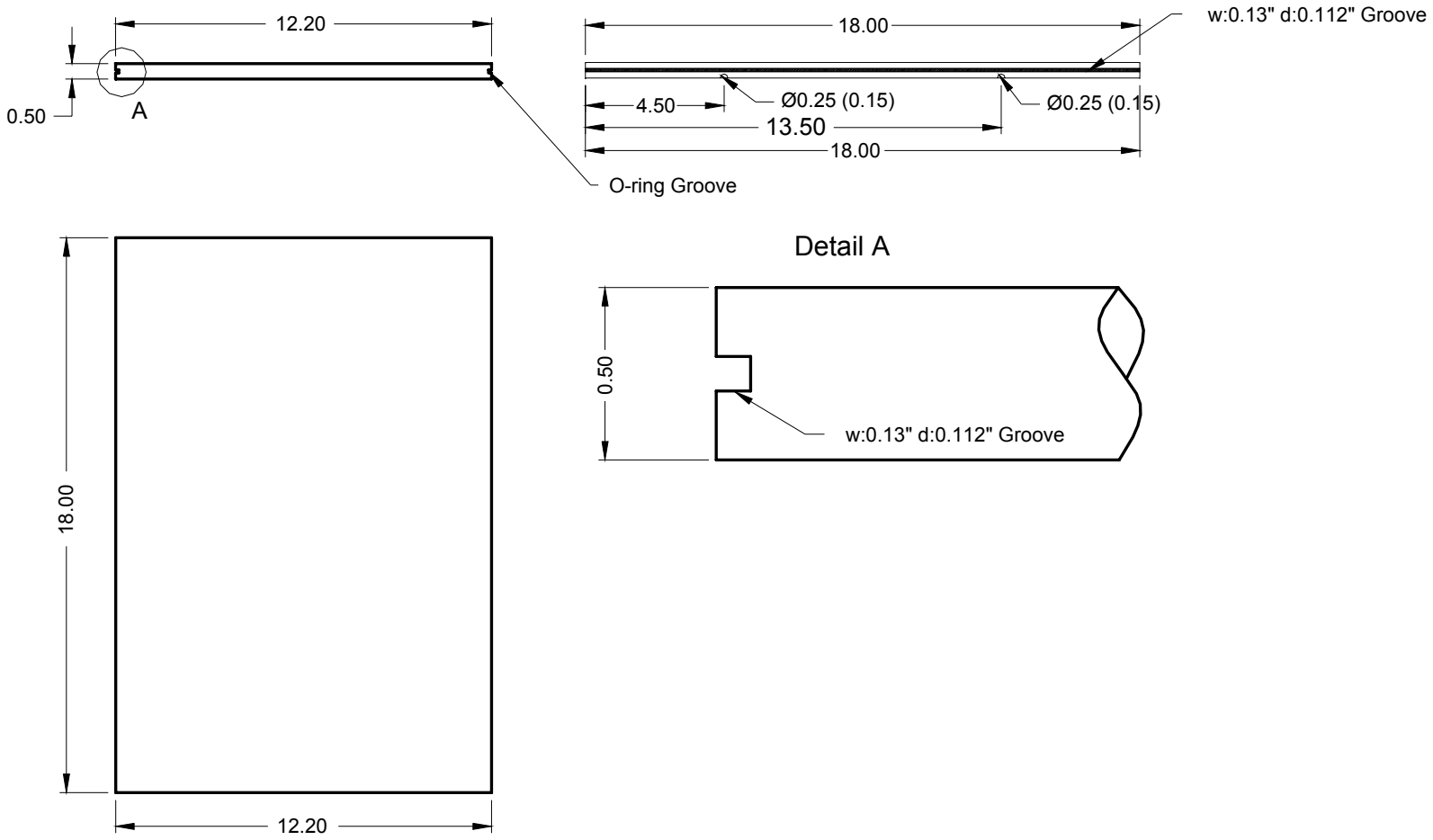

Figure B.57 Bottom panel

Front Panel

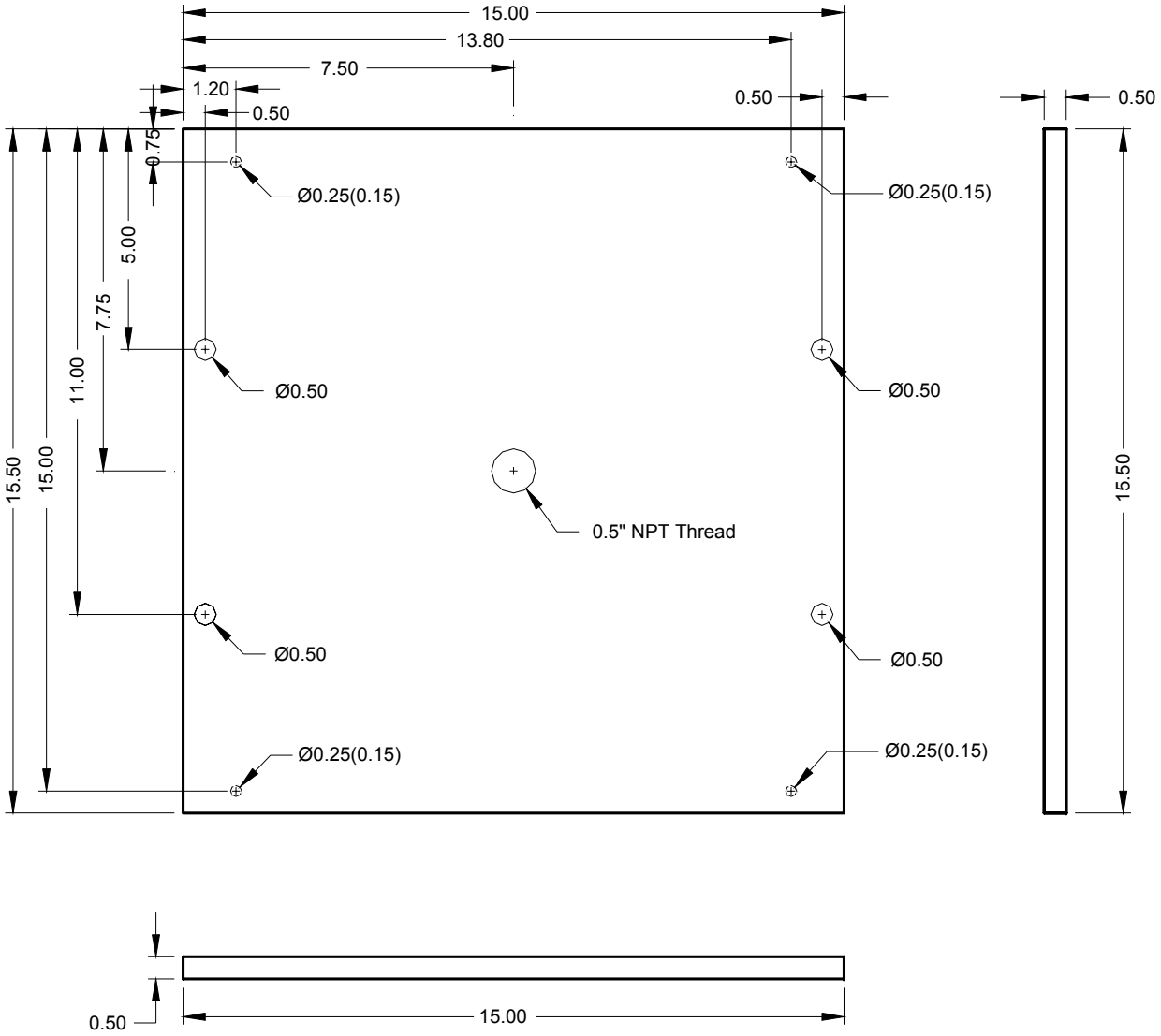

Figure B.58 Front panel

Back Panel

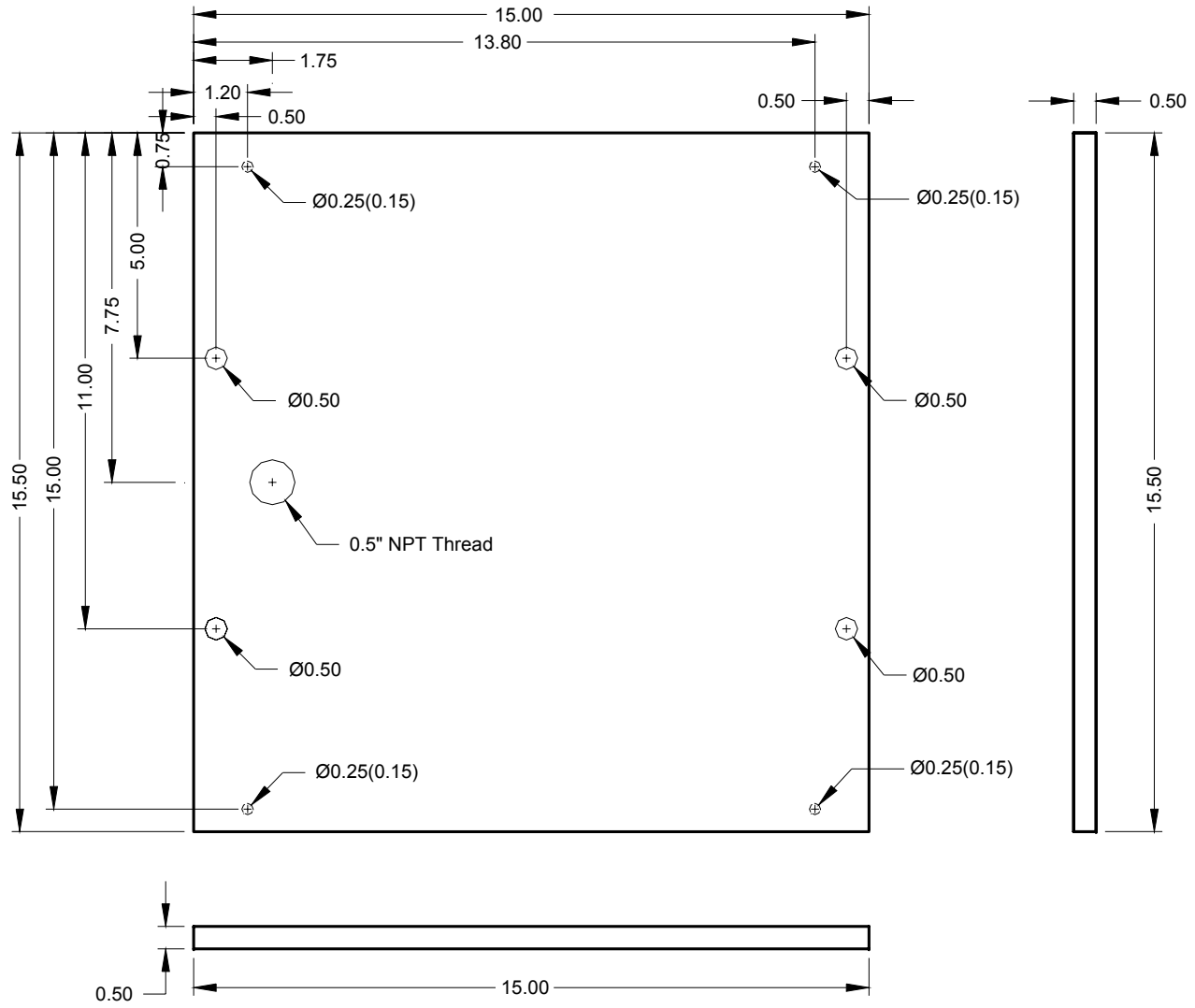

Figure B.59 Back panel

Compaction Plate

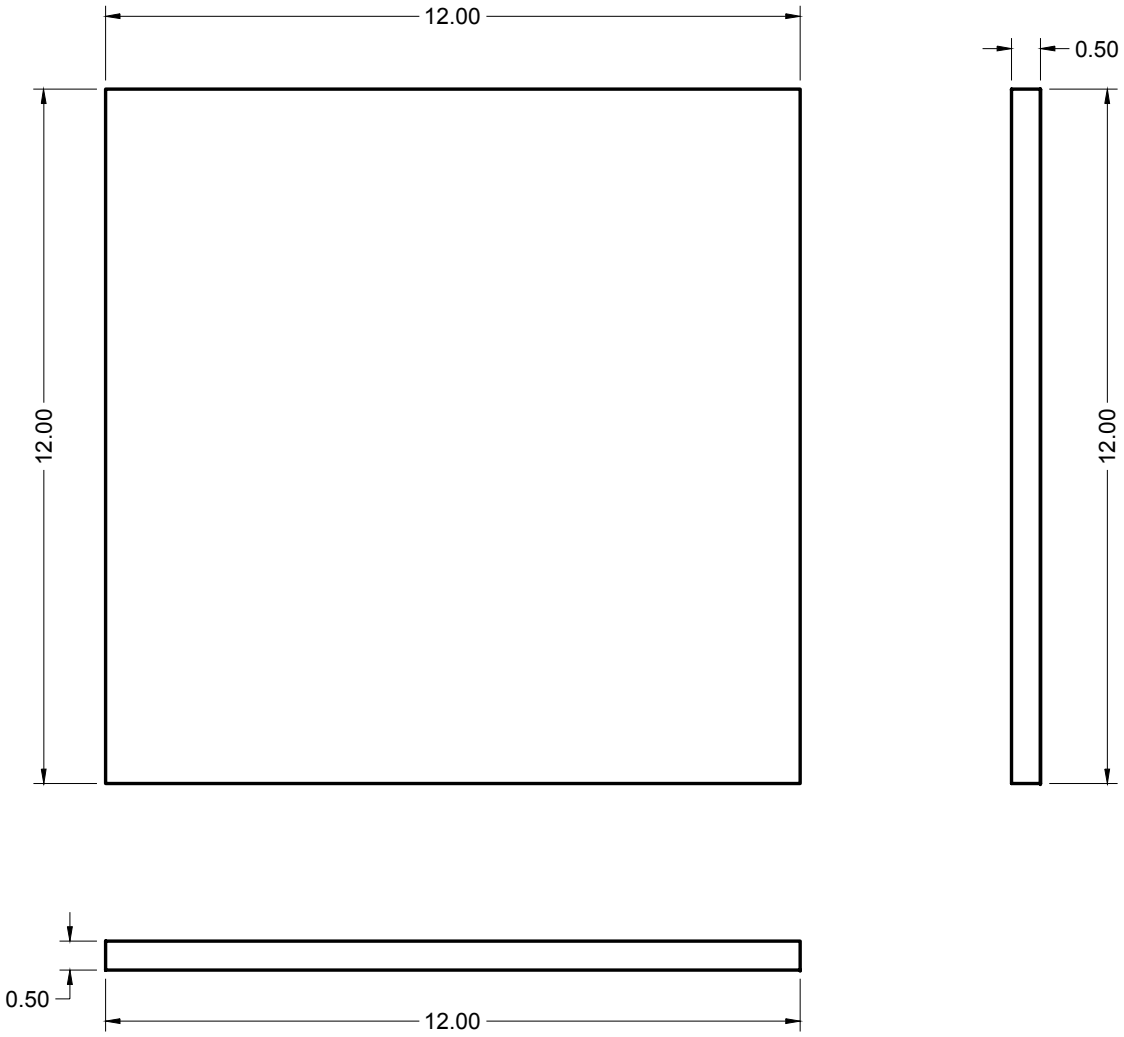

Figure B.60 Compaction panel

Compaction Plate Support

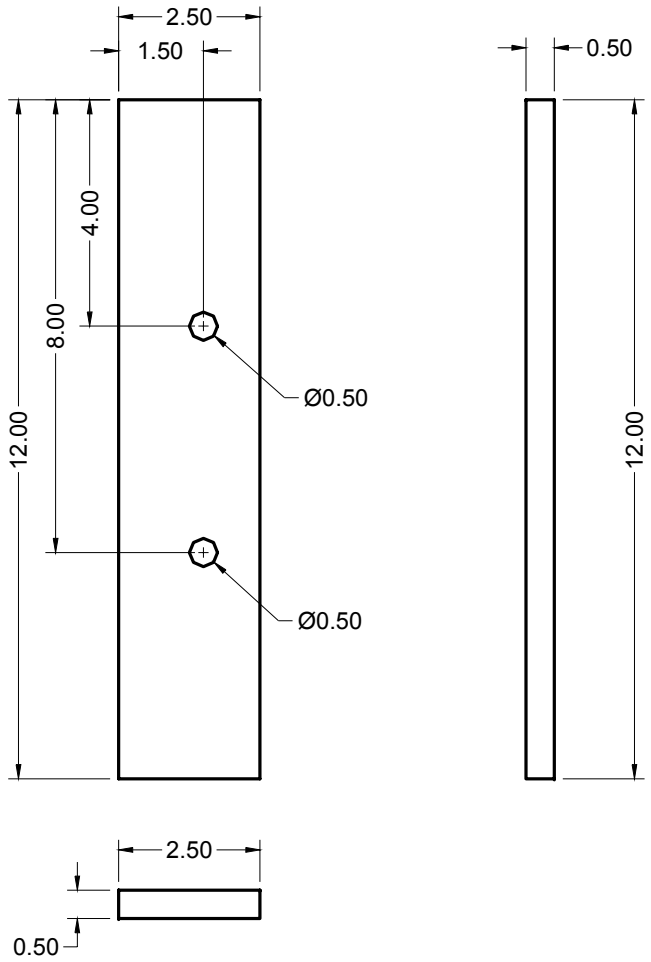

Figure B.61 Compaction plate support

Left Side Panel

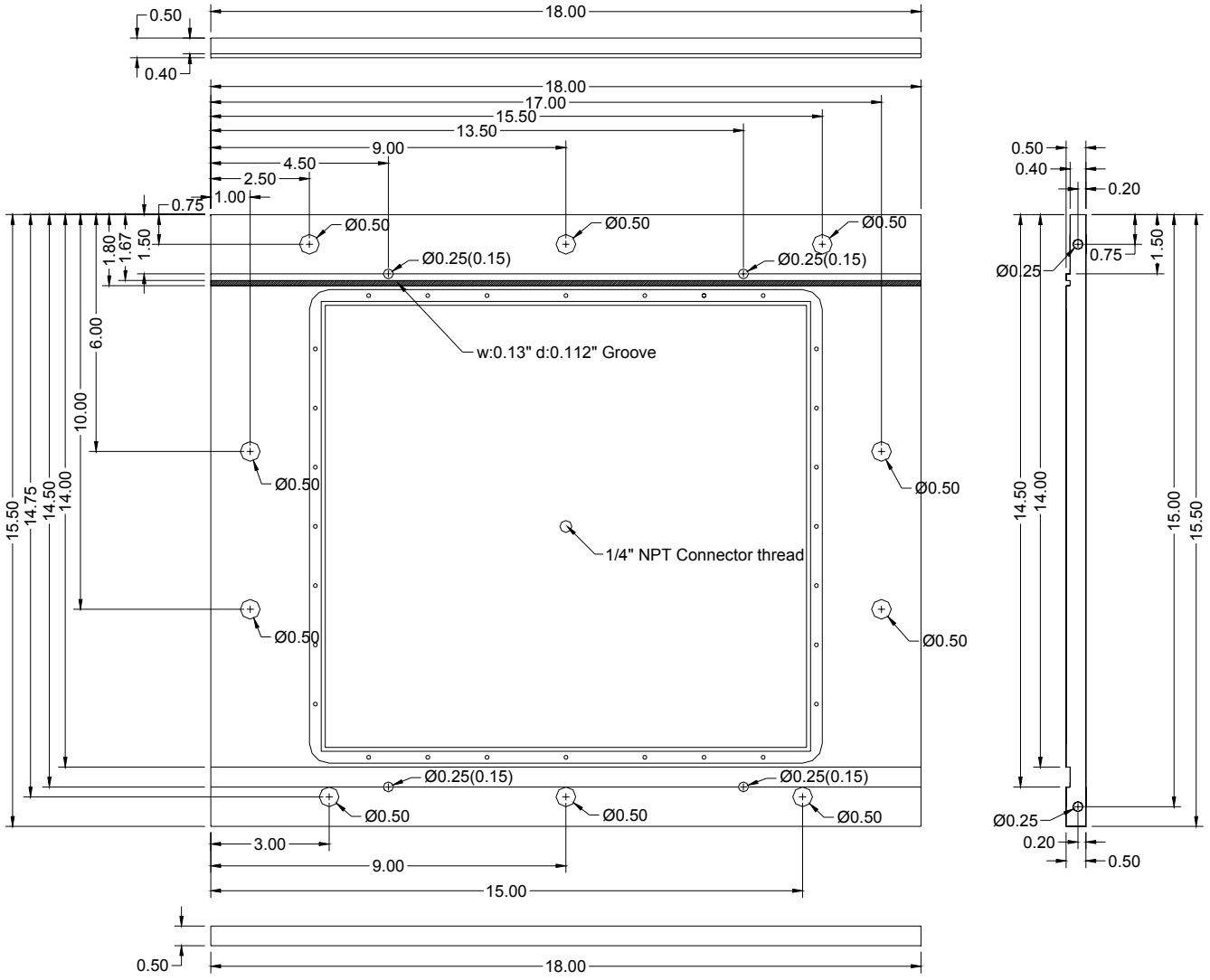

Figure B.62 Left side panel

Left Side Panel Insert

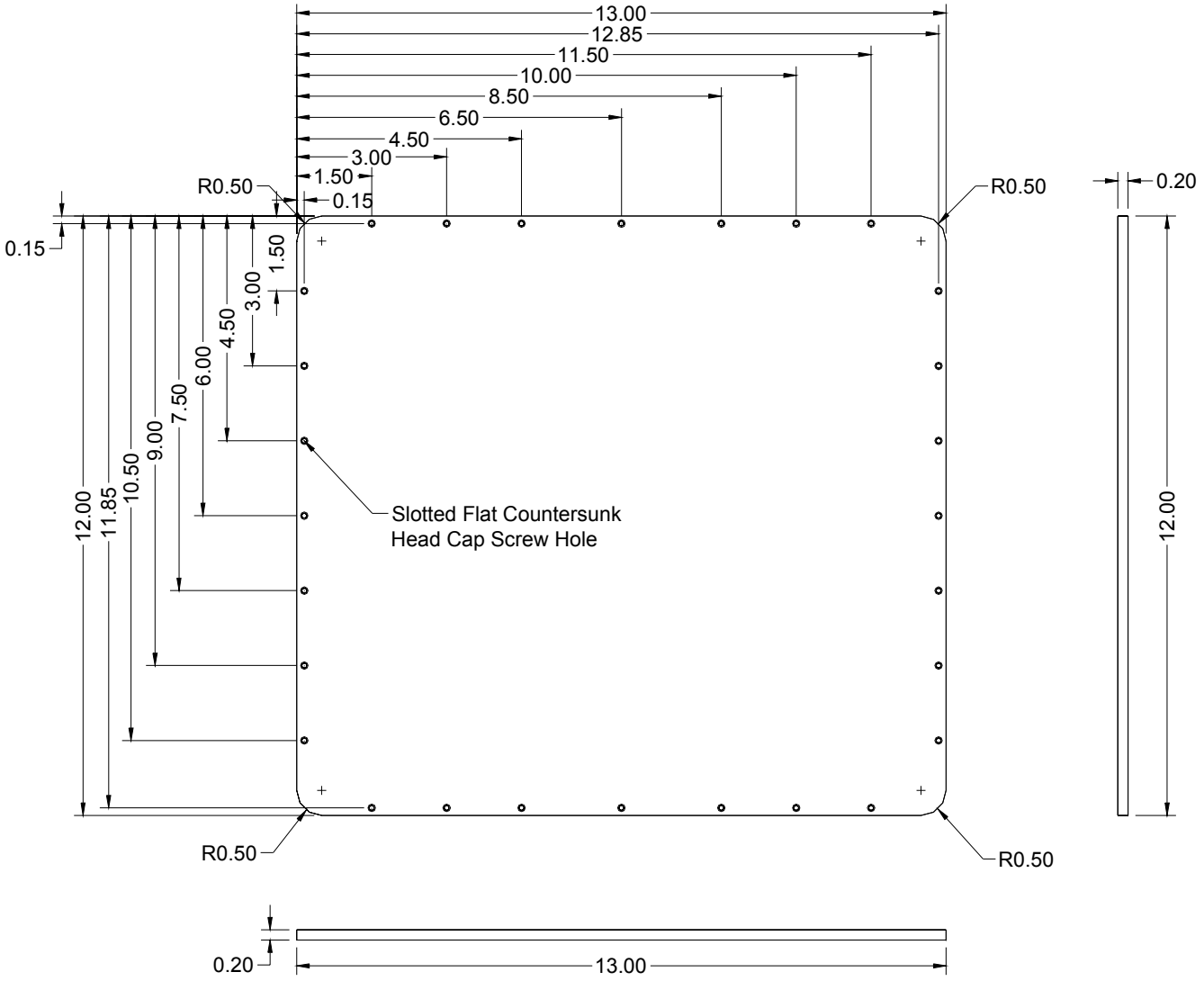

Figure B.63 Left side panel insert

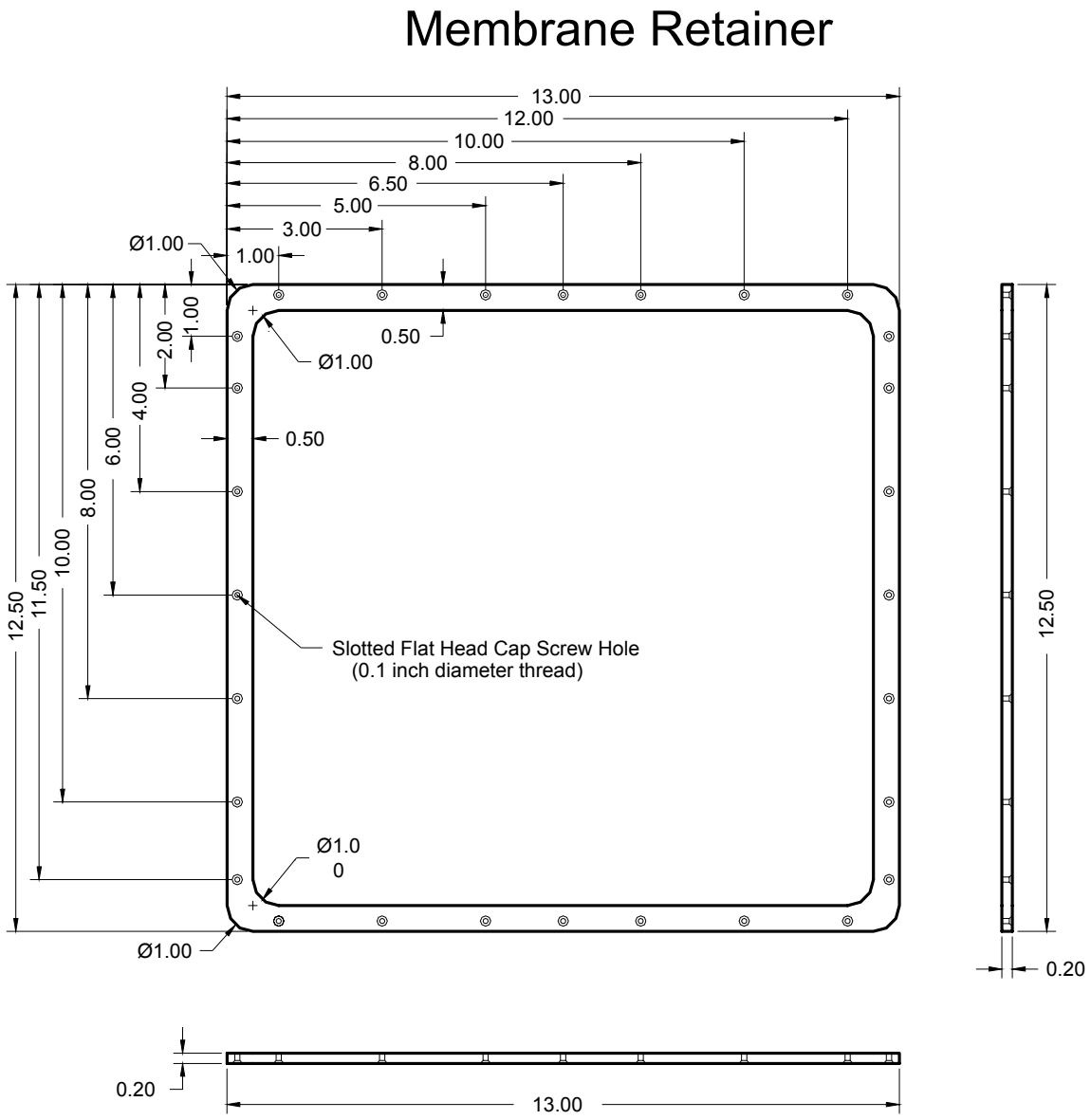

Figure B.64 Membrane retainer

Right Side Panel

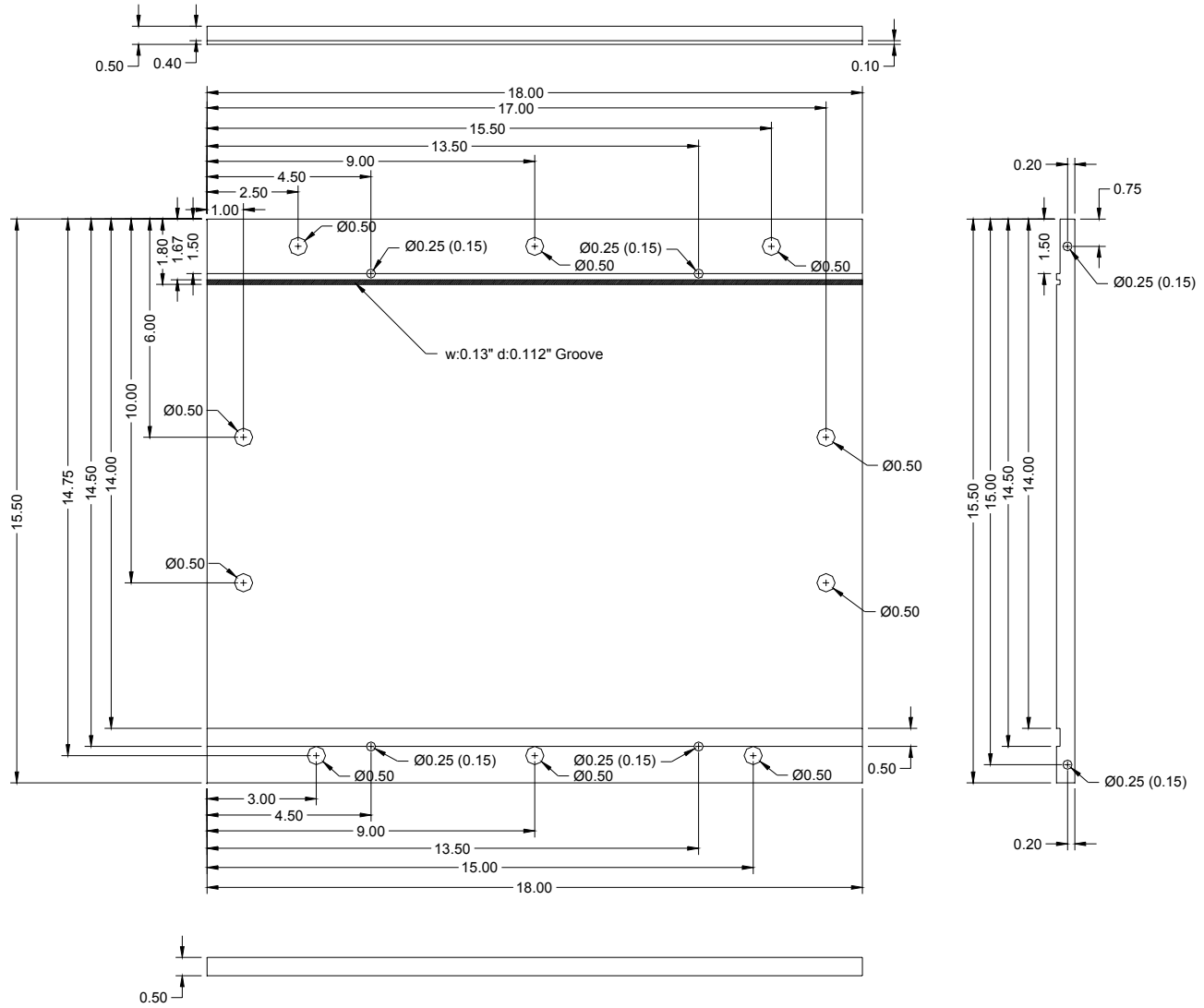

Figure B.65 Right side panel

Porous Plate

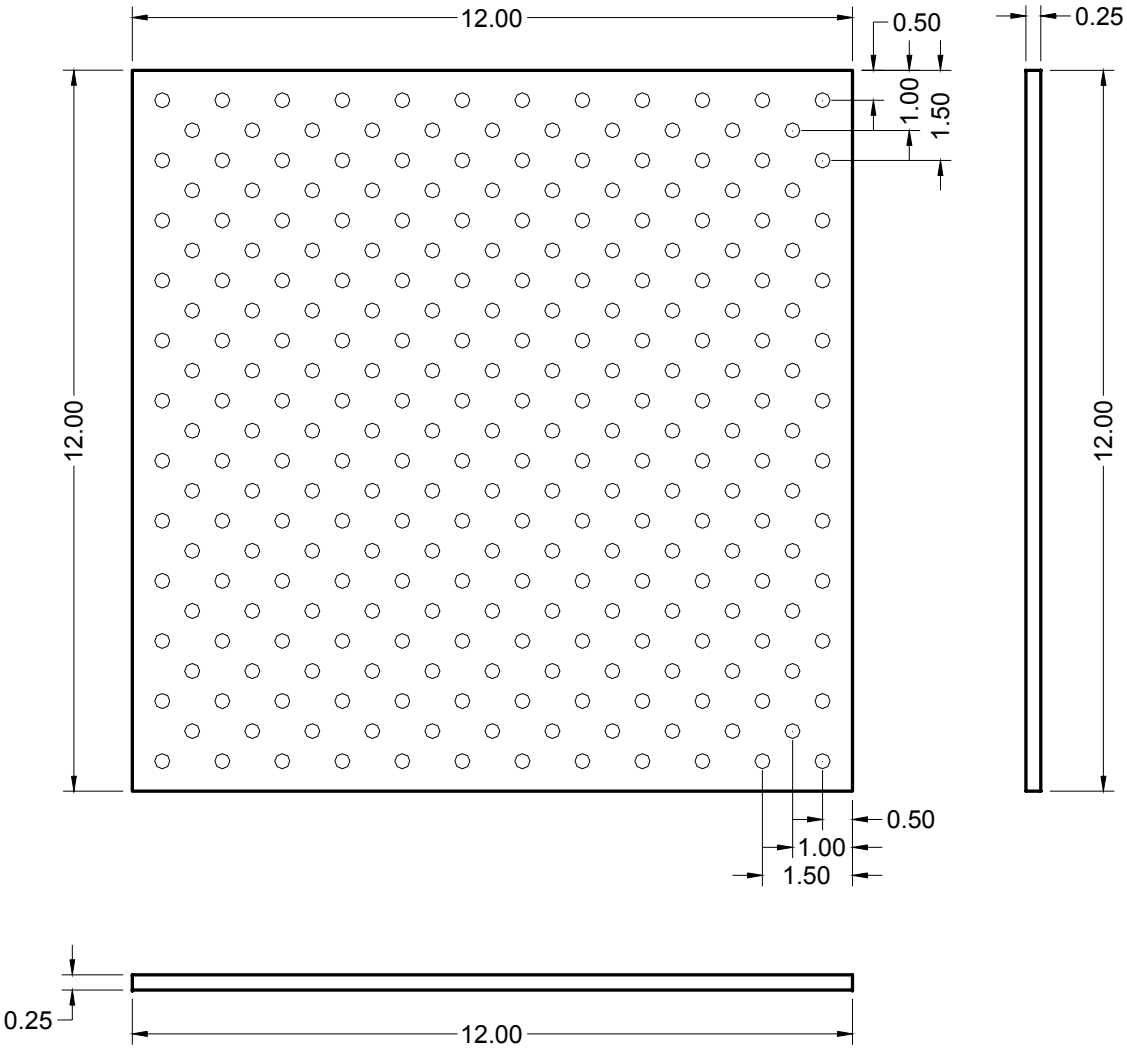

Figure B.66 Porous plate

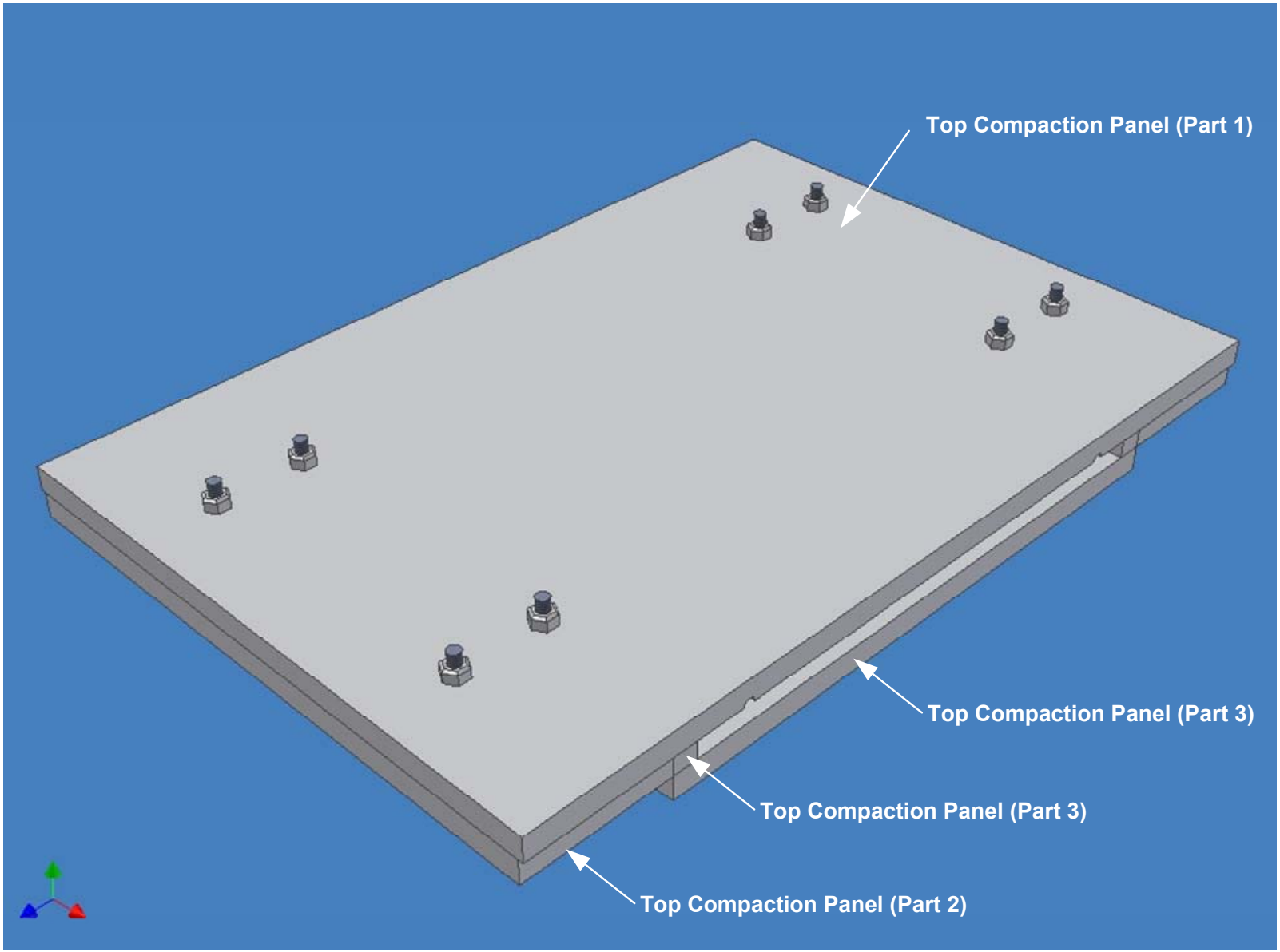

Figure B.67 Top compaction panel parts

Top Compaction Panel (Part 1)

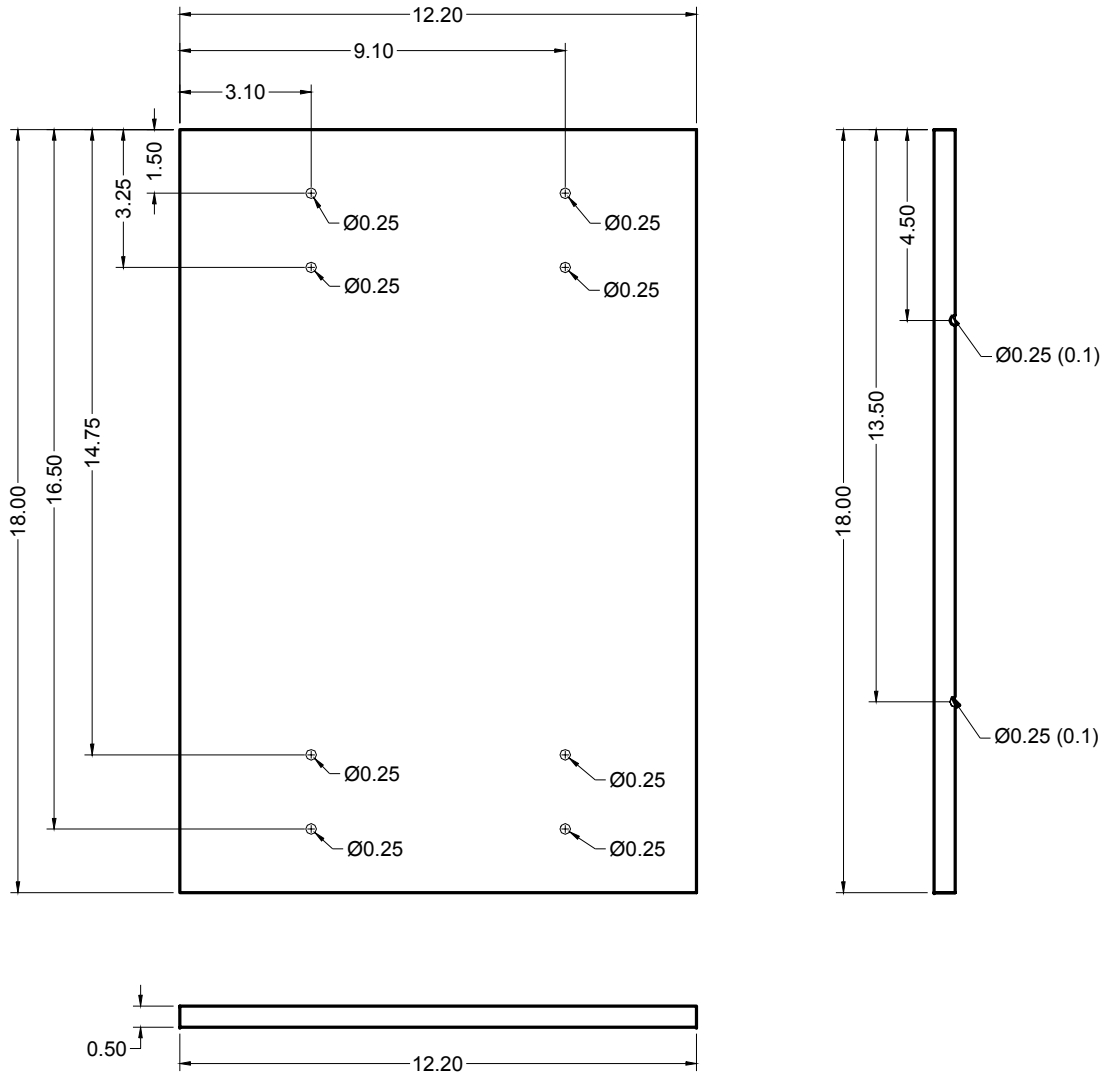

Figure B.68 Top compaction panel (part 1)

Top Compaction Panel (Part 2)

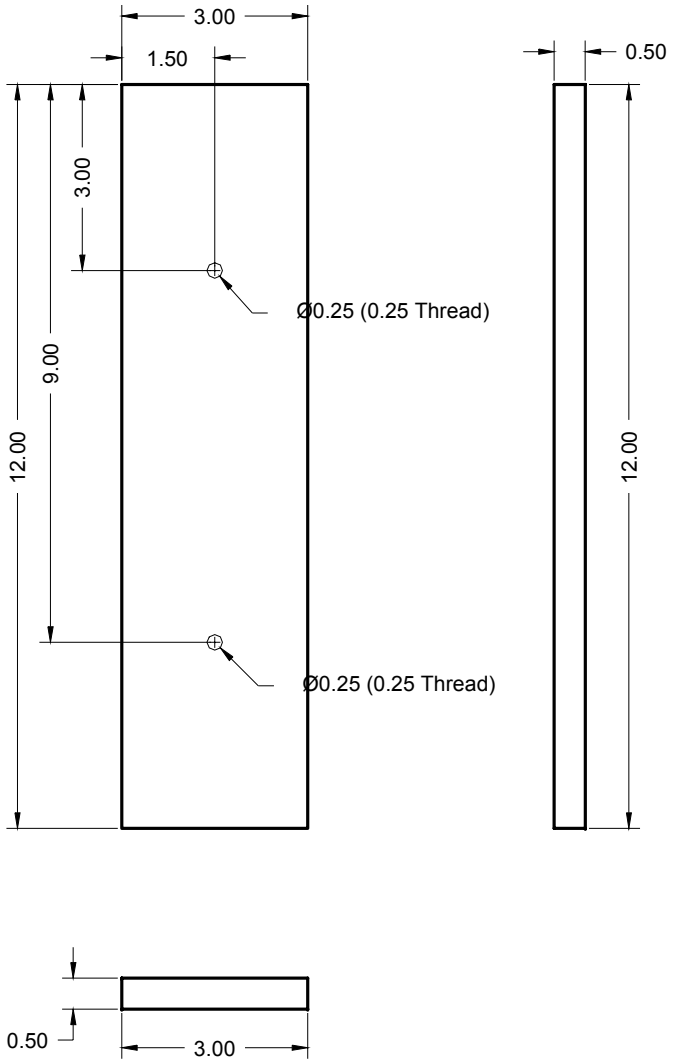

Figure B.69 Top compaction panel (part 2)

Top Compaction Panel (Part 3)

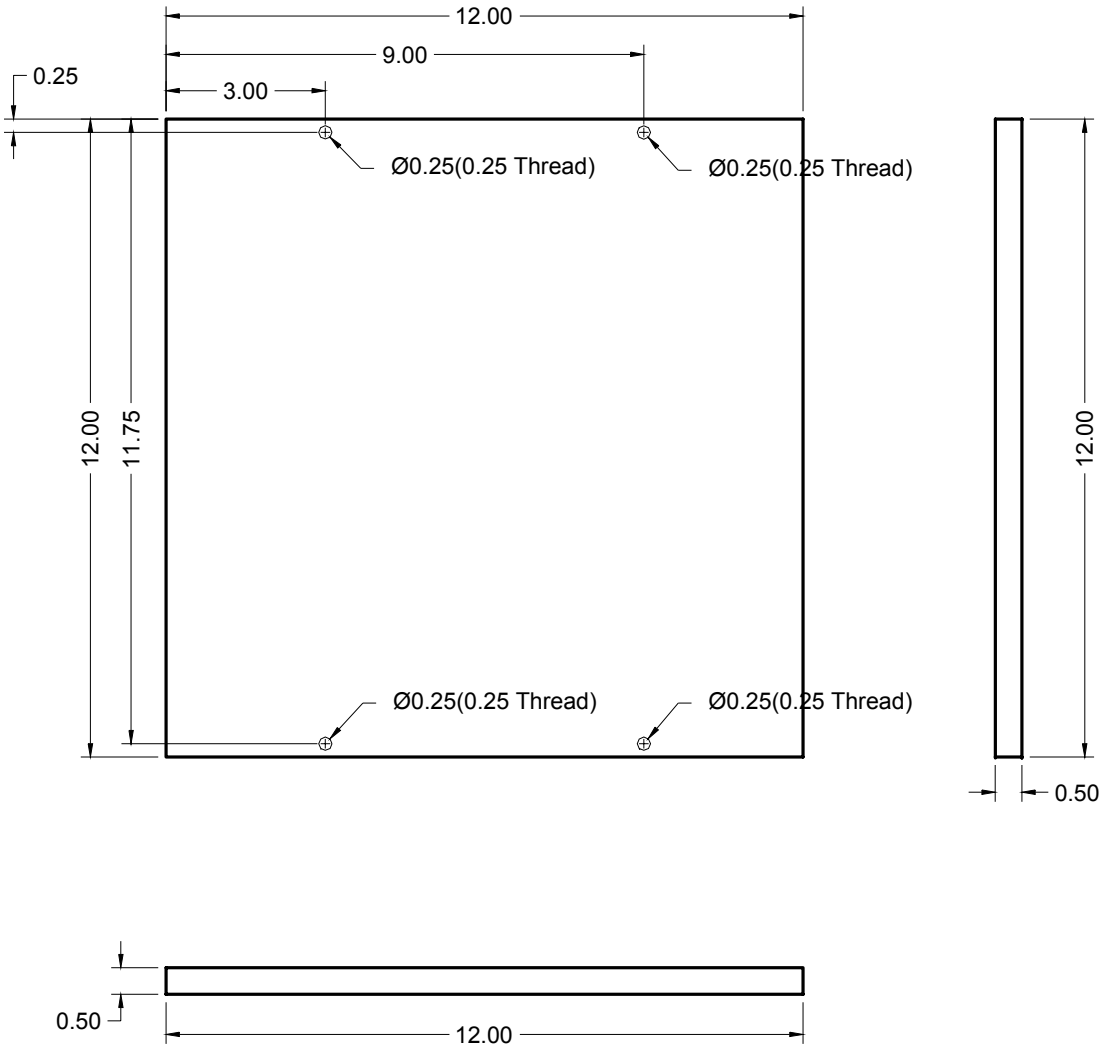

Figure B.70 Top compaction panel (part 3)

Top Compaction Panel (Part 4)

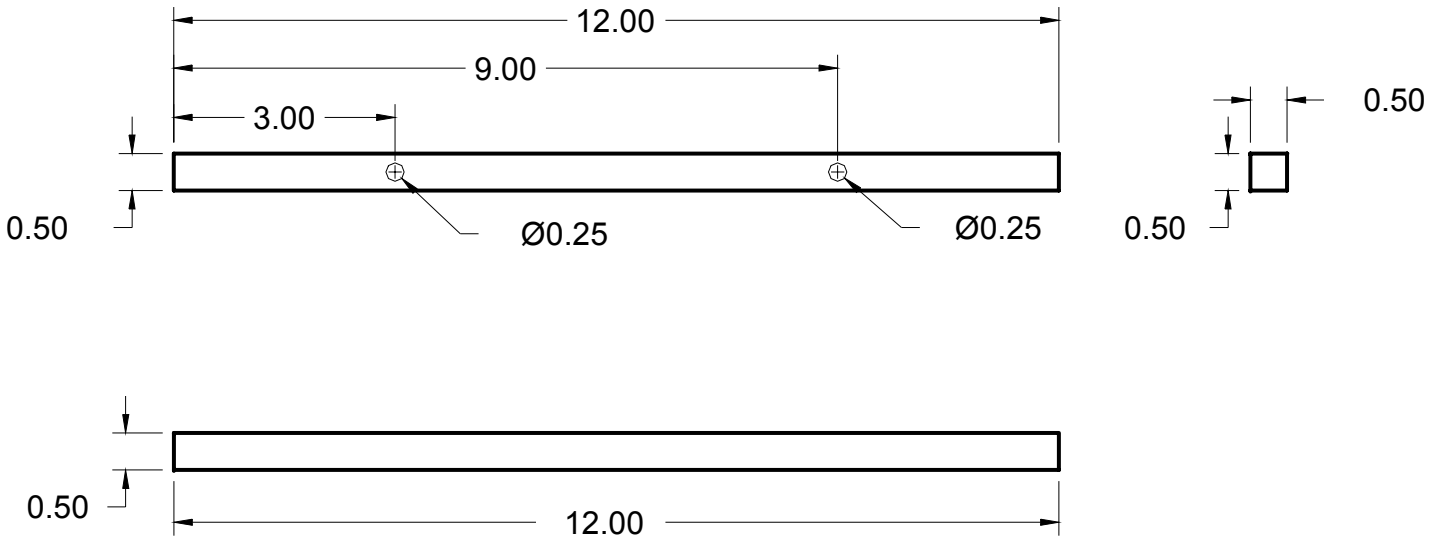

Figure B.71 Top compaction panel (part 4)

Top Transparent Plastic Panel

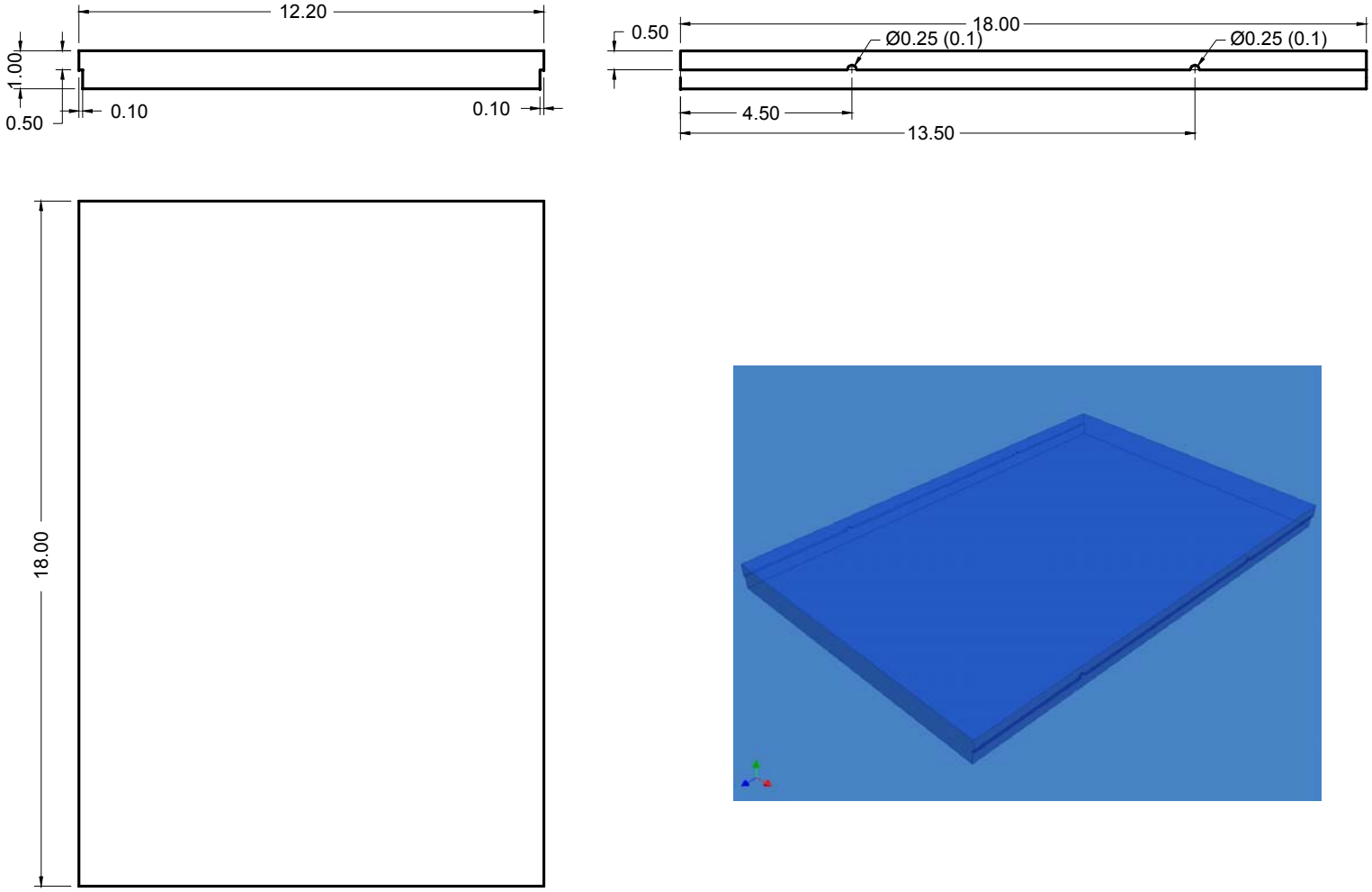

Figure B.72 Top transparent plastic panel